TECHNICAL REPORT NO. 1-674

AN EXPERIMENTAL STUDY OF ARCHING IN SAND

by

J. W. McNulty

May 1965

Sponsored by

Defense Atomic Support Agency

Conducted by

U. S. Army Engineer Waterways Experiment Station
CORPS OF ENGINEERS
Vicksburg, Mississippi

For Sale By
WATERWAYS EXPERIMENT STATION

$2.00

TECHNICAL REPORT NO. 1-674

AN EXPERIMENTAL STUDY OF ARCHING IN SAND

by

J. W. McNulty

May 1965

Sponsored by

Defense Atomic Support Agency

Conducted by

U. S. Army Engineer Waterways Experiment Station
CORPS OF ENGINEERS
Vicksburg, Mississippi

FOREWORD

This report was prepared by Captain James W. McNulty during his assignment as a research engineer to the Nuclear Weapons Effects Division, U. S. Army Engineer Waterways Experiment Station. The report is essentially a thesis submitted by Captain McNulty in partial fulfillment of the requirements for the degree of Doctor of Philosophy in Engineering in the Graduate College of the University of Illinois, and is an experimental study of arching in sand. The experimental arching study described was conducted by the Nuclear Weapons Effects Division under the sponsorship of the Defense Atomic Support Agency (Nuclear Weapons Effects Research Subtask 13.010, Interaction of Structures and Soils). The program of tests was accomplished under the supervision of Mr. W. J. Flathau, and under the general direction of Messrs. G. L. Arbuthnot, Jr., and F. R. Brown.

Colonels Alex G. Sutton, Jr., CE, and John R. Oswalt, Jr., CE, were Directors of the Waterways Experiment Station during the period of preparation and publication of this report. Mr. J. B. Tiffany was Technical Director.

AN EXPERIMENTAL STUDY OF ARCHING IN SAND

BY

JAMES WALSH McNULTY
B.S., United States Military Academy, 1956
M.S., University of Illinois, 1961

THESIS

**Submitted in partial fulfillment of the requirements
for the degree of Doctor of Philosophy in Civil Engineering
in the Graduate College of the
University of Illinois, 1965**

Urbana, Illinois

ACKNOWLEDGMENT

The author could not possibly acknowledge individually the assistance he has received from various staff members of the U. S. Army Engineer Waterways Experiment Station. Every phase of this work, which has been conducted intermittently over a period of two years, owes its success to the cooperation, enthusiasm, and professionalism of dozens of individuals, both technical and administrative. To WES the author offers his sincere thanks and appreciation.

In particular, the author wishes to thank Col. A. G. Sutton, Jr., Director of WES, 1961-64, his successor, Col. J. R. Oswalt, Jr., and Mr. W. J. Flathau, Chief, Protective Structures Branch, Nuclear Weapons Effects Division, for their constant interest and encouragement; Messrs. J. F. Gussio and J. E. Parrette for their outstanding help throughout many hundreds of hours of testing and data analysis; Mr. J. T. Ballard for his unfailing ability to design machines and later make them do things far beyond the scope of their original specifications; and 1st Lt. A. J. Hendron for invaluable suggestions, discussions, and constructive criticism.

For their encouragement and extreme patience the author thanks Majs. M. E. Barnes and F. H. Henk, Headquarters, Defense Atomic Support Agency, and Dr. N. M. Newmark, Professor and Head of the Civil Engineering Department, University of Illinois.

TABLE OF CONTENTS

TABLE OF CONTENTS (CONT'D)

TABLE OF CONTENTS (CONT'D)

NOTATION

(AR) Arching ratio = P_B/P_s

B Diameter of a circular trapdoor, width of a strip

c Cohesion intercept on a Mohr-Coulomb diagram

D Dimensionless deflection × 1000 = $\delta/B \times 1000$

D_r Relative density of a sand = $\frac{e_{max} - e}{e_{max} - e_{min}}$

e The base of natural logarithms; void ratio of a sand

E Young's modulus

h A variable indicating vertical position

H Depth of soil above a trapdoor or structure

K Coefficient of earth pressure = $\frac{\sigma_{Horizontal}}{\sigma_{Vertical}}$

K_o Coefficient of earth pressure at rest

L Total vertical load acting on a trapdoor or structure

M_{ct} Constrained (one-dimensional) tangent modulus

N A subscript denoting that (N × 100%) of the total change in some variable has been accomplished

P_B Average pressure acting on a trapdoor

P,p Pressure

P_s Surcharge pressure acting on the surface of a soil mass

r Polar coordinate for radial distance

S_N Slope of a secant from the initial point of an arching curve to the point on the curve where (N × 100%) of the total change in AR has taken place

T_i Slope of the initial tangent to an arching curve

ult A subscript denoting the ultimate value of a variable

v Shear stress

V Shear force

W	Weight of an object
x,y	Cartesian coordinates of position in plane
δ	Deflection of a trapdoor measured with respect to the base of soil bin
$\Delta(AR)_{max}$	The maximum change in arching ratio = $(AR)_{ult}$ - 1 or 1 - $(AR)_{ult}$
$\Delta(AR)_N$	The change in arching ratio when (N × 100%) $\Delta(AR)_{max}$ has been accomplished
γ	Unit weight of soil
ν	Poisson's ratio
ϕ	The angle of internal friction of a soil
σ	Normal stress
σ_o	Free-field normal stress
θ	Subscript indicating a circumferential stress

LIST OF TABLES

LIST OF FIGURES

AN EXPERIMENTAL STUDY OF ARCHING IN SAND

CHAPTER I: INTRODUCTION

1.1 Statement of the Problem

The present methods used to design buried protective structures do not produce economical designs. One of the major uncertainties is the interdependence of the load system acting upon a buried structure and the structural response caused by the load system. Unlike the load systems generally assumed in the design of surface structures which are essentially unchanged by any allowable structural deformation, the load system acting upon a buried structure is believed to be extremely sensitive to the deformational mode of the structure. One can imagine the process as taking place in steps comparable to those used in the moment distribution method of frame analysis. The structure, frozen in its initial configuration, is subjected to a system of loads applied by the surrounding soil which is also frozen. Allow the structure to respond to the loads. The adjacent soil, having been relaxed and subjected to the same deformations as the exterior of the structure, cannot now be applying the same loads. Hence, the response of the structure modifies the load system.

The interaction of a buried structure and its surrounding medium is primarily influenced by three factors: first, those physical properties of the structure which govern the nature and extent of structural response; second, the surrounding medium and its ability to transfer loads by the mobilization of shear stresses in response to relative displacements; and third, the state of stress described as free field which would have existed in the vicinity of the structure had the structure been absent.

The last factor is further dependent upon the source of energy which causes the free-field stress and certain properties of the medium.

Soil-structure interaction as defined above is not a problem unique to protective construction. All subsurface structures are influenced by interaction to some extent, and much research relevant to the problem had been conducted prior to the advent of nuclear weapons. Protective construction does have certain unique features which have necessitated additional research. The free-field stresses, which are the starting point for most designs, are usually large enough to be well outside the scope of previous civil engineering experience. As a result, many well-established theories, assumptions, and properties must be reconsidered at these greater magnitudes of load. Similarly, the well-established practice in soils engineering of modifying an initial design as the result of measurements made during construction cannot be readily applied because loads which begin to approximate the design loads are not available. In addition the economy which might be effected by some new concept applied to numerous smaller shelters or even a few large ones, and the reliability which will be required of such structures tend to justify research. Lastly, as the loads are dynamic, certain studies are necessary to investigate the dynamic response of the structures, the time-dependent properties of soil and structural materials, and other properties related to energy absorption and damping.

Soil-structure interaction may influence the structure in one or more of several ways. A buried vertical cylinder with stiff end caps and flexible walls, which allow the end caps to move relative to one another in response to vertical loads, may possess more or less vertical stiffness

than the soil it replaces. If more stiff, the vertical loads will be higher than the corresponding free-field loads. If less stiff, the opposite is true. This is a particularly simple example where the presence of soil simply changes the level of load. More complex is the buried structure with flexural stiffness, for example, a horizontal circular tunnel. The free-field loads may be taken as a system of uniform vertical and horizontal, normal compressive stresses, the vertical stress being about twice as great as the horizontal. In response to such loads, the tunnel should take an elliptical shape with the major axis horizontal. However, the downward motion of the crown and the outward motion of the sides cause a reduction in vertical stress and an increase in horizontal stress which result in a more uniform pressure on the tunnel. This changes the tunnel response from a flexural mode to a compressive mode and increases the load-carrying capacity. At the same time, it is possible that the tunnel, if more or less stiff than the soil it replaced, has been subjected to a stress system of generally different magnitude from the free-field stress system. Thus, soil structure interaction may change both the magnitude and distribution of loads acting on a buried structure. These changes may be either harmful or helpful.

Arching is defined here as the ability of a material to transfer loads from one location to another in response to a relative displacement between the locations. A system of shear stresses is the mechanism by which the loads are transferred. Arching of stresses in the medium is responsible for soil-structure interaction. It may act in a large sense and cause a stress change throughout a volume of soil because the structure located therein exhibits a different compressibility than does the

surrounding soil. It may act in a small sense, as around a tunnel, and cause a redistribution of stress as various elements of the tunnel attempt to move into or away from the surrounding soil. Arching is not interaction because it does not depend upon structural properties. Arching will be classified as active when the area or volume of interest undergoes a decrease in stress, and passive when the stress is increased.

A better understanding of soil arching is essential for the development of more economical designs of protective structures. In addition, it would serve the designer of conventional structures as well as the engineer trying to measure free-field earth pressures with gages which are themselves structures.

1.2 Purpose

The purpose of this study is to investigate experimentally soil arching apart from the other variables of the soil-structure interaction problem in order to determine the amount of load transfer possible in real soils, the relative deformations associated with arching, and the size of the zone in which the stresses transferred by arching are significant.

1.3 Scope

The change in load experienced by a trapdoor mounted in the stiff, horizontal base of a sand-filled soil container was measured as the trapdoor was moved vertically into or away from the soil mass. The soil mass itself was subjected to various pneumatic, static surcharges. The horizontal base was instrumented with flush-mounted pressure cells to indicate the distribution of transferred load.

The parameters varied in the tests were the following: the engineering properties of the medium (strength and stress vs. strain) by the

use of two different sands; the depth of soil cover above the trapdoor; the level of static surcharge pressure on the soil surface; the direction of motion of the trapdoor from the flush position leading to active and passive arching; and the size of the trapdoor.

An axially symmetrical test bin was used in order to minimize the influence of sidewall friction, the importance of which was demonstrated by preliminary tests in a long rectangular box. All tests were run by deflecting the trapdoor after the surcharge pressure on the soil surface had been established so that the influence of structural properties could be eliminated.

The next chapter contains a summary of the most relevant previous work. Chapter III describes the test apparatus and procedures as well as the soils used for the tests. Chapter IV presents the results of the tests and includes a discussion of the reliability of the data and of certain procedures followed to eliminate systematic errors in the data. In Chapter V the data are interpreted with respect to the major variables of the study and are compared with presently available arching theories. A semiempirical method of predicting a load-deflection curve is developed. The last chapter contains the summary, conclusions, and some recommendations for further research.

CHAPTER II: SUMMARY OF PREVIOUS RESEARCH

2.1 General

Arching is not a recent discovery; engineers have long known of phenomena associated with soil and other materials which are closely related to the subject of this research. For example, the stress concentration caused by a hole in a plate may be interpreted as an arching situation brought about by the lack of constraint at the surface of the hole which allows certain points to move with respect to others located farther away from the hole (Timoshenko and Goodier (1951), pp 78-85). The transfer of vertical load to the relatively rigid walls of a silo containing granular material is another well-known example. Terzaghi (1943, p 66) writes, "Arching is one of the most universal phenomena encountered in soils both in the field and in the laboratory."

It is the purpose of this chapter to review the most significant theoretical and experimental studies of arching in soils. In addition, certain studies of soil-structure interaction which clearly demonstrate the influence of arching upon structural response are reviewed.

2.2 Fundamental Analyses and Tests

Terzaghi (1936a) discusses arching in general and presents three examples which indicate the universality of the phenomenon: the reduction in lateral stress on the walls of a braced cut in sand; the reduction in load experienced by a yielding trapdoor; and the reduction in stress in the vicinity of a vertical shaft, a particularly interesting example of arching. Arching acts in two ways at the same time to reduce the stresses in the vicinity of the shaft. There is a bin-type arching induced

by the lateral expansion-vertical contraction around the hole which transfers vertical stress away. There is also ring-type arching around the hole induced by the same lateral (radial) expansion.

Experiments on arching above a yielding trapdoor were conducted by Terzaghi (1936b) in order to enhance his understanding of the stress distribution around tunnels. A trapdoor 7.3 cm wide and 46.3 cm long was mounted in the base of a bin containing about 31 cm of sand. Tests were conducted with both loose and dense ($\phi = 44^{\circ}$) sand. As the trapdoor was deflected downward, its movement and the total load upon it were measured. The horizontal and vertical stresses at various levels in the sand above the door were also measured by the friction tape method. Fig. 2.1A is a sketch of the experimental setup. The principal test results are shown in Figs. 2.1C-D. It can be observed that the total load on the door decreased to less than 10 percent of its original value by the time the trapdoor was deflected 0.005 to 0.010 times the door width, depending upon the density of the sand. After reaching the minimum value, the load increased slightly to about 13 percent at a deflection of 0.11 times the door width. During deflection, the vertical stress above the trapdoor decreased greatly in the soil located less than three door widths above the trapdoor, while the ratio of horizontal earth pressure to vertical earth pressure became as high as three times the at-rest coefficient of earth pressure K_o in the same region. The mechanism of this active arching is explained in two stages. During the first, which corresponds to the reduction in average trapdoor pressure from its hydrostatic value γH to its minimum value, the sand immediately above the trapdoor (Fig. 2.1A) expands vertically and contracts horizontally allowing the adjacent sand located in wedges b , a , c and

b_1 , a_1 , c_1 to expand horizontally and contract vertically. This subsidence causes a portion of the weight of the sand located between ac a$_1$c$_1$ to be transferred by shear across the shaded areas to the motionless sand masses. The subsequent slight increase in trapdoor pressure to the ultimate value is associated with the disintegration of structure in the sand above the door due to excessive expansion and shifting of the plane of minimum resistance to positions ab and a_1b_1 shown in Fig. 2.1B. It is well to note here that Terzaghi and Peck (1948, p 200) state that ultimate load on a trapdoor does not exceed the weight of a half cylinder of soil with a height and diameter equal to the trapdoor length and width, as shown by the shaded area of Fig. 2.1B. Terzaghi (1936b) also presents data from tests run by moving the trapdoor upward and downward in a cycle involving both passive and active arching. Hysteresis is very evident in both loose and dense sands. The initial portion of the passive arching curve is linear, and has about the same slope as the initial portion of the active arching curve. Terzaghi concludes with demonstrations that the state of soil stress associated with arching is not greatly changed by either seepage or "normal" vibrations. Several points of particular interest to protective construction research are not treated. In particular these are: the early portion of the arching curve where 90 percent of the load is lost, the ability of soil to arch loads of much greater magnitude than its own dead weight, and the influence of depths of soil cover considerably less than three door widths.

In Chapter V, Theoretical Soil Mechanics, Terzaghi (1943) presents an extensive discussion of trapdoor arching and the various theories available to compute the ultimate load upon a yielding trapdoor. It is

pointed out that observation shows that the surfaces of sliding formed in an active arching situation intersect the surface of the sand at right angles, and that the distance between the lines of intersection is always greater than the width of the door. Little else is known about the surfaces except some evidence that the average slope angle varies from 90° (vertical surfaces) for shallow burial to $45° + \phi/2$ for very deep burial. One theory of arching which assumes vertical slip planes above the edges of the trapdoor, and which is known to predict reasonable values for the ultimate arching ratio (the ratio of the load on the yielded door to the load on the undeflected door), is developed in detail for a soil in a state of plane strain with both frictional and cohesive strength components. The theory, when applied to a cohesionless soil with an angle of internal friction between 30° and 40°, predicts that cover two to three door widths deep will allow the load to reach a minimum value (about a 70 percent loss of dead load), which remains constant with further increases in depth. Since this and the experimental evidence discussed above (Fig. 2.1) indicate that the state of stress in soil higher than two or three widths above the trapdoor is unchanged, Terzaghi investigates the depth in which a surcharge pressure equal to the pressure due to this excess soil can be dissipated. The theory indicates that the same depth of soil which reduces the distributed dead load to its minimum value will reduce the soil pressure resulting from the surcharge to a negligible level. Terzaghi concludes that the pressure acting upon a yielding trapdoor is independent of the state of stress in any soil located more than two or three widths above the trapdoor. The theory developed, as well as Terzaghi's trapdoor experiments, is concerned only with a plane strain situation in which load is transferred across two

plane surfaces of sliding. Modification of the theory to fit three-dimensional situations is no great problem. When modified (Section 5.3), the theory indicates that cover equal to 1 or 1-1/2 diameters is sufficient for maximum arching and the dissipation of any surcharge pressures above a circular trapdoor.

A considerable amount of work, both theoretical and experimental concerning design of buried conduits has been conducted at Iowa State University by Professors Marston and Spangler and their associates during the last half century. The work, which is concerned both with arching and soil structure interaction, is well summarized by Spangler (1948). In general conduits are subdivided into two classes, ditch type and projecting. A ditch-type conduit is one buried in a relatively narrow ditch which is backfilled with material assumed to be more compressible than the undisturbed material. The tendency of the backfill material to settle causes a transfer of load across the sides of the ditch by shear. The result is a reduction in the total load on a plane at the level of the conduit top. The reduction in total load is independent of the conduit's properties. The analysis is very much like Terzaghi's in that the sides of the ditch become the vertical shear planes. Projecting conduits are covered by uniform material so that the problem becomes one of interaction in which the load on the structure is determined by its properties, the properties of the backfill, and the geometry. However, should one know in advance that a projecting-type conduit will deflect enough to allow shearing planes to form, the analysis is very much like a ditch-type conduit. At the other extreme is the very rigid conduit which collects load as the backfill settles around it. Between these extreme types of projecting conduits are

several indeterminate types, the analysis of which depends upon field observations. A concept important to this study is the plane of equal settlement which separates that soil in which stress is being transferred by shear from that soil which is acting merely as a surcharge. This plane fits in with Terzaghi's observation that the state of stress a certain distance above a yielding trapdoor remains unchanged. The definition of this plane as originally proposed by Marston has been modified by Spangler (1950) to include the effect of the weight of soil located between the plane of equal settlement and the structure, as well as the influence of that load transferred by shear upon the settlements of the soil columns adjacent to the structure. The modification is essential for situations in which large surcharges are considered. To locate the plane of equal settlement, a quantity known as the settlement ratio must be treated empirically. Spangler (1950) presents recommended values of the settlement ratio to be used for culvert design. Spangler's observations also indicate that flexible culverts are best constructed with well-compacted sidefills, which greatly increase the load-bearing capacity of the structure by limiting vertical deformation at the price of a minor increase in load. Van Horn (1963) has developed the Marston-Spangler approach for three-dimensional structures, and also a method of dynamic analysis for the various Marston-Spangler conditions.

Finn (1960) presents a closed form solution for distribution of stress in a plane, semi-infinite, elastic medium caused by rigid, vertical displacement of a trapdoor-like portion of its boundary. Chelapati (1964) modified Finn's solution to account for a variable depth of cover. The stresses due to lower boundary displacement (arching stresses) are

superimposed upon the stresses due to weight of the medium and a pressure on the upper boundary. Integration of the normal stress on the yielding portion of the base should lead to total load acting thereon so that arching can be expressed as a function of displacement. However, at the edge of the yielding strip the arching stress becomes unbounded so that the integral cannot be evaluated (Fig. 2.2). Chelapati, by assuming that tensile forces cannot be transmitted by soil, discards that portion of the stress distribution where the tensile normal stress associated with a displacement away from the medium (active arching) exceeds the compressive normal stress due to weight and the upper boundary pressure. The remaining compressive normal stress is then integrated to yield the load on the trapdoor. Chelapati's solution, not being in closed form, is presented graphically in terms of P_s (the surface pressure), δ (the deflection), H (depth of medium), E (Young's modulus), and the ratio of the average pressure on the trapdoor (P_B) to the surface pressure for specific values of Poisson's ratio and H/B (B being the width of the yielding strip). The above notation is a modification of Chelapati's notation so that it agrees with that used herein. Certain general observations can be made based on Chelapati work. Given H/B and a value of Poisson's ratio, a particular value of arching ratio (P_B/P_s) is associated with a particular value of the quantity $\frac{\delta E}{P_s H}$. If the three parameters, E, H, and P_s, are varied one at a time, it is possible to estimate their influence upon the deflection associated with a certain arching ratio. An increase in E will allow the same load transfer with less deflection. An increase in H demands more deflection together with an increase in B (so that H/B remains constant), but the relation is such that the dimensionless deflection

(δ/B) remains unchanged. An increase in P_s requires more deflection for the same percentage of load transfer. The solution also implies that the initial slope of an arching curve like those presented in Chapter IV should increase with H/B for a constant value of B. The data cannot be applied to passive arching in any obvious manner because of the technique used to remove the very large tensile stresses.

Bedesem (1964) presents a plane-strain plasticity solution for a trapdoor deflecting away from a medium which behaves according to the Mohr-Coulomb failure criterion, and which carries a uniform surcharge pressure. Although he concludes that the results should provide a good estimate of arching in a granular medium, the agreement between his results and experimental data depends upon increasing the angle of internal friction as a function of the cover-to-span ratio (H/B) for a particular problem in order to account for additional lateral restraint not found in the vicinity of shallow structures such as footings. In view of the surcharge pressure which ought to make depth effects negligible and the known tendency of sand to exhibit a lower angle of internal friction at higher confining pressures (Terzaghi and Peck (1948, p 82)), the correction seems unrealistic. However, since the test results against which Bedesem compares the theory were obtained in a plane strain configuration, it is probable that sidewall friction caused the measured loads to be too low, and the predictions to appear too high. It seems, too, that if the major principal stress were assumed vertical at the surface and horizontal immediately above the structure, the solution would yield more realistic results.

Sirieys (1964) presents in closed form an elastoplastic solution for the state of stress about a deep tunnel through rock which satisfies the

Mohr-Coulomb failure criterion. The boundary loads are a uniform radial stress applied at a great distance from the tunnel, and a uniform pressur acting on the inside of the tunnel. Although the solution may not be applied directly to the test results reported herein because of differin geometry and boundary conditions, the distribution of circumferential str along a radial line is of assistance in interpreting the changes in vert cal stress measured adjacent to the trapdoor. Fig. 2.3 shows the genera geometry and the circumferential stress distributions associated with active and passive arching about the tunnel. It is evident that the existence of the plastic regions severely modifies the stress distribution associated with a hole or inclusion in an elastic material. The radius of the boundary between the elastic and plastic regions is a variable which depends upon the properties of the medium and the boundar stresses.

2.3 Recent Arching Studies

Selig et al (1960) have developed a method of dynamic analysi based upon the assumption that the full shear strength of the soil is de veloped along vertical shear planes rising directly above the structure to the surface when the ultimate strength of the top structural members been developed. Selig (1960) presents additional experimental evidence support the method of analysis mentioned above. A series of plane tests were conducted in a glass-walled box with several types of structures lo cated at the bottom in order to observe the formation of shear planes. For flat roofs, vertical shear planes were observed, after the roof had been forced to deflect, rising above the structure to the surface for al depths of cover (a support-yielding situation). The only pressure-yield

structures shown are shallow, and although the disturbed zone above them runs to the surface, there is no major depression there like the depression associated with the support-yielding structures. The disturbance above the deeper support-yielding structures tends to discredit the idea of a plane of equal settlement. The writer is firmly convinced, however, that the deflections imposed upon the structure were many orders of magnitude greater than those required to cause arching of all load from the structure. As a result, the photographs presented by Selig (1960), although suitable for giving one a notion of the behavior of the soil, are unsuitable for determining the extent of disturbance. It is interesting that the distance between the vertical shear planes above a flexible roof panel is less than the width of the panel. The planes are separated by a distance equal to 0.8 the width of the panel.

Luscher and Höeg (1964) present the results of an extremely interesting series of tests concerned with both arching and interaction. Tests performed by hydrostatically loading both the inner and outer surfaces of hollow sand cylinders, with inside diameters of 1 in. and wall thicknesses of 1/4 and 1/2 in., demonstrated the capacity for ring-type arching. The cylinders with 1/2-in.-thick walls were subjected to ratios of external to internal pressure which varied between 13 and 20, depending on the void ratio. The cylinders with 1/4-in.-thick walls sustained pressure ratios between 4 and 6 before failing. The rate of loading was varied in some tests and with more rapid rates of loading, premature failure occurred at pressure ratios somewhat lower than those mentioned above. The sand cylinders underwent large radial deformations (3 to 7 percent of the original radius) prior to failure. After the tests on the sand cylinders,

flexible cylinders were tested to determine their strengths under hydrostatic loadings. Finally, soil-surrounded cylinders were tested so that the interaction between the soil and structure could be observed, and the effect of ring-type arching separated from the influence of the sand in preventing buckling of the tubes. Because the pressures acting on the outside of the interior cylinders were many times greater than the hydrostatic pressures for failure of the interior cylinders acting alone, it was concluded that the prevention of low-mode buckling far outweighs ring-type arching in causing the strength increase of the assembly. The symmetrical nature of these experiments tends to make direct application of the result to buried structures rather questionable.

Triandifilidis et al (1964) ran a series of static tests on rigid, vertical cylinders buried in sand. The cylinders were supported at the bottom of the test chamber. Passive arching was observed in all tests except those with very dense sand. The arching which was developed appeared to be independent of the surface pressure (0 to 80 psi).

2.4 Recent Studies of Soil-Structure Interaction

McDonough (1959) performed elastic analyses of two concentric spheres and cylinders subjected to uniform radial pressure P_o on the surface of the outer body. A relation is presented which gives the ratio of P_o to the pressure on the interior body as a function of the compressibility ratio of the bodies. A technique is developed for finding the compressiblity ratio of a buried structure and the surrounding medium so that the elastic results can be applied. The method is successfully used to predict the pressures experienced by buried drumlike structures in nuclear field tests. An elastic analysis of three concentric spheres is

also given. This analysis leads McDonough to conclude that an intermediate liner of either very high or very low modulus should be placed between a buried structure and the surrounding medium. The stiff liner attracts more load from the medium, but carries most of it around the structure. A weak liner forces the medium to carry the load around both the liner and the structure.

Wiedermann (1960) reports on several series of static interaction experiments conducted in dry sand. Although many of his test results are questionable for a variety of reasons, he is able to conclude that a dimensionless quantity called arching force is independent of free-field pressure, and that being close to the surface does not change the form of the arching force. The arching force is equal to the arching ratio minus 1, (AR - 1). Some of Wiedermann's tests were conducted with a footing-like punch pressed into the surface of a soil mass with a surcharge. With a surcharge of 10 psi, the load on the punch was increased to 40 psi before the deflection of the punch began to increase rapidly.

Whitman et al (1962) have conducted a series of static experiments on domes in sand. Arching was observed in tests of both rigidly and flexibly supported structures. The structures which were rigidly supported felt pressures slightly greater than the surface pressure until the domes failed by yielding at the support. The resulting crown deflection caused a relief of about half of the load on the structure. Yielding took place at about 100 psi with dense sand and 70 psi with loose sand. The flexibly supported domes never experienced loads equal to those associated with the surface pressure. The highest load was equivalent to about 0.6 of the surface pressure, and as this pressure increased from 10 to 200 psi the

load on the structure fell to 0.3 of the surface load.

Mason et al (1963) have studied the dynamic load on small vertical cylinders of varying vertical compressibility which were buried in sand at various depths. The input pressure at the surface of the sand had a rise time of about 1.5 msec and a very long duration. At all depths of burial and for all times, the stiffer structures over-registered, i.e. experienced pressures greater than free-field pressures. As the depth of burial was increased, the over-registration increased until a critical depth was reached below which no further increase was noted. For any given depth of burial, over-registration varied with time in such a manner that it was a maximum at about 2.0 msec, and a steady-state minimum at about 5.0 msec. Some less stiff structures under-registered slightly when the vertical cylinder walls were in contact with the sand, and under-registered greatly when the vertical cylinder walls were isolated from the sand by a cylinder of teflon. This indicates the stiffening effect, probably due to friction, which soil may have on a soft structure. Mason (1964) has taken the influence of the vertical stiffness of the soil and the vertical compressibility of the structure into account in an analysis based on a concept similar to the plane of equal settlement mentioned previously in Section 2.2. The analysis indicates that the over-registration experienced by a deeply buried, rigid structure should increase as the ratio of vertical length to span increases This is supported by limited experimental evidence. The analysis further indicates that as the ratio of soil stiffness to structural stiffness decreases, the over-registration will increase.

Allgood and Gill (1964) are of the opinion that arching (defined as follows) can only be developed in the vicinity of buried arches and

cylinders by rigid body motions like those induced by the failure of arch footings, or by placing flexible bedding beneath a cylinder. Arching is intended to mean the reduction in vertical load at the spring line from the total load acting at the surface directly over the arch. Their tests, supported by the evidence of Luscher and Höeg (1964), indicate that the influence of the surrounding soil in developing a load system close to hydrostatic limits vertical deflections enough to prevent load transfer to the adjacent soil. This is in general agreement with Spangler's (1950) comment that well-compacted sidewalls next to a flexible culvert more than compensate for a decrease in arching by increasing the strength of the culvert. However, in his analysis of the tunnel test section at Garrison Dam, Lane (1957) concludes that the influence of tunnel stiffness relative to that of the adjacent ground had a marked influence on vertical loads, horizontal loads, and bending moments. In addition to this, Donnellan (1964, p 79) observed considerable load relief in quasistatic tests on cylinders buried in dense sand. His tests indicate that the amount of load relief was essentially independent of the depth of cover. A discussion of this point is beyond the scope of this thesis, but it is the writer's opinion that the above definition of arching is unnecessarily restrictive, since the mechanism which might transfer load away from the general vicinity of a cylinder is essentially the same mechanism which transfers load from the deflecting crown of a cylinder to the more rigid areas (of the cylinder) adjacent to it. Allgood (1964) reports that dynamic arching (as defined above with a correction for inertia) was observed in tests of a semicircular arch with a 15-in. radius buried 6 in. deep (crown to surface). The arch was supported on footings 1.75 in. wide. At long times (greater than

40 msec), about 40 percent of the surface load was transferred by arching.

2.5 Buried Pressure Cell Research

Since buried pressure cells are small structures subject to the same interactions as larger structures, much of the research concerned with their design is relevant to protective construction. Many tests concerned with the influence of cell placement, geometry, and compressibility were conducted at the Waterways Experiment Station (1944). Most of the tests were conducted in loose Ottawa sand 10 in. deep using static pressures as high as 100 psi. The influence of cell projection from a rigid base was studied for various ratios of projection to diameter. The results indicate that if the projection is less than 1/25 the diameter, the pressure registered by the cell is essentially the same as that which a flush cell would register. A projection equal to the cell diameter was observed to cause registration as high as 160 percent of that experienced by a flush-mounted cell. The influence of compressibility was studied by mounting the cells on springs of various stiffness and positioning them flush with the rigid base. It was found that if the springs used were stiff enough to restrict the deflection to 0.001 diameter, the pressure cells would register about 90 percent of the applied pressure. The registration was not improved by increasing the stiffness. A cell which deflected about 0.01 diameter tended to register only about 60 percent of the applied pressure. It was noted that as the surface pressure increased, the indicated pressure varied linearly with it. The importance of cell proportions was studied by varying the ratio of overall thickness to diameter of soil-surrounded cells. It was found that as the ratio decreased the load experienced by a cell approached an asymptotic value which remained essentially constant. This

value was reached when the thickness equalled about 0.20 diameter. The last group of tests was concerned with the compressibility of soil-surrounded cells. Whenever the deflection was restricted to 0.0005 diameter, the output of the cell equalled a constant percentage of the surface pressure. Taylor (1947) has analyzed a simplified elastic model in order to develop a working hypothesis which might explain the experimental results summarized above. His model indicated that the conclusions are essentially correct.

An elastic analysis by Monfore (1950) of the stresses in the vicinity of a compressible cylindrical inclusion (vertically oriented) in an elastic medium indicates that, regardless of the relative moduli, the stress field resembles that predicted by Finn (1960) (Fig. 2.2), and that the magnitude of vertical arching stress adjacent to the inclusion is negligible beyond a circle with a diameter three times that of the inclusion.

CHAPTER III: EQUIPMENT, SOILS, AND PROCEDURES

3.1 General

The arching tests were conducted statically with a trapdoor so supported that it could not deflect until the desired level of pressure had been established on the surface of the overlying soil. The change in load could then be measured as the trapdoor was forced to move into or away from the soil mass. Thus, if the trapdoor were rigid, results would reflect only soil arching not soil-structure interaction which would occur if the trapdoor were more flexible and elastically supported. A circular trapdoor, located at the center of a cylindrical test chamber (Section 3.2) was used. With this geometry the possibility of bin friction was minimized, while the boundary conditions were kept fairly simple. Tests of this nature must necessarily be static in order to allow the surface pressure to reach the desired level before arching is induced by deflecting the trapdoor. The problem of ignoring time-dependent soil properties was avoided by the selection of dry sand as the test medium. Whitman (1964, p. 81) points out that the influence of strain rate upon the strength of sand is small, probably being less than a 15 percent increase due to loading times which range between one minute and five-thousandths of a second. Moore (1963, p. 121) has observed a reasonable agreement between the static moduli, dynamic moduli, and the modulus backfigured from seismic wave velocity in sands. The moisture content of each sand was checked occasionally during the course of the tests described. It varied between 0.1 and 0.2 percent. The surface of the sand was isolated from the air pressure by a diaphragm.

3.2 Test Apparatus

The tests were conducted in a cylindrical test chamber, with an inside diameter of 46-3/4 in., which was elevated above the level of the floor in order to provide space for the trapdoor support system and the associated instrumentation. The major components of the apparatus were the base, the trapdoor and its support system, the rings, and the bonnet. All of the components except the second are shown in Fig. 3.1.

3.2.1 Test Chamber Rings

The rings bolt between the base and the bonnet, and are the sidewalls for the test chamber. All except 2-in.-high rings were rolled from mild steel plate 5/8 in. thick and have flanges 1-1/2 in. high and 3 in. thick welded top and bottom. The flanges contain 40 bolt holes which have a diameter of 1-1/4 in. Access ports are located in the walls of the rings. Rings meeting the above description are available in heights of 6, 12, and 24 in. The nominal 2-in. ring (1-7/8 in.) is essentially a flange, 3-5/8 in. thick, with an interior diameter of 46-3/4 in. It also contains 40 bolt holes. Various rings are combined to give any desired depth of test chamber in nominal 2-in. increments.

3.2.2 Bonnet

The bonnet is a hemispherical top designed to contain static pressures as high as 500 psi. It contains three access ports which were used to contain an electronic pressure transducer, a Bourdon-type pressure gage, and the air valve. At the base of the bonnet is welded a drilled flange which is bolted to the upper ring. During these tests, a neoprene diaphragm 1/16 in. thick was placed over the soil surface to prevent the air pressure in the bonnet from penetrating the soil. The diaphragm was

anchored between the flanges of the bonnet and the upper ring.

3.2.3 Base

In addition to providing a bottom for the test chamber, the ba contained the pressure transducers used to measure the vertical earth pressure profile, and it provided alignment for the trapdoor. The top portion of the base is a horizontal, circular steel plate, 1 in. thick, with a diameter of 54 in. It is shown in Figs. 3.2 and 3.3. Its edges are drilled with bolt holes which line up with those in the rings and bonnet. In addition to the bolt holes, the plate contains a large cent hole into which was fitted the equipment necessary to guide the trapdoo and mount the two soil pressure cells closest to the trapdoor. The oth ten soil pressure cells were located in the plate itself as shown in Fig. 3.2. The steel plate is supported by the cylindrical structure sh in Fig. 3.3. It is somewhat similar to the soil rings described above, has a stiffening flange at its midheight and is bolted down to a frame e bedded in the thick concrete foundation. It is penetrated by three semi cular access ports, one of which is visible in Fig. 3.17. Twelve triang stiffening plates are welded to the interior surface of the cylinder and bottom of the top plate in order to limit the deflections of the plate. There is also an annular steel plate, 3/4 in. thick, which is welded bet the top plate and forms a shelf which carries the trapdoor cylinder and supporting flange. An irregular area, depressed about 1/32 in. and coat with mill scale covered about 17 percent of the area of the top plate (Fig. 3.2). One pressure cell (No. 6) was located within the area.

3.2.4 Trapdoor Support System

The trapdoor support system is shown in Fig. 3.3. A baseplat

underlain by grout and anchored by embedded bolts, rested in a shallow hole in the floor. To it was welded a plate containing four threaded holes which received the four jack support posts. A 25-ton jack, manufactured by the Joyce-Cridland Co. (Model WJ3228-6), which required 48 turns of the handle to make the platform move 1 in. was supported by the posts and locked in place by nuts. To the platform of the jack was bolted a stepped, circular plate with a center hole which contained a stud so threaded that it fitted the well in the base of a load cell. The load cell, securely fastened to the plate by the stud, had a standard, curved load button, which supported a bolt projecting from the bottom of the trapdoor, screwed into its top. Great care was taken to ensure good vertical alignment of the load-carrying elements. A deflection reference plate, through which the load-carrying elements passed, was mounted by bolts with spacers to the bottom of the trapdoor. The two sets of linear variable differential transformers (LVDT's) used to measure deflections were supported by the deflection reference plate. The upper LVDT's monitored the relative deflection between the deflection reference plate and the bottom of the flange which was welded to the trapdoor cylinder. This relative deflection was assumed equal to the deflection of the top surface of the trapdoor with respect to the upper surface of the horizontal top plate. By monitoring the output of the upper LVDT's and adjusting the jack so that the output remained constant during the buildup of pressure on the soil surface, it was possible to prevent most of relative deflection that would be caused by elastic compression of the load-carrying column and bending of the horizontal top plate. That considerable relative deflection is possible is indicated by the pressure versus deflection curves of several points on the horizontal top plate

and the freely deflecting trapdoors during several hydrostatic tests (Fig 3.4). The plate deflections were measured on the bottom of the top plate by dial gages mounted on the concrete floor. The deflection of the larger trapdoor was measured by the lower LVDT's during these hydrostatic tests as well as during the tests with soil. The lower LVDT mounts were clamped to round steel rods welded to the deflection reference plate as shown in Fig. 3.3. The average vertical deflection of these rods measured with respect to the floor was assumed equal to the vertical deflection of the center of the trapdoor. Since the trapdoor was held flush with the horizontal plate until relative deflection was desired, the lower LVDT's indicated deflection measured with respect to the top plate.

3.2.5 Trapdoors

Two trapdoors having diameters of 3 and 6 in. were used in this study. The major features and important dimensions of both doors are shown in Fig. 3.5. In order to minimize the possibility of a tilting of the vertical axis of the trapdoor without causing any unnecessary friction between the trapdoor and the cylinder walls, the trapdoor was built like steel piston with several permanent brass rings attached. The tolerance between the 6-in. trapdoor and the cylinder wall was 0.002 $\pm$ 0.001 in. The rings are visible in Fig. 3.6. The tolerances were such that the maximum possible tilt of the axis was about 0.033 degrees. Some tilt occurred as indicated by unequal outputs of the lower LVDT's during the first 0.002 in. of vertical relative displacement. The 3-in. trapdoor is shown in Figs. 3.5 and 3.7. A brass sleeve used to reduce the diameter of the hole to 3 in. was screwed to the lower edge of the trapdoor cylinder. The 3-in. trapdoor moved inside the sleeve. The trapdoor itself was made

of three components: the top, a stiff, aluminum pressure transducer described elsewhere (Waterways Experiment Station (1963a)); the middle, a hollow steel cylinder to which the top was bolted; and the bottom, which was the lower end of the 6-in. piston added so that the deflection reference plate and other items could be easily mounted.

3.3 Transducers and Instrumentation

The physical measurements made consisted of deflections, vertical soil pressures at the bottom of the soil mass, the air pressure on the soil surface, and the total force acting on the trapdoor, although this quantity has been treated as an average pressure in the analysis of test results. Each of the measurements will be discussed in the following paragraphs.

3.3.1 Load

Two strain-gage type load cells were used to measure the load on the trapdoors. A 5000-lb-capacity C&S Load Cell, manufactured by the Revere Corporation of America (Model 47C-44700-10), was used for all tests with the 6-in. trapdoor except those passive tests in which the depth of soil cover was greater than 6 in. A 10,000-lb-capacity load cell (Model D-1431), manufactured by the Baldwin, Lima, Hamilton Corporation, was used for the remaining passive tests with the 6-in. trapdoor, and all of the 3-in. trapdoor tests. The load cell calibrations were accomplished in place by conducting tests with air pressures as high as 110 psi directly on the trapdoors. The calibrations indicated that measurements associated with the larger trapdoor were accurate to within 2 psi, and that those associated with the smaller trapdoor were accurate to within 4 psi. Unfortunately, it was impossible to calibrate in place with pressures as high as

those experienced in the passive tests due to leaks in the apparatus and limitations on line pressure. However, since the output of the load cells during bench calibrations proved to be linear under loadings as high as those anticipated for the passive tests, the in-place calibrations were extended linearly for use during these tests. Load cell output was amplified by a CEC (Consolidated Electrodynamics Corporation) carrier amplifier, type 1-118, with a carrier frequency of 3000 cps. The amplified output was fed to a CEC galvanometer (type 7-319) and was recorded by a light beam oscillograph recorder on light-sensitive paper. Before each test, precision calibration resistors built into the amplifier were used to obtain calibration values for the test.

3.3.2 Pressures

Both the air pressures acting on the surface of the soil and the vertical stress at the bottom of the soil mass were measured by the same type of pressure cell, a CEC, type 4-312-0001, unbonded strain-gage pressure transducer with a range of 0-100 psia. The pressure-sensing element was a diaphragm with an overall diameter of 0.5 in. and an unsupported diameter of 0.45 in. When subjected to the rated pressure, distributed uniformly, the center of the diaphragm deflected 0.0008 in. The cell used to monitor air pressure was mounted in an adapter which was screwed to the end of a 2-in. length of 1/4-in. pipe projecting from the bonnet (Fig. 3.1). The cells used to monitor soil pressure were flush-mounted with the surface of the top plate of the base in brass adapters which screwed into the top plate from below. Before tests with soil were begun, the entire chamber was calibrated with air several times. The variation in the results indicated that air pressures could

be controlled to about 2 psi through the range of pressures used during the tests. These tests were used to establish an in-place calibration curve for the air-pressure gage, based upon the average pressure sensed by all pressure transducers in the apparatus. The 12 soil pressure cells were effectively calibrated in place under sand at the beginning of each test during the buildup of air pressure. In this way a calibration curve for each test to evaluate increases in soil pressure due to active arching with minor extrapolation was obtained. During certain tests, some pressure cells experienced reductions in soil pressure. Since it seemed probable that a different curve would be followed during unloading, several calibration tests, in which the trapdoor was held flush during loading and unloading of the soil surface, were conducted and the relation between loading and unloading curves established. The in-place loading calibrations run for each test minimized certain experimental errors associated with sand placement, gradual changes in the characteristics of the transducers, and the influence of friction at the soil ring boundary upon the pressure distribution at the base of the chamber. The calibration curves are presented and discussed in Appendix A. The amplification and recording equipment used with the pressure cells was the same as that used with the load cells.

3.3.3 Deflections

The LVDT's used to measure deflections were manufactured by the G. L. Collins Corporation (Model SS-102). They have a linear range of $\pm$0.10 in. and were excited by a common 6-volt, wet cell battery. The gages have two mechanical components, a gage body and a core which moves in a circular hole through the body. A change in the position of

the core changes the electrical coupling between two coils built into the gage body and causes a change in the output of the driven coil which is proportional to the position change. As the relative displacement between the body and the core is really the quantity measured, it is not important which component moves. During the tests the gage body moved, but during calibration the core was moved. A soft helical spring was compressed between the gage body and the end of the core so that the gage could follow the displacement of interest without the core being anchored. The lower LVDT's used to measure the deflection of the trap-door were installed as indicated in Fig. 3.3. The body of each was clamped to a vertical rod which ran down from the deflection reference plate. The spring-loaded core rested upon the end of a micrometer head which was securely anchored to the floor by a mounting bracket. The outputs from the lower LVDT's were recorded by a light beam oscillograph using a CEC, type 7-339 galvanometer. To obtain the desired linearity, it was necessary to place a high impedance network between the gage and the galvanometer. The gages were calibrated in place before each test by means of the micrometer head on which the core rested. Five or six calibration displacements of 0.005 in. each were given the core before each of the active tests, and the output (a deflection of the galvanometer trace which generally equaled 0.8-0.9 in.) was recorded. An analysis of these calibrations indicated that the deflections were known to an accuracy of 0.0004-0.0005 in. over the range of measurement (0-0.03 in.) throughout the active tests. For the passive arching tests, a much greater range of measurement without a corresponding loss of accuracy was desired. Because the linear range of the transducer was about three

times greater than the range of measurements made in the active tests, the problem was essentially one of being able to maintain the large scale of the record (to avoid errors in data reduction) without exceeding the already fully utilized capabilities of the recording equipment. This was accomplished by means of voltages which opposed the signal from the LVDT to the galvanometer. A technician, observing the displacement of the light beam reflected by the galvanometer mirror, introduced to the galvanometer a constant voltage of sufficient magnitude to make the galvanometer return to the vicinity of its initial position when he observed that it was about to leave its linear range. By taking the same action a second time, he could increase the capability of the recording equipment by a factor of three with no loss of sensitivity. However, the suddenly applied voltage acted like a dynamic load which the static galvanometer was unable to follow instantaneously, without oscillation. The records were corrected, as shown in Fig. 3.8, by construction of a trace through the approximate center of the oscillations parallel to the trace before the voltage was applied. This procedure may have resulted in a deflection error as high as 0.002 in. each time the voltage was applied, or a cumulative error of about 0.004 in. (about 5 percent) during the last third of test when the total deflection measurement approximated 0.06-0.09 in. The calibration procedure for passive tests was similar to that used for the active tests except that 25-30 calibration steps were applied.

The upper LVDT's, installed as shown in Fig. 3.3, measured relative deflection between trapdoor and top plate of the base; this relative deflection was monitored and nulled to zero during the buildup of

surface pressure. Because the vertical axis of the trapdoor exhibited the tendency to tilt mentioned above, it was necessary to install two LVDT's so that their combined output could be observed and thus the mid-point of the deflection reference plate held stationary. The gages were interconnected so that outputs associated with motion in the same direction would add, while the equal and opposite movements associated with rotation would cancel. Since both gages were operated close to their null points (as the jack was immediately used to reduce any combined output to zero), it was not necessary to calibrate the gages for each test. The combined output of the gages was monitored by a recording voltmeter manufactured by Varian Associates, which is visible in Fig. 3.17. The sensitivity of this instrument was such that it was possible to control the trapdoor's position to within 0.0005 in.

3.4 Description of Sands Tested

During the arching studies two sands were used because at high relative densities (D_r) which are comparatively easy to reproduce from test to test, the strengths and stress-deformation properties of the sands are quite different. As a result of this it was hoped that the influence of these properties upon arching could be ascertained. In addition to this, both sands were readily available at the Waterways Experiment Station (WES). The static properties of the sands used are listed in the following paragraphs. The results of constrained, dynamic tests on each sand have been reported by Durbin (1964).

3.4.1 Sand 1, Reid-Bedford Model Sand

Reid-Bedford Model Sand is a clean, uniform, fine sand (SP) obtained from a borrow pit in Campbell's Swamp near the Big Black River

in the vicinity of Yokena, Miss., about seven miles south of WES. The grain size distribution is shown in Fig. 3.9. The effective grain size (D_{10}) is 0.16 mm, and the uniformity coefficient is 1.15. A microscope examination shows that the grain shapes are predominately subangular to subrounded. The specific gravity of the solids is 2.65. The minimum and maximum densities are 86.0 pcf and 105.3 pcf, respectively, which correspond to void ratios of 0.924 and 0.570. The specific gravity, densities, and strength parameters listed herein were obtained by the methods specified by the Office of the Chief of Engineers (1964). The relation between the angle of internal friction and relative density is shown in Fig. 3.10 and was obtained by a series of stress-controlled, consolidated-drained, direct shear tests at several initial relative densities under normal pressures of 1, 3, and 6 kips per sq ft. A series of one-dimensional compression tests, described in a Waterways Experiment Station (1964) memorandum, was conducted in a 4.25-in. (diameter) by 1.245-in. (height) consolidometer using a ring 0.50 in. thick. The first cycles of loading and unloading for several initial relative densities are shown in Fig. 3.11. The loading portions of these and other tests are shown in Fig. 3.12. Figure 3.13 shows the constrained tangent modulus versus vertical stress curves for this sand at various relative densities.

3.4.2 Sand 2, Cook's Bayou No. 1

Cook's Bayou No. 1 is a clean, uniform, medium to fine sand (SP) obtained from Culkin Community, Miss., immediately northeast of Vicksburg, Miss. The sand is used commercially as a masonry sand.

The grain size distribution is shown in Fig. 3.9. The effective

grain size (D_{10}) is 0.22 mm, and the uniformity coefficient is 1.59. Individual particles vary in shape from angular to rounded with sub-rounded shapes predominating. The specific gravity of the solids is 2.65. The above determinations and the other results which follow were obtained by the same procedures used for sand 1 and the details are discussed in a Waterways Experiment Station (1963b) memorandum. The maximum and minimum dry densities are 110.8 pcf and 93.3 pcf, respectively, which correspond to void ratios of 0.495 and 0.775. The relation between the angle of internal friction and relative density, obtained by the procedures previously mentioned, is shown in Fig. 3.10. Static one-dimensional compression curves for this sand are shown in Fig. 3.14 and Fig. 3.15, and the accompanying constrained tangent modulus versus vertical stress curves are shown in Fig. 3.16.

3.5 Soil Placement Procedure

The sand specimens were built up by a sand-sprinkling technique which affords reasonable control over the density and uniformity of the soil, as well as rapid placement. The equipment used was a large sand container with 12 flexible hoses attached at the bottom which guide the sand to a 1/4-in. mesh screen through which it falls freely into the test chamber (Fig. 3.17). The container, supported by a crane above the test chamber, is rotated about its vertical axis and is guided by extra rings temporarily placed upon the test rings. By maintaining the distance between the screen and the surface on which the sand falls, and keeping the angular velocity of the container constant, it is possible to build a uniform, dense specimen of sand. For each of the sands used the height of fall selected was 24 $\pm$ 1 in., and the angular velocity at which

the container was rotated equaled 19 to 21 rpm. Several 12-in. specimens of each sand were built and sampled for density at various locations and depths. The results indicated that a specimen of sand 1 may be expected to be uniform with a maximum variation of ±1.2 pcf from the average density, while a specimen of sand 2 may show a maximum variation of ±0.7 pcf from the average. The average densities of the test specimens are listed in Tables 4.1 and 4.2. The average initial density of all specimens of sand 1 was 100.0 pcf, and the extreme values were 98.3 and 101.3 pcf. All specimens of sand 2 had an average initial density of 106.0 pcf, with extremes of 104.2 and 108.4 pcf. The variation in density from test to test was greater than was desired, and may be attributed to variations in the placement procedure associated with various operators. A level surface at the desired elevation above the chamber bottom was obtained by sprinkling sand about 1/2 in. deeper than the desired depth which always coincided with the top of a soil ring. Then, after the guide rings were removed, the surface was leveled using the flange of the upper ring as a guide and a length of steel angle as a screed.

3.6 Test Procedures

3.6.1 Pretest

The amplifiers, having been warmed up, were balanced and calibration steps were recorded for all load and pressure transducers. The jack was used to return the trapdoor to the flush position which was defined by a straightedge and reference to the output of the upper LVDT's. Generally, when in the flush position the surface of the trapdoor was not parallel to the top plate of the base, but projected about 0.001 in. on one side and was depressed about the same amount on the

opposite side. The electrical zero of the load cell was then checked on a strain gage indicator to remove any possibility of an apparent load due to friction. A circle of thin plastic membrane was placed over the trap door and the annular area immediately adjoining it, in order to help keep sand out of the space between the trapdoor and its cylinder. This plastic circle was held smoothly in place by a light film of oil previously placed on the trapdoor. Next, the lower LVDT's were nulled by adjusting the micrometer head and then the appropriate number of calibration steps was physically applied to the gages and the outputs were recorded. The lower LVDT's were then returned to the null position for the test. The sand sample was next constructed as described above, the neoprene diaphragm was placed on the level sand surface, and the bonnet was bolted to the uppermost ring. At this time the output of the upper LVDT's generally indicated that the trapdoor and the base had undergone some relative displacement (always less than 0.0005 in.) as a result of the sand placement and ring-bolting. If the direction of the relative displacement was such that the tendency to move during pressure buildup would be opposite to it, nothing was done about it at this time. If the tendency to move during pressure buildup was to increase the initial relative deflection, the jack was immediately used to eliminate it.

3.6.2 <u>During Test</u>

Air pressure was controlled manually by an operator who used a Bourdon-type pressure gage for reference. A second operator, who observed the output of the upper LVDT's adjusted the jack handle during pressure buildup in such a fashion that the upper LVDT output was kept at zero. During tests with the 6-in. trapdoor this invariably required moving

the jack upward, while the opposite was invariably true during tests with the 3-in. door. Occasionally pretest operations left the trapdoor with a residual deflection opposite in sense to the direction in which the door would tend to move. When this was the case, the jack was not adjusted until the pressure buildup was sufficient to return the trapdoor to the null position. The trapdoor was then continuously nulled until the desired level of air pressure was established. At this time the trapdoor was raised or lowered by turning the jack handle 4-1/2 to 5 revolutions in the appropriate direction. Generally 15 sec were required for this, although in some of the deeper passive tests it was necessary to use a pipe wrench for leverage on the jack handle, which took about twice as long due to the necessity of getting a new grip on the jack handle every 2/3 turn. After the trapdoor had been raised or lowered, the surface pressure was released. This concluded the test.

3.7 Data Reduction

All of the test records were read manually to the nearest 0.01 in. using an engineer's scale. The zeros for the soil pressure cells and the trapdoor reaction were taken just before the buildup of surface pressure was initiated. As a result, the dead weight of the soil was effectively omitted from the measurements, but as this was never more than 2 psi and generally considerably less, its contribution to any pressure reading was negligible.

CHAPTER IV: TEST RESULTS

4.1 General

The test program was composed of three series of arching tests. The first and second series consisted of active arching tests on sands 1 and 2, while the third series consisted of passive arching tests on sand 2. In each series of tests the ratio of depth of cover to trapdoor diameter (H/B) was the major variable. In the second series the surface pressure was varied in some tests and the diameter of the trapdoor was treated as a variable in both the second and third series. The most important test parameters are summarized in Tables 4.1 and 4.2. The redistribution of normal stress on the base of the soil container was also measured in all tests with the 6-in.-diameter trapdoor.

4.2 Arching Curves

Throughout this study the load on the trapdoor has been divided by the area of the trapdoor and treated as an average, uniform pressure P_B This average pressure has been made dimensionless by dividing it by the air pressure P_s acting at the surface, and this ratio has been termed the arching ratio. Whenever the arching ratio is equal to 1.0, no arching exists, and the actual distribution of pressure on the trapdoor and the surrounding base should be uniform. Active arching is indicated by an arching ratio less than 1.0, but not less than zero. An arching ratio greater than 1.0 is associated with passive arching. The average deflection of the trapdoor δ has been made dimensionless by dividing it by the diameter of the trapdoor B . Arching ratio (P_B/P_s) versus dimensionless deflection (δ/B) data are plotted in Figs. 4.1-4.26. Series I data are presented in

Figs. 4.1-4.6, Series II in Figs. 4.7-4.17, and Series III in Figs. 4.18-4.25. Certain passive arching curves, which were obtained from tests with the 3-in.-diameter trapdoor, are replotted in Fig. 4.26 to a smaller scale so that the reader may observe the behavior of the arching ratio at the very large values of dimensionless deflection which could be measured in a few tests.

4.3 Experimental Errors in Arching Curves

An examination of the data points presented in Figs. 4.1-4.25 reveals that the initial value of the arching ratio is very seldom equal to 1.0, and that the curves traced by the points in the active tests generally demonstrate a reversal in curvature during the initial deflections when δ/B is less than 0.0002. The data points for test 31 in Fig. 4.11 provide a typical example. The initial point indicates that the undeflected trapdoor felt about 95 percent of the surface pressure. The inability to maintain the full surface pressure on the trapdoor is associated with three factors. The first is the inability of the operator to hold the trapdoor perfectly flush during the buildup of surface pressure. As mentioned in Chapter III, the trapdoor could be held flush to within 0.0005 in. For a 6-in. trapdoor, this error is equal to a dimensionless deflection (δ/B) of approximately 0.1×10^{-3}. The general slope of the early data points is such that this much trapdoor deflection, if downward with respect to the base, could easily account for much of the load loss. During the tests with the 6-in. trapdoor, the door tended to move downward with respect to the base. As a result, the operator manipulating the jack in order to keep the output of the upper LVDT's null was trying to hold the downward-tending trapdoor flush, and his tendency was to undercorrect rather than

overcorrect. This is borne out by tests using the 3-in. trapdoor which had a tendency to move upward relative to base during the application of the air pressure. The operator's tendency to undercorrect would lead to an arching ratio close to or greater than 1. This was the case for most tests with the smaller door. The second factor is indicated by Fig. 3.4 which shows that the top plate of the base undergoes measurable bending deflections when loaded uniformly. The deflections, being greater toward the center of the plate, would tend to arch load toward the outer edges and thus contribute to the reduction in arching ratio at the center. Last of all, the possibility of wall friction not allowing the load to reach the bottom must be considered. It is not believed to be significant for the majority of tests, because the ratio of soil depth to tank diameter was kept small. However, the tests run with 36 in. of sand 1 (Fig. 4.6) show a maximum arching ratio of 0.6 and bin friction is probably the major cause. As a result of this, the 36-in. tests are not analyzed in the next chapter. The reverse curvature observed in the early portions of the arching curves is associated with the tilt of the vertical axis of the trapdoor. Reversal in direction causes a small amount of backlash in the jack which makes the platform move slightly in other than a vertical direction for a short time. This backlash, by slightly changing the alignment of the load-carrying elements, causes a slight tilting of the trapdoor. The tilting is observable in the outputs of the lower LVDT's which move in opposite directions, although their average is generally nonzero and of the proper sense. As the top surface of the trapdoor tilts, one side moves in the wrong direction, or at least at a lesser rate in the proper direction. This situation causes the rate of load change to be less than it should be until the tilting stops. The reversals in

curvature should be evident during active tests with the 6-in. door and passive tests with the 3-in. door because these are the only tests requiring a reversal in jack direction to initiate relative deflection. An examination of the data reveals that the reversal in curvature is found only in active tests with the 6-in. door. The absence of the tendency from the passive tests with the smaller door indicates that the error associated with this small tilt occurs at deflections smaller than the accuracy of the LVDT's.

4.4 Correction of Experimental Error

The experimental errors mentioned above are associated with the inability to begin all tests with an arching ratio of 1, and the reversal in curvature in the very early portions of the active arching curves. Since both of these errors are associated with an inability to control and measure deflections precisely at the beginning of a test, some method was sought whereby the curves might be adjusted by minor changes in deflection. This approach is justifiable because the total load acting on the trapdoor is known with a high degree of certainty so that any deviations in its value from other than ideal conditions must really exist and should be due to some unmeasured deflection. Also, any adjustment based upon the load measurement (for example, calling the initially measured load all of the applied load and thereby forcing the initial arching ratio to equal 1) would change the value of the ultimate arching ratio which ought to be independent of deflection. A similar situation would exist if one attempted to measure the ultimate bearing capacity of a footing and ignored a non-trivial load already acting before the start of the test.

Physical reasoning requires one to assume that the initial

slopes of corresponding active and passive arching curves ought to be identical. In order to test the hypothesis, the data points for corresponding active and passive tests are plotted together in Figs. 4.27-4.30. The general identity of slope on both sides of the crossover point is apparent in these figures. The straight lines drawn on the figures approximate quite well the initial slopes of corresponding sets of data points. The lines, in general, do not go through the ideal crossover points. An assumption that the error is associated with deflection would justify correcting each of the curves by translating them to the right far enough that each curve begins at its proper initial point. Because the errors are of the same magnitude as the error associated with holding the trapdoor flush with the base (0.0005 in.) the correction seems reasonable. Thus, the curves drawn in Figs. 4.1-4.25 represent an average of the plotted points except in the vicinity of the reversals in curvature. Here the best straight line which could be drawn through the points lying just beyond the vicinity of the reversals in curvature has been used as the initial tangent. Whenever the active arching curves from this chapter are used in the chapters which follow, this initial tangent is extended to the point where it crosses the arching-ratio-equals-1.0 line and this intersection is taken to be a new initial point for deflections.

4.5 Stress Redistribution Due to Arching

Figs. 4.31-4.45 present profiles of changes in vertical stress at the surface of the top plate of the base as a function of the dimensionless deflection of the trapdoor. The data from Series 1 are shown in Figs. 4.31-4.34, while the data from those tests of Series 2 and 3 conducted with the 6-in. trapdoor and a surface pressure of 75 psi are shown in

Figs. 4.35-4.37 and Figs. 4.38-4.43, respectively. The profiles from tests run with pressures of 40 and 110 psi are shown in Figs. 4.44 and 4.45. Positive stress changes are associated with increases in vertical stress. The values presented are the average stress change of two pressure cells located the same distance from the center of the trapdoor.

4.6 Influence of Experimental Error on Stress Data

Because the soil pressure cells were calibrated in place during the buildup of air pressure for each test, it is felt that errors associated with soil placement have been minimized for cells which undergo only increases in pressure during a test. However, since a buried pressure cell follows a different unloading path, special unloading calibration tests had to be conducted. The relation between loading and unloading stress for a given level of transducer output (Appendix A) is quite consistent for three tests of two different transducers even though one of the loading-unloading calibration curves was markedly different from the others. The extrapolation of the calibration curves to levels of pressure beyond that of the surface pressure is a potential source of error. This is a minor factor for cells subjected to only increasing loads because the slope of the calibration curves between 75 and 110 psi is essentially the same as the slope between 60 and 75 psi as shown in Appendix A. However, certain cells occasionally underwent increases in pressure followed by decreases. There is no calibration information available to cover these situations and Fig. A7, which relates loading and unloading pressures from 75 psi, was used. The result of these uncertainties is believed to be a variation of about ± 2 psi in any pressure change. This variation is of the same magnitude as many of the pressure changes observed and so the data, while

adequate to qualitatively indicate magnitudes and distribution of pressure changes, should not be used quantitatively to predict small changes in pressure.

CHAPTER V: ANALYSIS OF TEST DATA

5.1 General

The data presented in the previous chapter indicate that under certain conditions arching may be a very significant factor in determining the total load which acts upon a buried structure. The potential influence of arching on the distribution of load is also apparent and could well prove to be more important to a designer than gross load changes. In this chapter the influence of the test variables on the arching curve, and the usefulness of available analytical solutions in predicting arching are assessed. A method of constructing an arching curve is presented; and the redistribution of stress over the area adjacent to the trapdoor is analyzed.

5.2 Influence of Test Variables on Arching Curves

5.2.1 Active and Passive Arching

Striking differences exist between the plots of arching ratio versus dimensionless deflection measured in active and passive tests at equal values of H/B. For very small values of dimensionless deflection ($-1 < \frac{\delta}{B} \times 1000 < 1$) comparable active and passive arching curves are symmetrical about their common point (1.0,0) as indicated by Fig. 5.1 and Figs. 4.27-4.30. Beyond these bounds, the arching ratio falls off quickly to zero or some finite limiting va ue (called hereafter the ultimate arching ratio) for active curves, hile for passive curves, the approach to an ultimate value requires much larger deflections (especially for large values of H/B).

5.2.2 Influence of Surface Pressure

Active arching tests with sand 2 were conducted with P_s nominally equal to 40, 75, and 110 psi for values of H/B equal to 1/3, 2/3, and 1. The summary arching curves for these tests have been plotted together in Fig. 5.2. For a fixed value of H/B, the final portion of each curve (i.e. the value of the ultimate arching ratio) is associated with the angle of internal friction which is, for all practical purposes, a constant for pressures in this range. Fig. 5.2 indicates that this is the case. The variations among final portions of comparable curves are small and attributable to experimental variation. The influence of P_s on the initial slope of the arching curve (T_i) cannot be evaluated directly from Fig. 5.2, because of the interrelation between P_s and the constrained tangent modulus M_{ct} of the soil. The elastic solution of Chelapati (1964) indicates that the slope of an arching curve will increase if Young's modulus (E) is increased, and will decrease if P_s is increased. A similar relation is indicated by equation 5.3.2 (page 50) which is derived from an equation relating the load and deflection of a rigid circular die on an elastic half-space. The dependence of T_i on P_s as given in equation 5.3.2 is a result of the use of P_s as a normalizing factor for the ordinates of the arching curve. The relation between T_i and M_{ct}/P_s (since M_{ct} is related to the E given in equation 5.3.2) is indicated by Table 5.1. Although there are variations which may be the result of experimental error and the writer's ability to represent the data by a single curve, the initial slope of the arching curve decreases as the ratio M_{ct}/P_s decreases. For most sands at low values of vertical stress (less than 400 psi) the ratio M_{ct}/P_s is fairly constant (Whitman (1964), page 41),

Table 5.1

Influence of Surface Pressure P_s and Constrained [illegible]nt Modulus M_{ct} on Initial Slope of Arching Curve T_i

and	P_s psi	M_{ct} psi	$\frac{M_{ct}}{100 \times P_s}$	T_i H/B = 1/3	T_i H/B = 2/3	T_i H/B = 1
2	40	32,000	8.0	0.84	1.40	1.60
2	75	48,000	6.4	0.80	1.10	1.36
2	110	62,000	5.6	0.78	1.16	1.60
1	75	24,000	3.2	0.55-0.88	1.00	1.20

and so the dependence of the arching curve on P_s is not evident. Although the influence of P_s on passive arching was not studied experimentally, the writer concludes that the passive arching curves for a given sand would be essentially independent of P_s. This conclusion is based on the ultimate arching ratio's lack of dependence on P_s, the general identity of active and passive initial slopes for the same value of H/B, and the evidence of Kriandifilidis et al (196[illegible]).

5.2.3 Influence of Soil Properties

The influence which the various strengths and stress-deformation properties of the soils tested have upon active arching may be determined readily by a comparison of the data summarized in Fig. 5.3. The top plot of Fig. 5.3 shows that throughout the range of comparable tests the stronger soil (sand 2) was capable of transferring more load than was sand 1. For H/B equal to 4, the ultimate arching ratios are almost the same, but the middle plot of Fig. 5.3 indicates that about twice the deflection was required to reach this ratio with sand 1. For the two most shallow burial ratios (H/B = 1/3, 2/3) the ultimate arching ratios varied by about 0.1, sand 2 exhibiting the lower, although the trapdoor underwent

about the same displacement for both sands in developing the ultimate arching ratio. The above behavior is not unexpected because shallow depth of soil is quickly brought to a state of plastic equilibrium by a small downward deflection. The load transfer capacity is then dependent only on the angle of internal friction, which is greater for sand 2. When the depth of cover is increased so that small deflections do not bring the entire depth to a condition of plastic equilibrium, the load transfer capacity above the trapdoor depends not only on the angle of internal friction, but also on the height of soil above the door through which the shearing strength is mobilized. Hence, at great depths of cover the effect of a smaller value of angle of internal friction is compensated for by increased deflections which mobilize the strength of more material. Similarly, the behavior of the initial slopes of the arching curves as shown in the bottom plot of Fig. 5.3 is reasonable. Because of the reversals in curvature indicated in Fig. 4.1, an upper and lower bound had to be set on one value of initial slope, but within these limits the behavior is such that sand 2, which has the higher constrained tangent moduli, manifests the higher initial slopes. This is in accord with certain theoretical solutions which will be discussed in Section 5.3.

5.2.4 Ratio of Soil Depth to Trapdoor Diameter (H/B)

The arching curves in Chapter IV make it quite apparent that H/B is the only significant geometrical variable treated in this study. The results from tests with both sizes of trapdoor are the same in all significant respects for a constant value of H/B . The influence of the H/B ratio is substantial. The ultimate arching ratios depend upon the H/B ratio as shown in Figs. 5.3 and 5.7 for active and passive tests. The

influence on active tests is greater when H/B is less than 1, because a plane of equal settlement is not established in the sand above the trapdoor. For passive tests, changes in H/B continue to have an influence on the ultimate arching ratio to the extreme value (H/B equal to 2-2/3) tested. However, the passive data points for H/B greater than or equal to 2 follow the same curve out to high values of dimensionless deflection (0.015) before leaving the common curve (Fig. 4.26). Therefore, the influence of the H/B ratio on the passive arching curves for values of H/B greater than 2 is insignificant for values of δ/B likely to be encountered in practical problems. One geometrical variable not significant to this study which could prove significant in situations where the weight of soil is not negligible is the diameter of the trapdoor, because the area to perimeter ratio of the trapdoor varies linearly with the diameter.

5.3 Theoretical Solutions as a Basis for Predictions

5.3.1 General

The writer knows of no available elastoplastic solutions with which the results of the tests may be directly compared. Therefore, in the following sections certain elastic solutions which may prove of value in estimating the initial slope of an arching curve, and certain plastic solutions which may help with estimates of the ultimate arching ratio are considered.

5.3.2 Elastic Solutions

Unfortunately, the solutions of Finn (1960) and Chelapati (1964) cannot be compared directly with the test results because they are plane solutions. However, the general behavior of the arching curves which the solutions imply ought to exist during active arching (Section 2.2) was

observed in every respect but one. As explained in Section 5.2, P_s did not influence the initial slope of the arching curves because the modulus M_{ct} varies nearly linearly with P_s. Timoshenko and Goodier (1951, p 372) present an elastic solution which relates the load and deflection of a rigid circular die resting on the surface of a semi-infinite, elastic medium. Because of the axially symmetric nature of this solution, it is of possible interest in spite of different boundary conditions adjacent to the die. The equation in modified notation is

$$\delta = \frac{\left(P_B - P_s\right)\left(\frac{\pi B^2}{4}\right)\left(1 - \nu^2\right)}{B E} \qquad 5.3.1$$

which may be manipulated to give Young's modulus as a function of the initial slope of the arching curve, T_i, the surface pressure, and Poisson's ratio (ν).

$$E = 250\pi \left(1 - \nu^2\right) P_s T_i \qquad 5.3.2$$

where

$$T_i = \frac{\left(P_B/P_s - 1\right)}{\delta/B \times 1000}$$

Based upon the initial slopes taken from test data and listed in Tables 4.1 and 4.2, it is possible to compute an effective value of Young's modulus for comparison with the constrained tangent modul' of the sands. The comparison is made on Fig. 5.4 for an assumed value of ν equal to 0.3. It is apparent that the difference in constraint on the material adjacent to the trapdoor and that adjacent to the die is not negligible because at the smaller values of H/B where the difference between a semi-infinite solid and a finite solid ought to be most apparent, the agreement is best. At the higher values of H/B the ratio E/M_{ct} approaches a constant

value of approximately 3. This behavior is reasonable because at these greater depths the experimental setup more closely resembles a semi-infinite space and only the difference in constraint should play a major role. The heavy line in Fig. 5.4 is a reasonable representation of the observed trend for later use in the construction of an arching curve.

5.3.3 Plastic Solutions

Because of the state of plane strain considered by Bedesem (1964), Terzaghi (1943), Spangler (1948), and others, it is difficult to make a direct comparison between their analyses and the values of the ultimate arching ratio observed in these tests. However, it is not difficult to modify the approach of Terzaghi and Spangler in order to derive an axially symmetric solution based on the assumption of vertical shearing planes rising above the circumference of the trapdoor to the surface. Equation 5.3.3 is the solution of the differential equation obtained from a summation of the vertical forces acting on the differential element shown in Fig. 5.5. The details of the solution have been presented by Van Horn (1963, p 3).

$$P_B = P_s e^{\mp 4K \tan \phi \frac{H}{B}} + \frac{(+\gamma B - 4c)}{4K \tan \phi}\left(1 - e^{\mp 4K \tan \phi \frac{H}{B}}\right) \qquad 5.3.3$$

where c is the cohesion of the soil, γ is the unit weight, and K is an effective earth-pressure coefficient. The upper signs of those in pairs apply to active arching, while the lower apply to passive arching. If, as is often the case, the surface pressure is large enough to make the weight of the soil negligible, and if the soil is assumed cohesionless, the following expression for arching ratio results.

$$\frac{P_B}{P_s} = e^{\mp 4K \tan \phi \frac{H}{B}} \qquad 5.3.4$$

The paired signs have the same significance as indicated above. The derivation of this equation will be referred to as the differential approach. It is also possible to consider the sand cylinder above the trapdoor a rigid body which transfers load across the cylinder wall by shear at a uniform rate from surface to trapdoor. That is, the change in normal stress due to arching will be neglected within the cylinder, and P_s will be taken as the vertical stress down to the level of the trapdoor. The following relations result, if cohesion and soil weight are neglected.

$$P_B\left(\frac{\pi B^2}{4}\right) = P_s\left(\frac{\pi B^2}{4}\right) \mp P_s\ (K \tan \phi)(\pi\ B\ H)$$

or

$$\frac{P_B}{P_s} = 1 \mp 4\ K \tan \phi \frac{H}{B} \qquad 5.3.5$$

This line of reasoning will be termed the rigid-body approach. Figs. 5.6 and 5.7 indicate that neither approach is adequate to predict the ultimate loads due to both active and passive arching. The active arching data points on Fig. 5.6 do generally plot as equation 5.3.4 predicts, while the plot of equation 5.3.5, which was fitted to pass through one data point, bears no resemblance at all to the form of the data. The opposite is true in the case of passive arching, as the various curves on Fig. 5.7 indicate. Here the rigid-body approach follows the data points quite well when H/B is less than 2. The effective earth-pressure coefficients (K) indicated beside the curves of Figs. 5.6 and 5.7 were back-calculated by treating

them as unknowns in equations 5.3.4 and 5.3.5. The concept of treating K as a variable which depends on H/B is in consonance with Terzaghi's (1936b) observation that K varies above a yielding trapdoor (Fig. 2.1). The situation studied by Terzaghi was one in which the plane of equal settlement was well below the surface of the soil. Since the soil above the plane of equal settlement does not undergo any major reduction in vertical stress, one would expect an effective value of K , based upon the assumption of a fully developed shearing surface, to become less as the depth of cover increases. Fig. 5.8 shows the manner in which K , back-calculated from equation 5.3.4, varies with H/B for both active and passive arching. The values of K associated with active arching increase from about 0.7 for H/B equal to 1/3 to about 1.25 for H/B equal to 1, and then decrease to 0.7 and 0.3 for H/B equal to 2 and 4. The increase in K between small values of H/B and H/B equal to 1 is attributable to the fact that the true surface of sliding probably resembles more nearly the surface of a truncated cone than the surface of a right circular cylinder. Since the surface area of a cylinder increases directly with the height while the surface area of a cone depends upon the height squared, the increased value of K compensates for an increase in shearing surface not accounted for in the theories. The decrease in K when H/B is greater than 1 is in accordance with the concept discussed above in connection with Terzaghi's experiment. The values of K associated with active arching in sand 2 when H/B is greater than 2 (Fig. 5.8) are actually hypothetical since they are based upon an assumed ultimate arching ratio of 0.01. The actual value of the ultimate active arching ratio, (0.00), is associated with infinite depths of cover. The values of K

associated with passive arching decrease from about 0.59 to about 0.34 as H/B varies from 1/3 to 1-1/3, and then remain fairly constant as H/B increases to a value of 2. The decrease in the value of K which accompanies the first few increases in H/B is associated with the success of rigid-body approach in predicting these ultimate arching ratios. When H/B is small, a cylindrical mass of soil is pushed upward by the trapdoor. The vertical stress varies from a very high level right above the center of the trapdoor down to P_s at the surface of the soil where K is probably about the same as K_o. However, at the level of the trapdoor, but over its perimeter, the disturbance caused by the door deflection is felt as shear accompanied by a dilation perpendicular to the failure plane. This tendency to dilate causes an increase in horizontal stress greater than that associated with K_o. As a result, the effective value of K is higher than K_o. As the depth is increased, the extreme values of K at the upper and lower surfaces have less influence on the effective value of K and it decreases. As the depth increases, the variation in K becomes more uniform from top to bottom and, therefore, more like the model used in the differential approach. This explains the inability of equation 5.3.4 to predict ultimate passive arching ratios until rather large H/B ratios are reached (Fig. 5.7). For lower values of H/B, the rigid-body approach happens to work because the underestimation of vertical stress in the soil cylinder caused by assuming that it does not vary is compensated for by the high value of K (0.9) obtained from fitting the equation through the points of Fig. 5.7. As the depth increases, the underestimation of vertical stress becomes more serious, but the constant value of K continues to compensate because the actual effective value

of K is decreasing. At the value of H/B where the actual value of K becomes stable, the rigid-body approach ceases to work satisfactorily. Equation 5.3.4 is considered better than equation 5.3.5 for the prediction of ultimate arching ratios, both active and passive, because the differential approach is based upon a more realistic model. The variation of effective earth-pressure coefficient with H/B must be taken into account, however. Table 5.2 contains a list of recommended values based upon the results of these tests.

The arching curves indicate that a plane of equal settlement for active arching associated with an ultimate arching ratio of zero is located about one diameter above the trapdoor. Increases in cover above this depth change the form of the arching curves very little. A maximum value of ultimate arching ratio was not observed during passive tests. This seems reasonable since a large enough deflection into the soil should be able to disturb any finite depth of soil cover. On the other hand, the initial portions of the arching curves for large values of H/B are very much alike (Figs. 4.23-4.25). This suggests that the curves follow a common line, and each breaks off in the vicinity of its own ultimate arching ratio. The nature of these curves is discussed in more detail in the next section.

5.4 Secant Analysis of Arching Curves

5.4.1 General

The methods of elasticity and plasticity (based upon an assumed slip plane) having been used to predict reasonable values of the initial slopes and final values of the arching curves, do not help with the problem of constructing the intermediate curve. No general method is known to the

writer which can describe the transition from a quasielastic condition to a state of plastic equilibrium. The shape of the arching curves reflects this transition. An empirical method of analysis is described below which uses both the initial slope and final value of the active arching curves, thus taking into account both extremes of behavior, and allows prediction of curves for other soils. A similar method is described for passive arching curves, but it is based purely on the final value. The analysis below is based upon the arching curves of Chapter IV corrected as indicated in Section 4.4.

5.4.2 Definitions of Terms

Fig. 5.9 illustrates the terms and methods used in the secant analysis. A general active arching curve is used for the sake of example. The maximum change in the arching ratio between the initial point and final value is termed $\Delta (AR)_{max}$ and defined as follows:

$$\text{Active Arching } \Delta (AR)_{max} = 1.00 - (AR)_{ult}$$

$$\text{Passive Arching } \Delta (AR)_{max} = (AR)_{ult} - 1.00$$

The value of $(AR)_{ult}$ is termed $(AR)_{1.00}$ because all of the change in arching ratio has taken place when it reaches this value. Other values of arching ratio between 1.00 and $(AR)_{1.00}$ are represented by $(AR)_N$, where the subscript indicates how much of the change, $\Delta (AR)_{max}$, has been accomplished when the arching ratio reaches this value. Four values of the arching ratio $(AR)_{0.25}$, $(AR)_{0.50}$, $(AR)_{0.75}$, and $(AR)_{0.90}$ are of interest in this analysis. Secants drawn from the initial point of the arching curve (0, 1.00) to a point of interest on the curve are identified by S_N which stands for the slope of the secant to the point of interest associated with $(AR)_N$. S_o is the slope of the initial tangent also designated by T_i.

5.4.3 Results of Analysis

Fig. 5.10 presents the results of the analysis. The upper plots show the variation in secant slope associated with certain percentages of $\Delta\,(AR)_{max}$. The lower plots show how the secant slopes, having been normalized by division by the appropriate T_i, vary with these same percentages of $\Delta\,(AR)_{max}$. The secants taken from the active arching curves show no general agreement with one another. However, their variation from T_i as load is lost generally follows the same pattern. This is very evident in the lower left plot of Fig. 5.10 wherein each has been normalized by T_i. The maximum spread between extreme points is 0.16; it is associated with the 75% and 90% values of $\Delta\,(AR)_{max}$. This variation, if applied to the arching curve for H/B equal to 4 can result in extreme values of $S_{0.90}$ of 0.61 to 1.01 for sand 2 and 0.32 to 0.53 for sand 1. The widest variation in normalized slope is associated with the lowest values of arching ratio, where a variation in secant slope will cause the greatest error in dimensionless deflection (see, for example, how the horizontal distance between $S_{0.75}$ and $S_{0.90}$ in Fig. 5.9 increases with decreasing values of the arching ratio). This maximum error, being associated with low values of arching ratio, is not apt to cause serious trouble because of the self-limiting nature of the interaction which tends to make the initial portions of an arching curve more significant than the later portions.

The analysis of the passive arching curves is shown on the right side of Fig. 5.10. This analysis shows that for passive arching the slopes themselves collapse much better than the normalized slopes. If the points for H/B equal to 2 are omitted, the spread is greatest for

the secants associated with values of arching ratio close to the ultimate value. The possible errors at the large values of dimensionless deflection associated with these large arching ratios are not particularly significant. The error associated with an average value of slope at these large arching ratios may be minimized by specifying a range of slopes which increases with H/B, as indicated by the order of the data points (again omitting H/B equal to 2). The failure of the points associated with H/B equal to 2 to fall into the vicinity of and the sequence indicated by the other points seems to reflect an underestimation of the ultimate arching ratio. For this test and the deeper tests the arching ratios were determined by extrapolation. The major results of the secant analysis are summarized in Table 5.3.

5.4.4 Prediction of Arching Curves

An arching curve for sand may be predicted with reasonable accuracy using the results contained herein for H/B less than 4 for the active case, and less than 2 for the passive. It is necessary to know beforehand the angle of internal friction (ϕ) and the constrained tangent modulus versus pressure relation for the sand. Using ϕ and an appropriate value of K (Table 5.1), the ultimate arching ratio can be estimated by the use of equation 5.3.4. Next, an effective Young's modulus, based upon the constrained tangent modulus, can be estimated by using Fig. 5.4. This effective modulus is used in equation 5.3.2 with Poisson's ratio equal to 0.3 to estimate the slope of the initial tangent to the arching curve, T_i. It is now possible to construct the initial tangent and the horizontal lines associated with $\Delta\ (AR)_{max}$ and 0.9Δ to 0.25Δ, as shown in Fig. 5.9. Next the slopes of the secants, $S_{0.25}$ to $S_{0.90}$, can

e obtained directly for passive arching or in normalized form for active rching from Table 5.3. The slopes can be used to construct the appropriate secants and locate the points of intersection with the corresponding orizontal lines. Finally, based upon the initial slope and ultimate rching ratio together with four intermediate points, the arching curve an be drawn as a smooth curve or a series of line segments. Because of he limitations on surface pressure in the tests, it is felt that this onstruction should not be used for pressures greater than 200 psi.

.5 Transfer of Vertical Stress Due to Arching

5.5.1 General

The elastic solution of Finn (1960) and the elastoplastic olution of Sirieys (1964) each has its place in describing the observed edistribution of vertical stress adjacent to the trapdoor. Passive arching stresses are best described by the former, and active stresses by the atter. In the following sections the most significant observations are iscussed, compared with theory, and reasons for the inability of one heory to describe all of the data are discussed.

5.5.2 Active Arching

The most striking feature of the stress distributions associated ith active arching is the reduction in stress observed with large values f H/B and deflection (Figs. 4.33 and 4.34) in sand 1 and its failure to ppear under similar conditions in sand 2. If the ratio p/σ_o in Sirieys' lastoplastic solution (Fig. 2.3) is interpreted as the arching ratio, $\frac{B}{s}$, the solution predicts that for small values of the arching ratio he boundary between the elastic and plastic regions will be farther from he perimeter of the trapdoor in sand 1 than it is in sand 2. Hence,

because there were no pressure cells closer to the edge of the trapdoor than 2-3/4 in., the plastic region in sand 2 could not be detected. The size of the plastic region appears to be limited by shallow depths of cover which do not begin to approximate the geometry of the solution. This is indicated by Figs. 4.31, 4.32, 4.35, and 4.36, which show that no reduction in vertical stress was observed for values of H/B equal to or less than 2. That a plastic region exists at all depths of cover seems to be unquestionable because of the abrupt discontinuity existing at the edge of the trapdoor when it has deflected a small amount. This contention is supported by the continual redistribution of pressure as the deflection of the trapdoor continues after the load on the trapdoor has stopped changing. The continued deflection of the trapdoor under constant load enables more sand to flow, which causes the plastic region to grow with an accompanying reduction in vertical stress adjacent to the trapdoor and a buildup farther away. Consider the behavior of the closest cells at H/ equal to 2/3 (Figs. 4.31 and 4.35). In each of the tests the arching ratio assumed a nearly constant value at a dimensionless deflection of about 4 (Figs. 4.2 and 4.11), yet as the deflection increased further to a value of about 16 the maximum change in vertical stress grew from about 10 to 16 psi. This indicates that a secondary arching of load, induced by the plastification of the sand in the vicinity of the trapdoor, takes place. The extent of the area over which significant arching stress was observed is a function of the H/B ratio and the soil as indicated by Fig. 5.11. The curves appear to be tending toward a maximum radius which is independent of depth of cover for H/B greater than 4. The maximum radius is estimated at six to eight trapdoor radii. The influence of surface

essure P_s can be estimated by studying Figs. 4.44 and 4.45 which show ie results of tests run at 40 and 110 psi. There appears to be a direct elation between arching stress and the air pressure on the sand surface.

5.5.3 Passive Arching

The arching stress distributions associated with passive arching re shown in Figs. 4.38 to 4.43. These distributions resemble the elastic tress distribution (Fig. 2.2) much more than elastoplastic distributions. severe reduction in stress close to the trapdoor is evident. Within short distance, the change in stress passes through zero and becomes slight increase. The passive arching stress distributions indicated uch greater stress changes than did the active distributions, but it is ifficult to quantitatively assess them because of the difficulty in btaining an in-place unloading calibration. However, the tendency toward xtreme stress changes distributed over small areas is clear. The peak eductions in stress increase with deflection and H/B for values of H/B ess than or equal to 1.

CHAPTER VI: SUMMARY AND CONCLUSIONS

6.1 Summary

In order to better define the capability of real soil to transfer load away from or on to flexible and stiff buried structures, a series of active and passive arching tests was conducted with two sands. A circular trapdoor, mounted flush with the bottom of a circular soil container, was used in order to minimize the influence of sidewall friction. The trapdoor was held in the flush position until a preselected level of air pressure was established at the sand surface; then the trapdoor was forced to move into or away from the soil mass. The load acting on the trapdoor and the average deflection of the trapdoor were measured. The influence of depth of soil cover, trapdoor diameter, surface pressure, and the strength and stress-strain properties of the soils used were investigated. The test results have been presented as arching curves which show the relation between the ratio of the average pressure on the trapdoor to the air pressure on the soil surface and the dimensionless ratio of the deflection of the trapdoor divided by the door diameter. The influence of the variables has been assessed; the influence of small deflections is known quantitatively; and a semiempirical method of analysis has been developed which allows prediction of the arching curves associated with various sands. In addition, the changes in vertical stress on the area adjacent to the trapdoor have been measured and certain conclusions drawn concerning their extent and magnitude. Certain aspects of the physical behavior of the soil adjacent to the trapdoor have been inferred by means of the stress measurements.

6.2 Conclusions

As a result of the experimental program it is concluded that the dimensionless plot of pressure versus deflection, called herein the arching curve, may be successfully used to predict soil arching in a simple, easily visualized form. The arching data contained herein indicate that the importance of very small relative deflections can hardly be overestimated. A structural deflection as small as 0.0002 times the major dimension of an area is capable of causing the load on the area to change by as much as 50 percent. Greater deflections can cause much greater changes in load, but the relation is far from linear and depends upon many variables.

The influence of soil properties may be satisfactorily taken into account for cohesionless soils similar to those tested as part of this program, if one knows the angle of internal friction at the relative density of interest, and the constrained tangent modulus at the relative density and pressure of interest. The free-field stress has little influence upon the shape of the arching curve for a given sand, within the range of pressures utilized (40-110 psi), due to the tendency of the constrained tangent modulus to increase with confining pressure.

The results of the tests may probably be extrapolated to larger structures, because the size of the trapdoor did not influence the arching curves within the sizes studied.

Most active arching takes place in the soil immediately above the structure so that soil cover in excess of one to two diameters changes the arching curve very little. Passive arching, however, is greatly influenced by each addition to the H/B ratio, within the range of tests ($1/3 \leq H/B \leq 2\text{-}2/3$). However, even this dependence seems minimal when the

data of Fig. 4.26 are examined. Here it is evident that the influence of cover in excess of two diameters is small until very large deflections are reached. Since the interaction between soil and a real structure is self-limiting, it is concluded that the influence of H/B on passive arching curves is minor in the ranges of δ/B of interest in practical problems, if H/B is greater than 2.

The semiempirical secant analysis method which takes both the initial slope and final value of the arching curve into account is satisfactory for the prediction of both active and passive arching curves within reasonable limits for dense, cohesionless soil. However, the differences in method of application to active and passive arching considered together with the success of the rigid-body approach in predicting ultimate passive arching ratios (for small values of H/B), and the inability of a single analytical solution to predict stress distributions for both active and passive arching lead the author to conclude that, except at very small values of δ/B, the phenomena of active and passive arching are quite different. This conclusion is further confirmed by the fact that much larger values of dimensionless deflection are required in passive arching tests to develop certain arching ratios than are required in active tests; e.g., even for H/B equal to 1/3 the ultimate passive arching ratio requires a deflection five times greater than the ultimate active arching ratio.

The measurements of stress redistribution indicate that a stress increase as high as a quarter of the free-field stress may be expected in the vicinity of a yielding structure, and that a stress reduction as high as the free-field stress itself may be expected in the vicinity of a rigid structure. If structures or gages are to be isolated from interaction with

one another, Fig. 5.11 can be used to estimate the required spacing. For structures having about equal dimensions in plan, the figure can be used directly. If Fig. 5.11 is used for rigid structures, as well as flexible structures, the results should be conservative. For long structures, like tunnels, the distance from the figure should be squared.

6.3 Suggestions for Research

Certain items which have come to light in the course of this study, or which seem to be natural continuations of the work, are offered for consideration:

a. A test program, similar to that described herein, should be conducted on cohesive materials in order to determine the significant strength and stress-deformation parameters.

b. A brief number of tests above an elastically supported trapdoor should be run in order to test the applicability of these data to simplified soil-structure interaction.

c. The role of arching in a dynamic environment has yet to be established. A dynamic test program on an elastically supported, low mass trapdoor would prove or disprove the role. A long-duration pulse should be used if possible so that changes in load due to arching could be separated from those due to decay.

d. The work of McDonough (1959), Luscher and Höeg (1964), and Sirieys (1964) all suggests that some internal confining pressure greatly enhances the ability of the material around a tunnel to develop ring-type arching. It is

suggested that the design of tunnel linings be studied from this point of view.

BIBLIOGRAPHY

1. Allgood, J. R., (1964), "Blast Loading of Small Buried Arches," Proceedings, ASCE, 90, ST5, 39-61, October.

2. Allgood, J. R., and H. L. Gill, (1964), Static and Blast Loading of Small Buried Cylinders, Technical Report R332, U. S. Naval Civil Engineering Laboratory, Port Hueneme, Calif., November.

3. Bedesem, W. B., (1964), A Continuum Theory of Soil-Structure Interaction in Granular Media, Ph. D. Thesis, University of Illinois, Urbana, Ill.

4. Chelapati, C. V., (1964), Arching in Soil Due to the Deflection of a Rigid Horizontal Strip, Technical Note N-591, U. S. Naval Civil Engineering Laboratory, Port Hueneme, Calif., October.

5. Donnellan, B. A., (1964), The Response of Buried Cylinders to Quasi-static Overpressures, Ph. D. Thesis, University of Illinois, Urbana, Ill., May.

6. Durbin, W. L., (1964), "Correlation of Stress-Strain and Wave-Propagation Parameters in Shock-Loaded Dry Sands," Study of the Dynamic Stress-Strain and Wave-Propagation Characteristics of Soils, Report 2 by United Research Services, Inc., to U. S. Army Engineer Waterways Experiment Station, Vicksburg, Miss., November.

7. Finn, W. D., (1960), Stresses in Soil Masses Under Various Boundary Conditions, Ph. D. Thesis, University of Washington, November.

8. Lane, K. S., (1957), "Garrison Dam--Evaluation of Results from Tunnel Tests Section," Proceedings, ASCE, 83, SM4, Paper 1439, November.

9. Luscher, U., and K. Höeg, (1964), The Interaction Between a Structural Tube and the Surrounding Soil, RTD TDR-63-3109, Air Force Weapons Laboratory, Kirtland AFB, New Mexico, January.

10. Mason, H. G., (1964), Effects of Structural Compressibility on Soil-Structure Interaction, Progress Report Draft prepared for Defense Atomic Support Agency, URS Corporation, Burlingame, Calif., October.

11. Mason, H. G., O. H. Criner, R. Waissar, and N. R. Wallace, (1963), A Study of the Dynamic Soil-Structure Interaction Characteristics of Real Soil Media, RTD TDR-63-3075, Air Force Special Weapons Center, Kirtland AFB, New Mexico, September.

12. McDonough, G. F., Jr., (1959), Dynamic Loads on Buried Structures, Ph. D. Thesis, University of Illinois, Urbana, Ill., May.

13. Monfore, G. E., (1950), An Analysis of the Stress Distributions In and Near Stress Gages Embedded in Elastic Solids, Laboratory Report No. SP-26, Structural Research Section, U. S. Department of the Interior, Bureau of Reclamation, Denver, Colo., June.

14. Moore, P. J., (1963), "One Dimensional Compression and Wave Propagation," The Response of Soils to Dynamic Loadings, Massachusetts Institute of Technology, Cambridge 39, Mass., Report 21 to U. S. Army Engineer Waterways Experiment Station, June.

15. Office of the Chief of Engineers, U. S. Army, (1964), Soils Laboratory Test Methods, Engineer Manual in preparation.

16. Selig, E. T., (1960), "An Analytical Method for the Design of Underground Structures," Shock, Vibration and Associated Environments, Part III, Bulletin No. 28, 36-47, Office of the Secretary of Defense, Washington, D. C., September.

17. Selig, E. T., K. E. McKee, and E. Vey, (1960), "Underground Structures Subject to Air Overpressure," Transactions, ASCE, 3258, 1627-1649, August.

18. Sirieys, P. M., (1964), "Champs de Contraintes Autour des Tunnels Circulaires en Elastoplasticite," Rock Mechanics and Engineering Geology, II, 1, 68-75.

19. Spangler, M. G., (1948), "Underground Conduits--An Appraisal of Modern Research," Transactions, ASCE, 113, 316-343.

20. Spangler, M. G., (1950), Field Measurements of the Settlement Ratios of Various Highway Culverts, Bulletin 170 of the Iowa Engineering Experiment Station, Iowa State College, Ames, Iowa, August.

21. Taylor, D. W., (1947), "Pressure Distribution Theories, Earth Pressure Cell Investigations and Pressure Distribution Data," Soil Mechanics Fact Finding Survey Progress Report, Waterways Experiment Station, Vicksburg, Miss., April.

22. Terzaghi, K., (1936a), "Arching in Sands," Engineering News-Record, 116:690-693, May.

23. Terzaghi, K., (1936b), "Stress Distribution in Dry and in Saturated Sand above a Yielding Trap Door," Proceedings 1st International Congress on Soil Mechanics and Foundation Engineering, Cambridge, Mass., 1, 307-311, June.

24. Terzaghi, K., (1943), Theoretical Soil Mechanics, John Wiley and Sons, Inc., New York.

25. Terzaghi, K., and R. B. Peck, (1948), Soil Mechanics in Engineering Practice, John Wiley and Sons, Inc., New York.

26. Timoshenko, S., and J. N. Goodier, (1951), Theory of Elasticity, 2nd ed., McGraw-Hill Book Company, Inc., New York.

27. Triandafilidis, G. E., D. Hampton, and M. Spanovich, (1964), "An Experimental Evaluation of Soil Arching," text of paper presented at a Symposium on Soil-Structure Interaction held at the University of Arizona, Tucson, Ariz., June.

28. U. S. Army Engineer Waterways Experiment Station, (1944), Soil Pressure Cell Investigation--Interim Report, Technical Memorandum 210-1, U. S. Waterways Experiment Station, Vicksburg, Miss., July.

29. U. S. Army Engineer Waterways Experiment Station, (1963a), Design of a Transducer for Pressure Measurements on Buried Concrete Structures, Miscellaneous Paper No. 1-593, by B. C. Chan, Vicksburg, Miss., August.

30. U. S. Army Engineer Waterways Experiment Station, (1963b), Soils Laboratory Tests on Cook's Bayou No. 1 Sand, Unpublished Memorandum for Record, Soils Division, U. S. Army Engineer Waterways Experiment Station, Vicksburg, Miss, September.

31. U. S. Army Engineer Waterways Experiment Station, (1964), Static One-Dimensional Compression Tests on Reid-Bedford Model Sand, Unpublished Memorandum for Record, Soils Division, U. S. Army Engineer Waterways Experiment Station, Vicksburg, Miss., August.

32. Van Horn, A. D., (1963), "An Analytical Method for Determining Loads," A Study of Loads on Underground Structures, Part III, Iowa Engineering Experiment Station, Iowa State University, Ames, Iowa, May.

33. Whitman, R. V., (1964), "Mechanical Properties of Earth Materials," Nuclear Geoplosics, Part Two, DASA-1285(II), Defense Atomic Support Agency, Washington 25, D. C., June.

34. Whitman, R. V., Z. Getsler, and K. Höeg, (1962), "Static Tests Upon Thin Domes Buried in Sand," The Response of Soils to Dynamic Loadings, Massachusetts Institute of Technology, Cambridge 39, Mass., Report 12 to U. S. Army Engineer Waterways Experiment Station, December.

35. Wiedermann, A. H., (1961), Static Experiments for the Study of the Interaction of Buried Structures with Ground Shock Waves, AFSWC TR-61-32, Air Force Special Weapons Center, Kirtland Air Force Base, New Mexico, April.

Table 4.1

Summary of Active Arching Tests, Series I and II

Test No.	Date 1964	Depth of Cover in.	Trap-door Diam-eter in.	Depth to Diam-eter Ratio (H/B)	Measured Surface Pressure psi	Measured Unit Weight of Soil pcf	Average Unit Weight of Soil for Each Group of Tests, pcf	Initial Slope of Arching Curve $\left(\frac{P_B/P_s - 1}{\delta/B \times 1000}\right)$	Ultimate Value of Arching Ratio $(P_B/P_s)_{ult}$	Approximat Dimensionle Deflectior at Ultimat Arching Rat
						Series I, Sand 1				
1	8-4	2	6	1/3	75	98.3				
2	9-4	2	6	1/3	73	98.9	99.5	0.55-0.88	0.55	4
3	13-4	2	6	1/3	74	99.7				
4	6-5	2	6	1/3	74	101.0				
5	6-5	4	6	2/3	73	100.6				
6	12-5	4	6	2/3	74	100.4	99.8	1.00	0.25	4
7	26-5	4	6	2/3	74	98.3				
8	7-4	6	6	1	73	99.7				
9	7-4	6	6	1	74	99.3	100.4	1.20	0.05	4.5
10	13-5	6	6	1	74	100.2				
11	10-3	12	6	2	76	101.1				
12	12-3	12	6	2	75	101.3	100.8	1.30	0.03	4
13	12-3	12	6	2	≈75	100.5				
14	13-5	12	6	2	75	100.5				
15	20-3	24	6	4	74	99.8				
16	20-3	24	6	4	75	99.4	99.9	1.40	0.02	3.5
17	14-5	24	6	4	74	100.4				
18	23-3	36	6	6	74	100.2				
19	24-3	36	6	6	74	100.0	100.1	--	0.02	--
20	15-5	36	6	6	74	100.0				
						Series II, Sand 2				
21	10-6	2	6	1/3	38	105.0	105.4	0.84	0.45	3.5
22	11-6	2	6	1/3	37	105.8				
23	9-6	2	6	1/3	72	104.5				
24	9-6	2	6	1/3	72	104.2	104.8	0.80	0.45	4
25	10-6	2	6	1/3	73	105.8				
26	11-6	2	6	1/3	≈110	106.3	106.7	0.78	0.40	4.5
27	11-6	2	6	1/3	≈110	107.1				
28	17-6	4	6	2/3	38	107.6	108.0	1.40	0.05	4
29	17-6	4	6	2/3	38	108.4				
30	16-6	4	6	2/3	73	107.0				
31	16-6	4	6	2/3	73	107.0				
32	17-6	4	6	2/3	72	106.3	106.9	1.10	0.15	4
33	6-10	2	3	2/3	71	107.1				
34	6-10	2	3	2/3	73	107.1				
35	17-6	4	6	2/3	108	106.3	106.3	1.16	0.10	4
36	18-6	4	6	2/3	107	106.3				
37	3-6	6	6	1	39	106.2	106.1	1.60	0.00	2.5
38	4-6	6	6	1	40	106.0				
39	28-5	6	6	1	72	105.5				
40	28-5	6	6	1	75	105.7	105.9	1.36	0.00	3
41	3-6	6	6	1	75	106.2				
42	4-6	6	6	1	74	106.0				
43	7-7	6	6	1	95	105.7				
44	8-7	6	6	1	109	105.5	105.6	1.60	0.02	3.5
45	8-7	6	6	1	102	105.5				
46	5-6	12	6	2	73	106.5				
47	5-6	12	6	2	73	106.2	105.8	2.32	0.00	2
48	7-10	6	3	2	73	104.5				
49	7-10	6	3	2	72	105.9				
50	18-6	24	6	4	74	106.5				
51	25-6	24	6	4	72	106.2	106.1	2.60	0.00	1.5
52	9-7	24	6	4	73	105.5				

Table 4.2

Summary of Passive Arching Tests, Series III, Sand 2

Test No.	Date 1964	Depth of Cover in.	Trap-door Diam-eter in.	Depth to Diam-eter Ratio (H/B)	Measured Surface Pressure psi	Measured Unit Weight of Soil pcf	Average Unit Weight of Soil for Each Group of Tests, pcf	Initial Slope of Arching Curve $\left(\frac{P_B/P_s - 1}{\delta/B \times 1000}\right)$	Ultimate Value of Arching Ratio $(P_B/P_s)_{ult}$	Approximate Dimensionless Deflection at Ultimate Arching Ratio
53	3-8	2	6	1/3	72	107.6				
54	4-8	2	6	1/3	72	106.8	107.3	0.80	1.95	-10
55	4-8	2	6	1/3	74	107.6				
56	7-8	4	6	2/3	74	106.3				
57	10-8	4	6	2/3	73	105.0				
58	10-8	4	6	2/3	74	105.0	105.7	1.10	3.00	-13
59	16-10	2	3	2/3	73	106.3				
60	20-10	2	3	2/3	73	105.8				
61	13-8	6	6	1	72	106.1				
62	13-8	6	6	1	73	105.7	105.7	1.36	3.60	-15
63	14-8	6	6	1	73	105.2				
64	19-8	8	6	1-1/3	73	105.6	105.4	1.50	4.5	-15
65	20-8	8	6	1-1/3	72	105.1				
66	21-8	10	6	1-2/3	73	105.3	105.4	1.65	≈6.0	-20
67	21-8	10	6	1-2/3	73	105.6				
68	24-8	12	6	2	72	106.5				
69	24-8	12	6	2	73	106.3				
70	20-10	6	3	2	73	105.8	106.1	2.32	≈10.0	-50
71	21-10	6	3	2	73	105.5				
72	3-11	6	3	2	72	105.8				
73	4-11	6	3	2	72	106.7				
74	11-9	14	6	2-1/3	73	106.5				
75	14-9	14	6	2-1/3	73	106.5	106.3	2.30	--	--
76	16-9	14	6	2-1/3	72	105.9				
77	27-10	8	3	2-2/3	72	105.7	105.5	2.70-3.00	--	--
78	27-10	8	3	2-2/3	72	105.3				

Table 5.2

Prediction of Ultimate Arching Ratio in Dry Sands

Equation 5.3.4

Burial	Effective Earth-Pressure Coefficient K
Active Arching	
$H/B \leq 1/3$	0.7
$1/3 < H/B \leq 2/3$	0.8
$2/3 < H/B \leq 1$	1.0
$1 < H/B \leq 2$	0.9
$2 < H/B$	-- $AR_{ult} = 0$
Passive Arching	
$H/B \leq 1/3$	0.7
$1/3 < H/B \leq 2/3$	0.5
$2/3 < H/B \leq 2$	0.4

Table 5.3

Results of Secant Analysis of Arching Curves

Percent Completion of Total Change in $\Delta (AR)_{max}$.)	$*\left(\frac{S_n}{T_i}\right) \pm$ Range Interval
Active Arching $H/B \leq 4$	
0%	1.00
25%	$0.94\ ^{+.06}_{-.05}$
50%	$0.84\ ^{+.03}_{-.03}$
75%	$0.53\ ^{+.08}_{-.07}$
90%	$0.32\ ^{+.06}_{-.09}$
Percent Completion of Total Change in $\Delta (AR)_{max}$.)	$**S_n \pm$ Range Interval
Passive Arching $H/B < 2$	
0%	T_i
25%	$0.73\ ^{+.05}_{-.04}$
50%	$0.44\ ^{+.07}_{-.07}$
75%	$**0.28\ ^{+.11}_{-.11}$
90%	$**0.21\ ^{+.11}_{-.12}$

* The principal value of $\left(\frac{S_n}{T_i}\right)$ associated with each N for active arching is the mean of the observed values. The range interval represents the variation of the extreme observed values from the mean. The variation may be neglected.

* The principal value of S_n associated with each value of N for passive arching is the value observed for H/B equal to 1. The positive side of the range interval is associated with H/B equal to 1-2/3, and the negative side with H/B = 1/3. The variation of S_n may be neglected except for N equal to 75 percent and 90 percent.

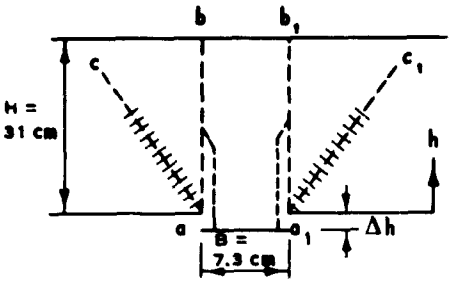

A. TEST SETUP AND SOIL BEHAVIOR ASSOCIATED WITH SMALL DEFLECTIONS

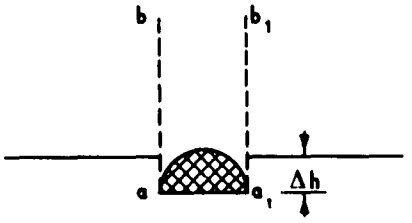

B. BEHAVIOR ASSOCIATED WITH LARGE DEFLECTIONS

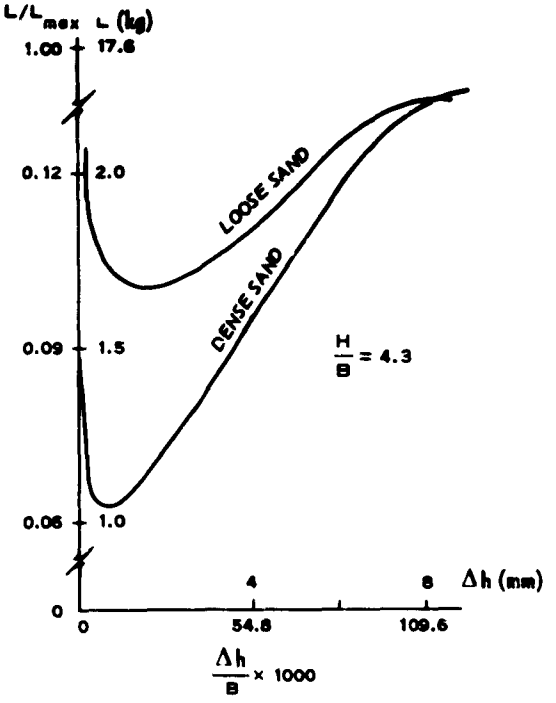

C. TRAPDOOR REACTION VS DEFLECTION

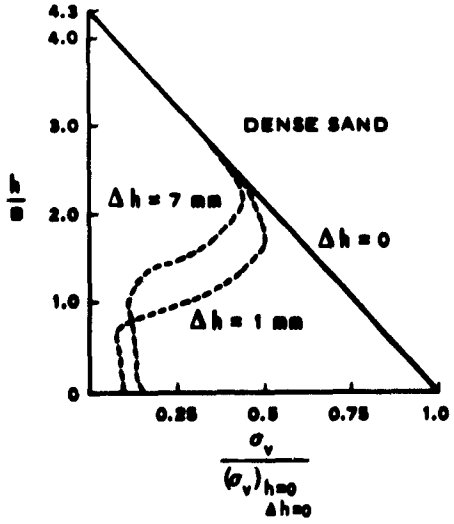

D. VARIATION OF VERTICAL SOIL STRESS ABOVE CENTER LINE OF TRAPDOOR

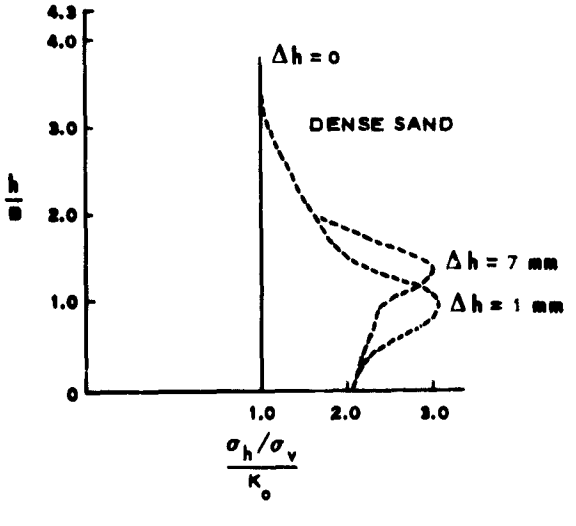

E. VARIATION OF EARTH PRESSURE COEFFICIENT ABOVE CENTER LINE OF TRAPDOOR

Fig. 2.1 Terzaghi's (1936b) trapdoor experiment

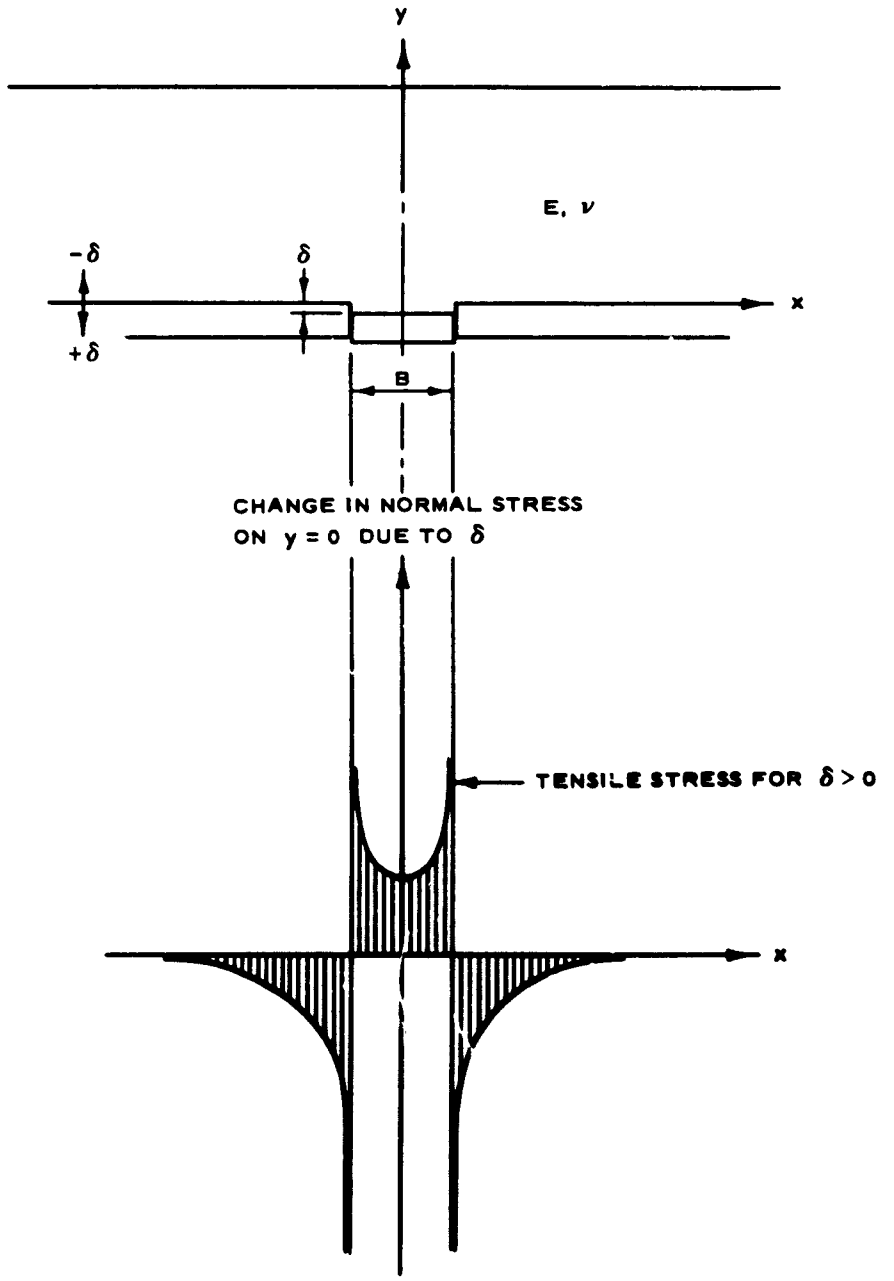

Fig. 2.2 Distribution of arching stresses from Finn's (1960) elastic solution

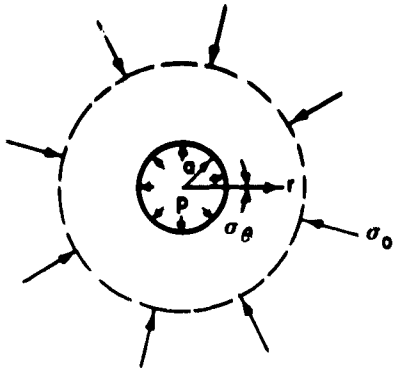

(a) GEOMETRY AND BOUNDARY CONDITIONS

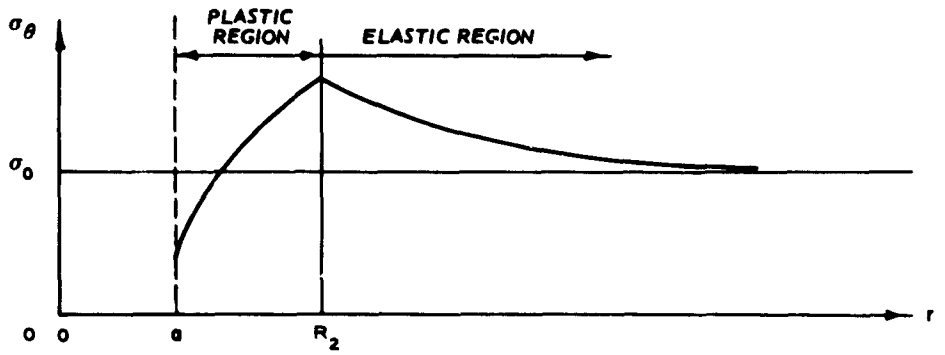

(b) ACTIVE ARCHING – $p << \sigma_0$

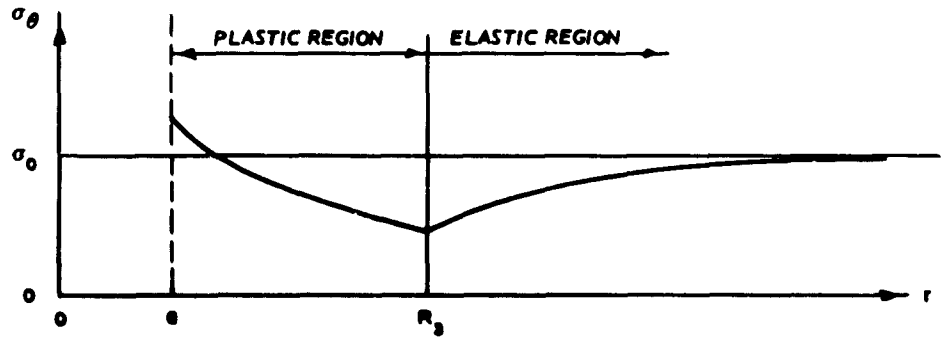

(c) PASSIVE ARCHING – $p >> \sigma_0$

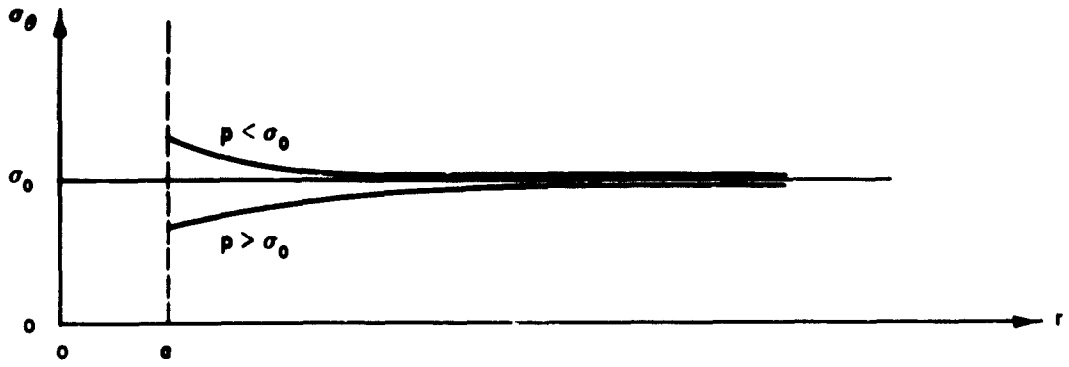

(d) ELASTIC SITUATION – $p \approx \sigma_0$

Fig. 2.3 Circumferential stress distributions from Sirieys' (1964) elastoplastic solution

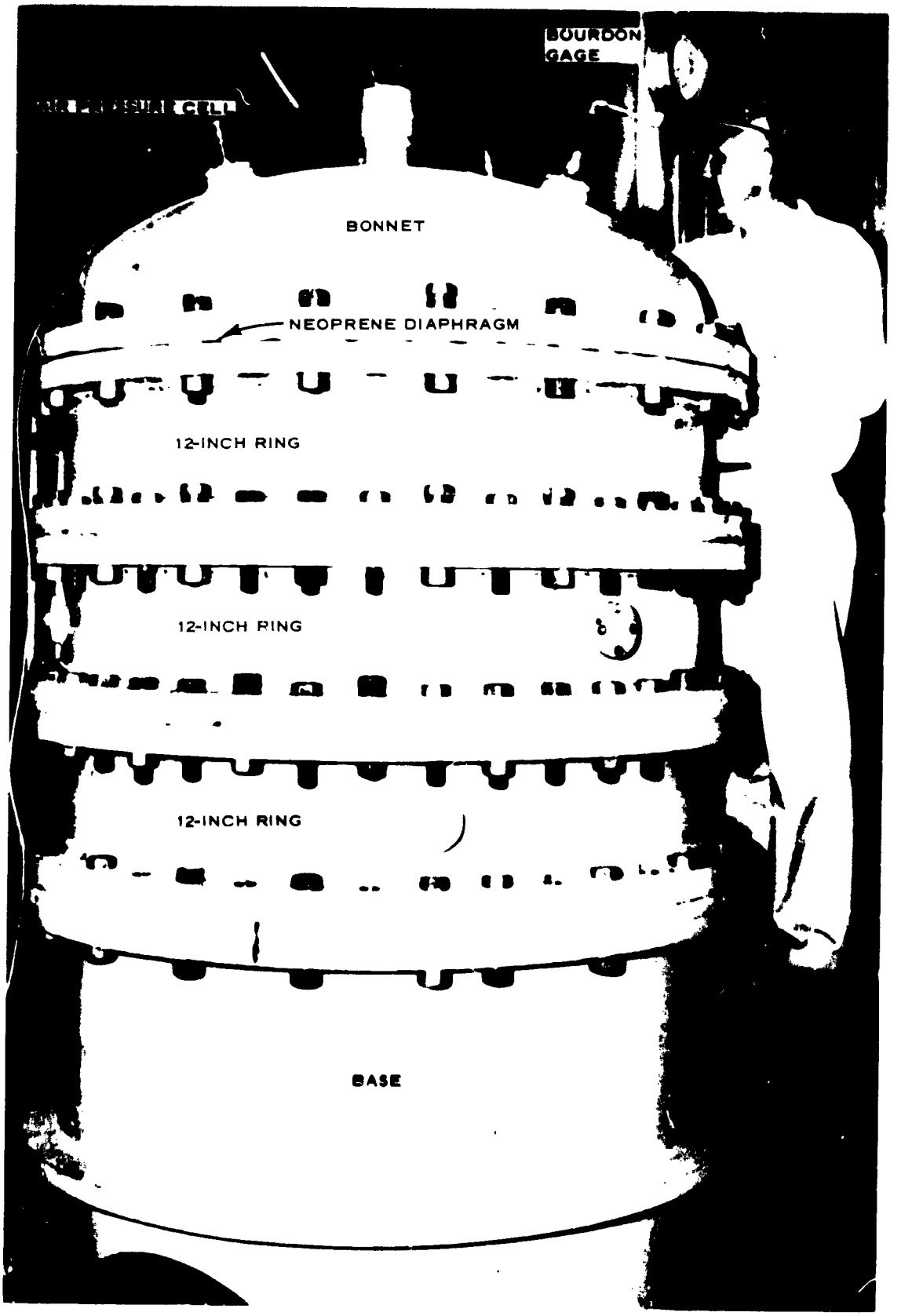

Fig. 3.1 Test apparatus during a 36-in. test

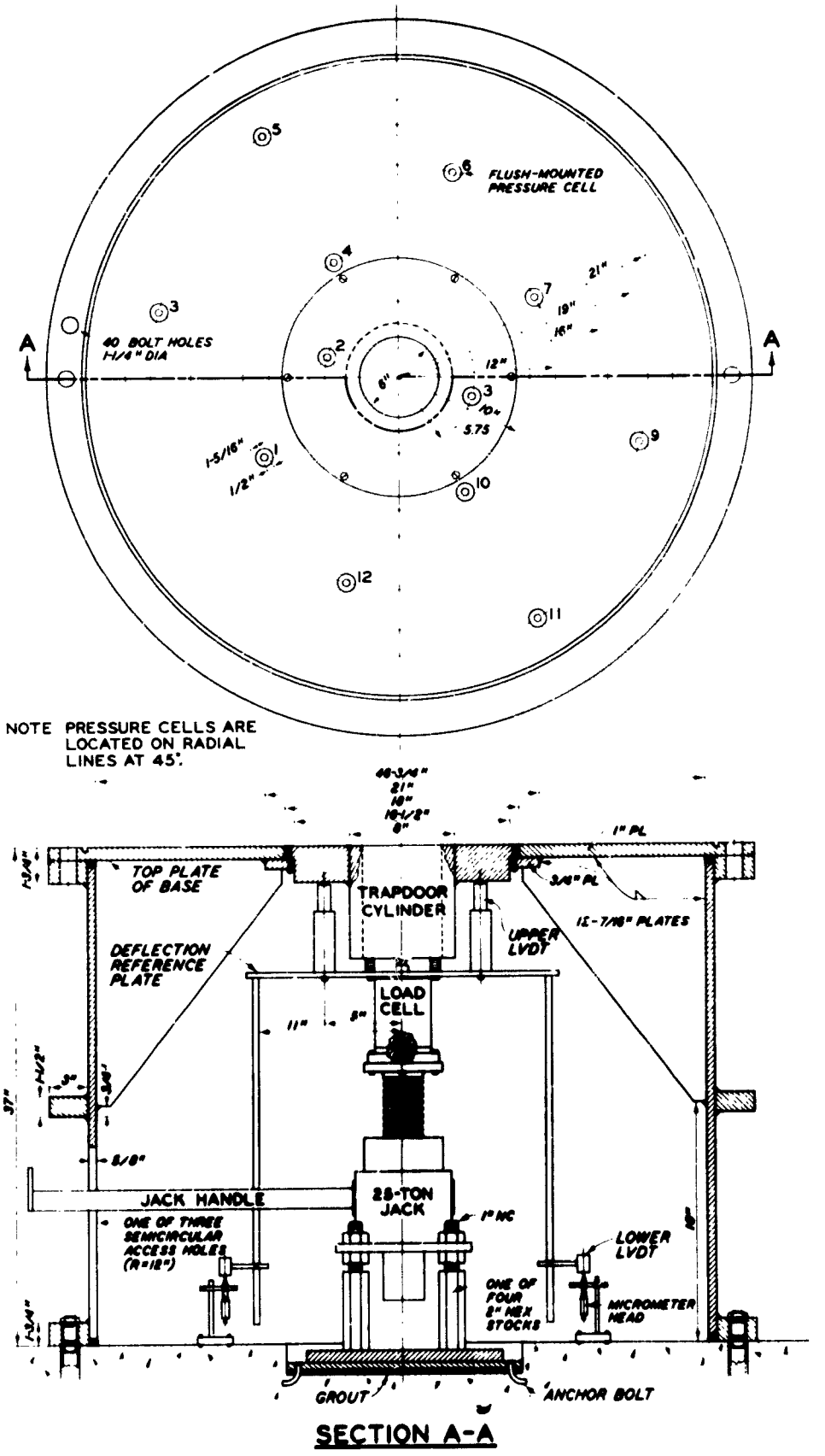

Fig. 3.3 Base of test apparatus and trapdoor support system

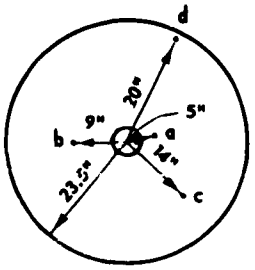

BOTTOM OF TEST CHAMBER

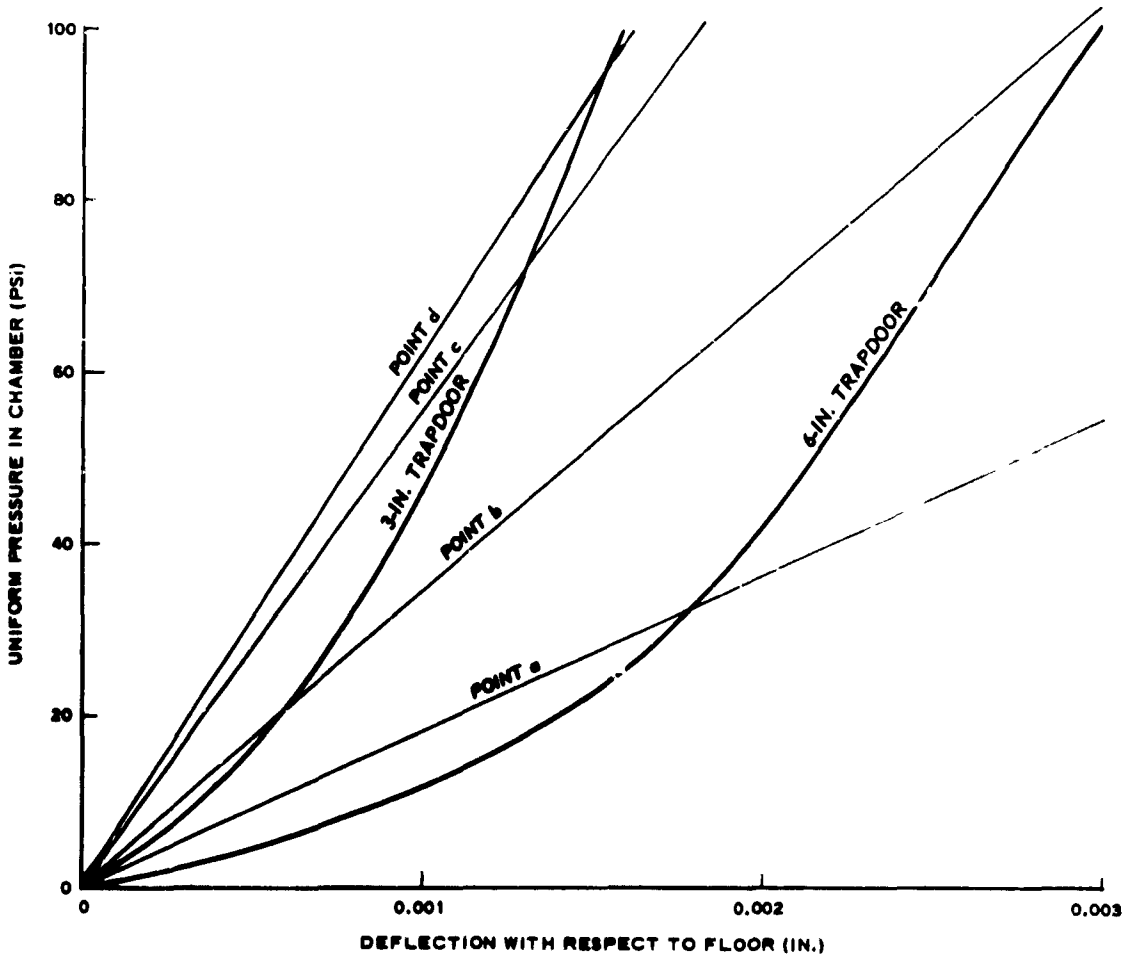

Fig. 3.4 Pressure vs. deflection curves for the trapdoors and various points on the top plate

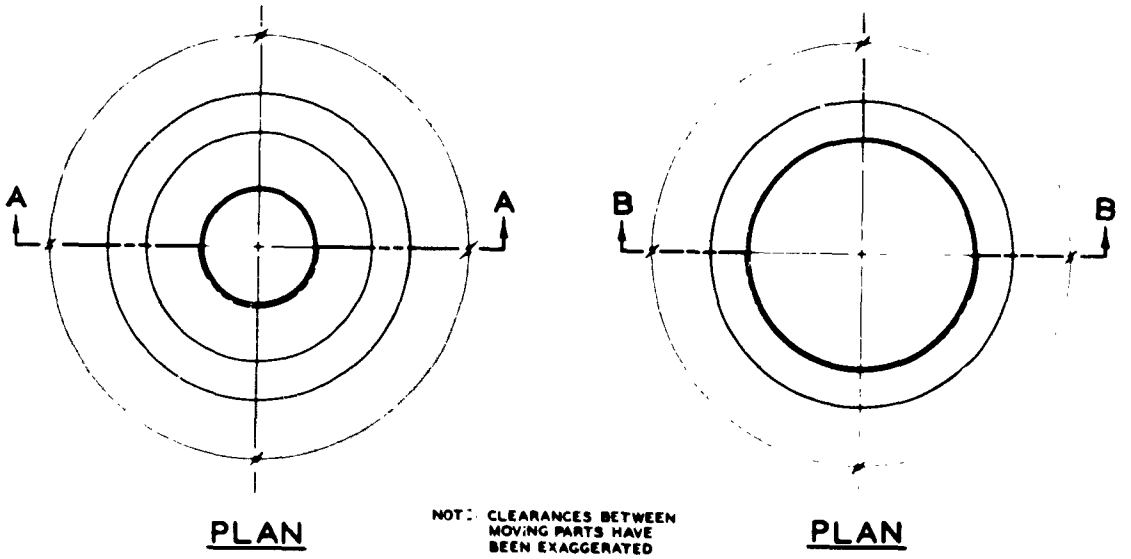

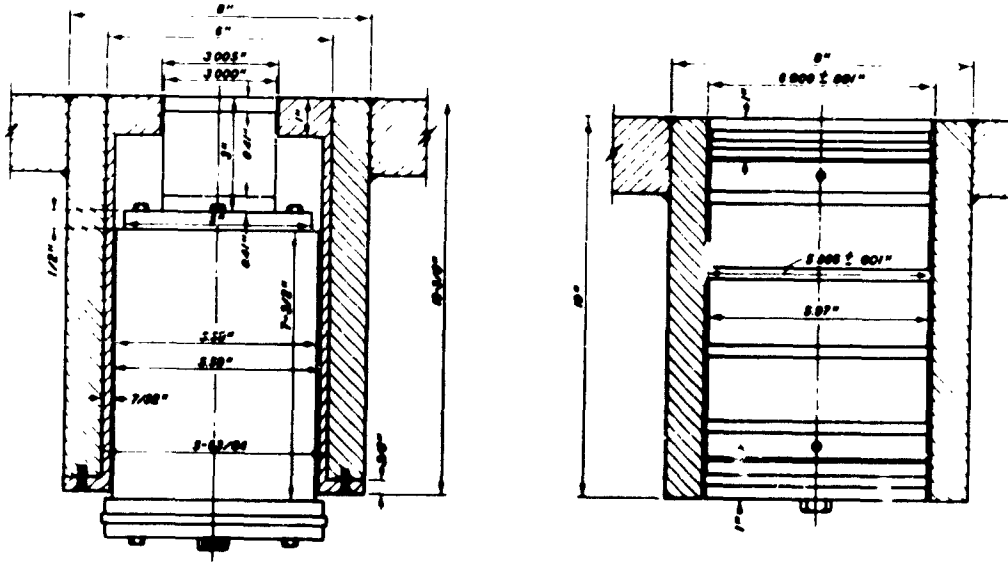

Fig. 3.5 Details of the trapdoors

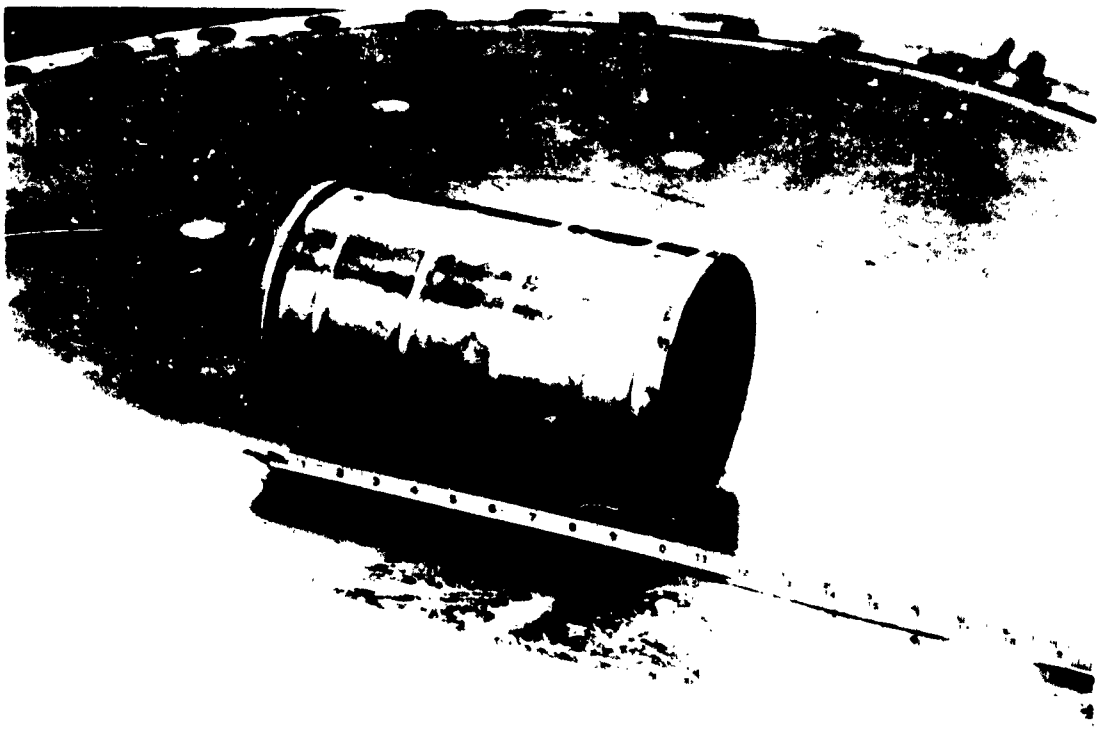

Fig. 3.6 The 6-in.-diameter trapdoor

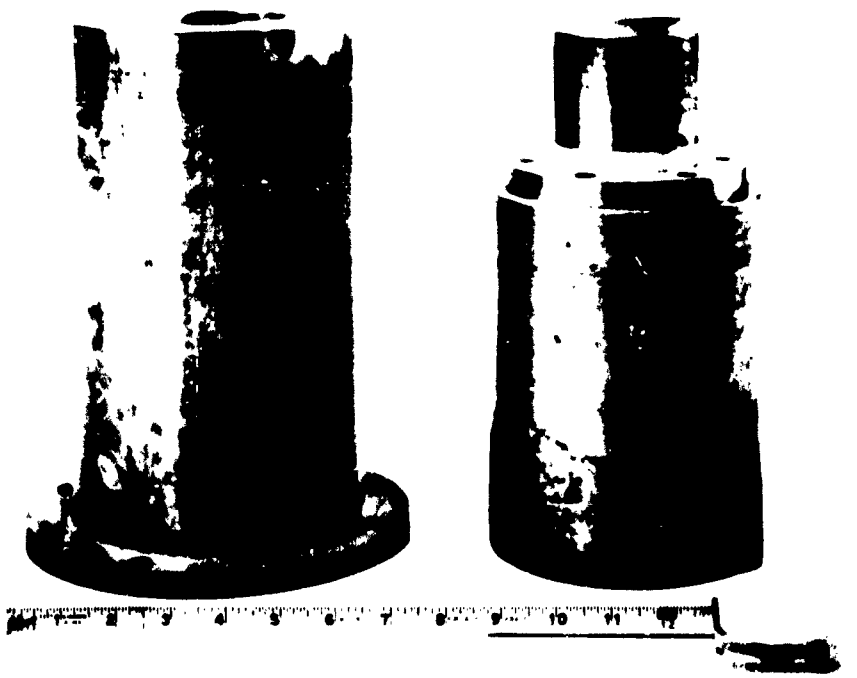

Fig. 3.7 The 3-in.-diameter trapdoor assembly

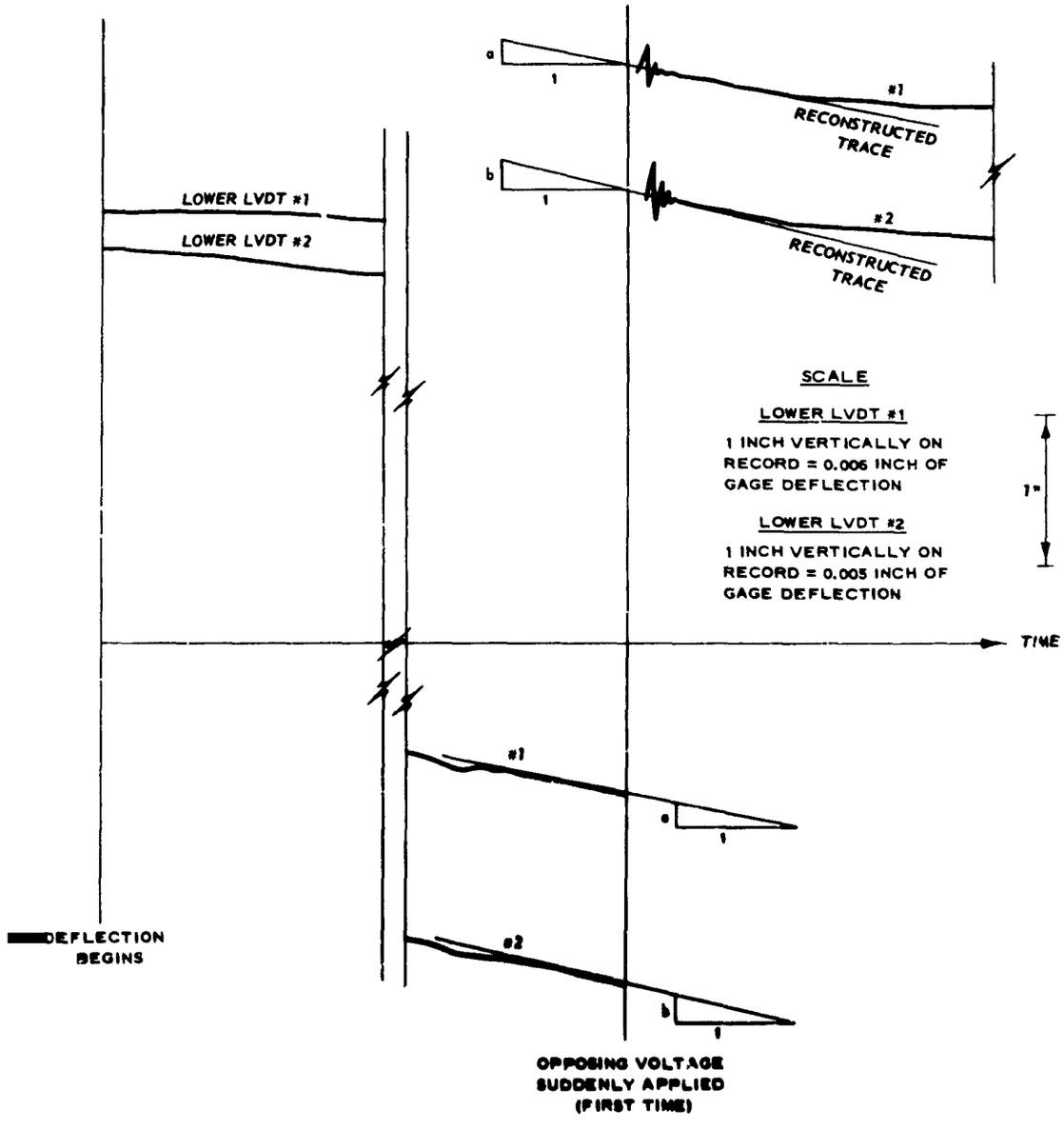

Fig. 3.8 Discontinuities in deflection traces during a typical passive arching test

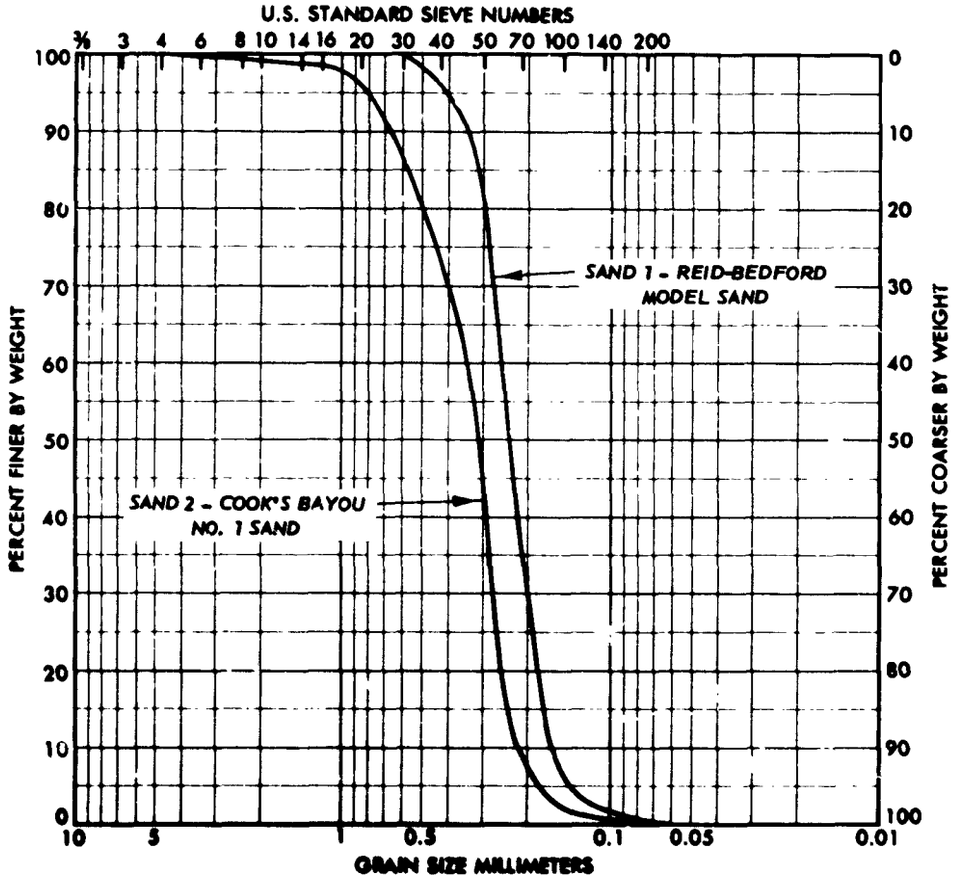

Fig. 3.9 Grain size distribution curves of sands tested

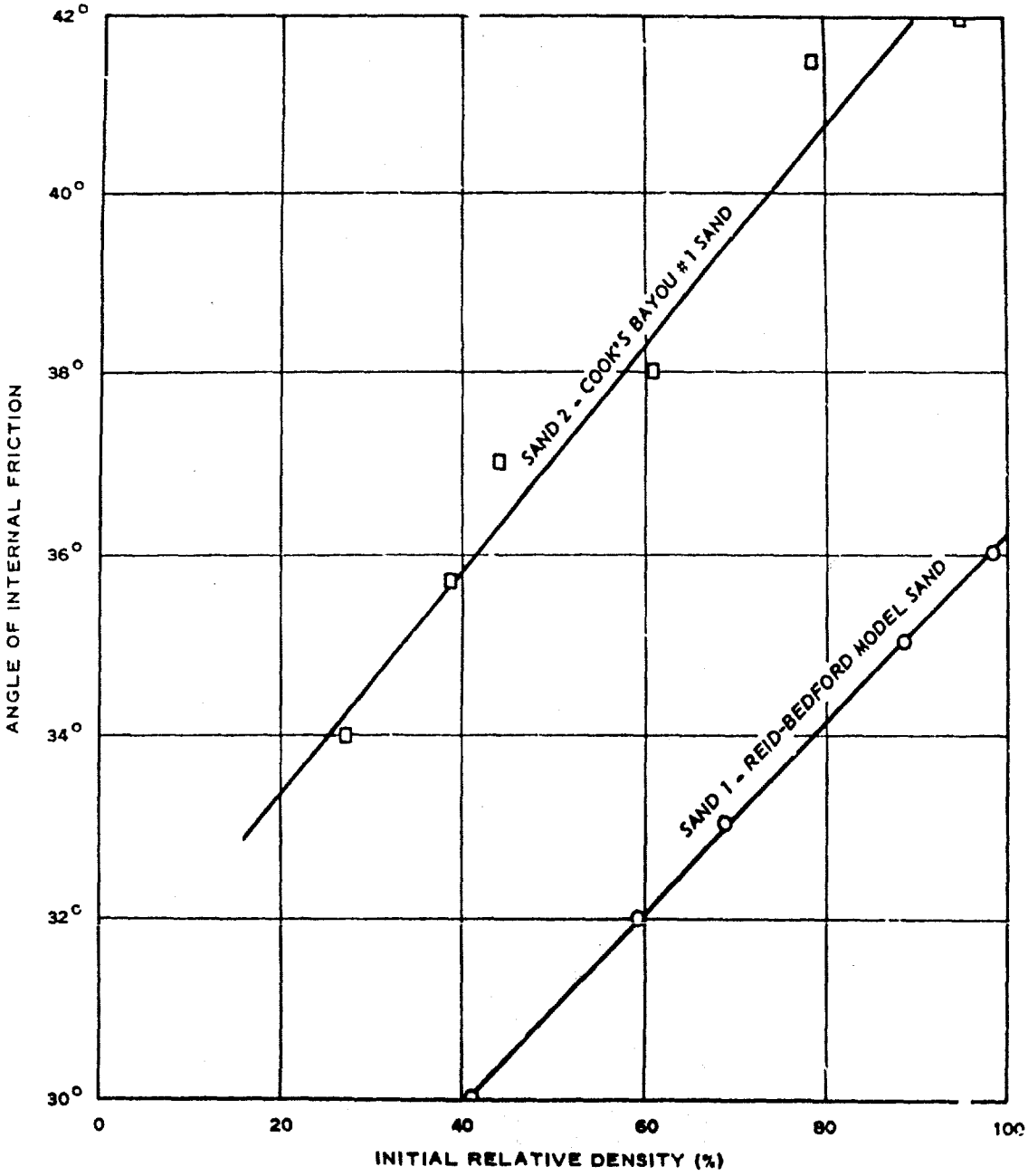

SAND 1	0.92	0.85	0.78	0.71	0.64	0.57
SAND 2	0.77	0.71	0.65	0.60	0.54	0.49

INITIAL VOID RATIO

SAND 1	86.0	89.9	93.7	97.6	101.4	105.3
SAND 2	93.3	96.8	100.3	103.8	107.3	110.8

INITIAL DRY DENSITY (PCF)

Fig. 3.10 The relation between angle of internal friction and density for the sands tested

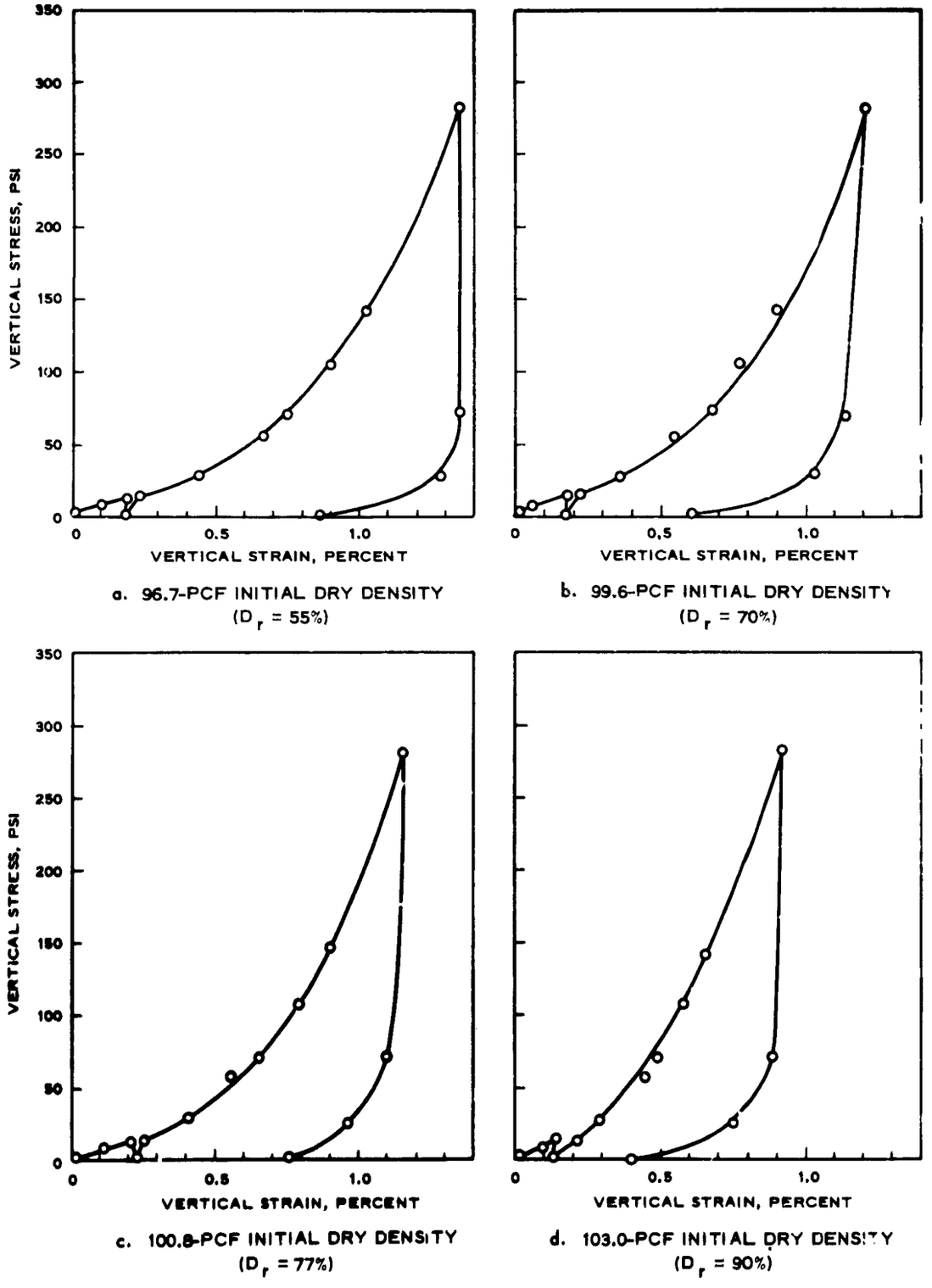

Fig. 3.11 One-dimensional compression stress-strain curves for sand 1

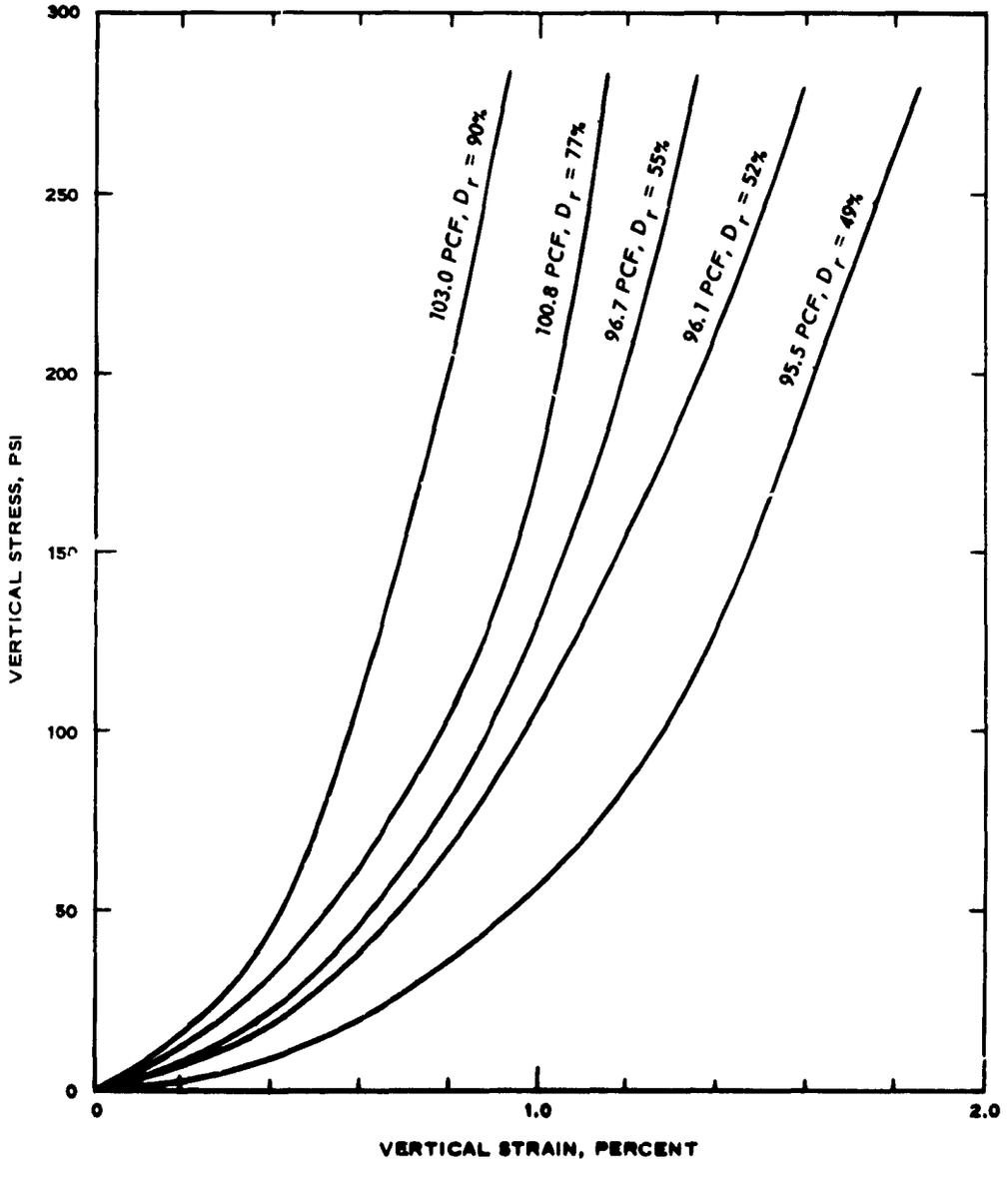

Fig. 3.12 Comparison of one-dimensional loading curves for sand 1

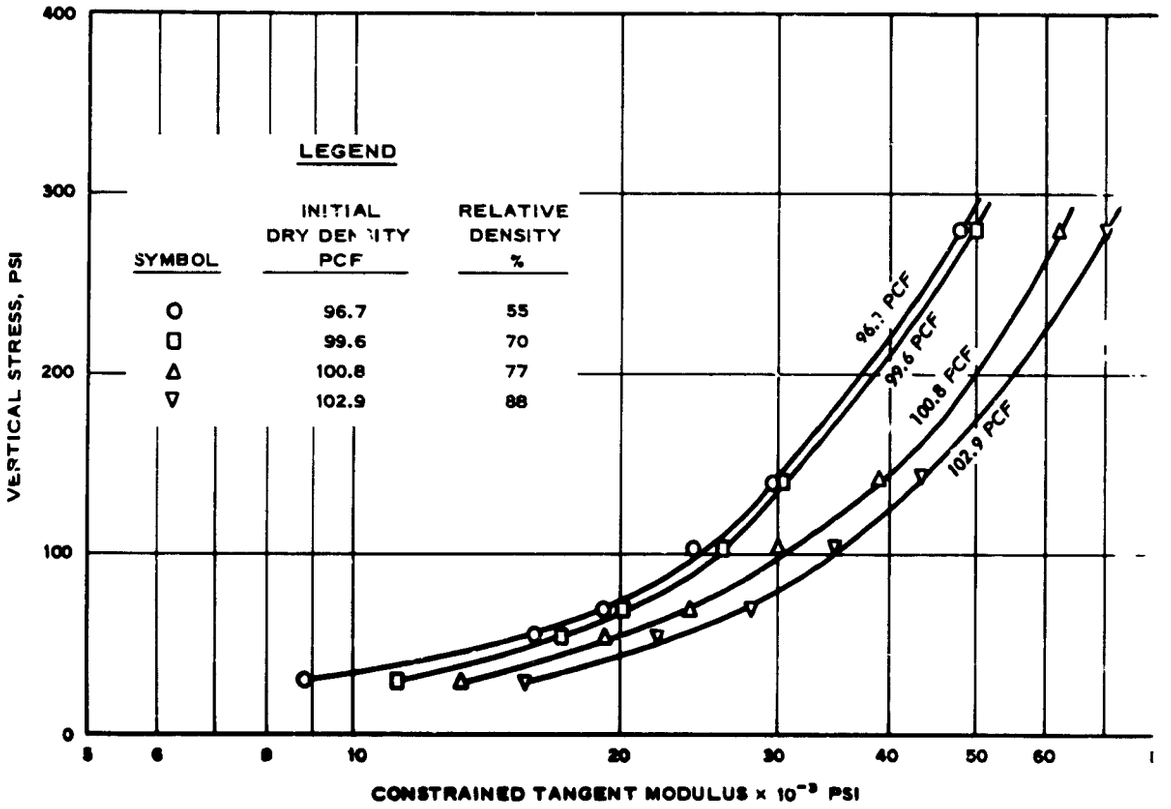

Fig. 3.13 Constrained tangent modulus vs. vertical stress for sand 1

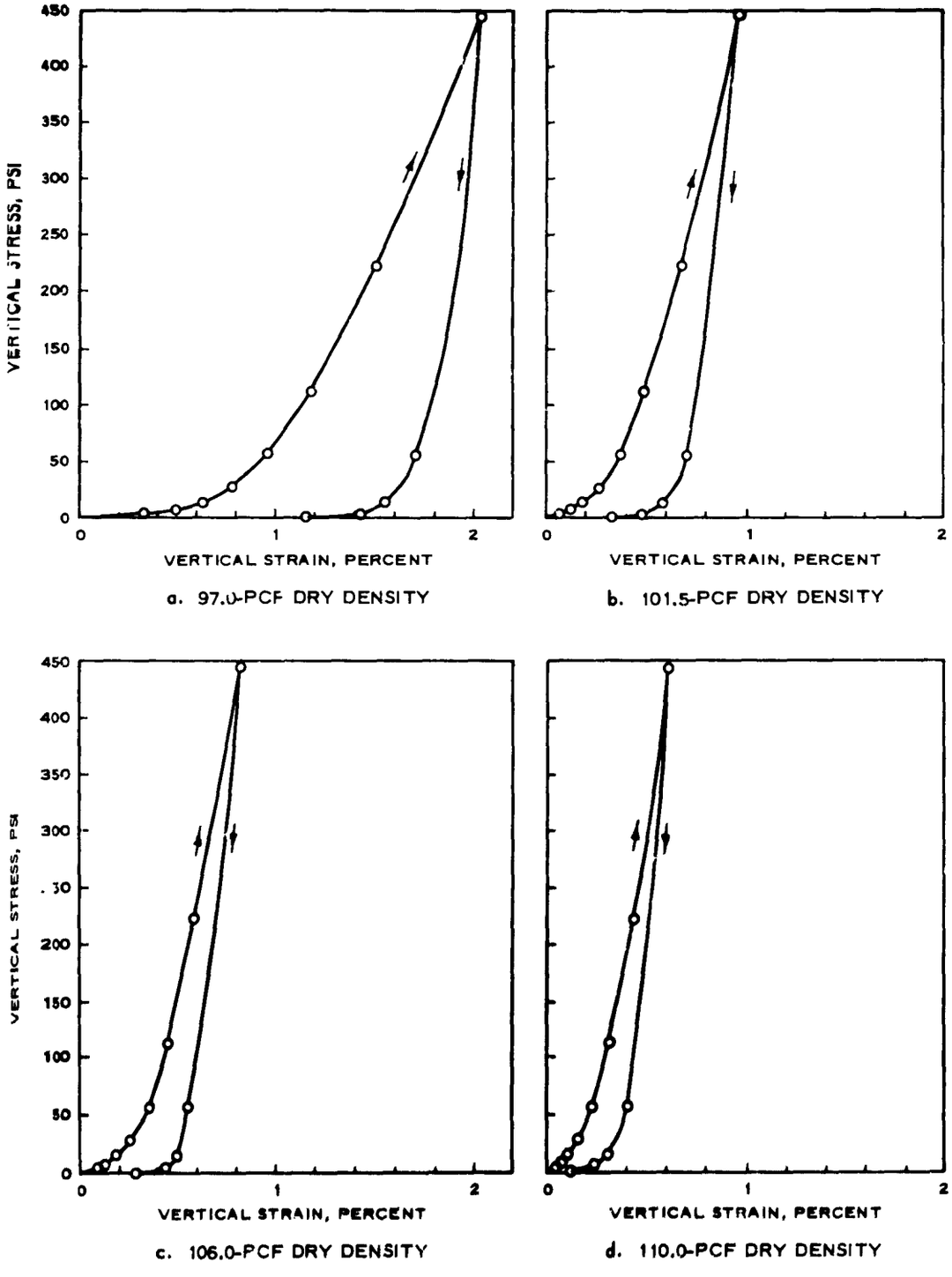

Fig. 3.14 One-dimensional compression stress-strain curves for sand 2

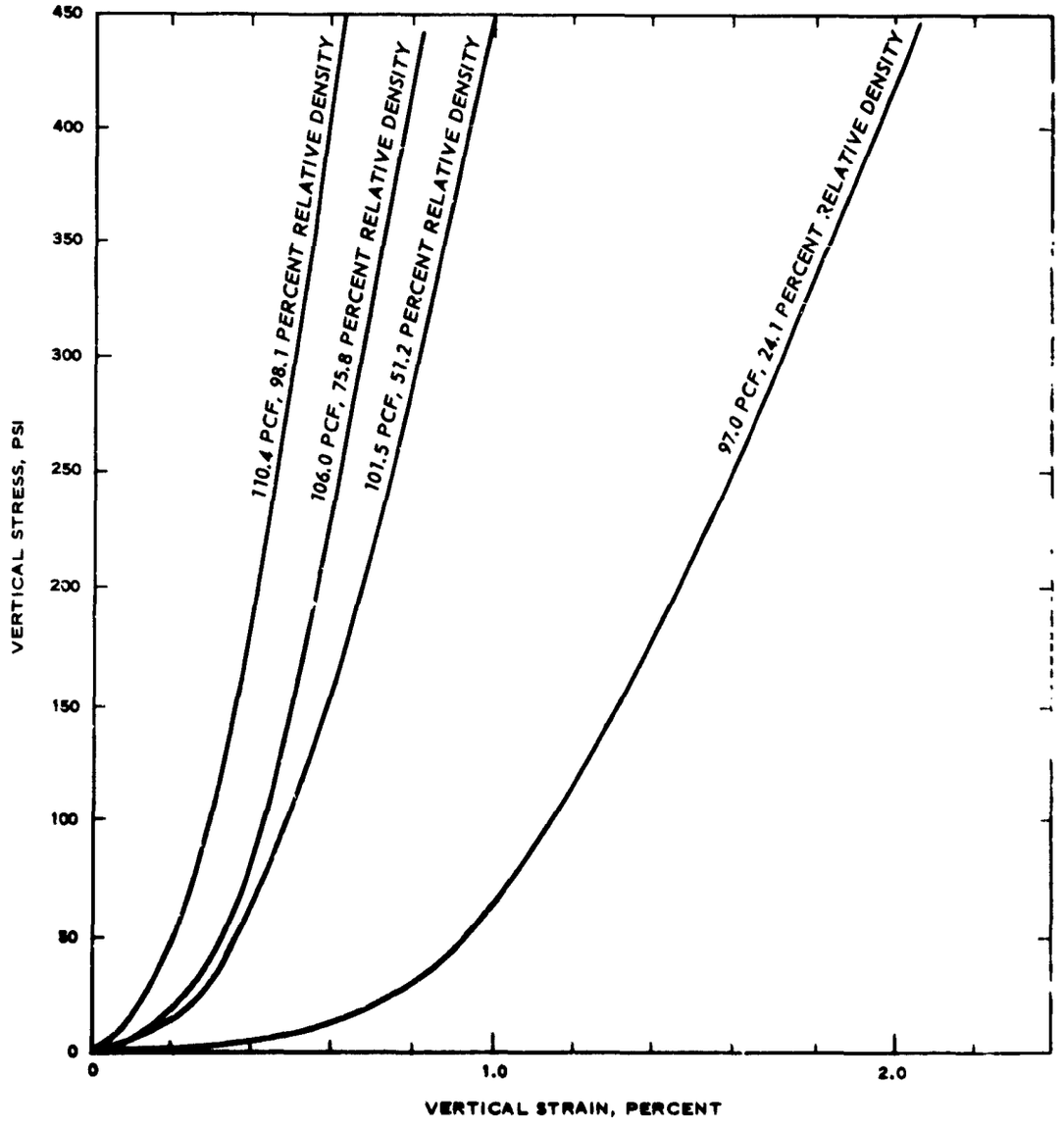

Fig. 3.15 Comparison of one-dimensional loading curves for sand 2

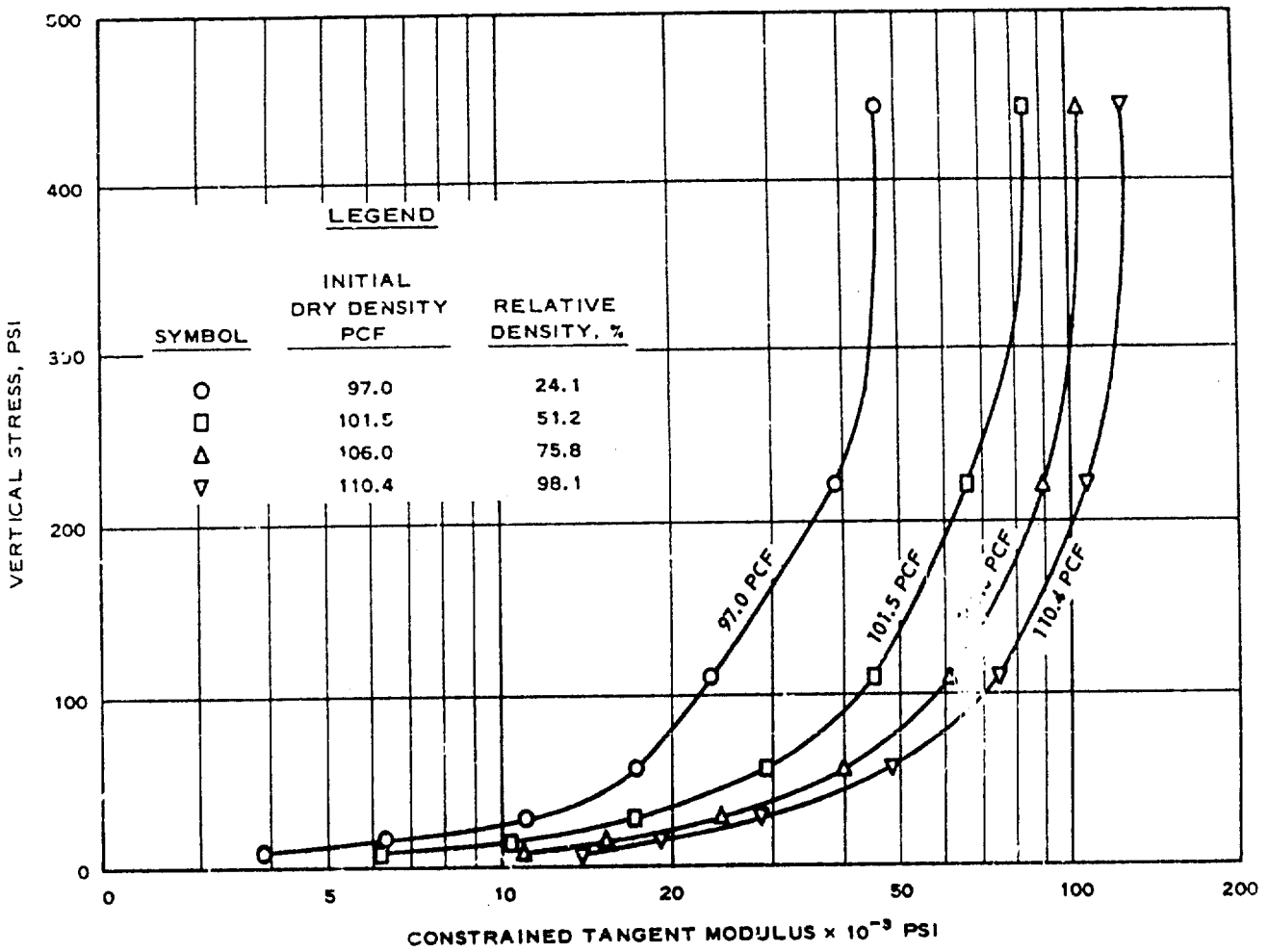

Fig. 3.16 Constrained tangent modulus vs. vertical stress for sand 2

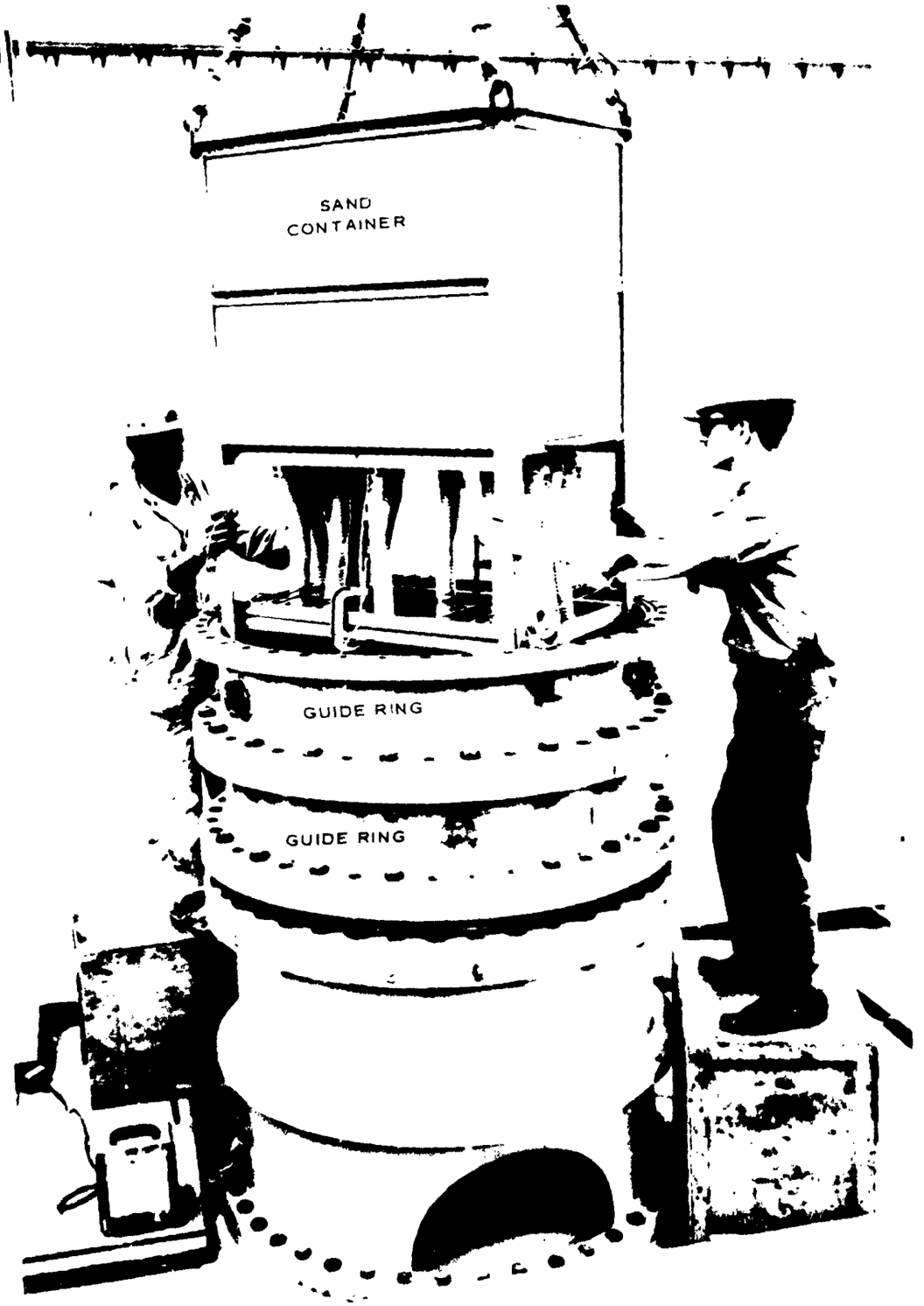

Fig. 3.17 Preparation of sand specimen for a 6-in.-deep test

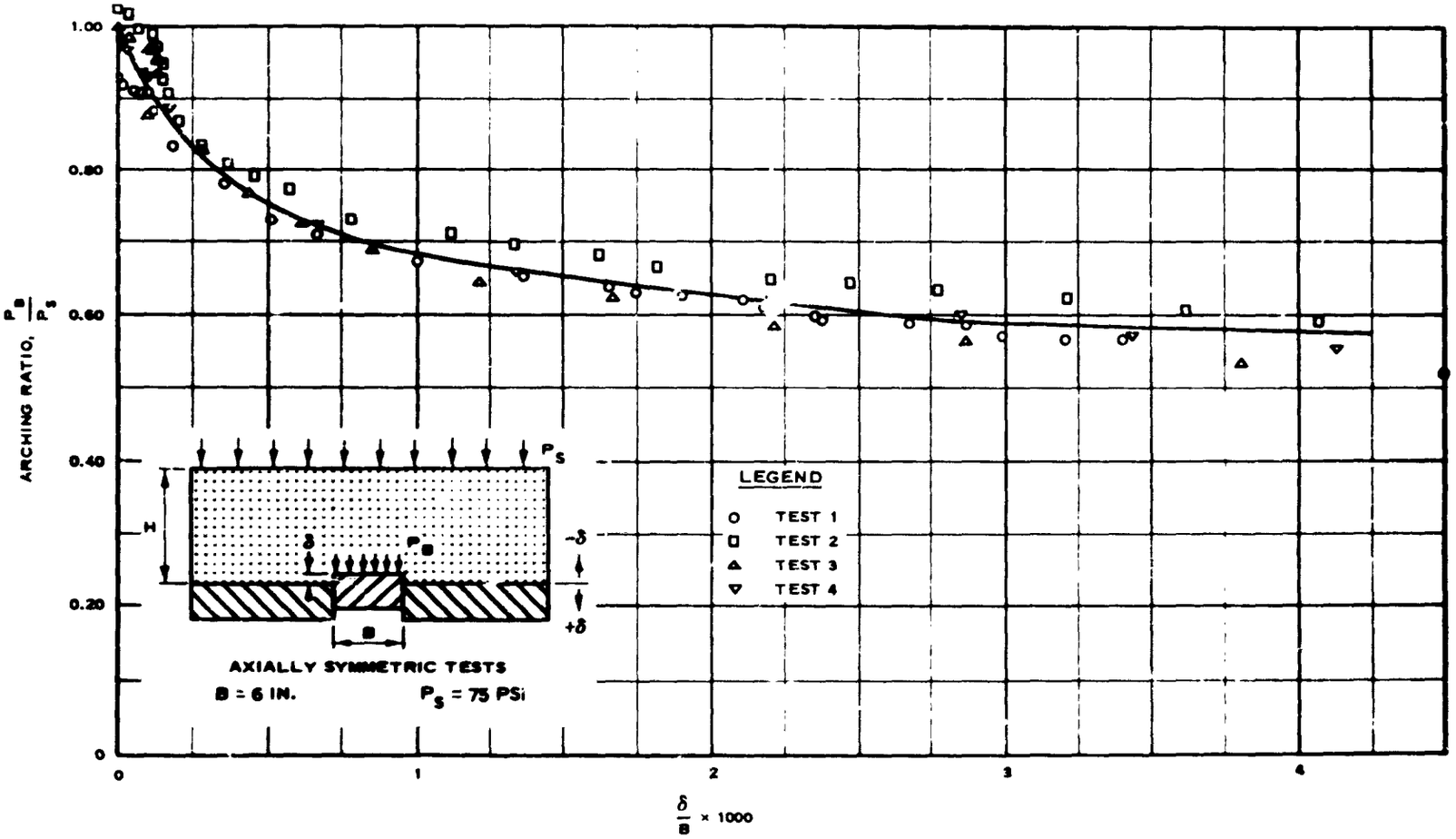

Fig. 4.1 Dimensionless plot of pressure vs. deflection for active arching tests with sand 1, H/B = 1/3 , P_S = 75 psi

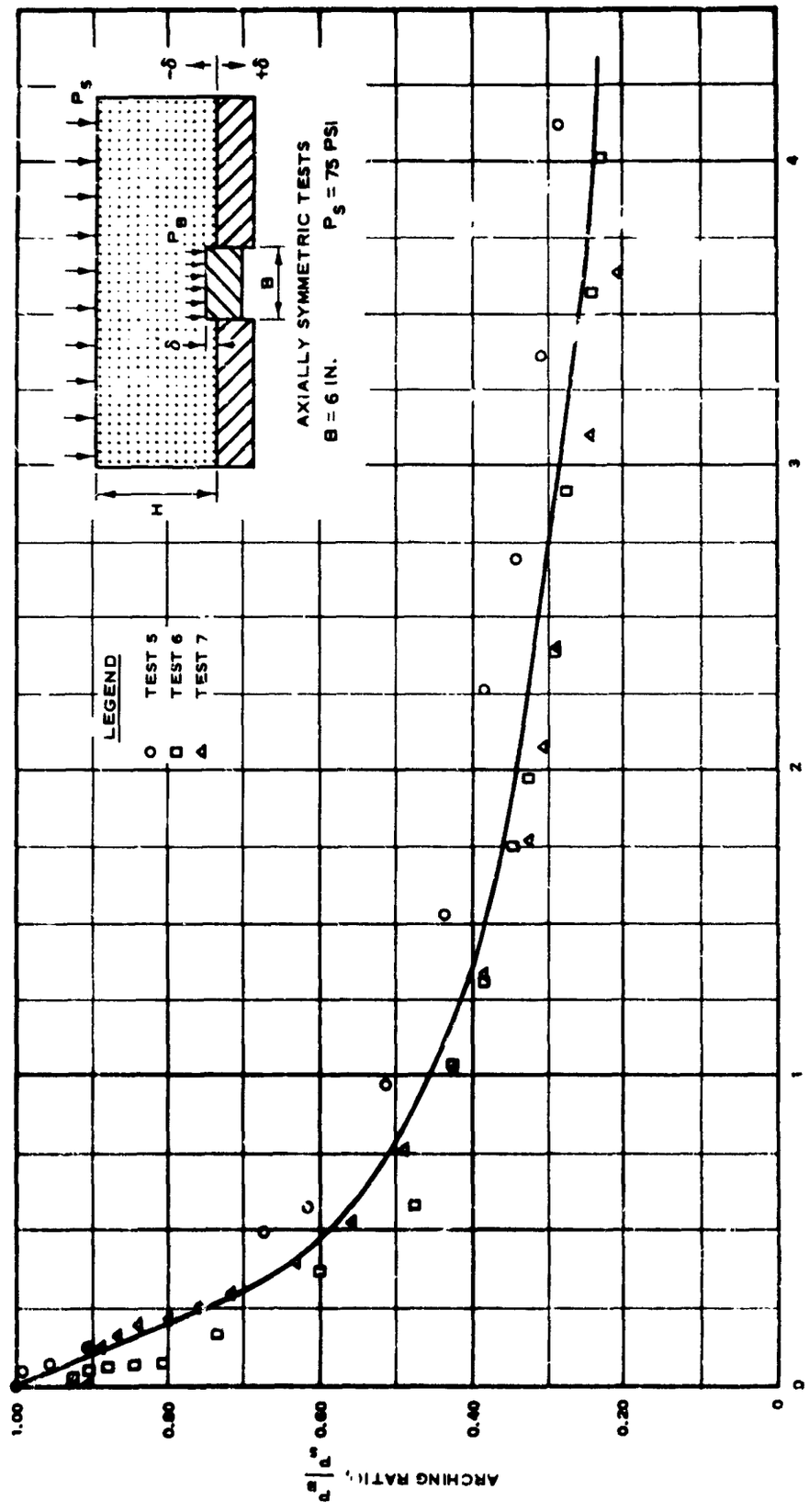

Fig. 4.4 Dimensionless plot of pressure vs. deflection for active arching tests with sand

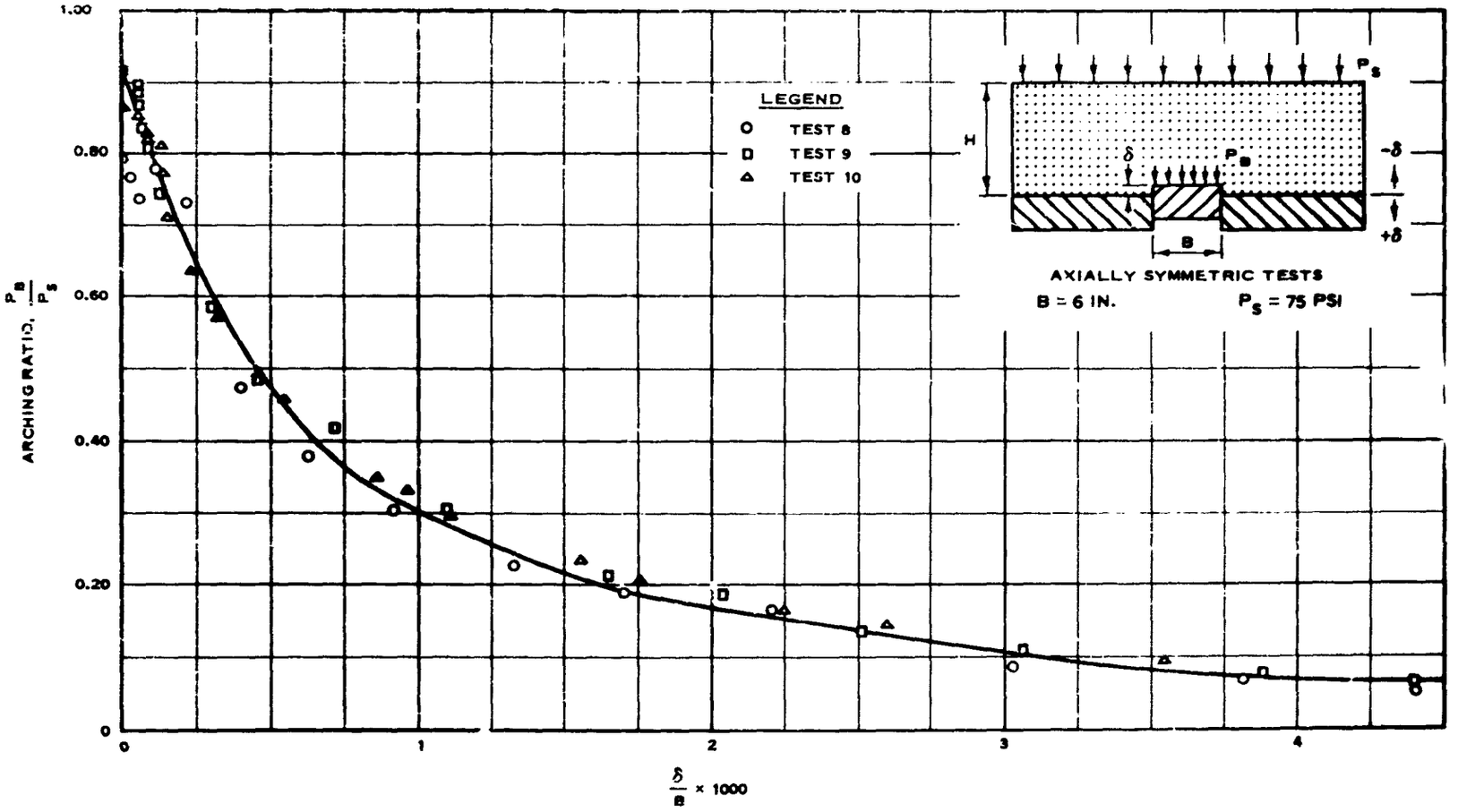

Fig. 4.3 Dimensionless plot of pressure vs. deflection for active arching tests with sand 1, H/B = 1 , P_s = 75 psi

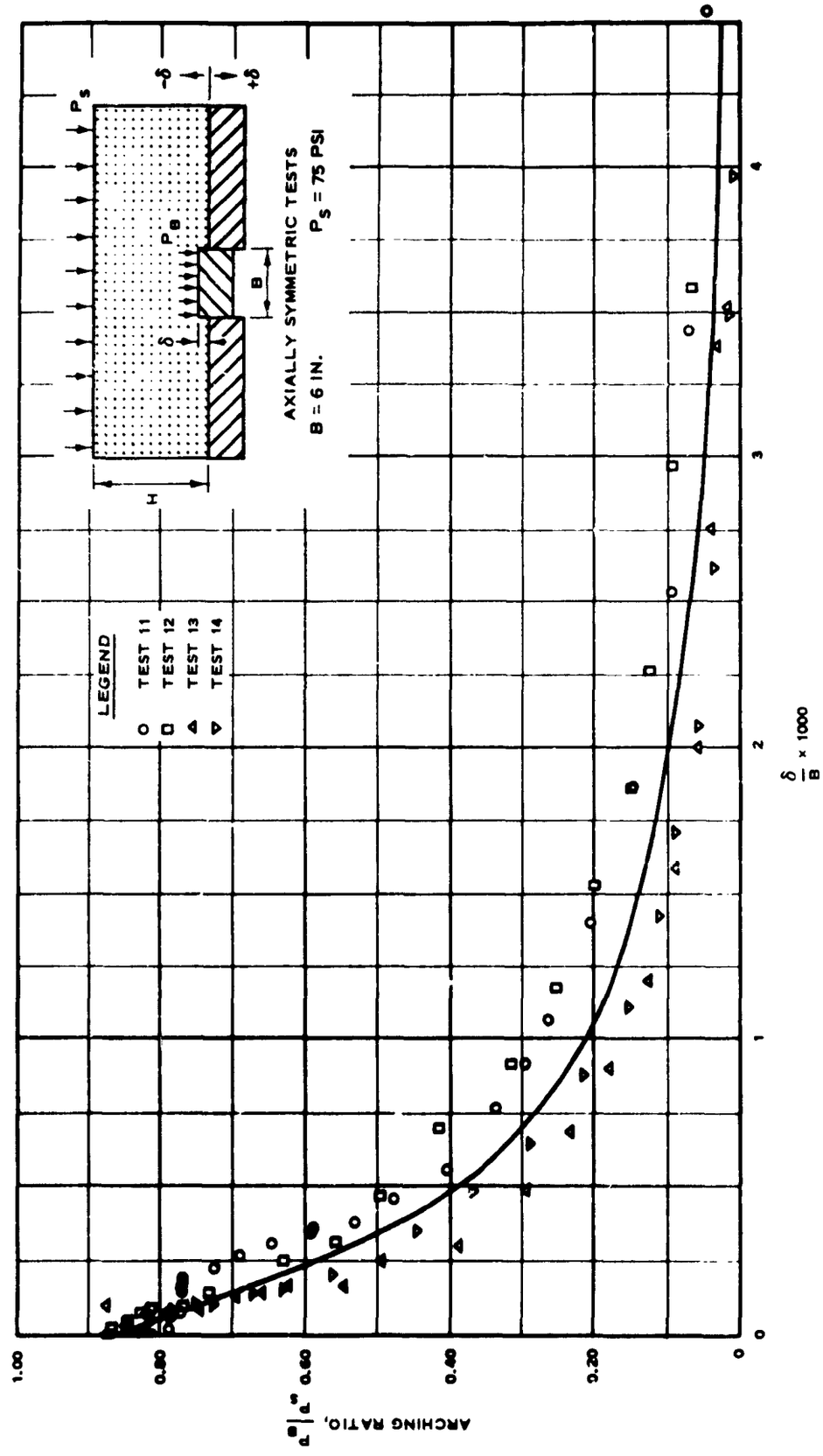

Fig. 4.4 Dimensionless plot of pressure vs. deflection for active arching tests

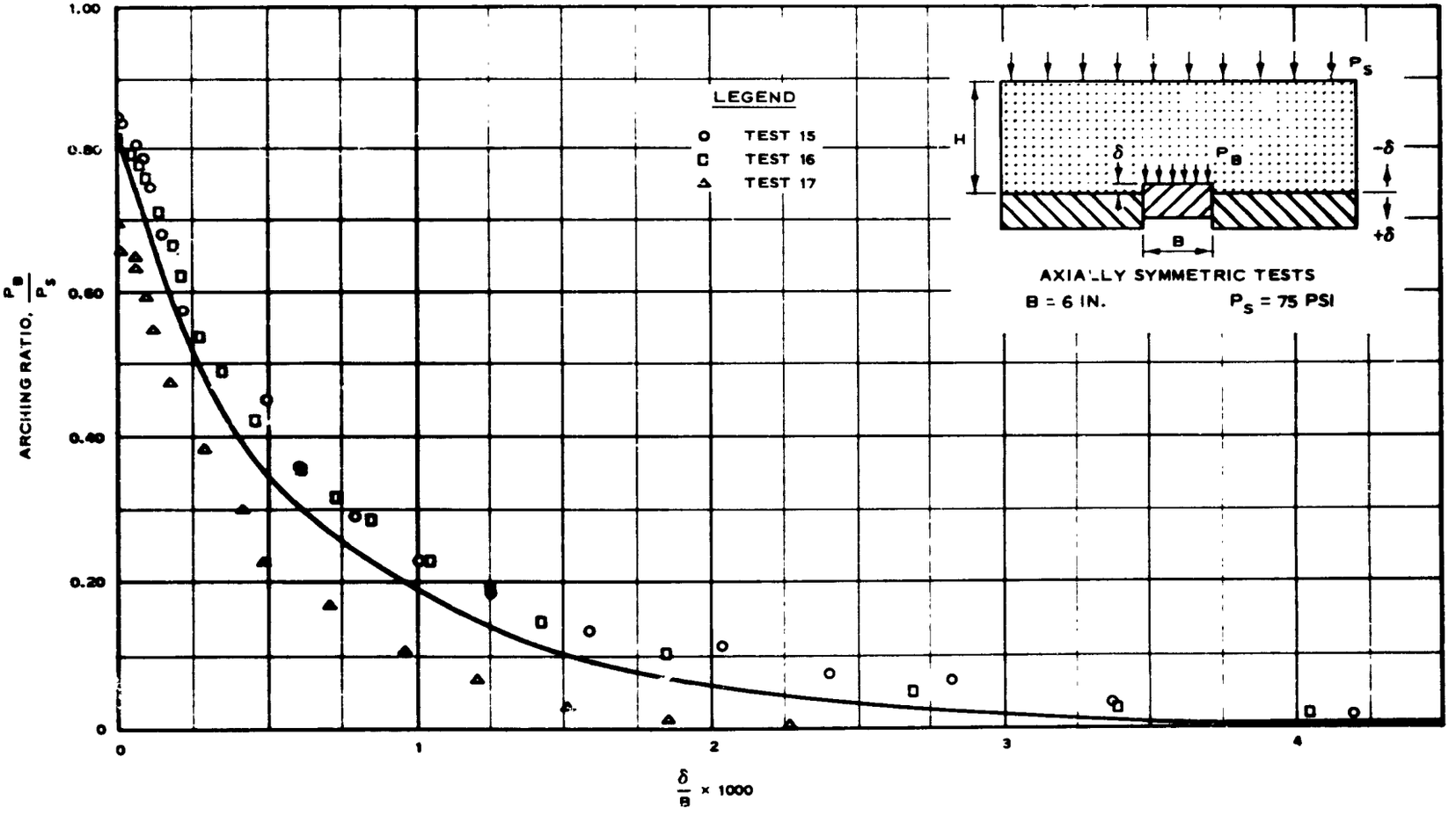

Fig. 4.5 Dimensionless plot of pressure vs deflection for active arching tests with sand 1, H/B = 4 , P_s = 75 psi

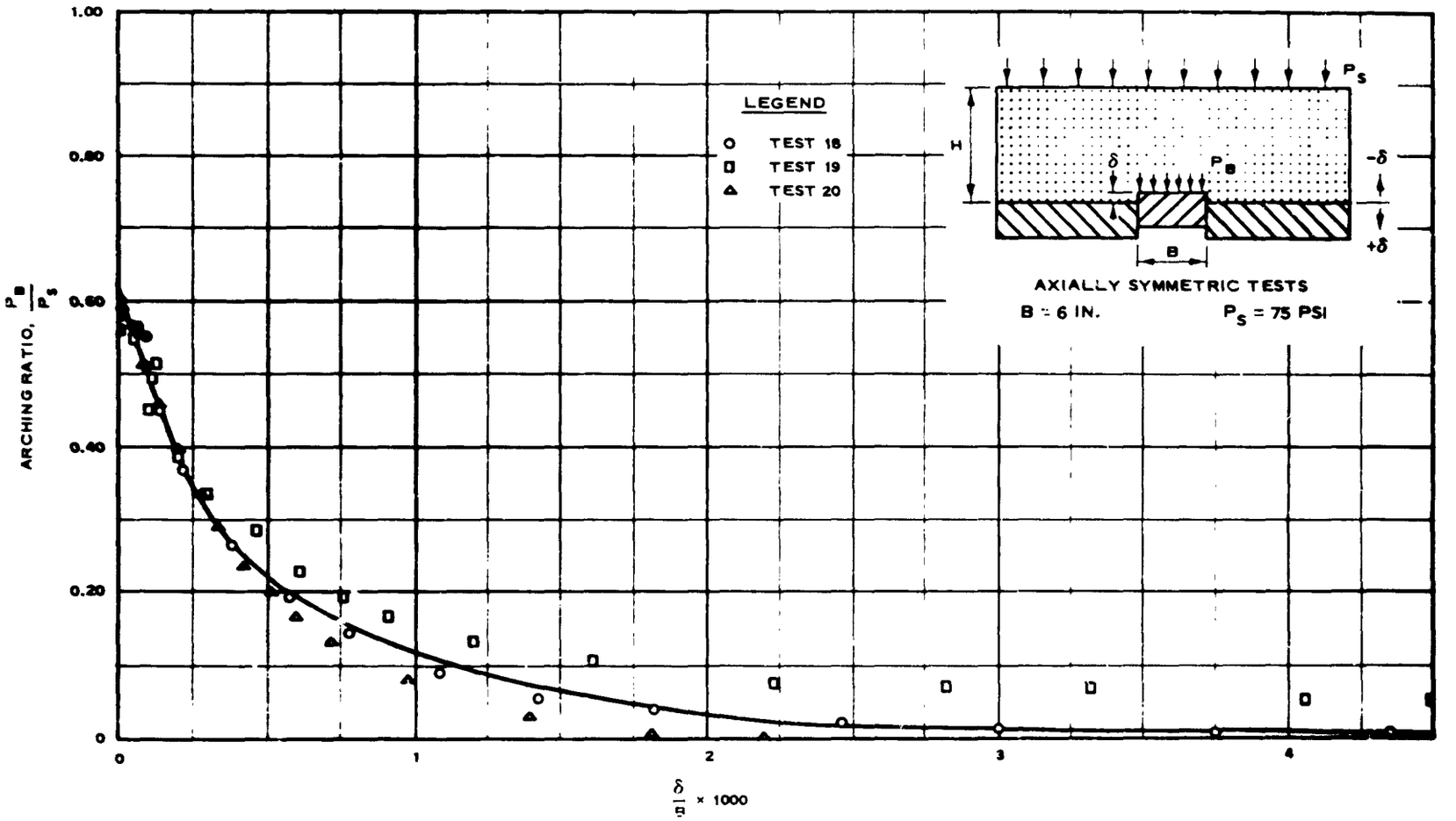

Fig. 4.6 Dimensionless plot of pressure vs. deflection for active arching tests

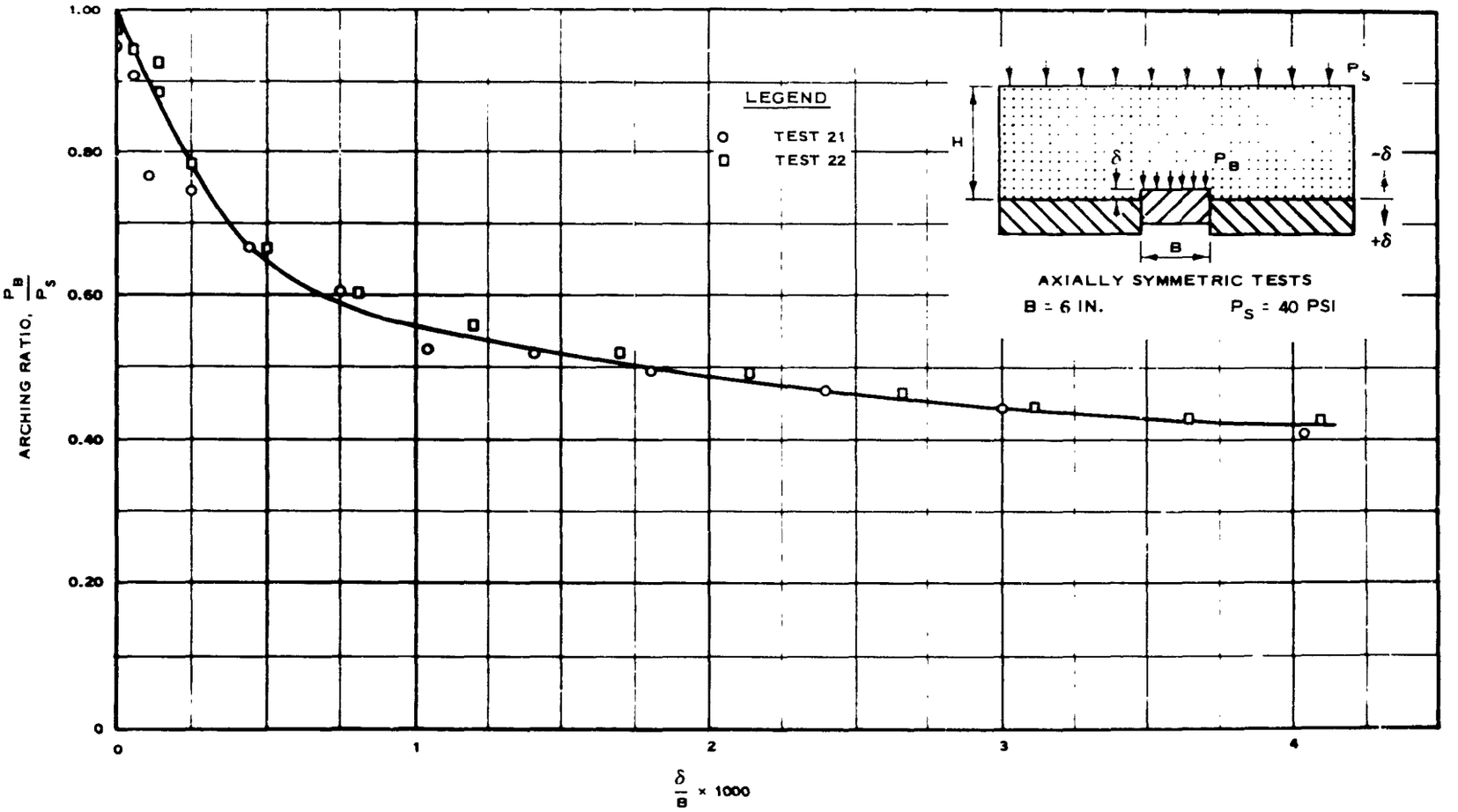

Fig. 4.7 Dimensionless plot of pressure vs. deflection for active arching tests with sand 2, H/B = 1/3, P_s = 40 psi

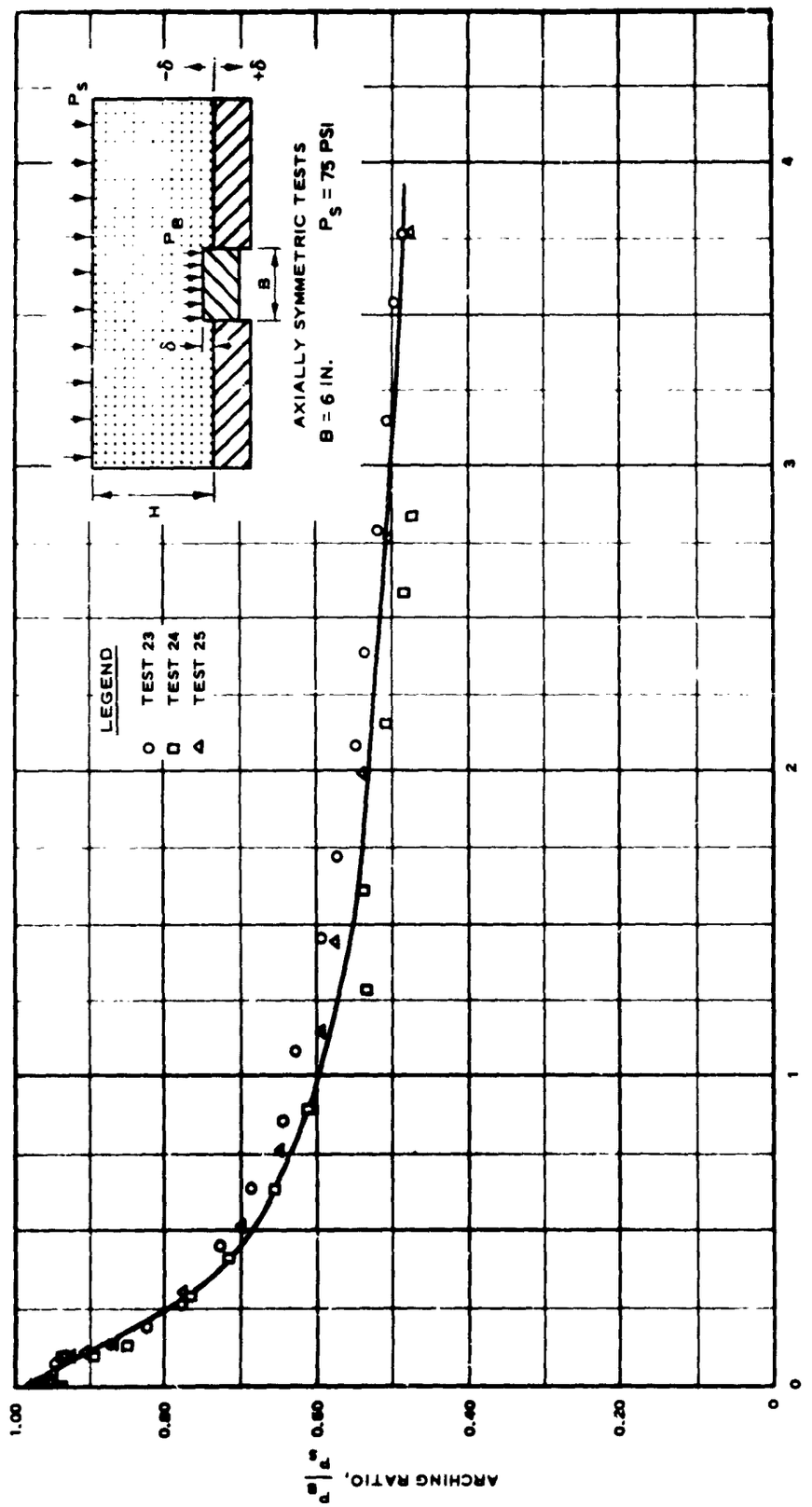

Fig. 4.5 Dimensionless plot of pressure vs. deflection for active arching tests with sand

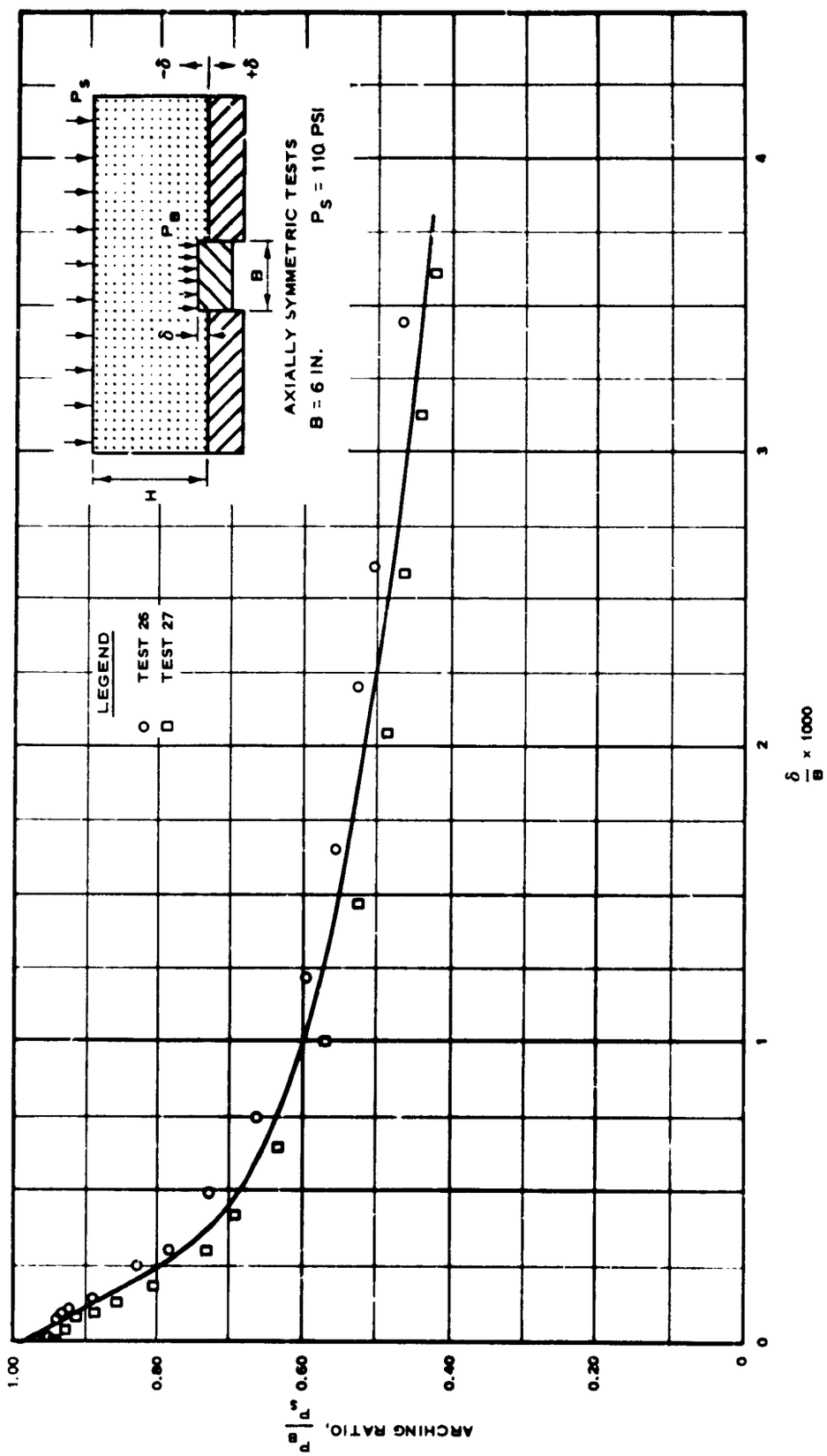

Fig. 4.9 Dimensionless plot of pressure vs. deflection for active arching tests with sand 2, H/B = 1/3 , P_s = 110 psi

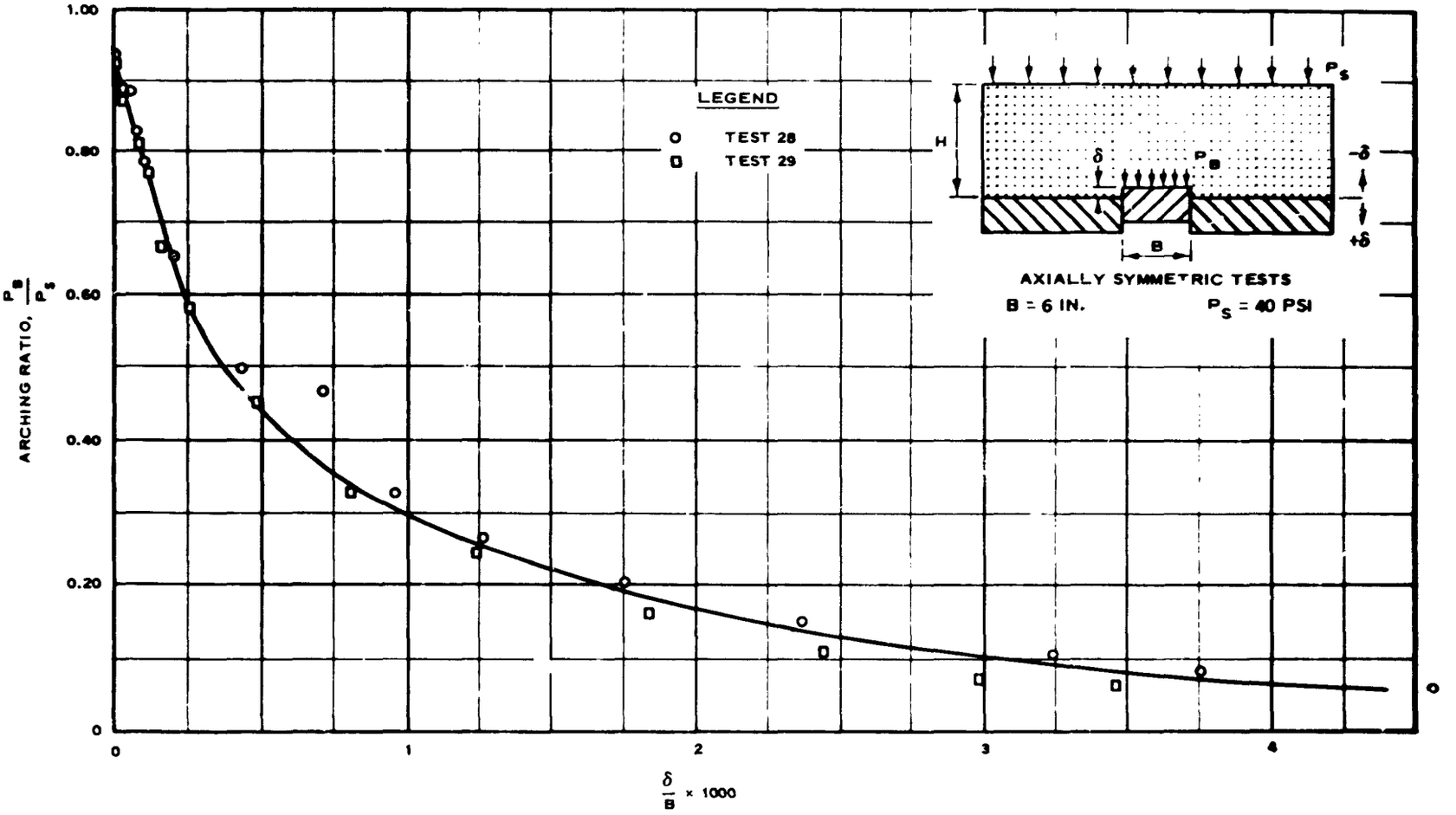

Fig. 4.10 Dimensionless plot of pressure vs. deflection for active arching tests

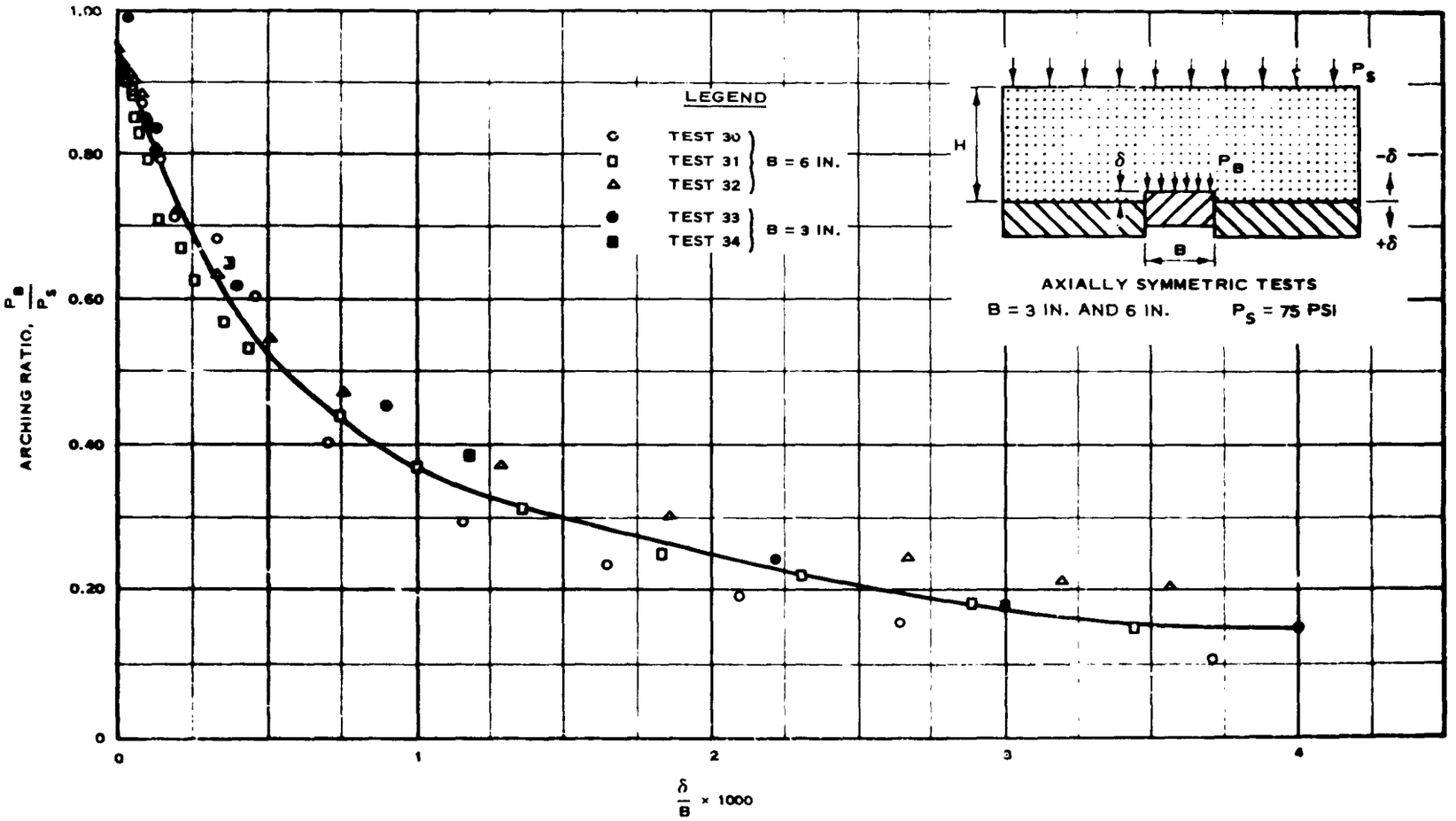

Fig. 4.11 Dimensionless plot of pressure vs. deflection for active arching tests with sand 2, H/B = 2/3 , P_s = 75 psi

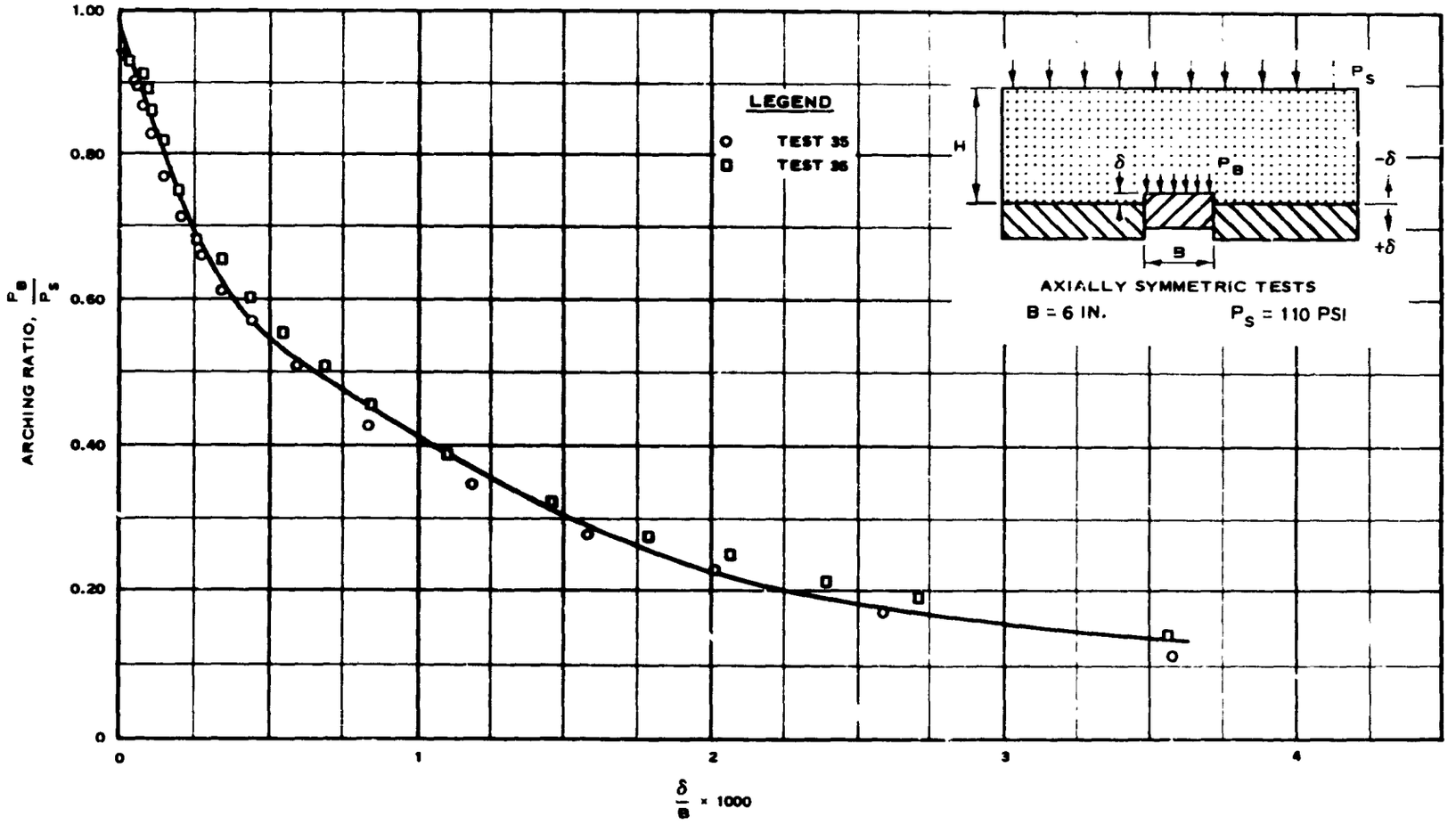

Fig. 4.12 Dimensionless plot of pressure vs. deflection for active arching tests with sand 2, H/B = 2/3 . P_s = 110 psi

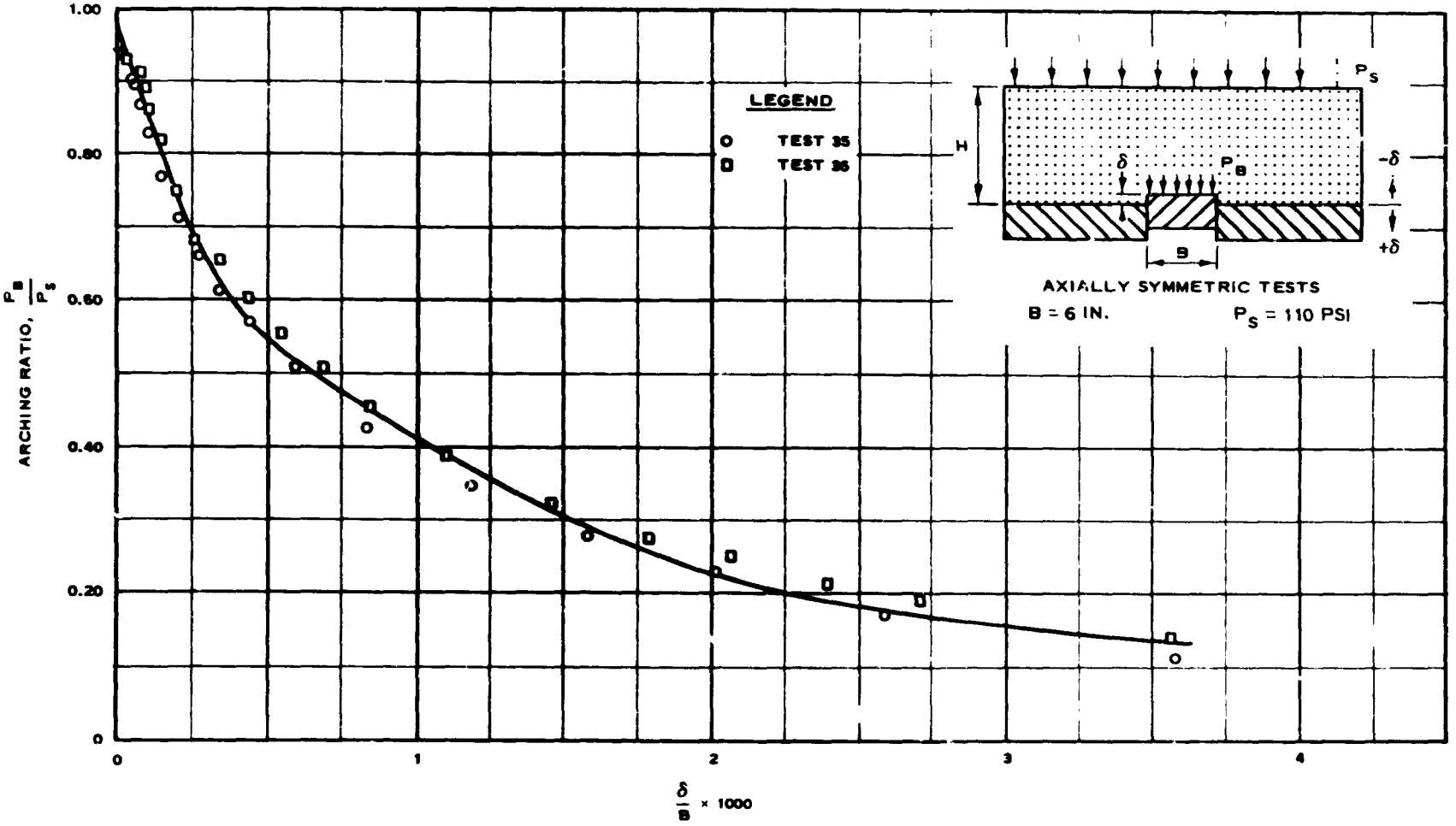

Fig. 4.12 Dimensionless plot of pressure vs. deflection for active arching tests with sand 2, H/B = 2/3 , P_s = 110 psi

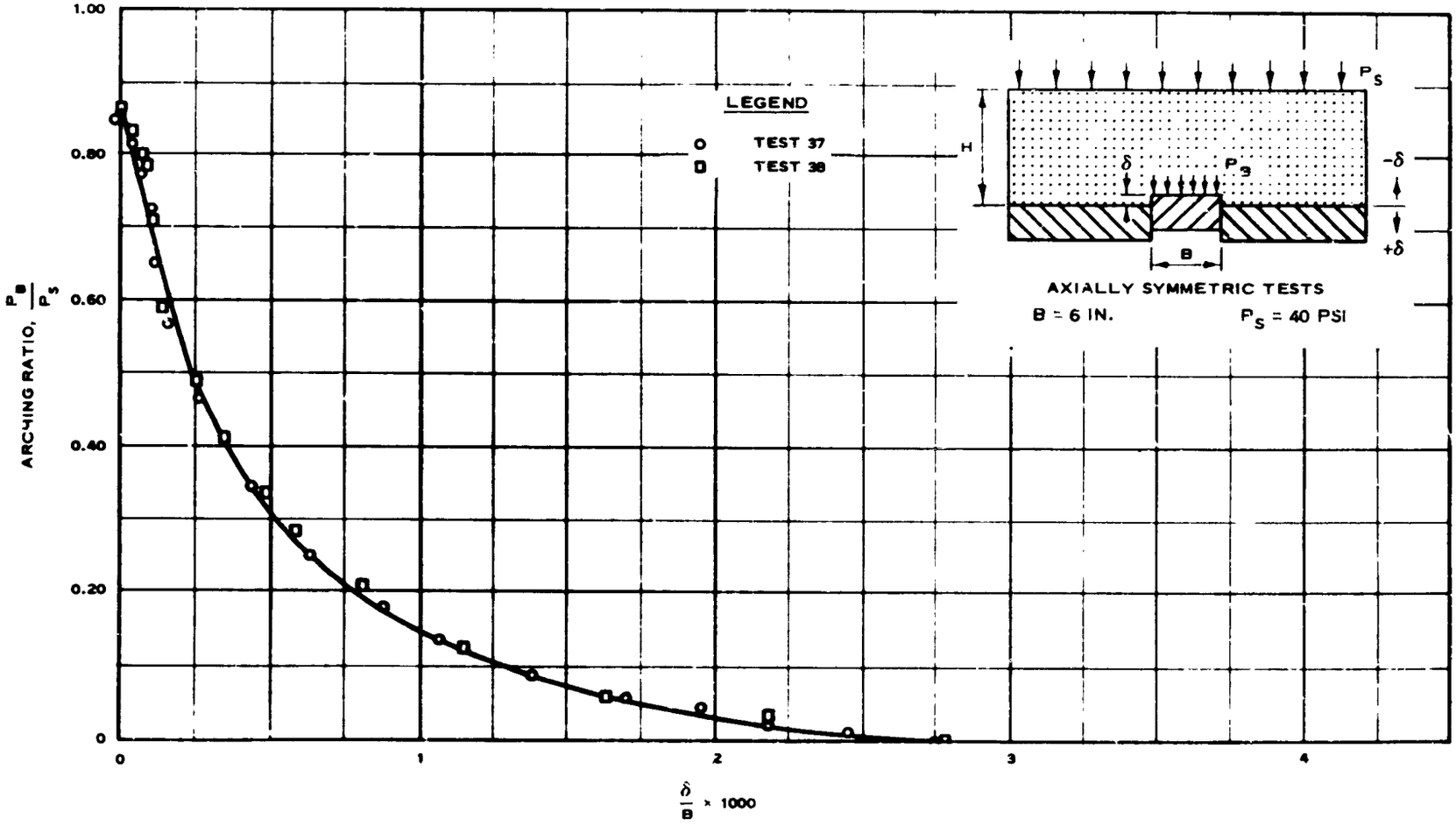

Fig. 4.13 Dimensionless plot of pressure vs. deflection for active arching tests with sand 2, H/B = 1 , P_s = 40 psi

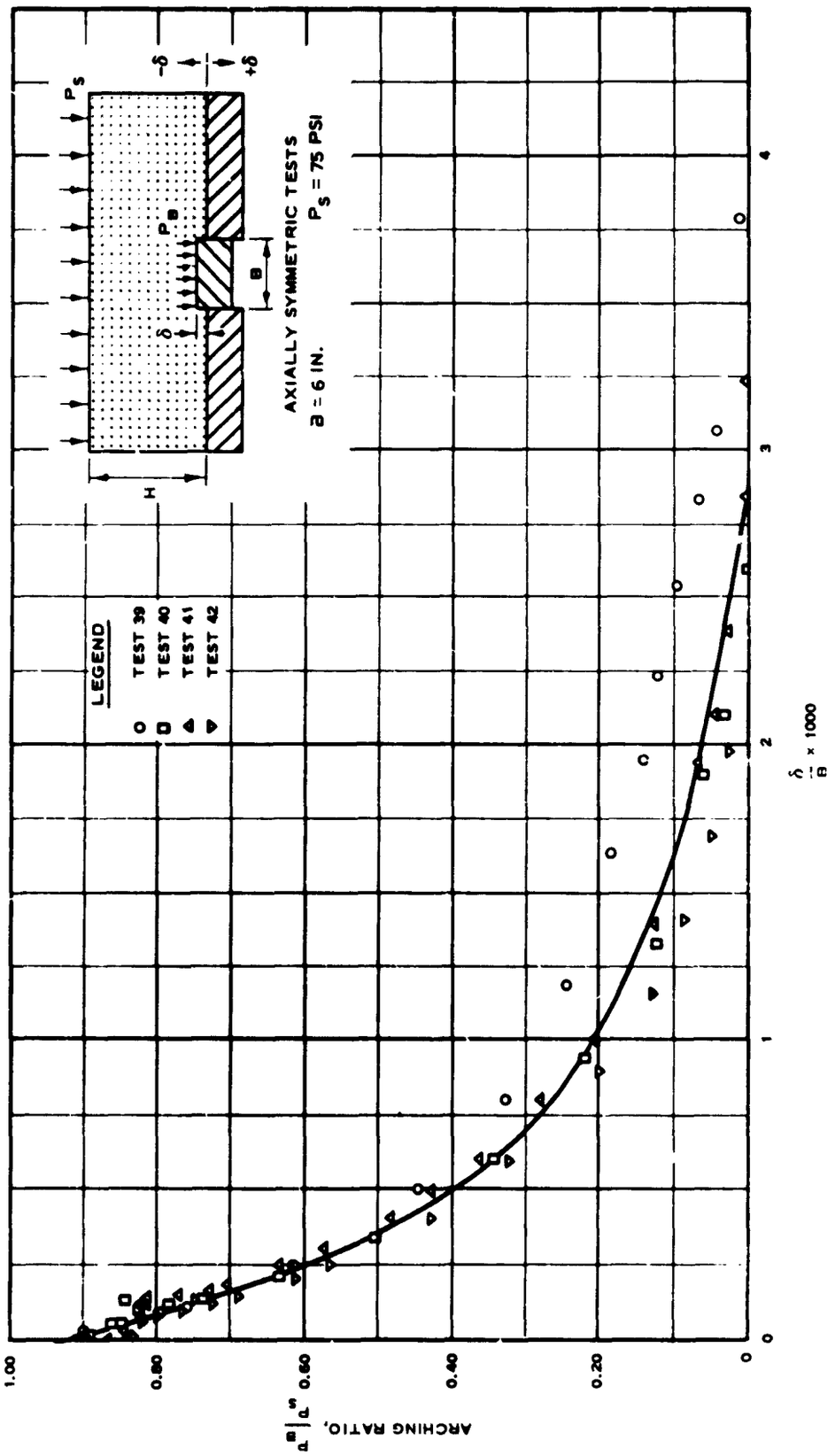

Fig. 4.14 Dimensionless plot of pressure vs. deflection for active arching tests

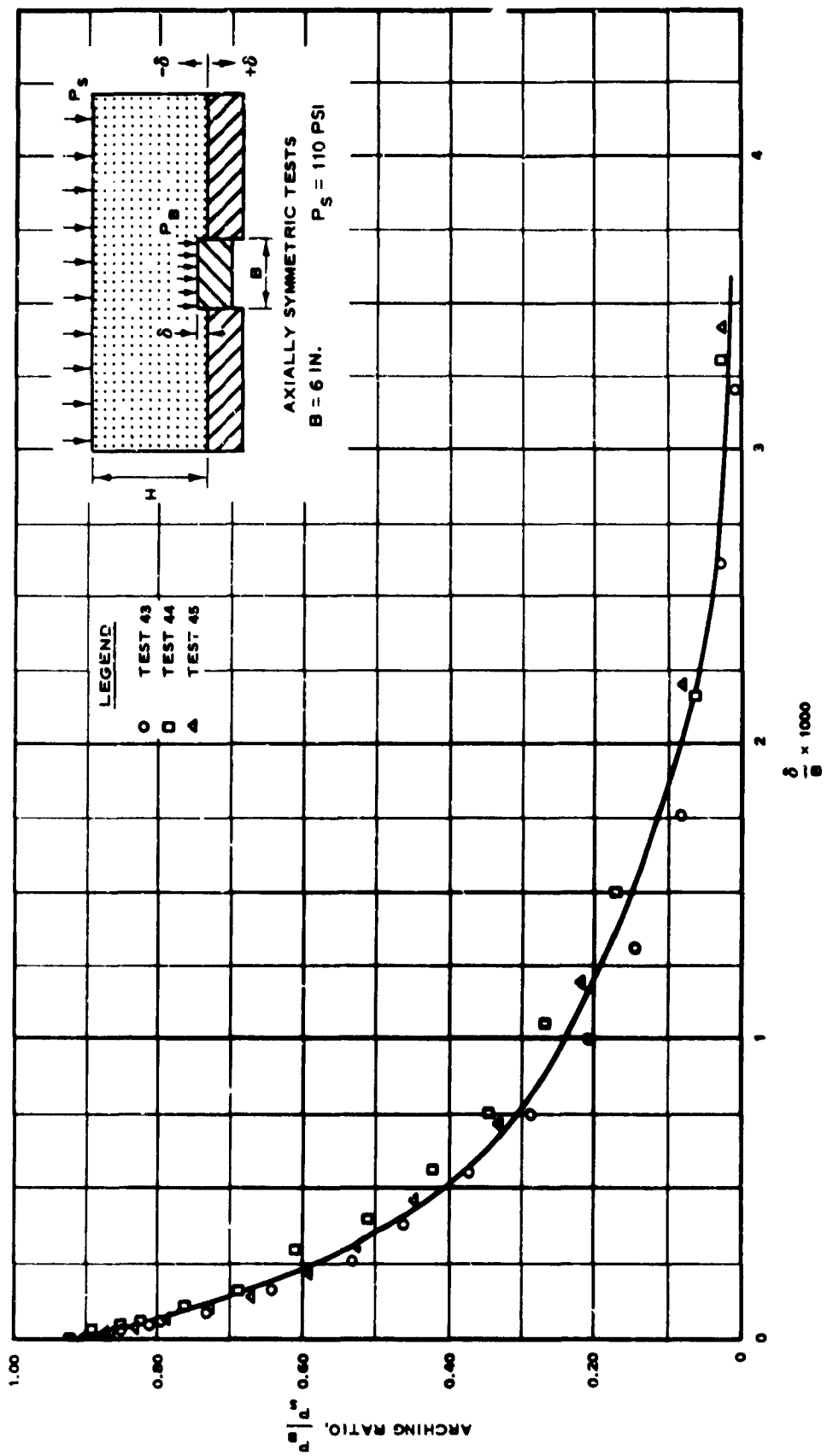

Fig. 4.15 Dimensionless plot of pressure vs. deflection for active arching tests with sand 2, H/B = 1 , P_s = 110 psi

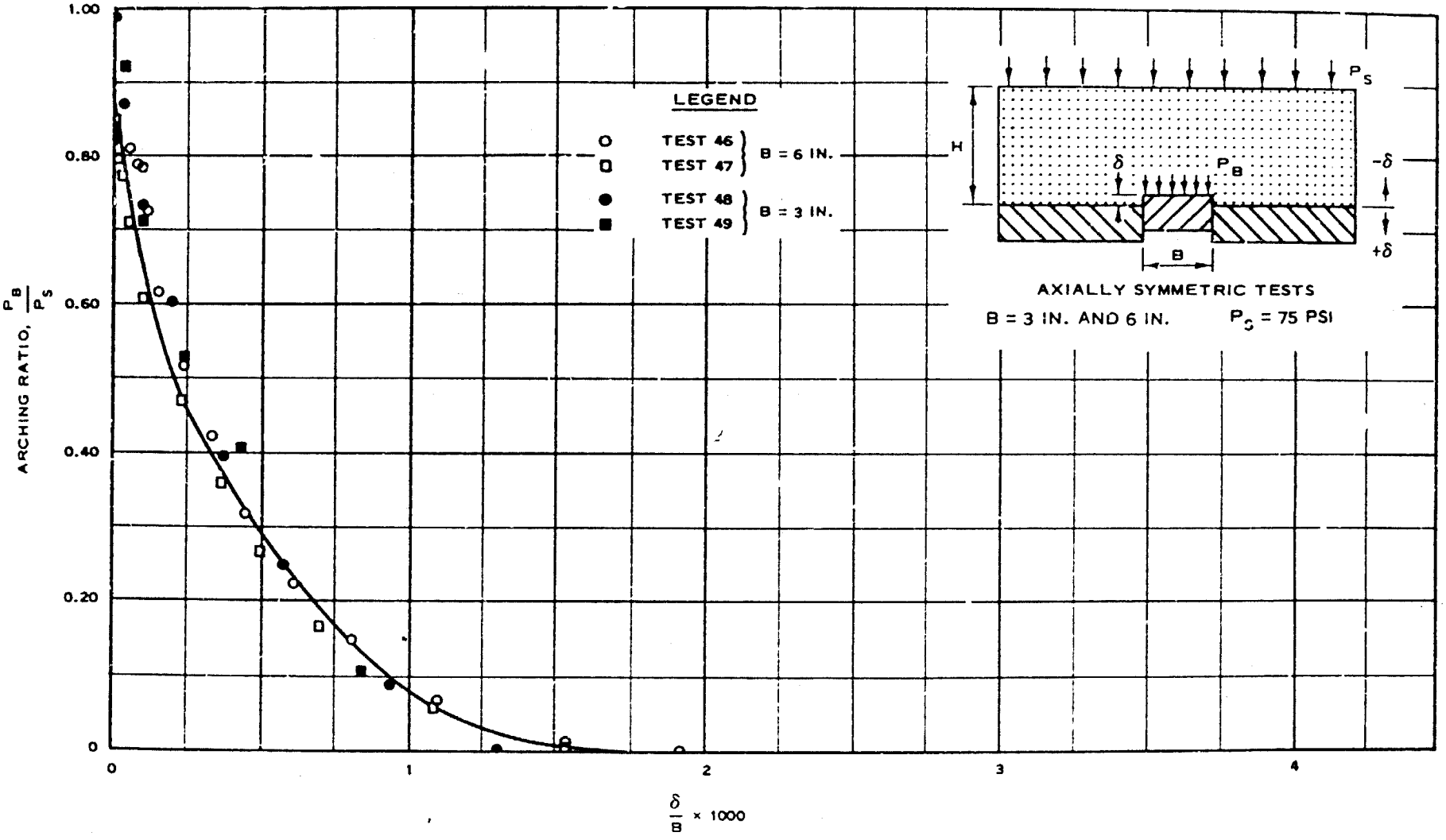

Fig. 4.16 Dimensionless plot of pressure [illegible] tests

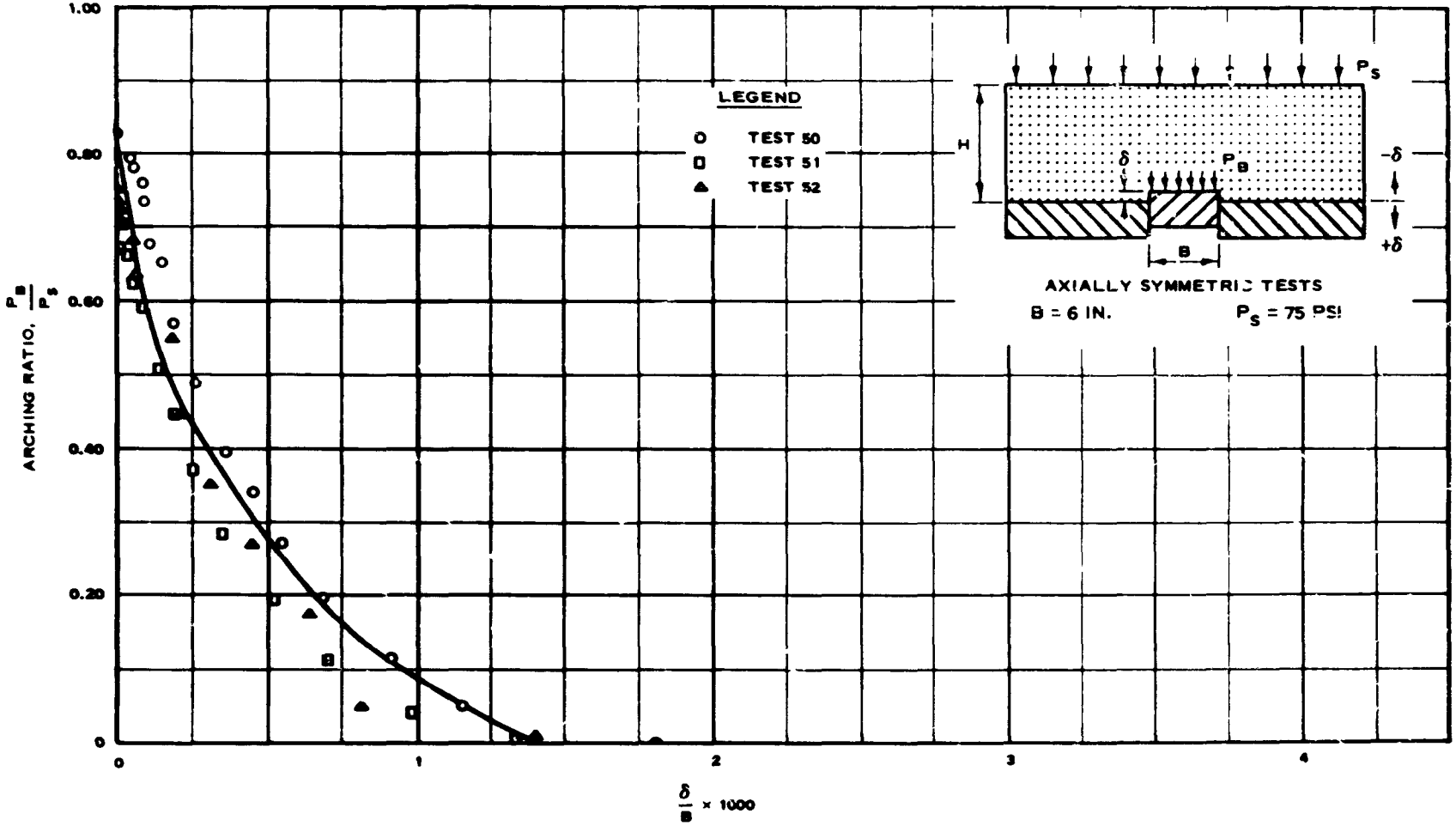

Fig. 4.17 Dimensionless plot of pressure vs. deflection for active arching tests with sand 2. H/B = 4 , P_s = 75 psi

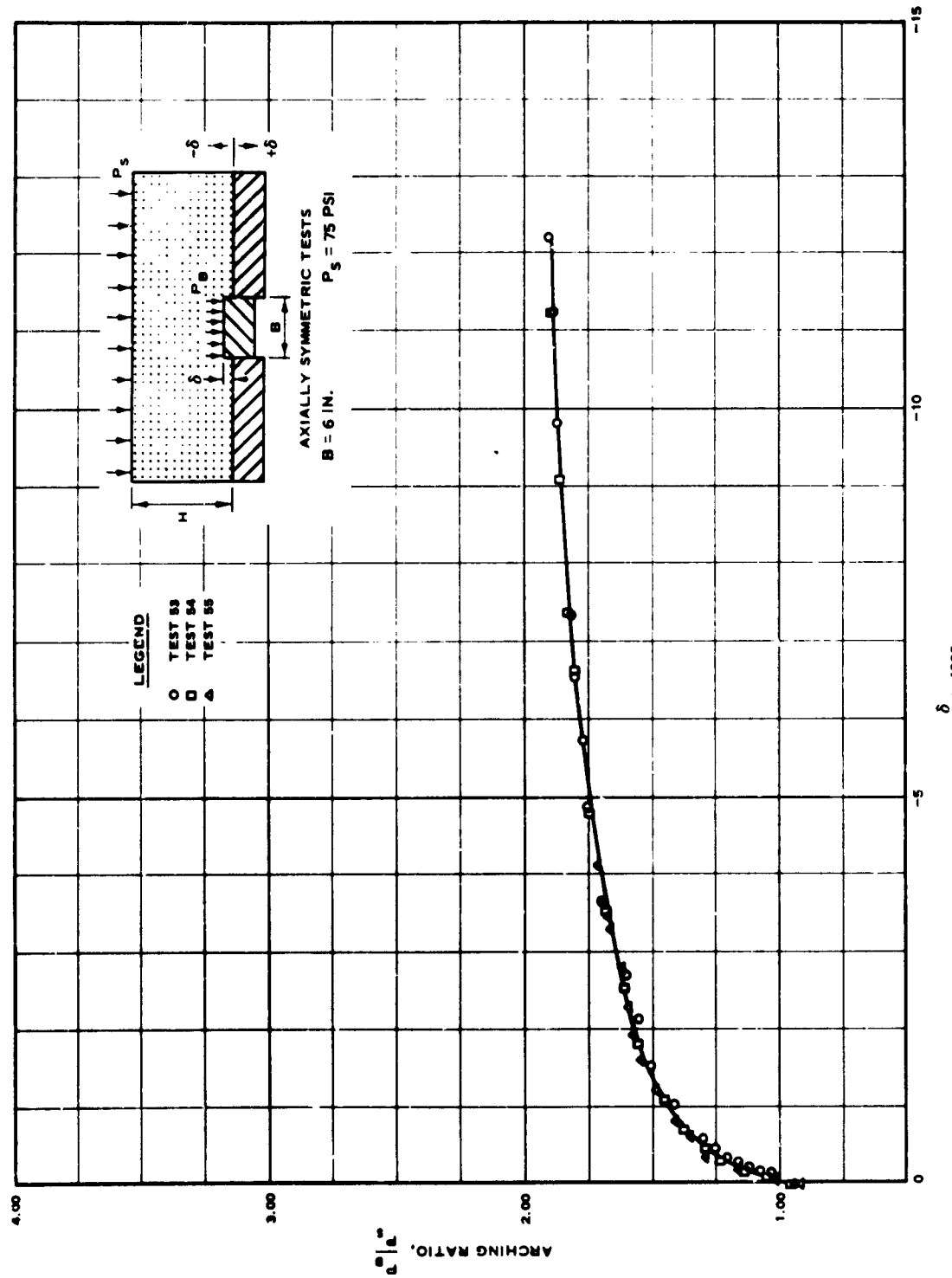

Fig. 4.18 Dimensionless plot of pressure vs. deflection for passive arching tests

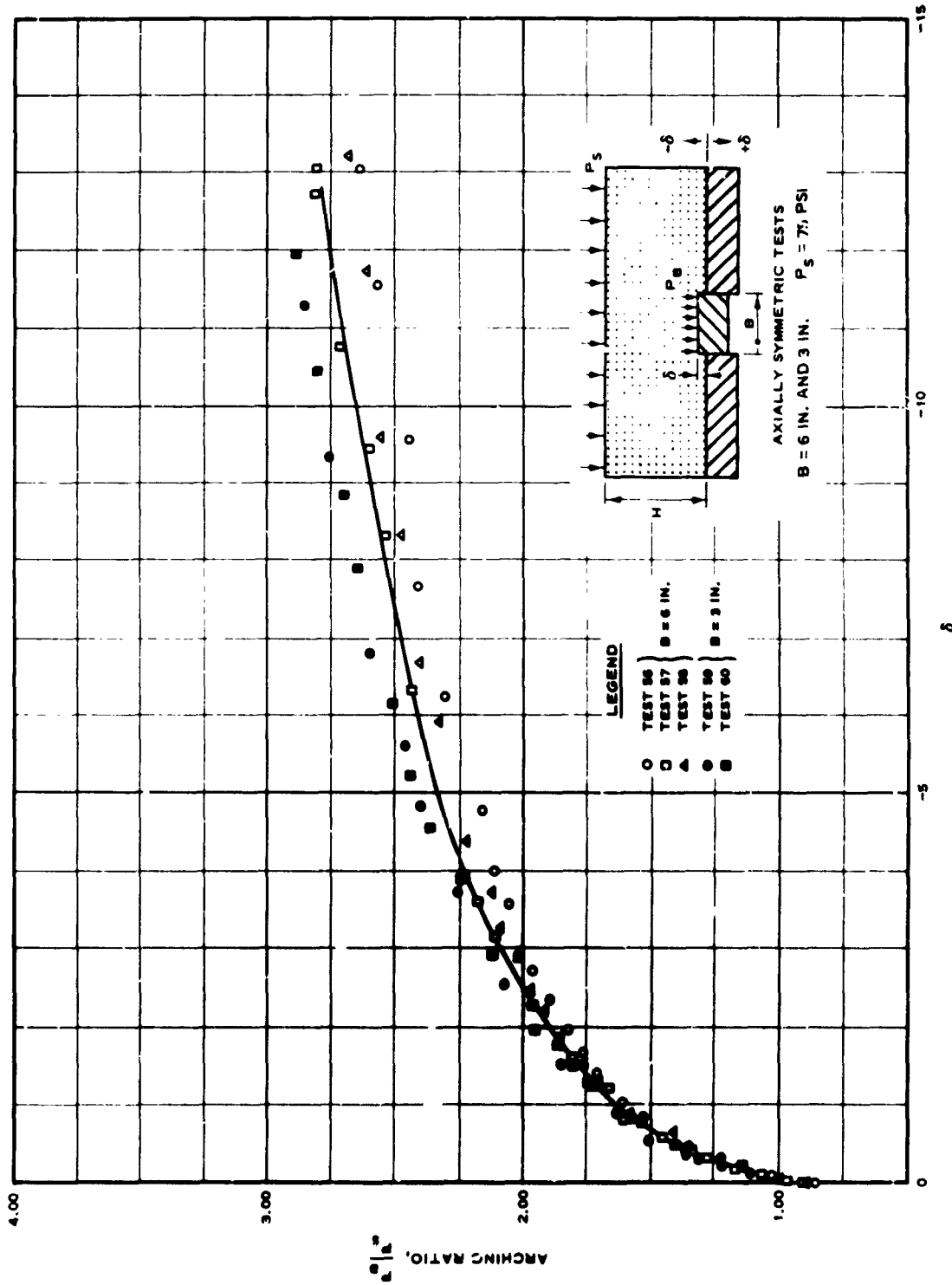

Fig. 4.19 Dimensionless plot of pressure vs. deflection for passive arching tests with sand 2, H/B = 2/3, P_s = 75 psi

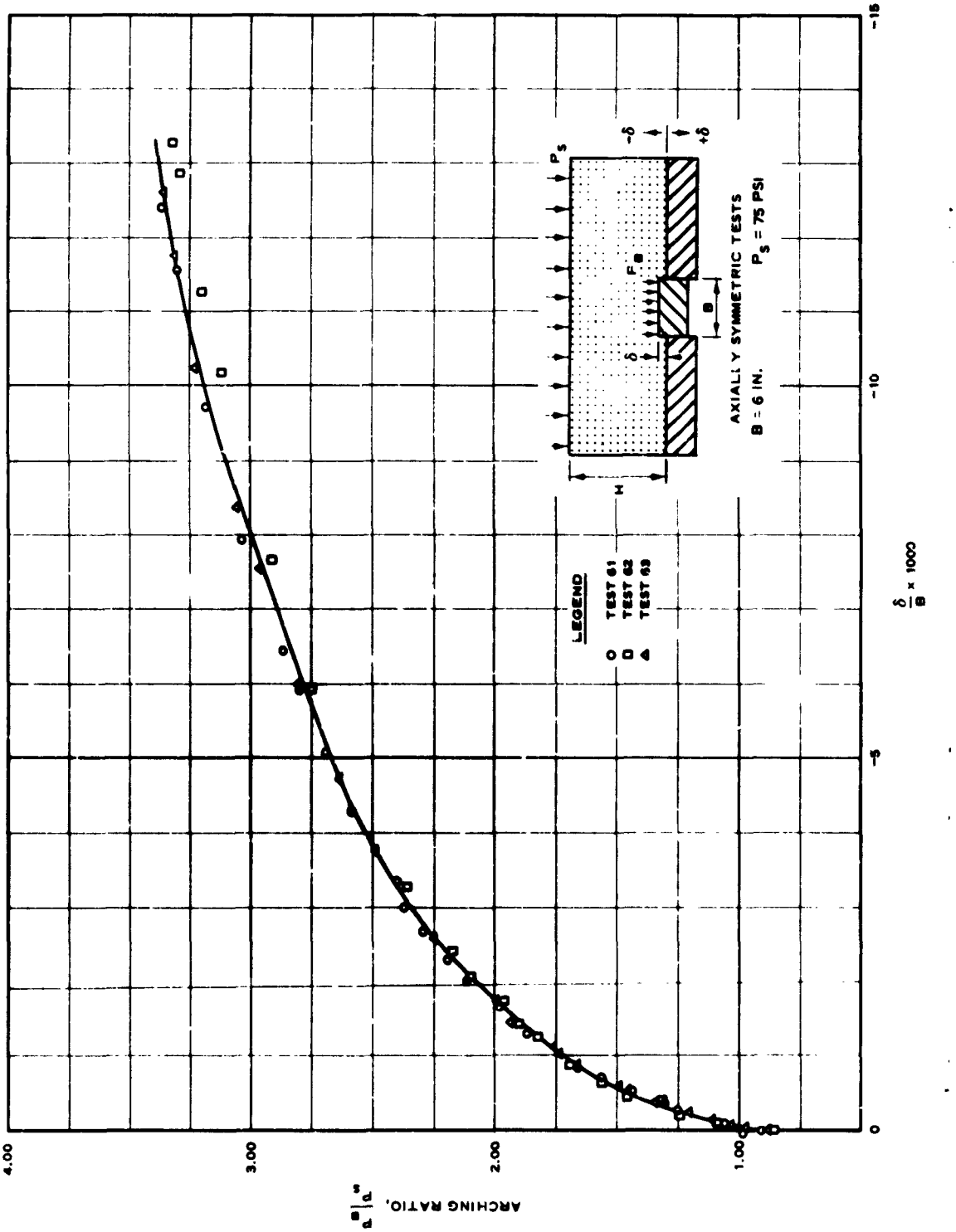
ARCHING RATIO, $\frac{P_s}{P}$
4.00
3.00
2.00
1.00
0
-5
-10
-15
$\frac{\delta}{B} \times 1000$
LEGEND
TEST 61
TEST 62
TEST 63
AXIALLY SYMMETRIC TESTS
B = 6 IN.
P_s = 75 PSI
P_s
F_B
B
H
δ
$-\delta$
$+\delta$

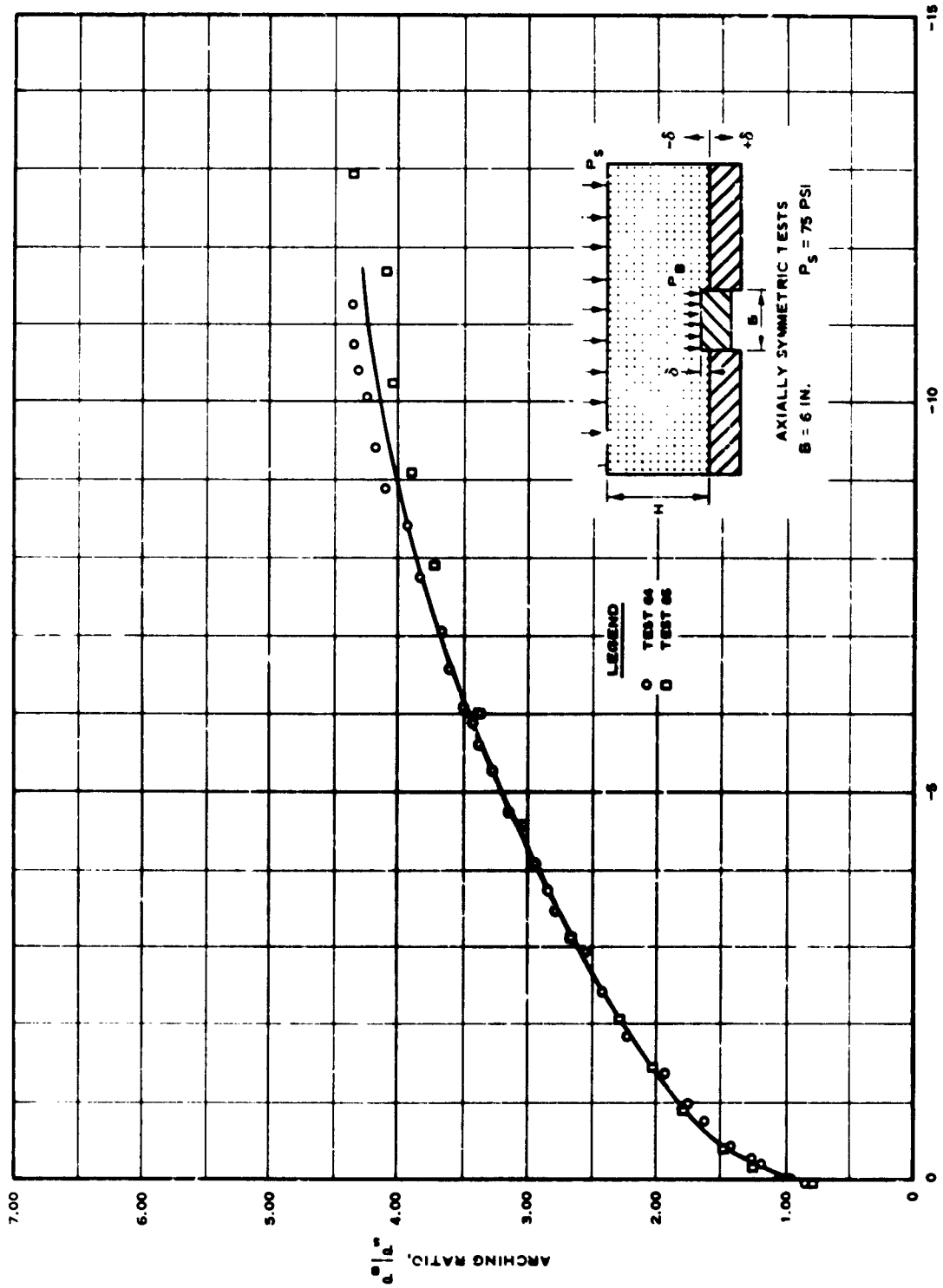

Fig. 4.21 Dimensionless plot of pressure vs. deflection for passive arching tests with sand 2, H/B = 1-1/3 , P_s = 75 psi

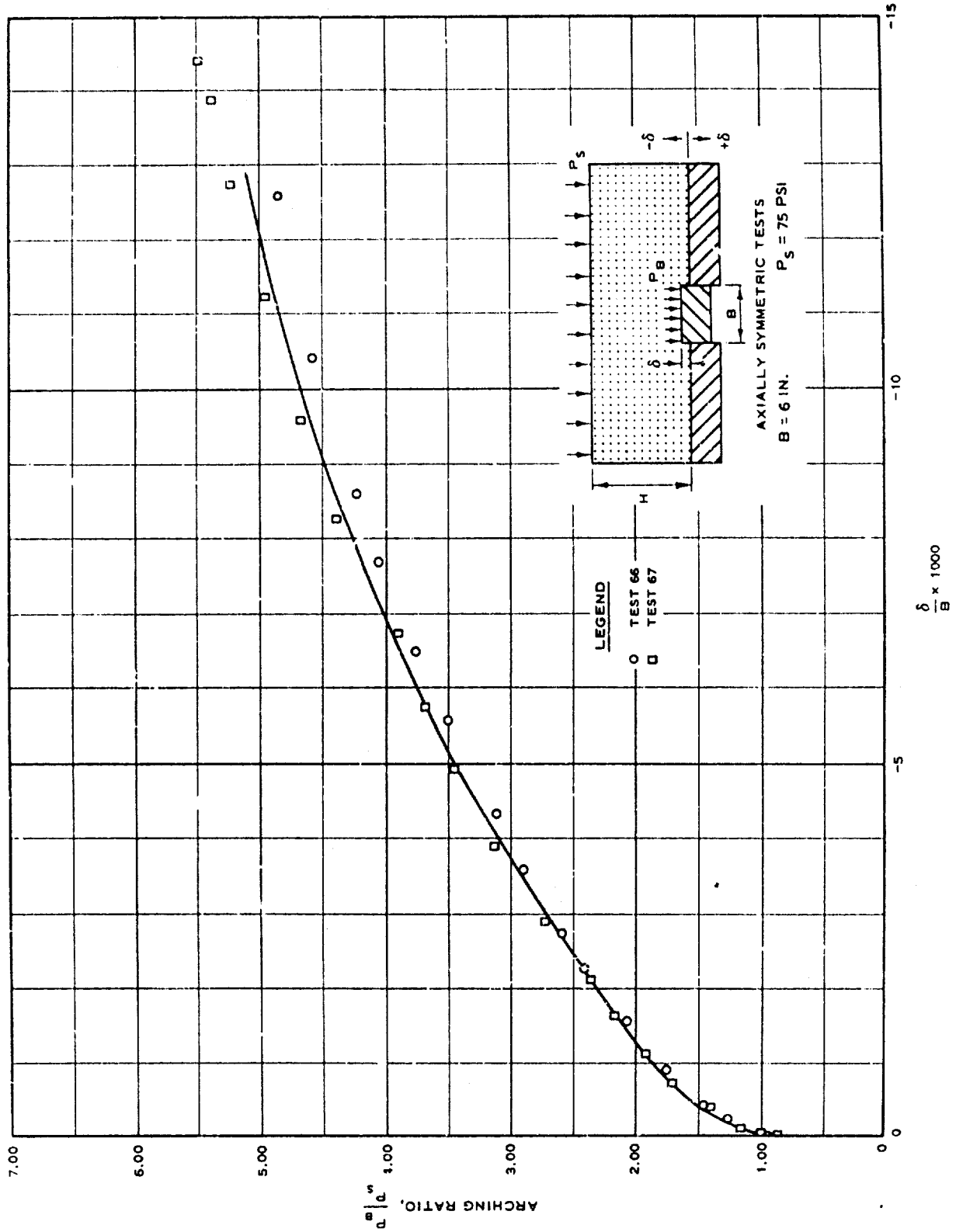
ARCHING RATIO, $\frac{p}{q_s}$
7.00
6.00
5.00
4.00
3.00
2.00
1.00
0
-5
-10
-15
$\frac{\delta}{B} \times 1000$
LEGEND
TEST 66
TEST 67
AXIALLY SYMMETRIC TESTS
P_s = 75 PSI
B = 6 IN.
P_s
P_B
B
H
$-\delta$
$+\delta$

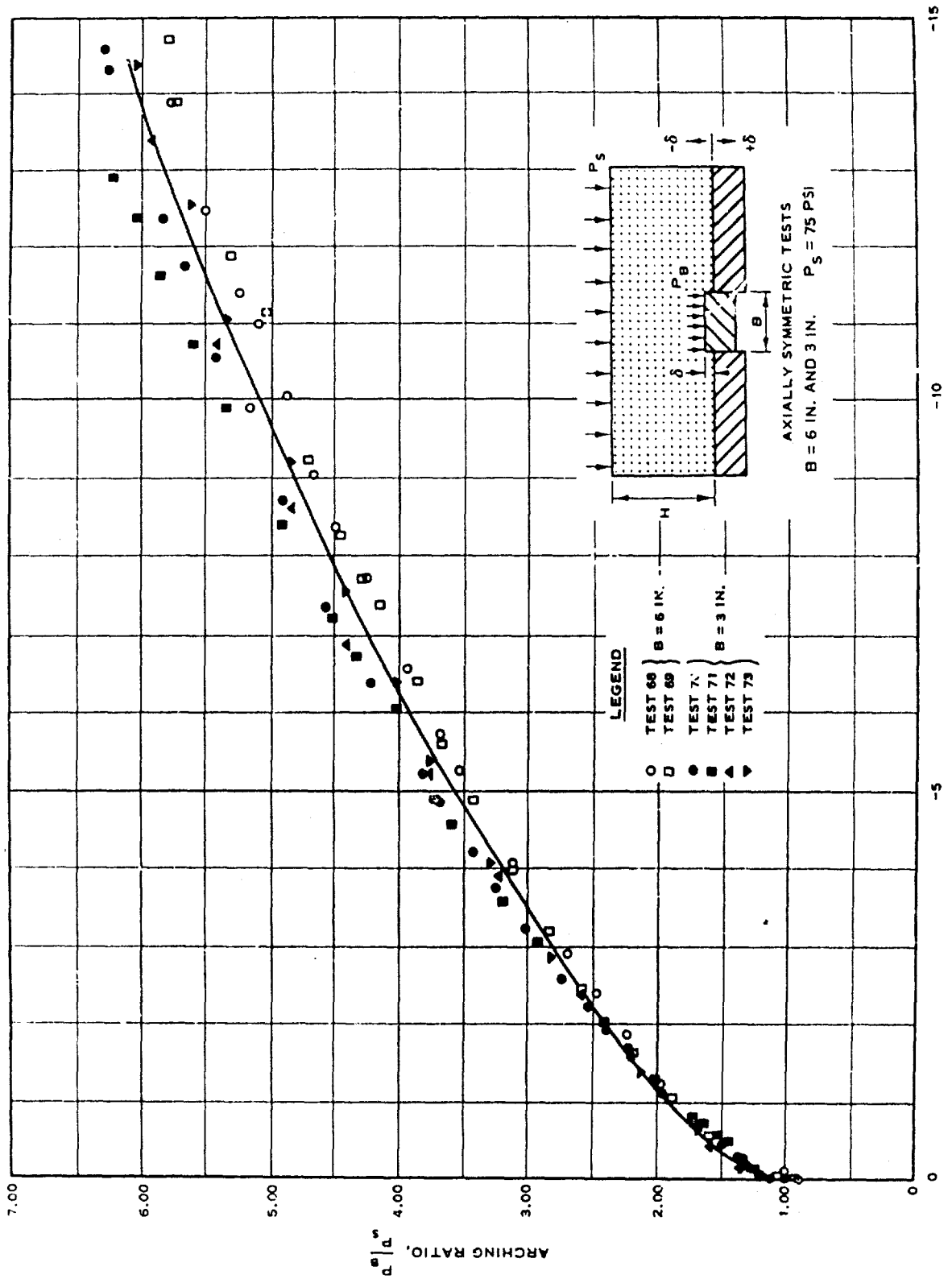

Fig. 4.23 Dimensionless plot of pressure vs. deflection for passive arching tests with sand 2, H/B = 2 , P_s = 75 psi

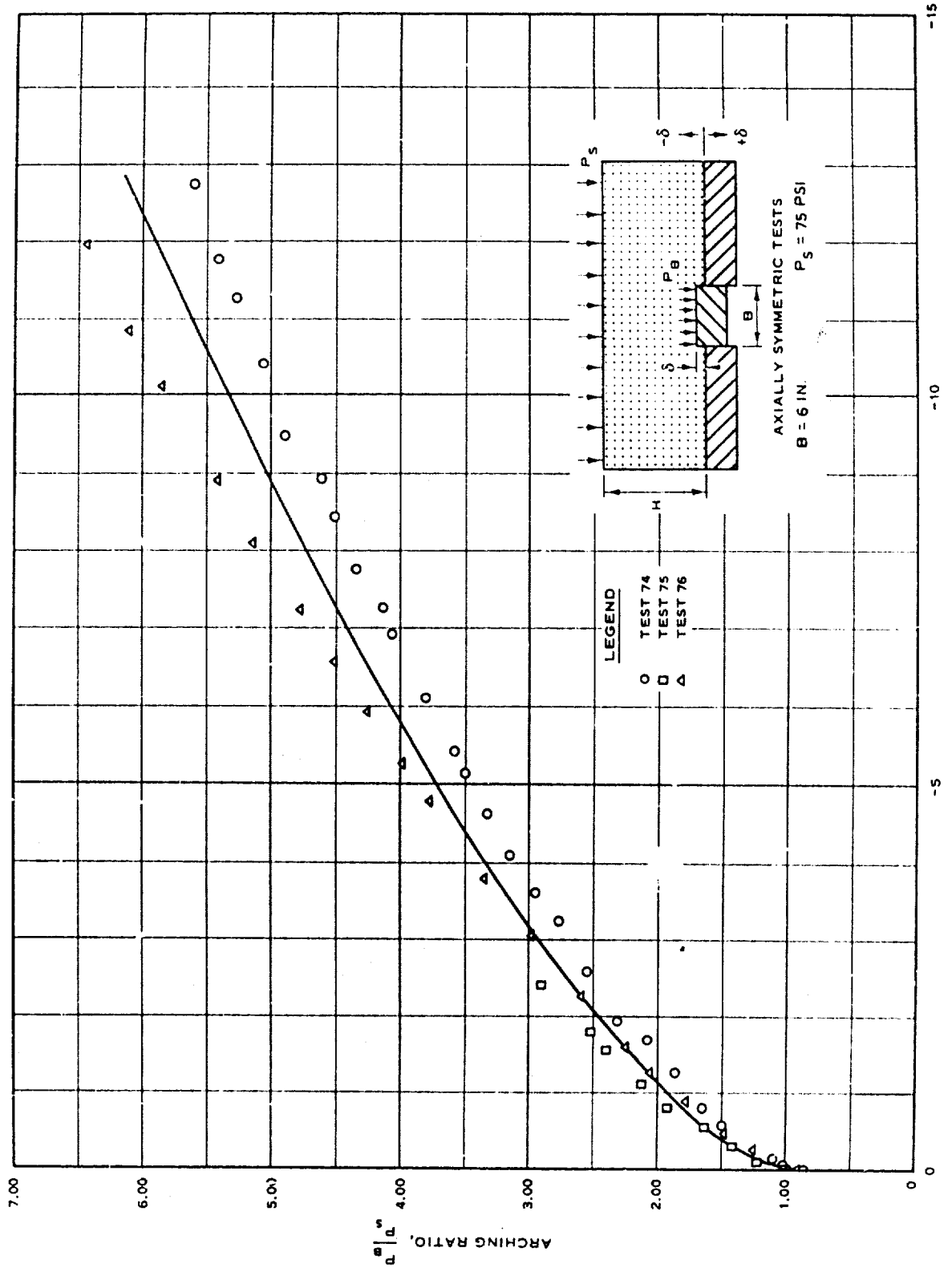

Fig. 4.21 Dimensionless plot of pressure ratio for rigid piston tests

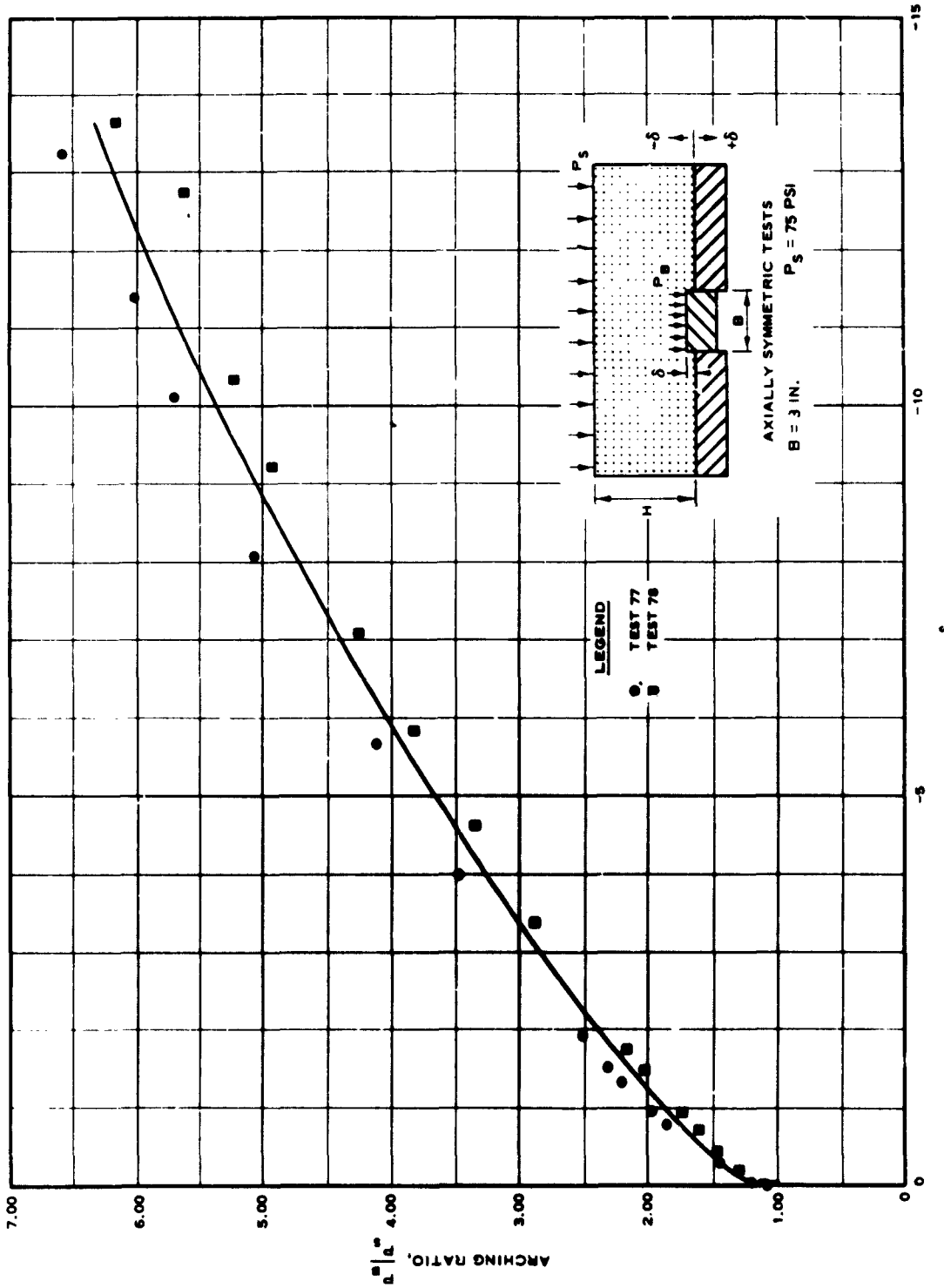

Fig. 4.25 Dimensionless plot of pressure vs. deflection for passive arching tests with sand 2, H/B = 2-2/3 , P_s = 75 psi

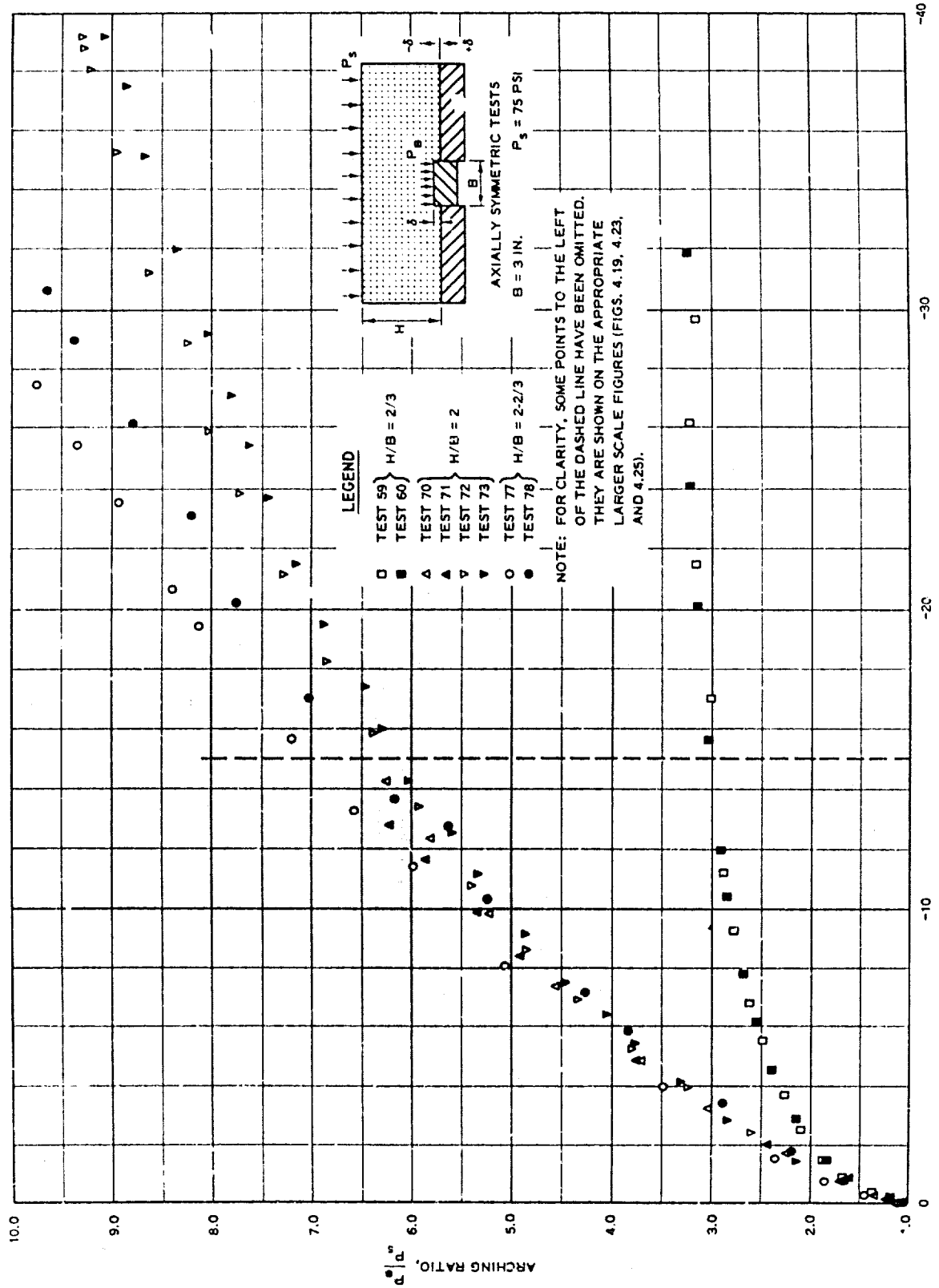

Fig. 4.26 Small-scale dimensionless plot of pressure vs. deflection for passive arching tests

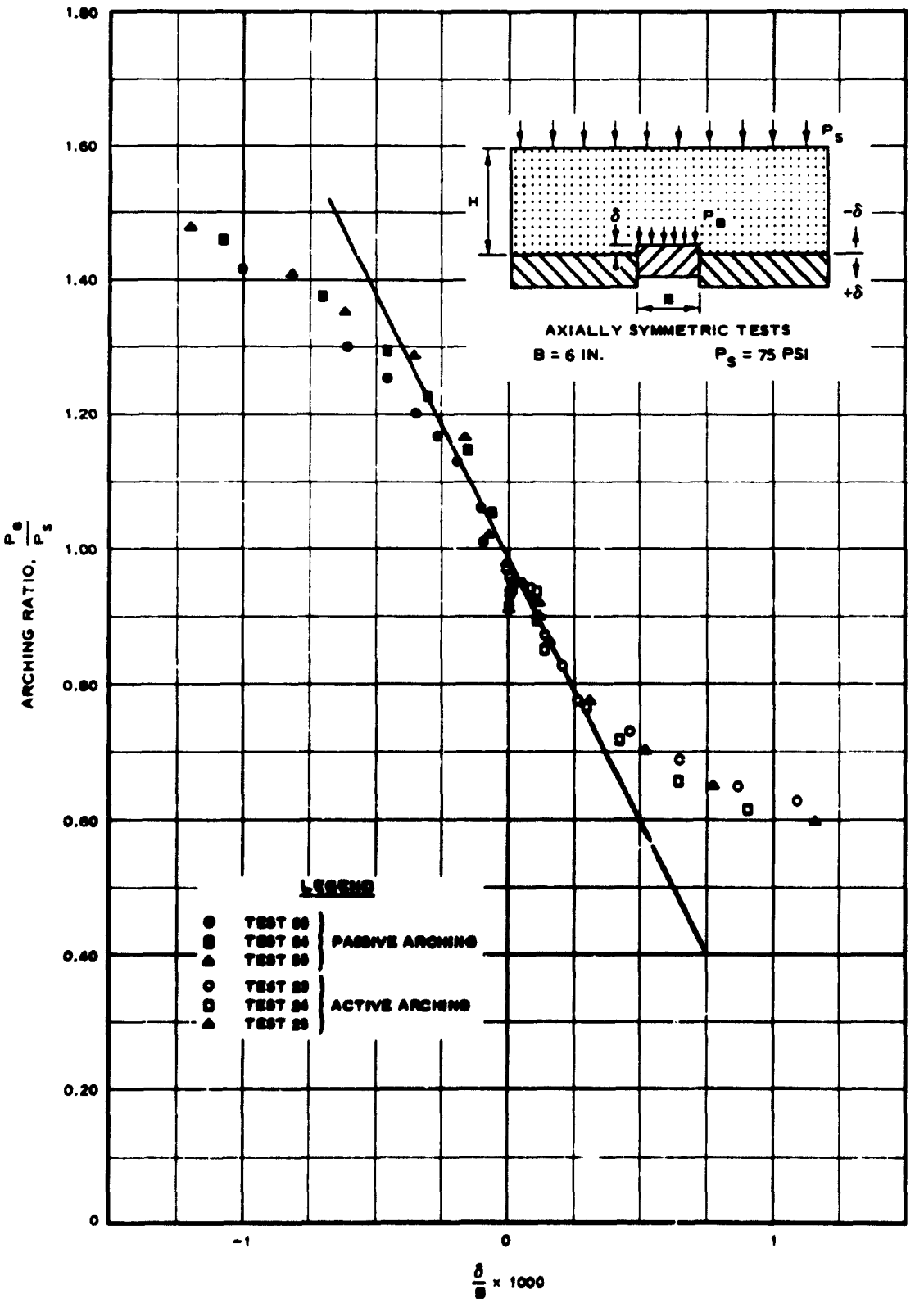

Fig. 4.27 Dimensionless plot of initial portions of pressure vs. deflection data for active and passive arching tests with sand 2, H/B = 1/3

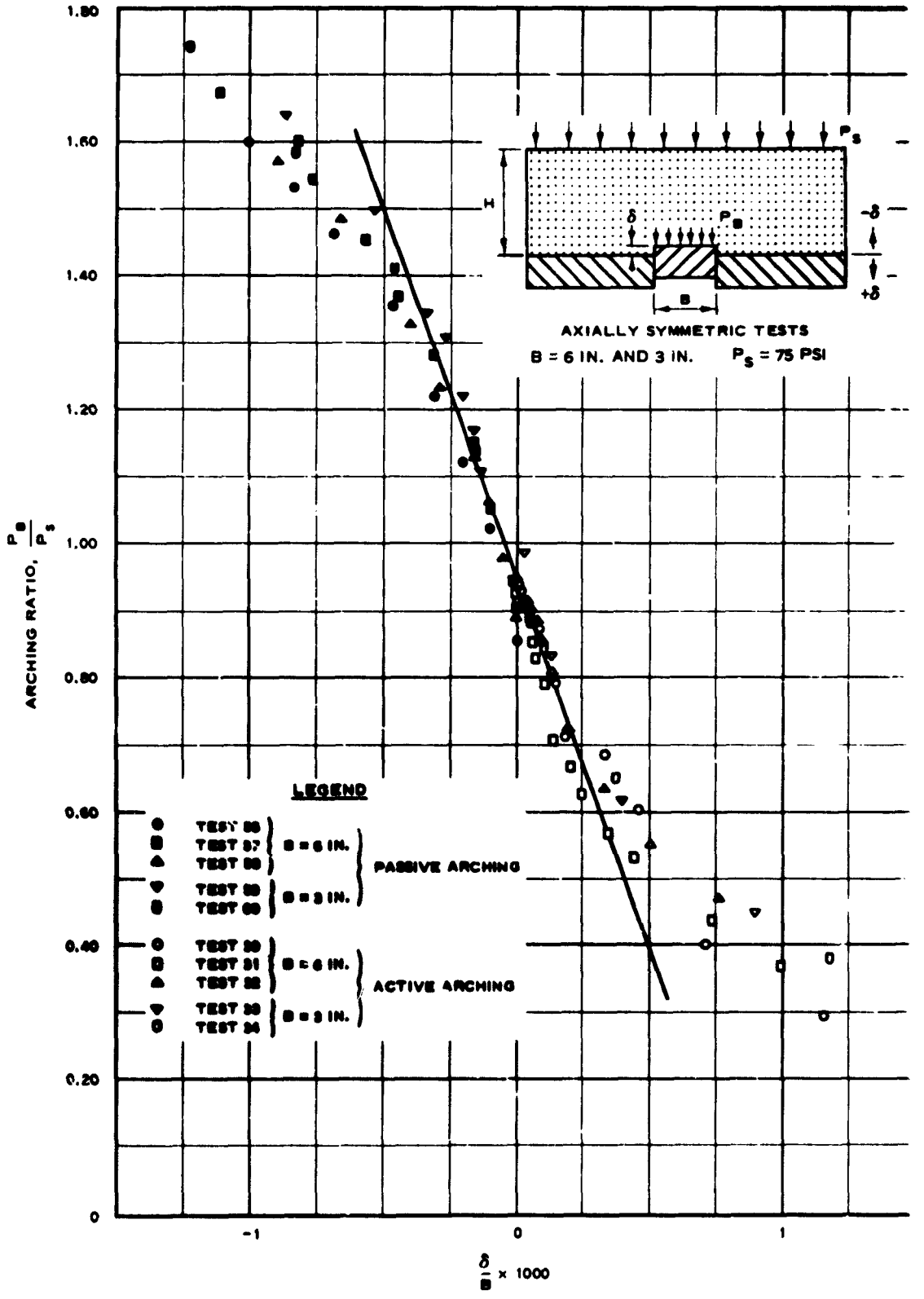

Fig. 4.28 Dimensionless plot of initial portions of pressure vs. deflecti data for active and passive arching tests with sand 2, H/B = 2/3

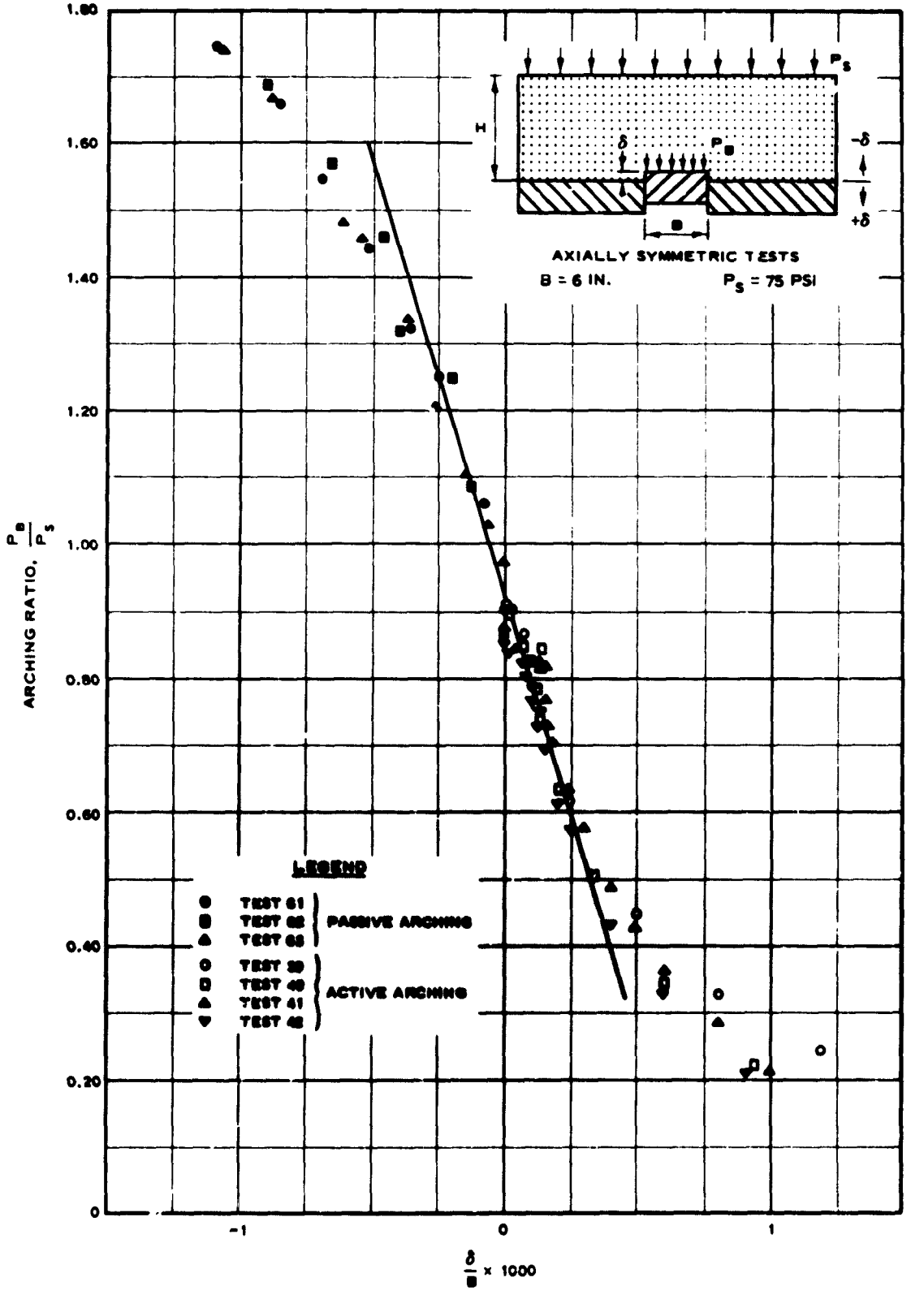

Fig. 4.29 Dimensionless plot of initial portions of pressure vs. deflection data for active and passive arching tests with sand 2, H/B = 1

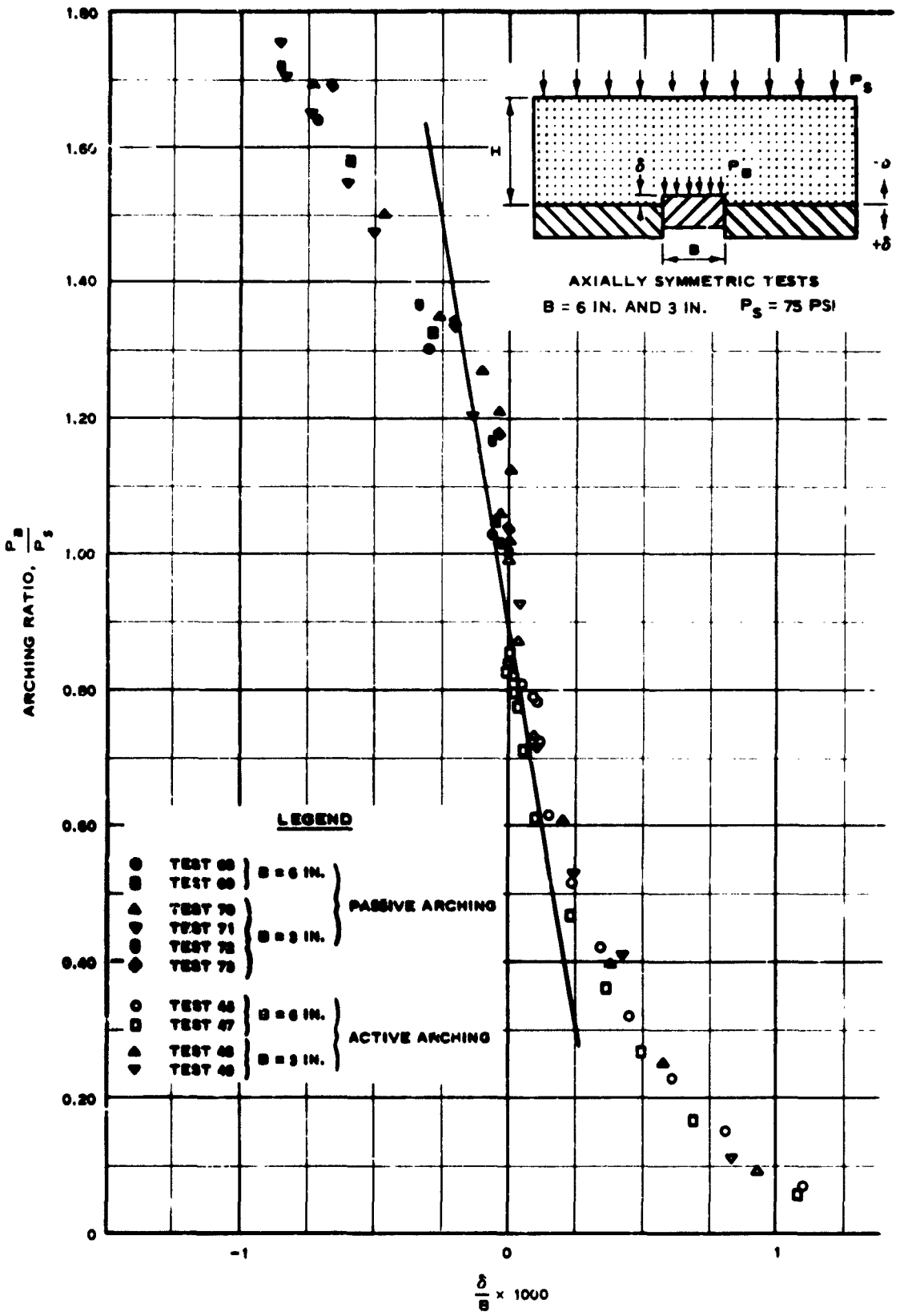

Fig. 4.30 Dimensionless plot of initial portions of pressure vs. deflec data for active and passive arching tests with sand 2, H/B = 2

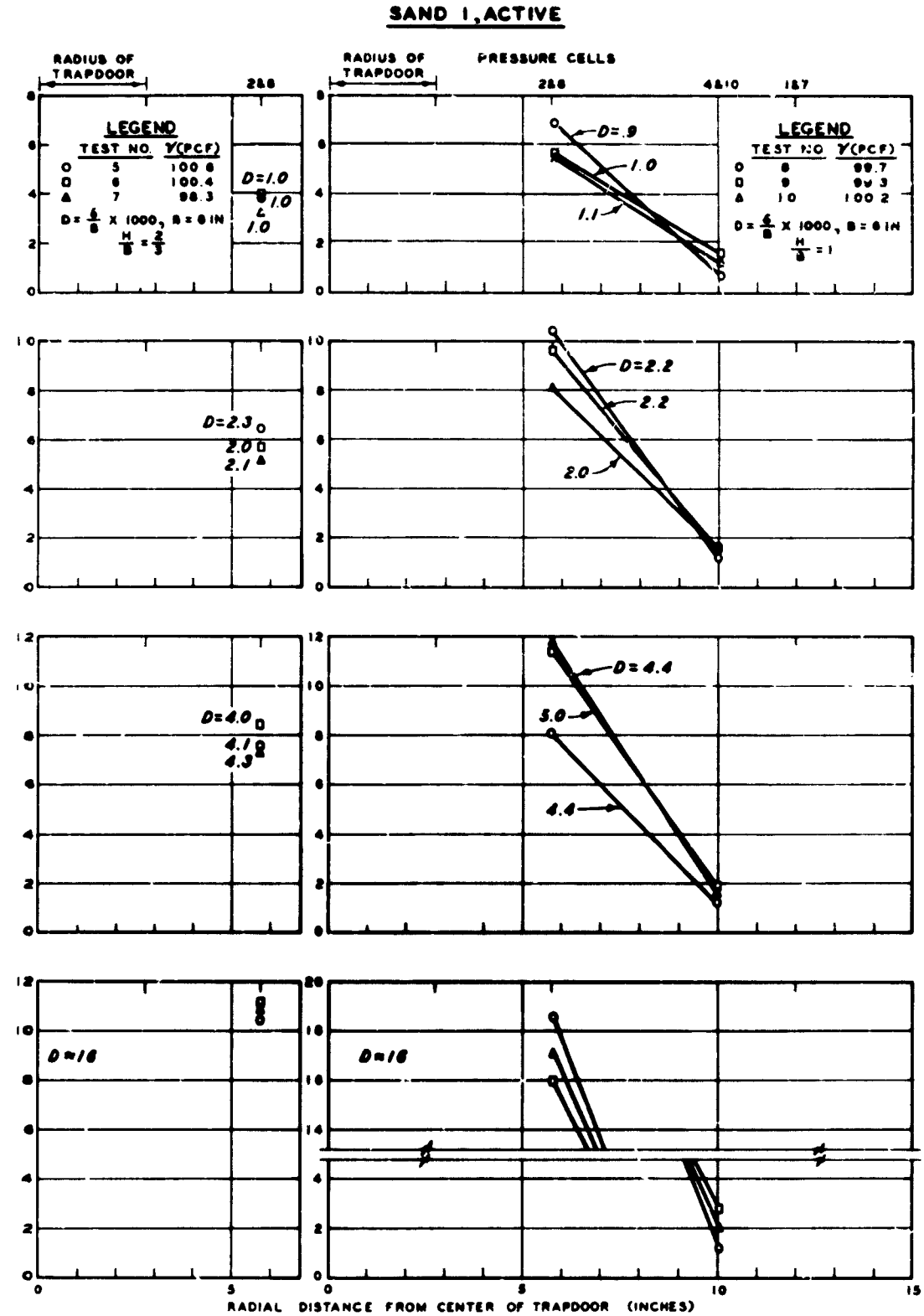

Fig. 4.31 Change in vertical stress due to active arching vs. radial distance from center of trapdoor; sand 1; H/B = 2/3 , 1 ; P_s = 75 psi

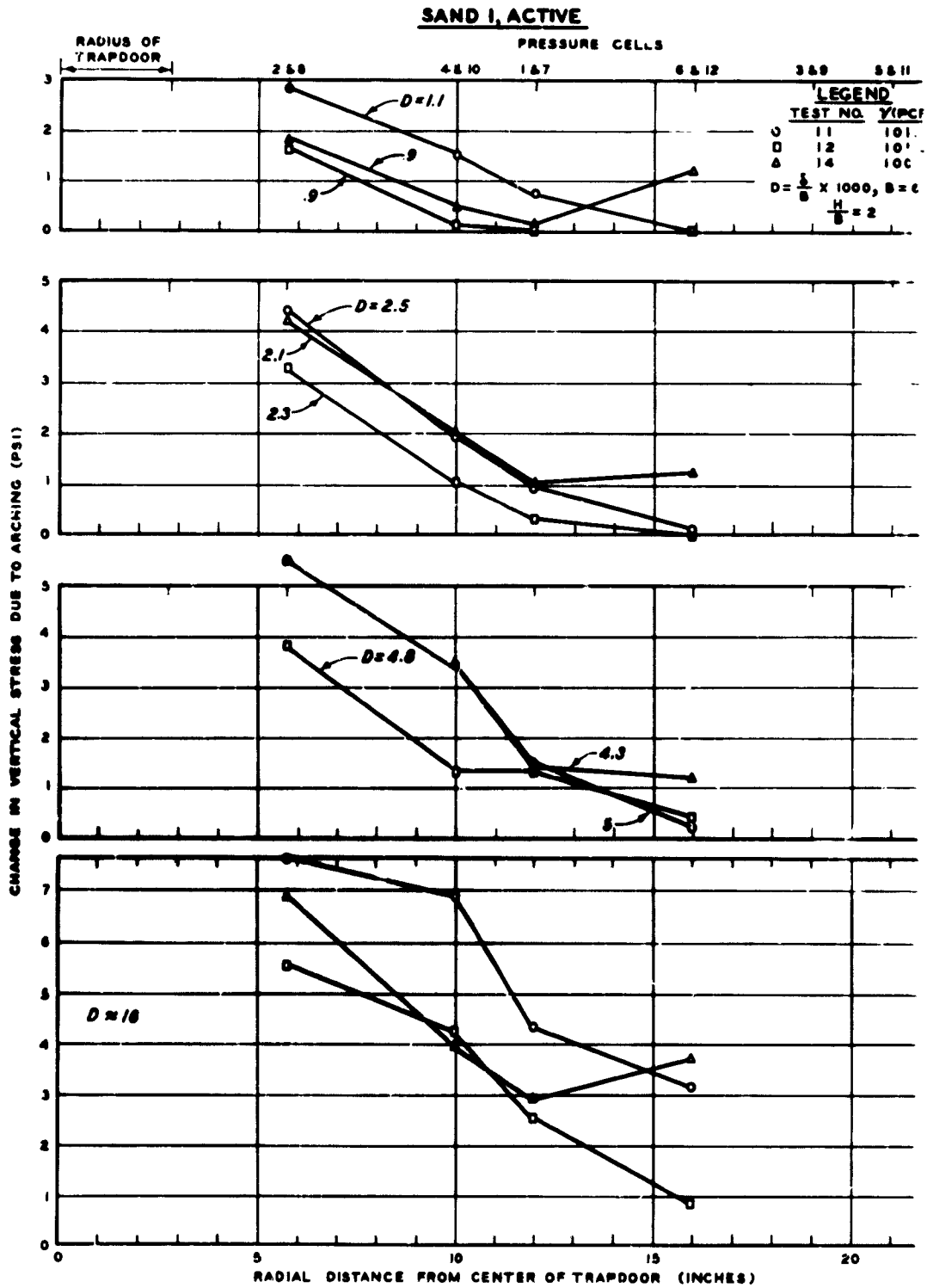

Fig. 4.32 Change in vertical stress due to active arching vs. radi distance from center of trapdoor; sand 1; H/B = 2 ; P_s = 75 psi

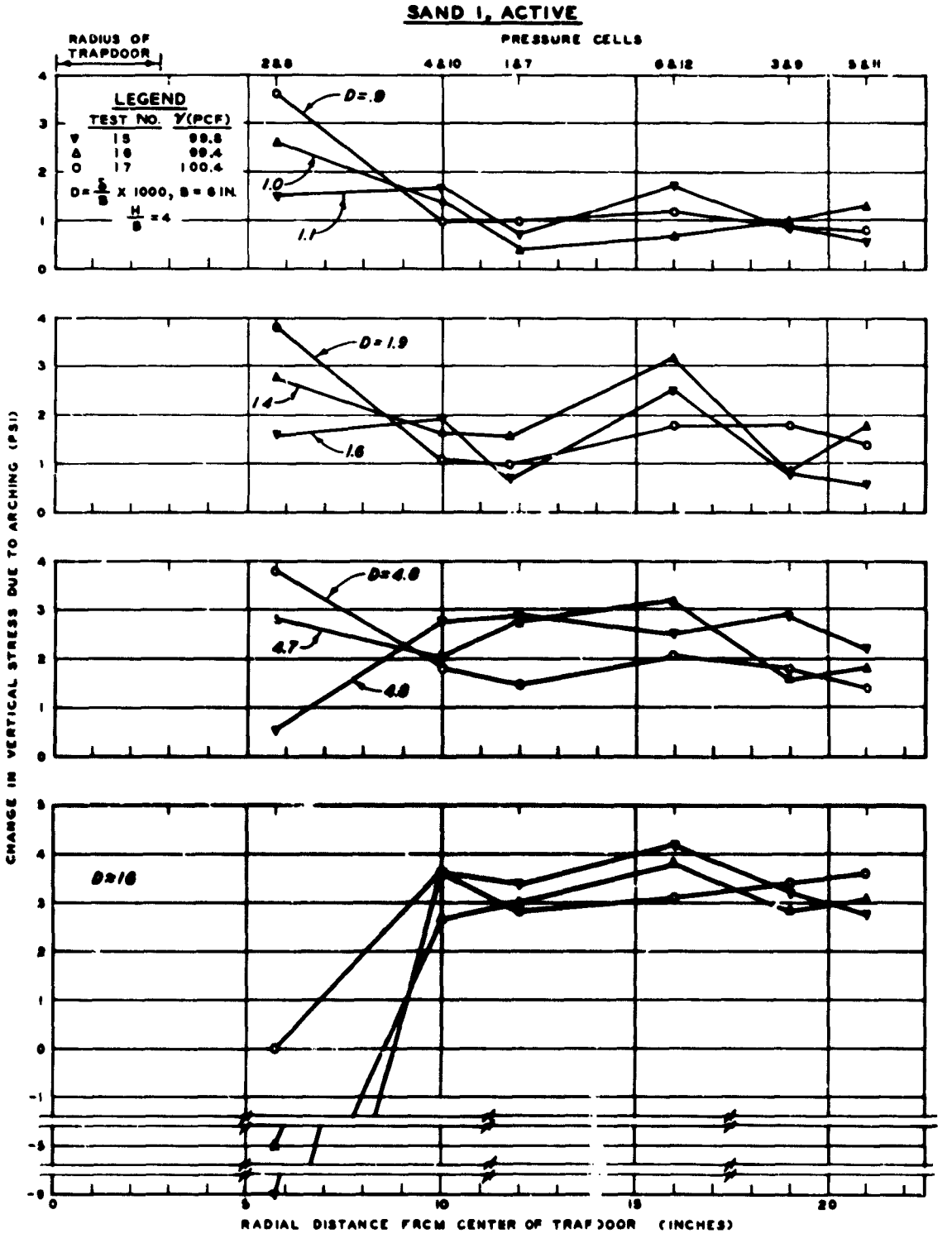

Fig. 4.33 Change in vertical stress due to active arching vs. radial distance from center of trapdoor; sand 1; H/B = 4 ; P_s = 75 psi

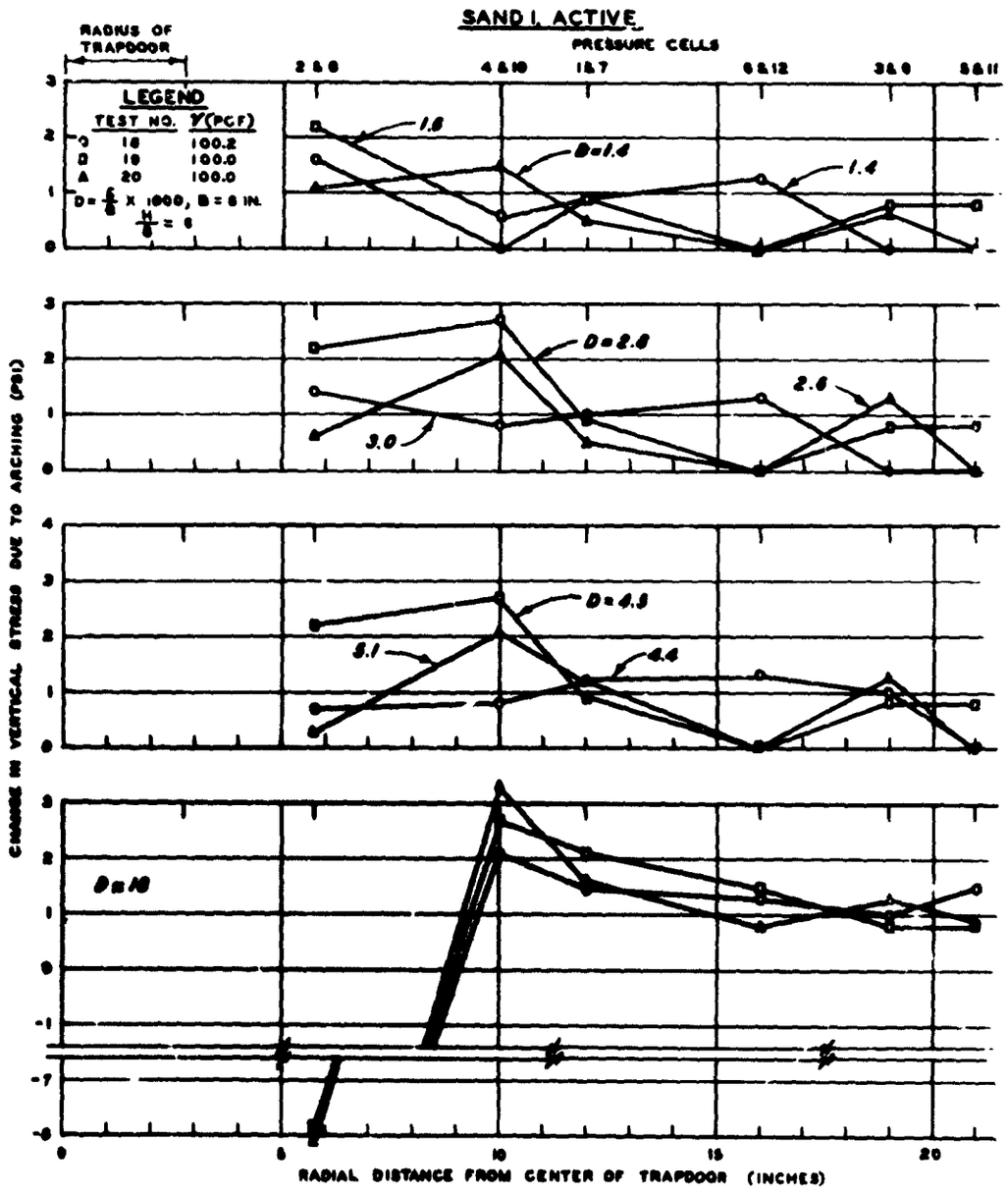

Fig. 4.34 Change in vertical stress due to active arching vs. radi distance from center of trapdoor; sand 1; H/B = 6 ; P_s = 75 psi

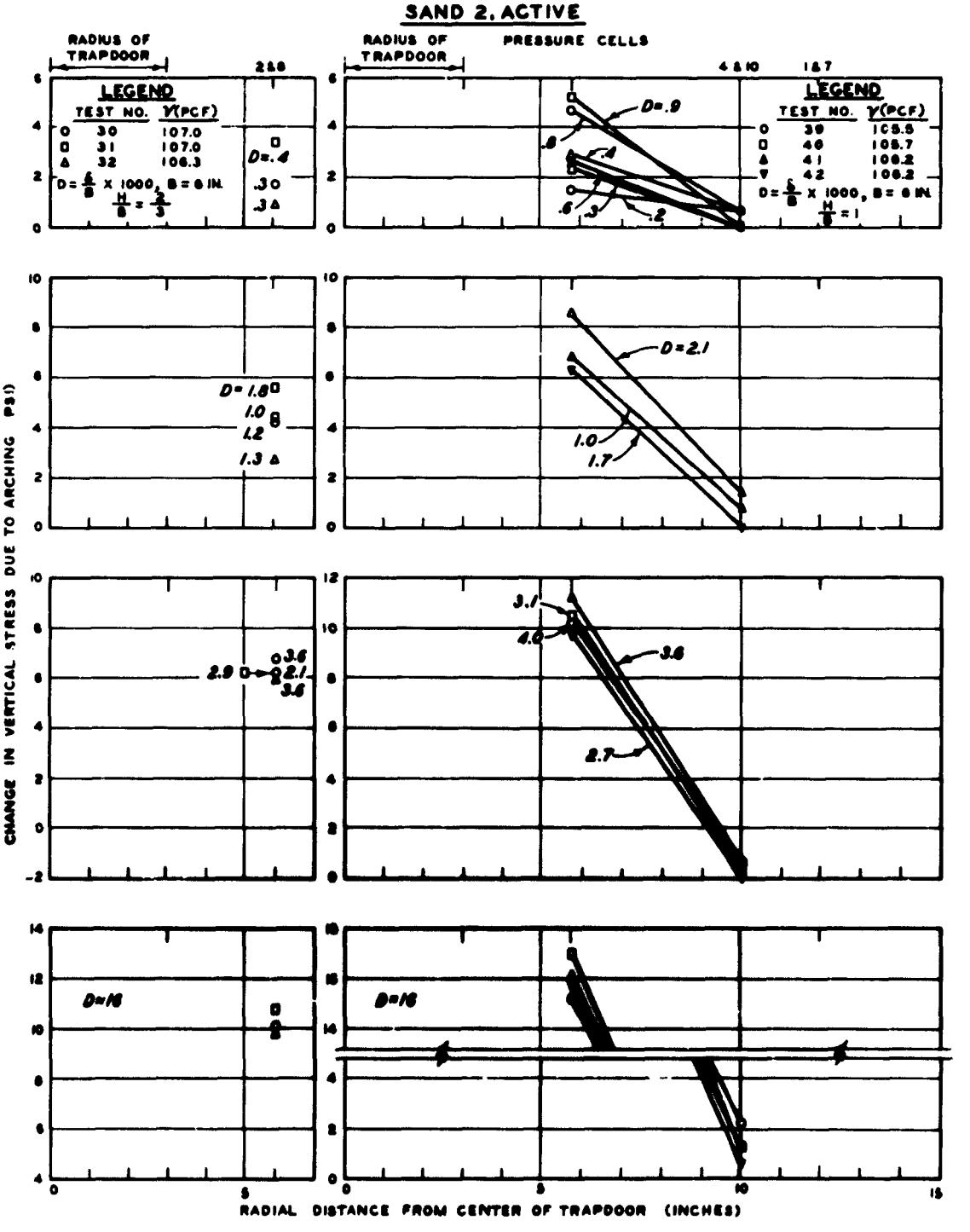

Fig. 4.35 Change in vertical stress due to active arching vs. radial distance from center of trapdoor; sand 2; H/B = 2/3 , 1 ; P_s = 75 psi

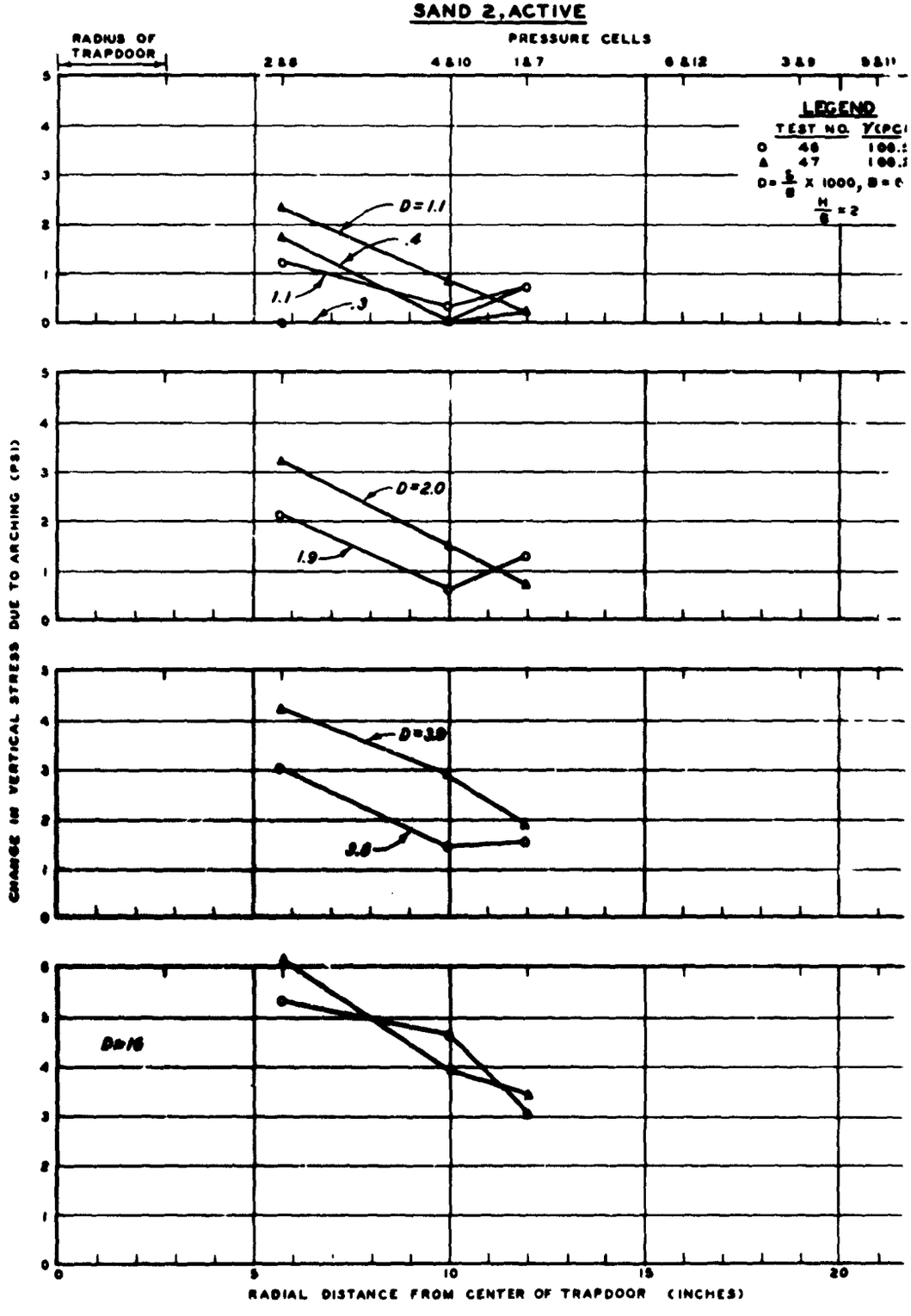

Fig. 4.36 Change in vertical stress due to active arching vs. radia distance from center of trapdoor; sand 2; H/B = 2 ; P_s = 75 psi

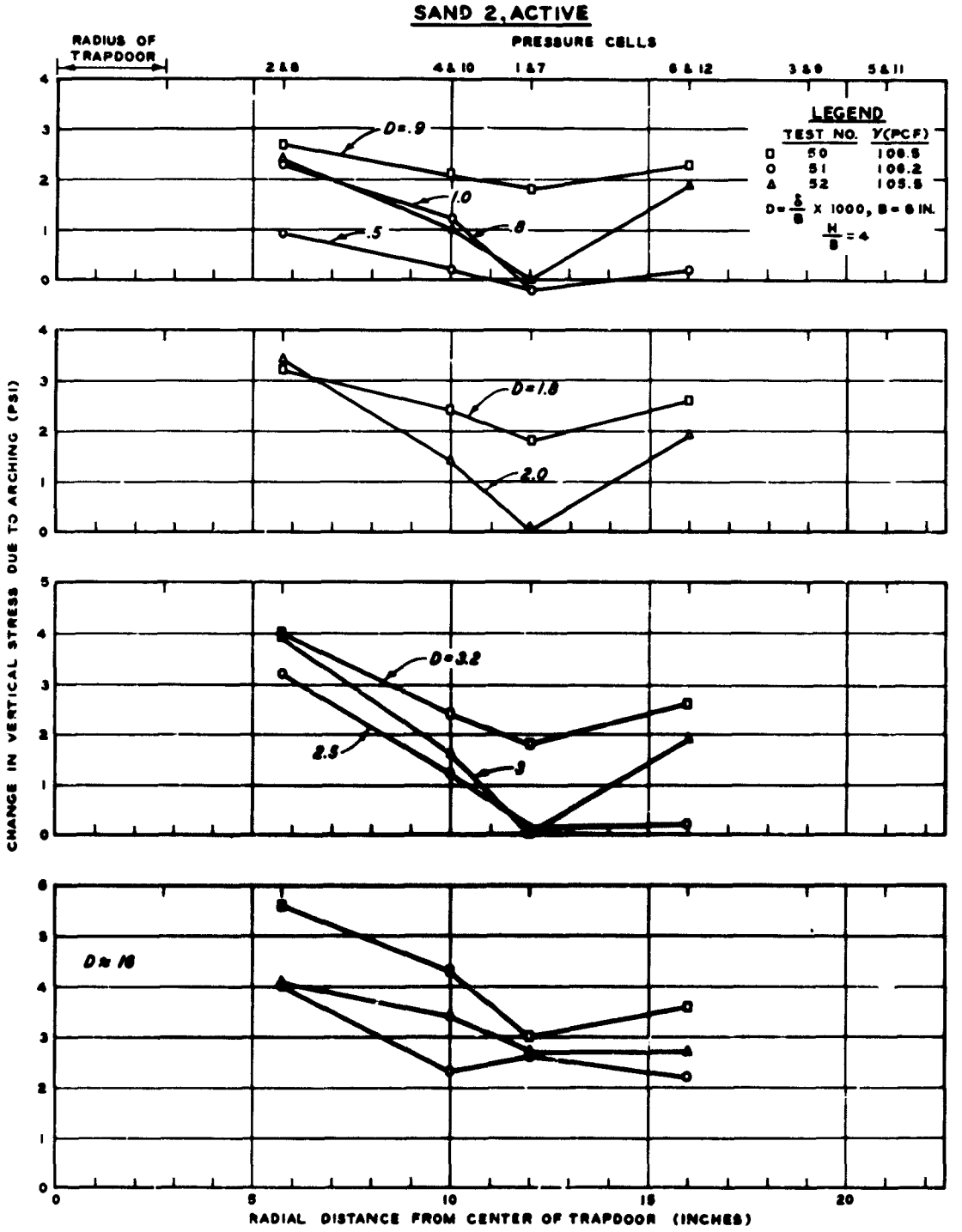

Fig. 4.37 Change in vertical stress due to active arching vs. radial distance from center of trapdoor; sand 2; $H/B = 4$; $P_s = 75$ psi

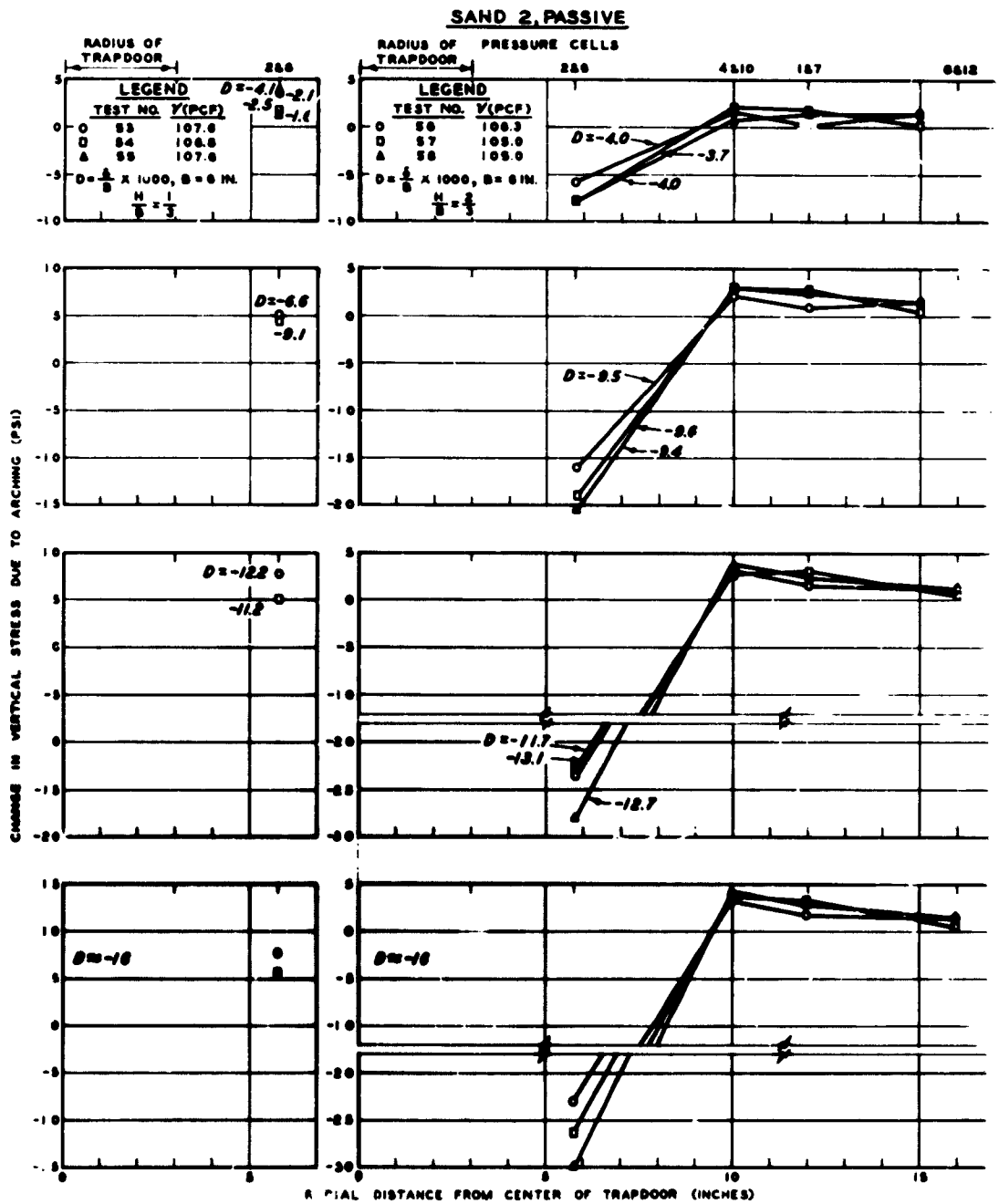

Fig. 4.38 Change in vertical stress due to passive arching vs. radi distance from center of trapdoor; sand 2; H/B = 1/3 , 2/3 ; P_s = 75 l

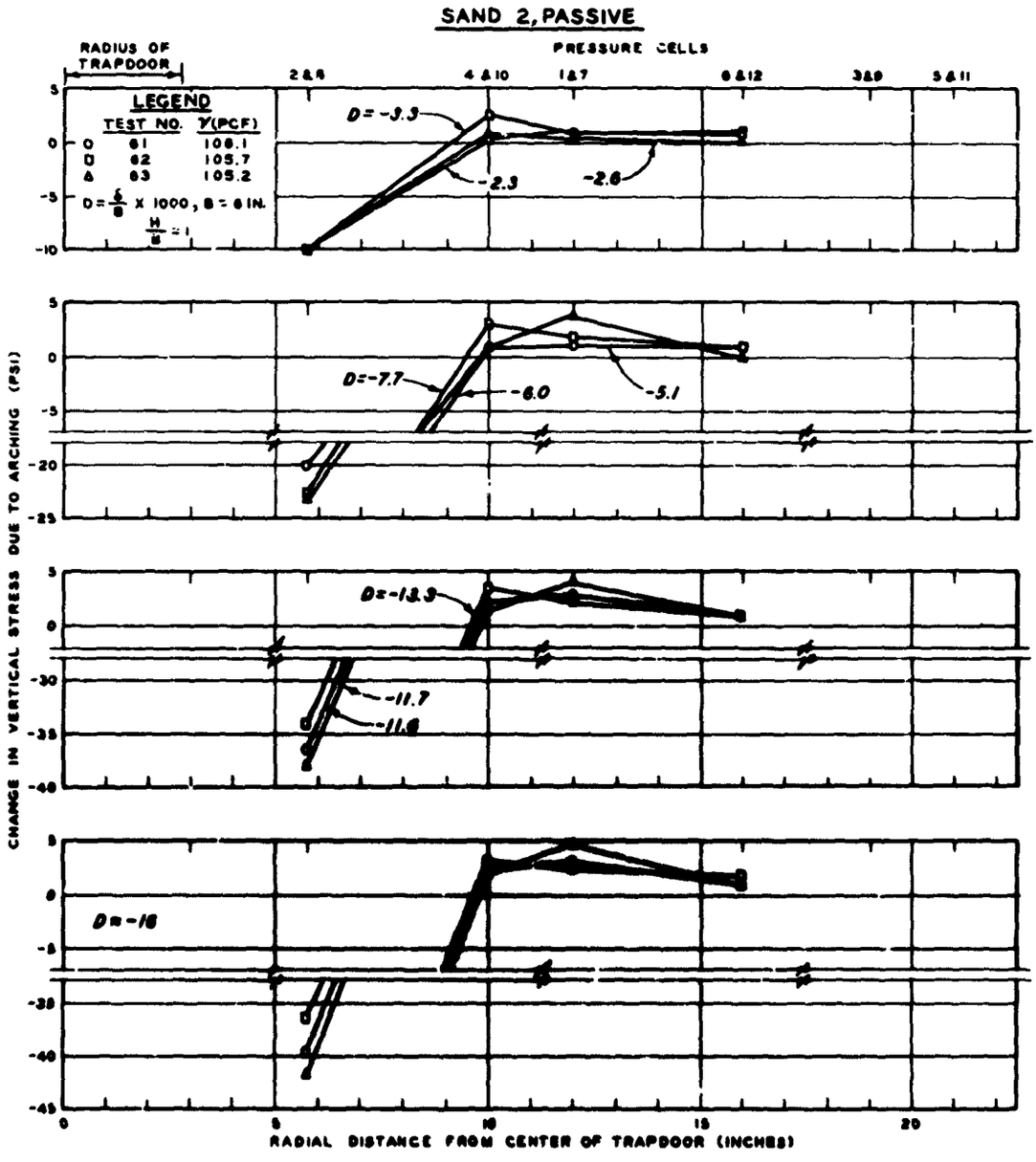

Fig. 4.39 Change in vertical stress due to passive arching vs. radial distance from center of trapdoor; sand 2; $H/B = 1$; $P_s = 75$ psi

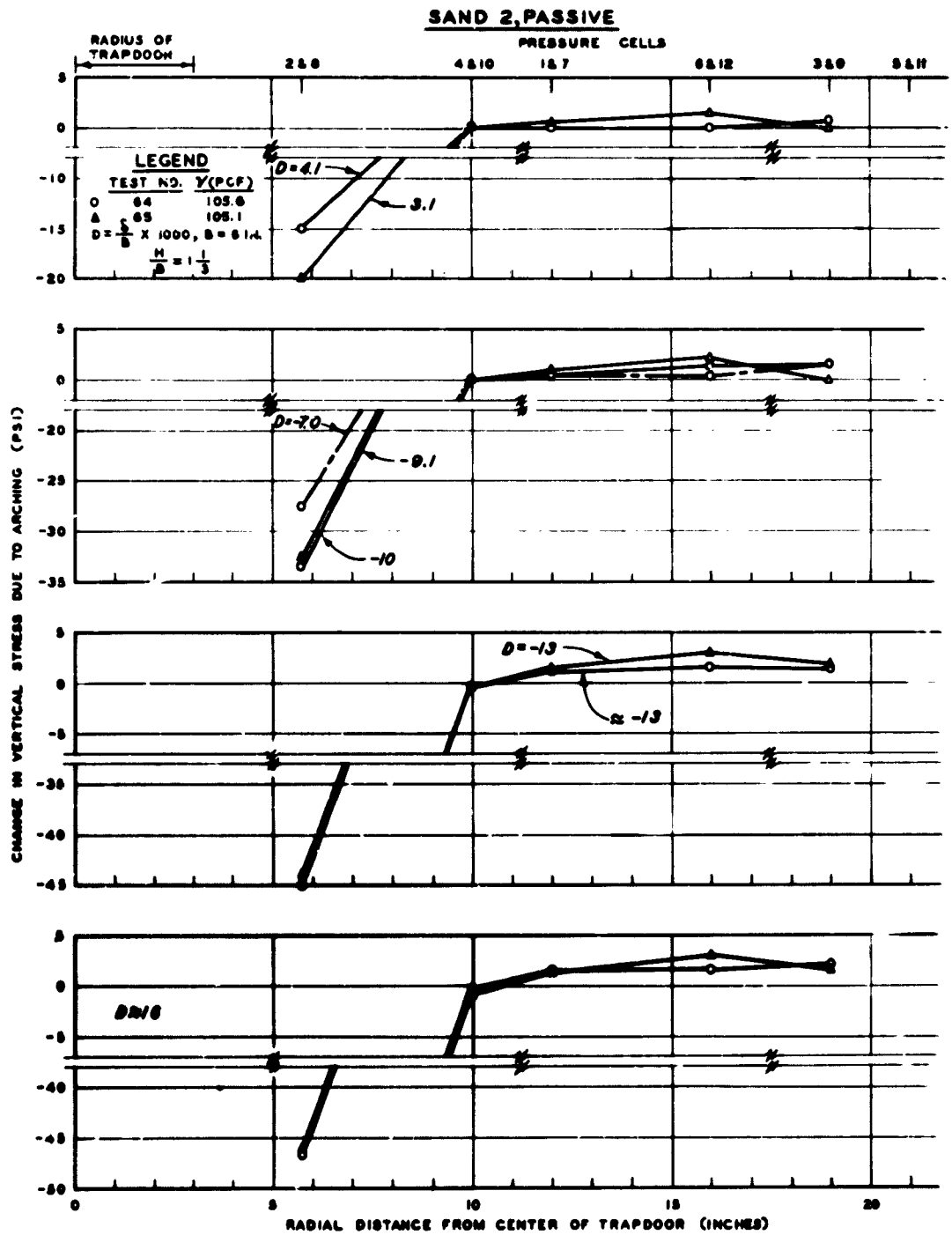

Fig. 4.40 Change in vertical stress due to passive arching vs. radi distance from center of trapdoor; sand 2; H/B = 1-1/3 ; P_s = 75 p

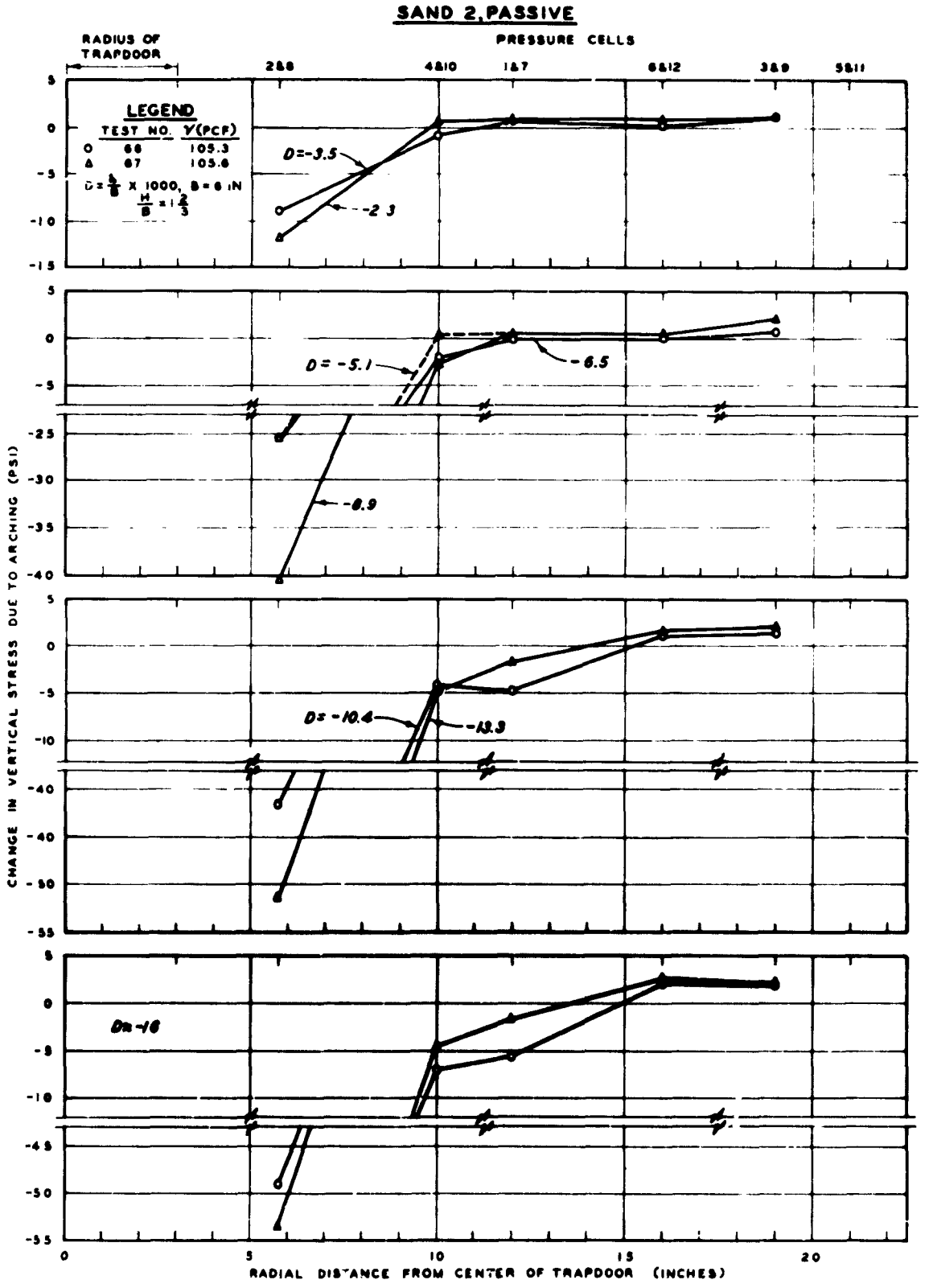

Fig. 4.41 Change in vertical stress due to passive arching vs. radial distance from center of trapdoor; sand 2; H/B = 1-2/3 ; P_s = 75 psi

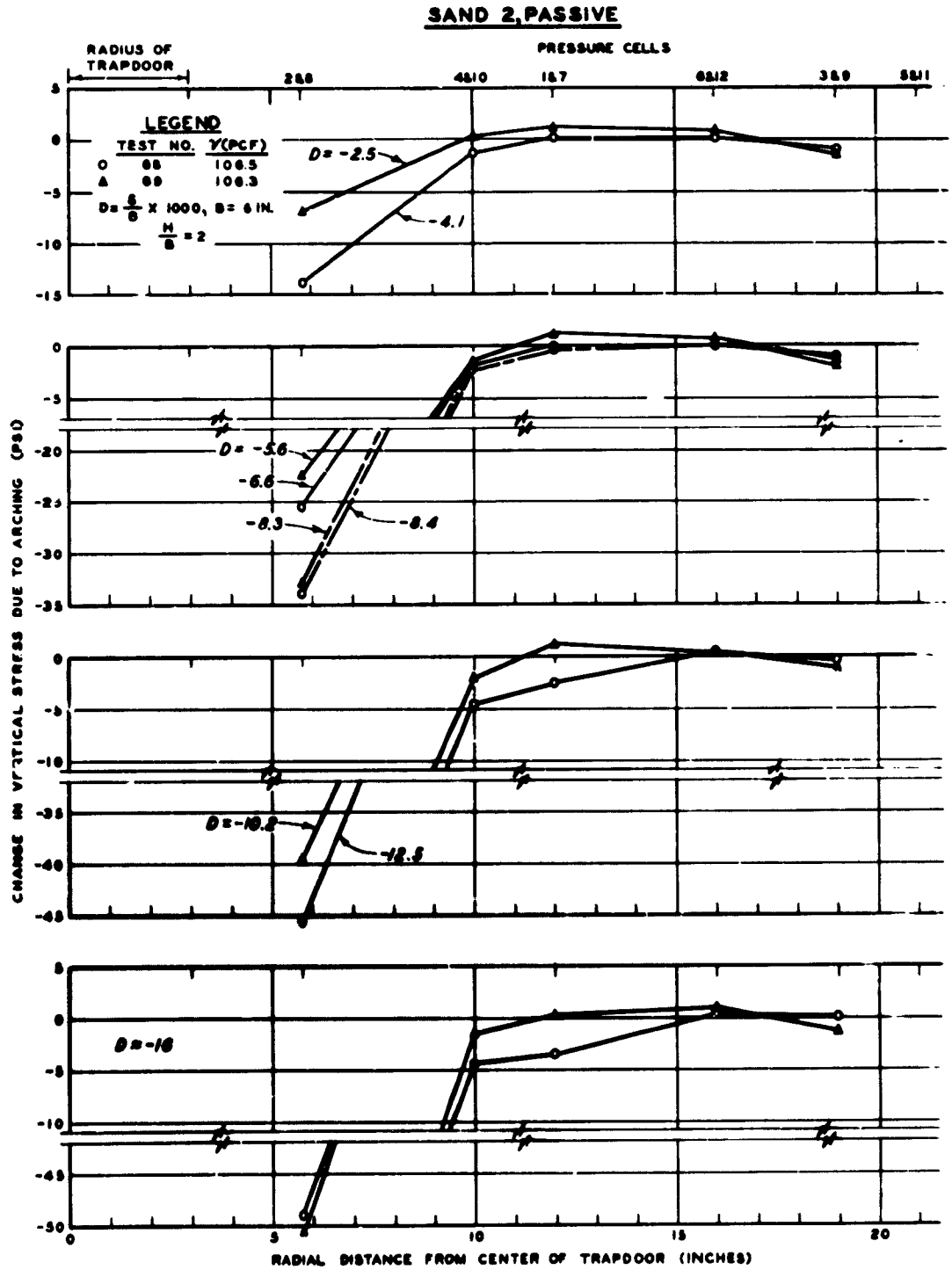

Fig. 4.42 Change in vertical stress due to passive arching vs. radi distance from center of trapdoor; sand 2; H/B = 2 ; P_s = 75 psi

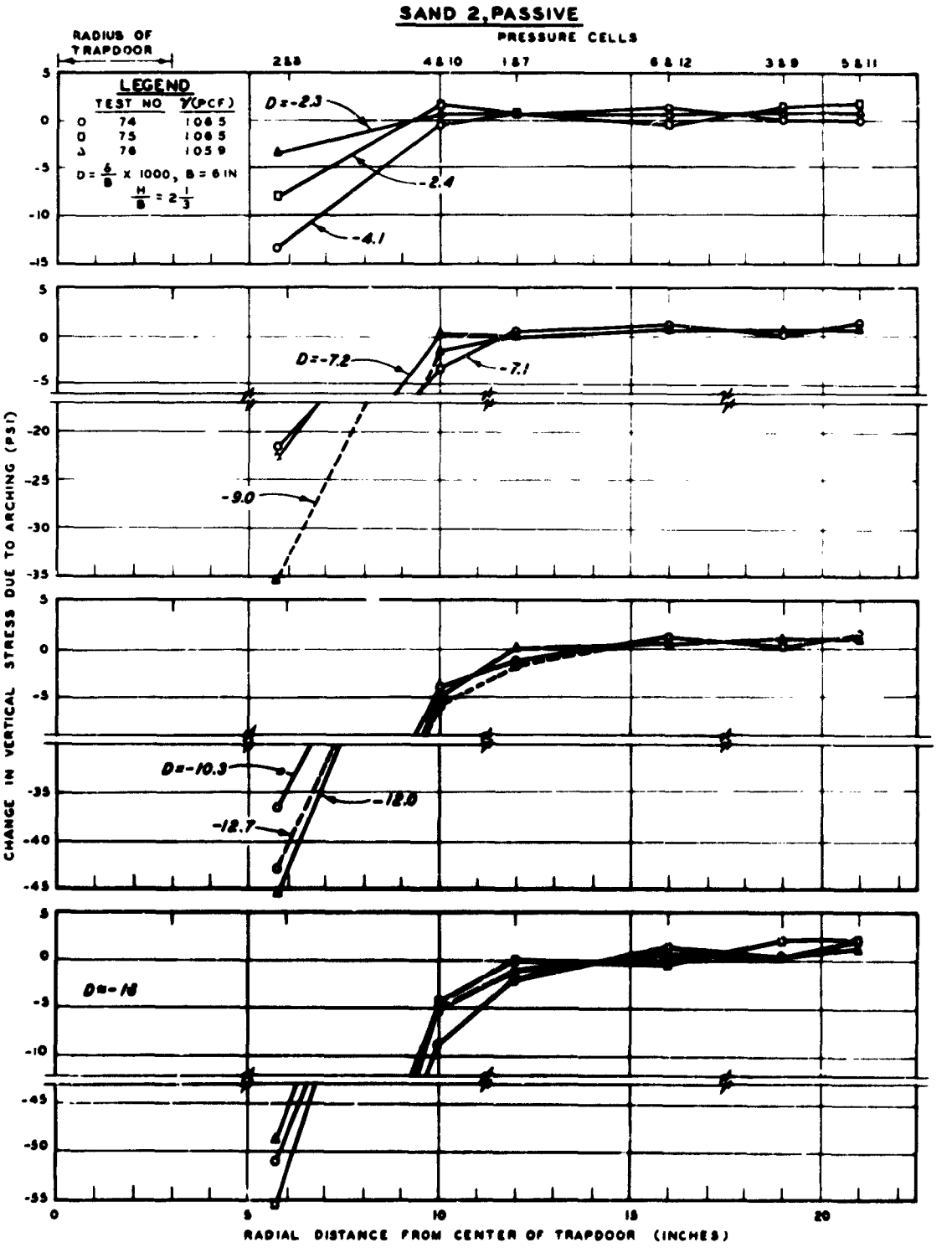

Fig. 4.43 Change in vertical stress due to passive arching vs. radial distance from center of trapdoor; sand 2; H/B = 2-1/3 ; P_c 75 psi

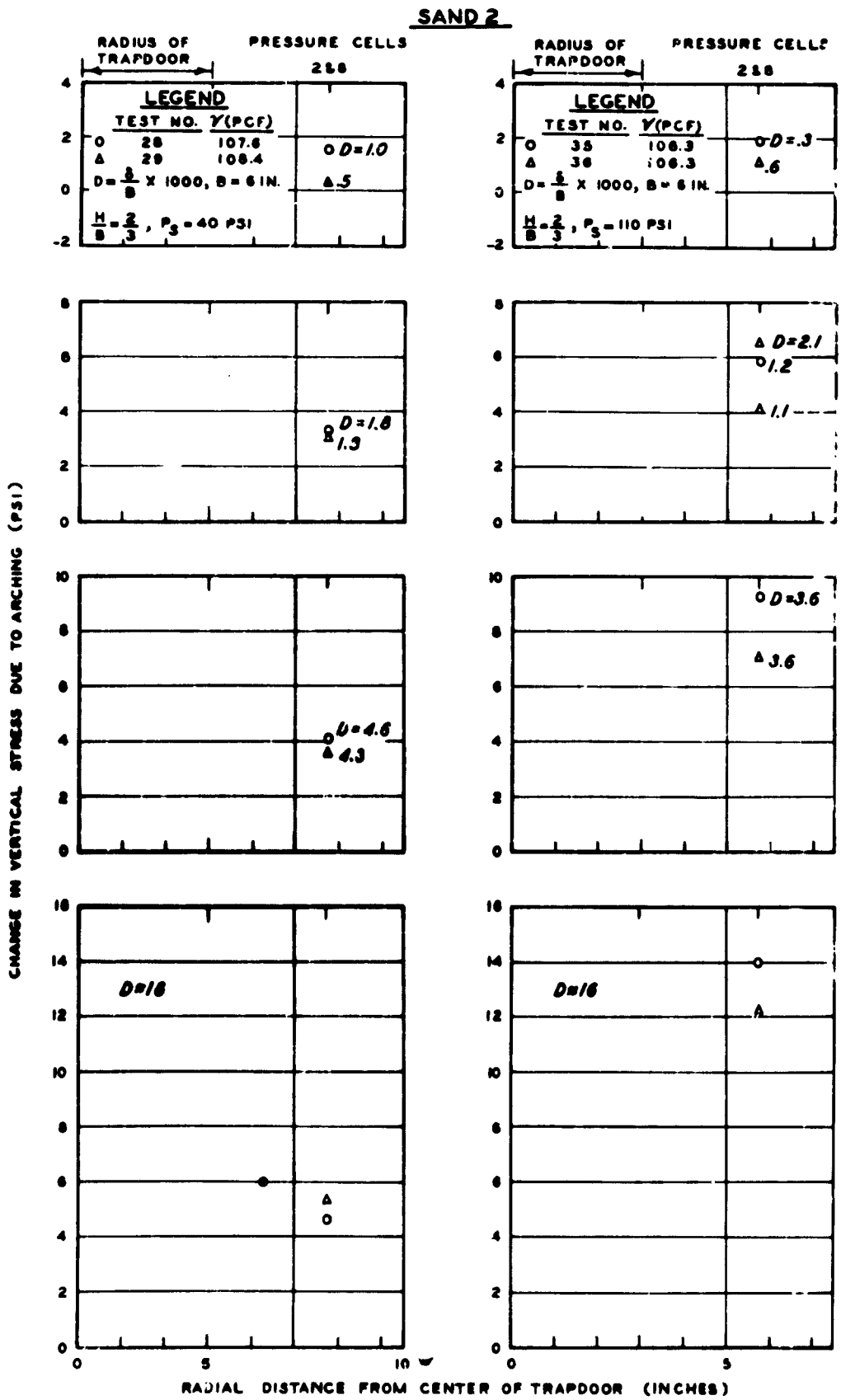

Fig. 4.44 Change in vertical stress due to active arching vs. radial d

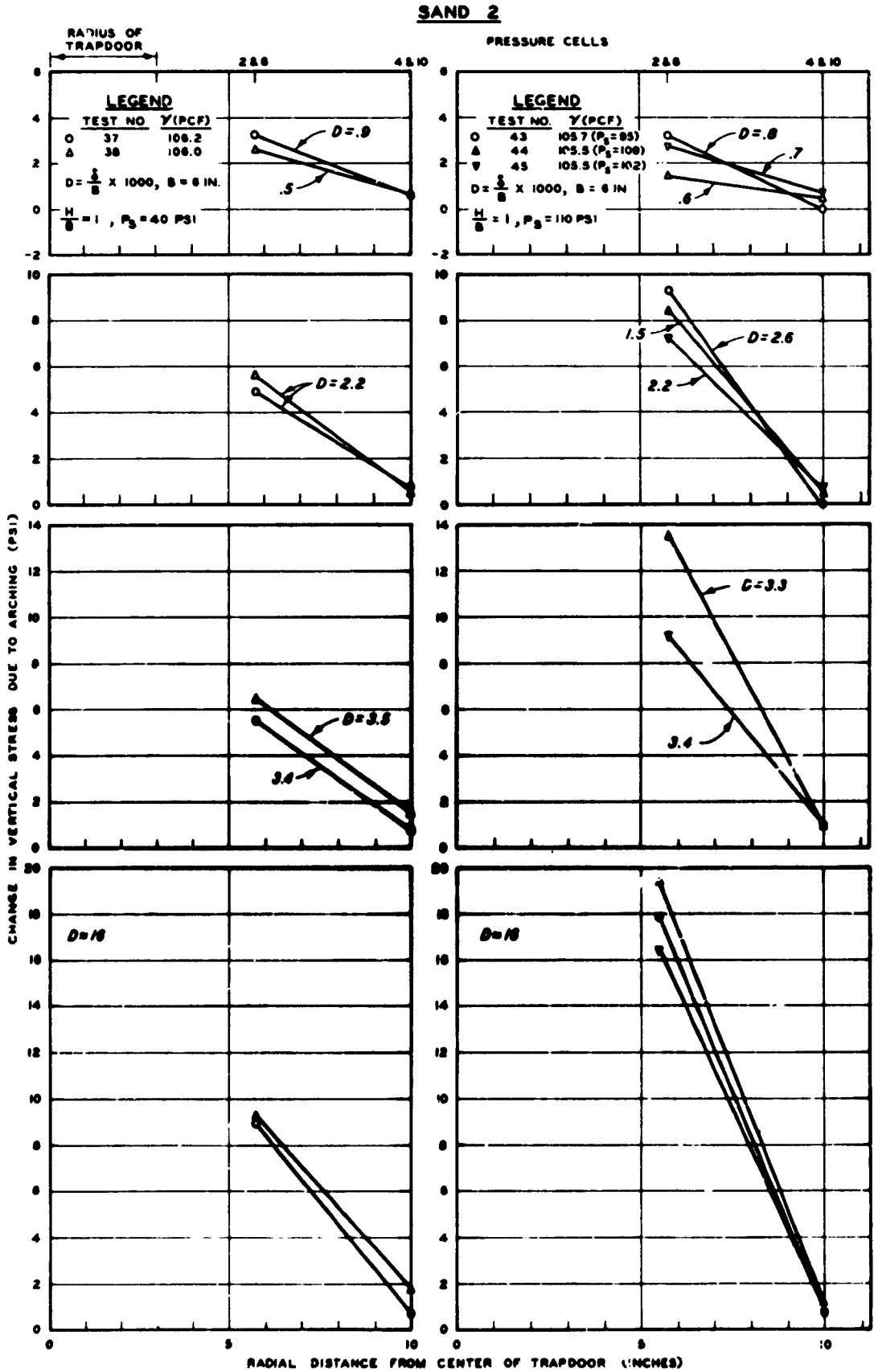

Fig. 4.45 Change in vertical stress due to active arching vs. radial distance

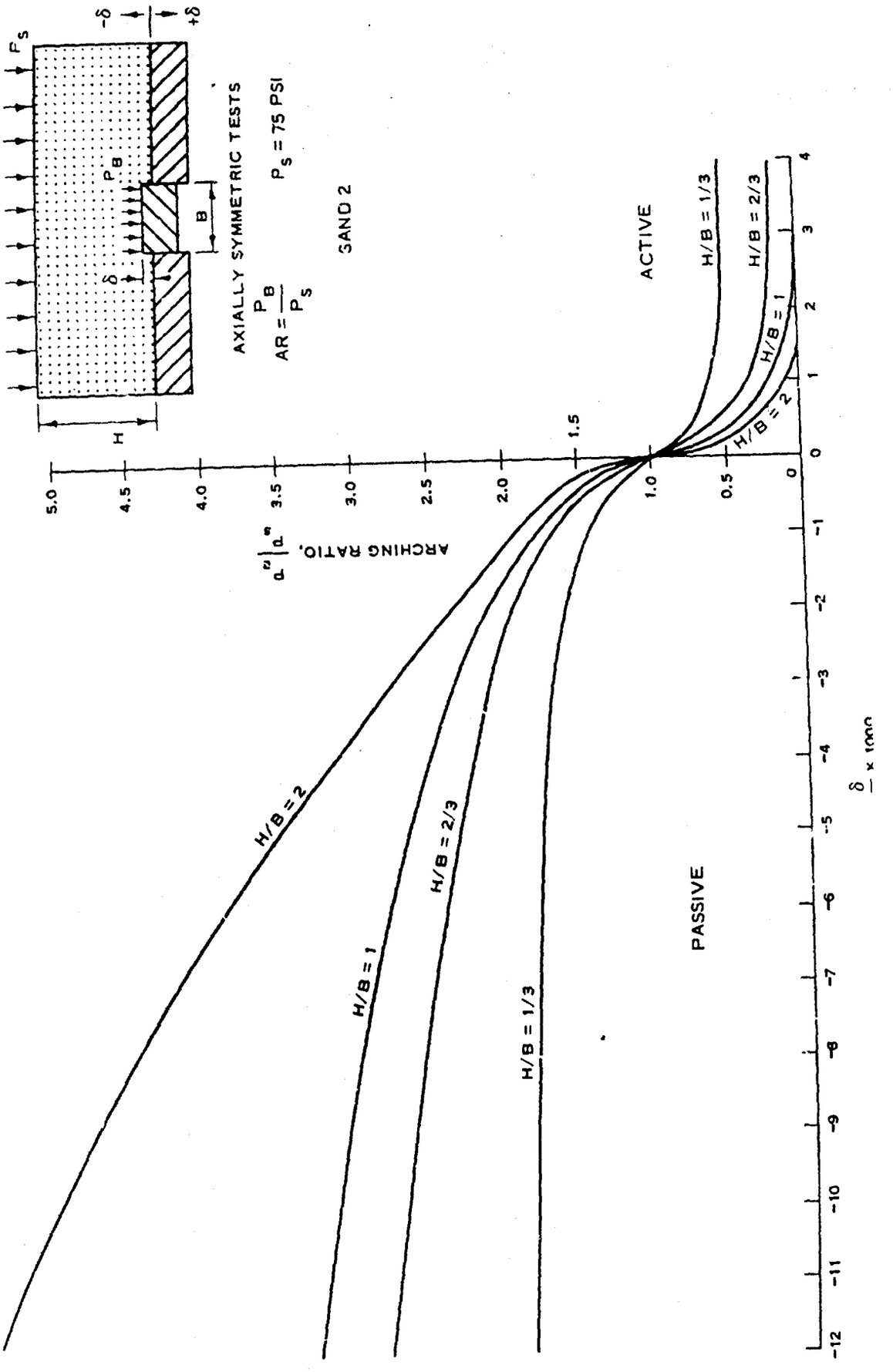
AXIALLY SYMMETRIC TESTS
$AR = \frac{P_B}{P_S}$
P_S = 75 PSI
SAND 2
ACTIVE
PASSIVE
H/B = 1/3
H/B = 2/3
H/B = 1
H/B = 2
ARCHING RATIO, σ_v / σ_v^*
$\frac{\delta}{}$ x 1000
P_S
P_B
B
H
δ
$-\delta$
$+\delta$

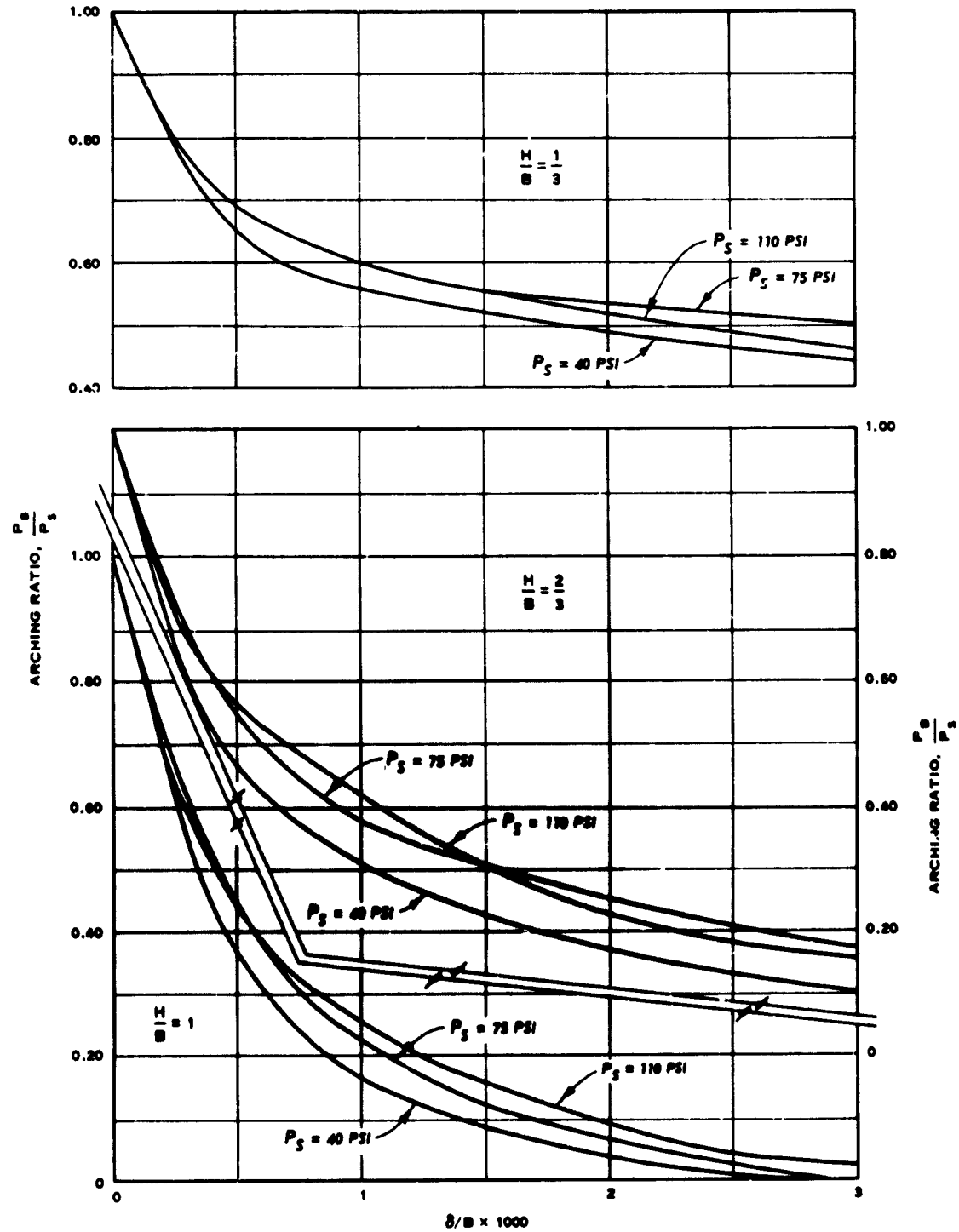

Fig. 5.2 Influence of surface pressure on active arching

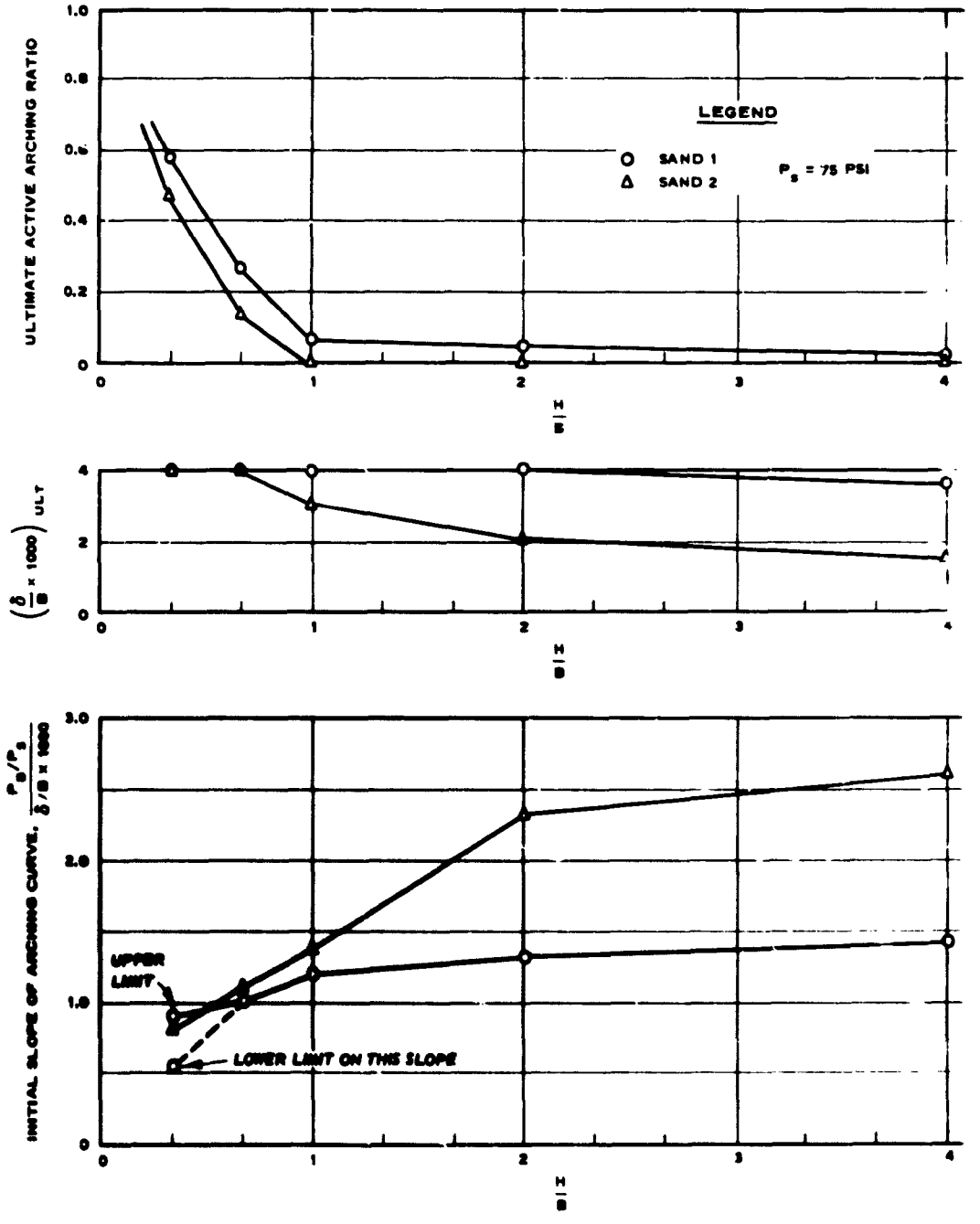

Fig. 5.3 Influence of soil properties and depth of cover on activ arching

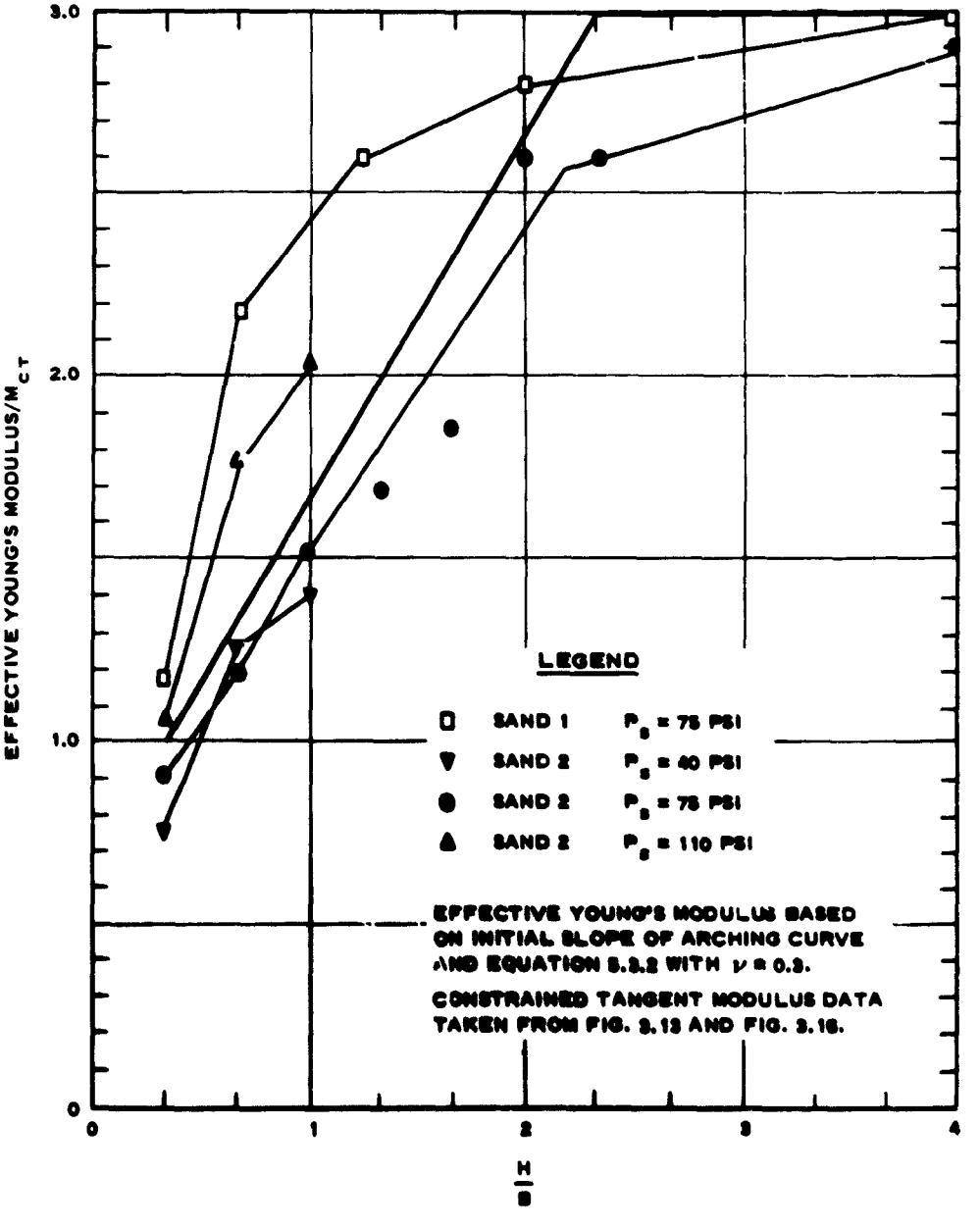

Fig. 5.4 Relation between ratio of constrained tangent modulus to effective Young's modulus and H/B

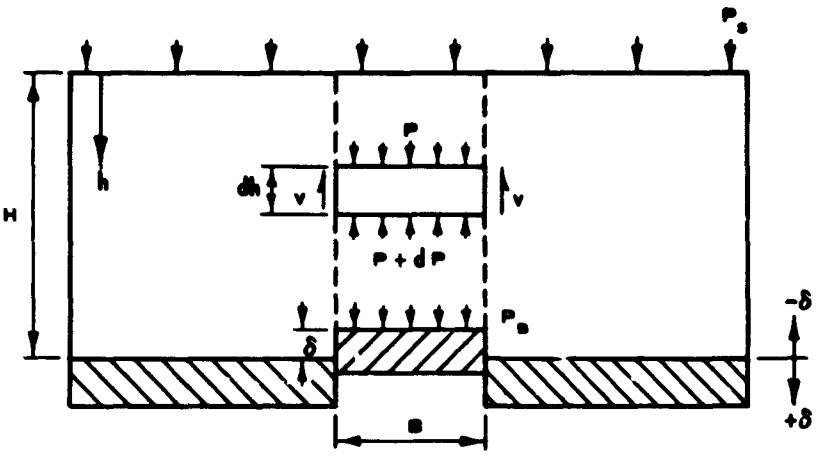

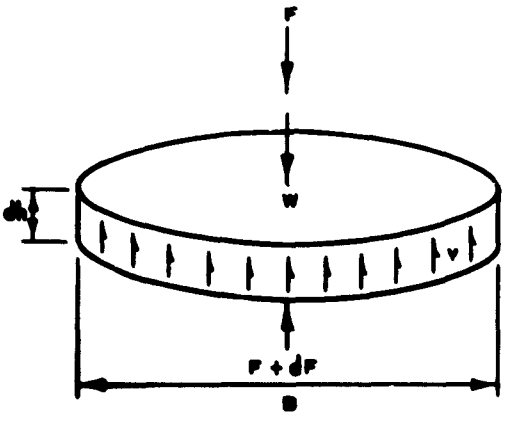

$$W = \gamma \left(\frac{\pi B^2}{4}\right) dh$$

$$F = P \frac{\pi B^2}{4} \qquad dF = dP \frac{\pi B^2}{4}$$

$$v = c + KP \tan \phi \qquad V = v (\pi B)\, dh$$

$$\Sigma (\text{FORCE})_{vert} = 0$$

$$W + F = (F + dF) + V$$

$$dF = W - V$$

$$dP = \left(\gamma - \frac{4}{B}(c + KP \tan \phi)\right) dh$$

BOUNDARY CONDITION: $P = P_s$ AT $h = 0$.

Fig. 5.5 The differential approach to ultimate arching

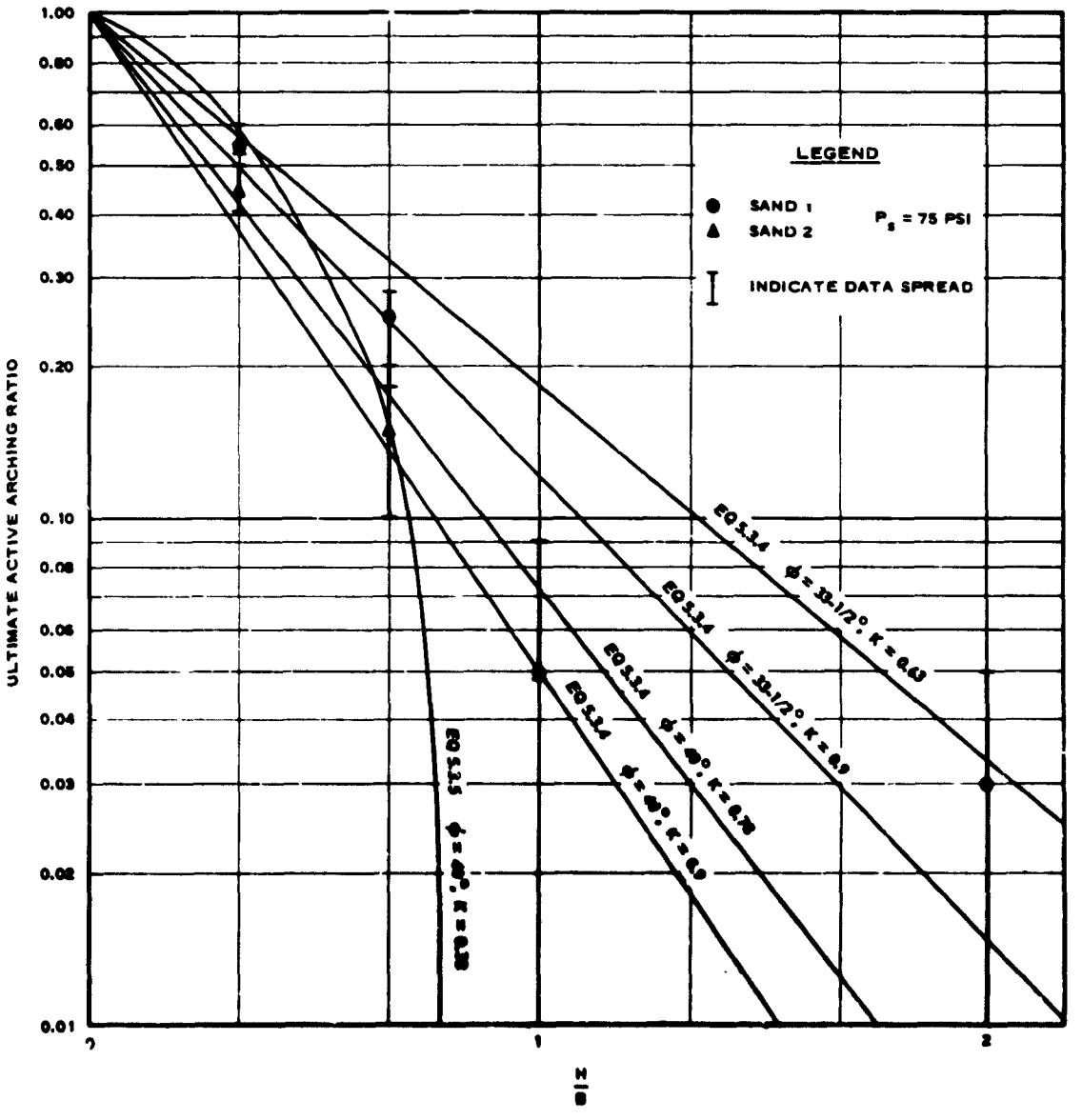

Fig. 5.6 Relation between ultimate active arching ratio and H/B

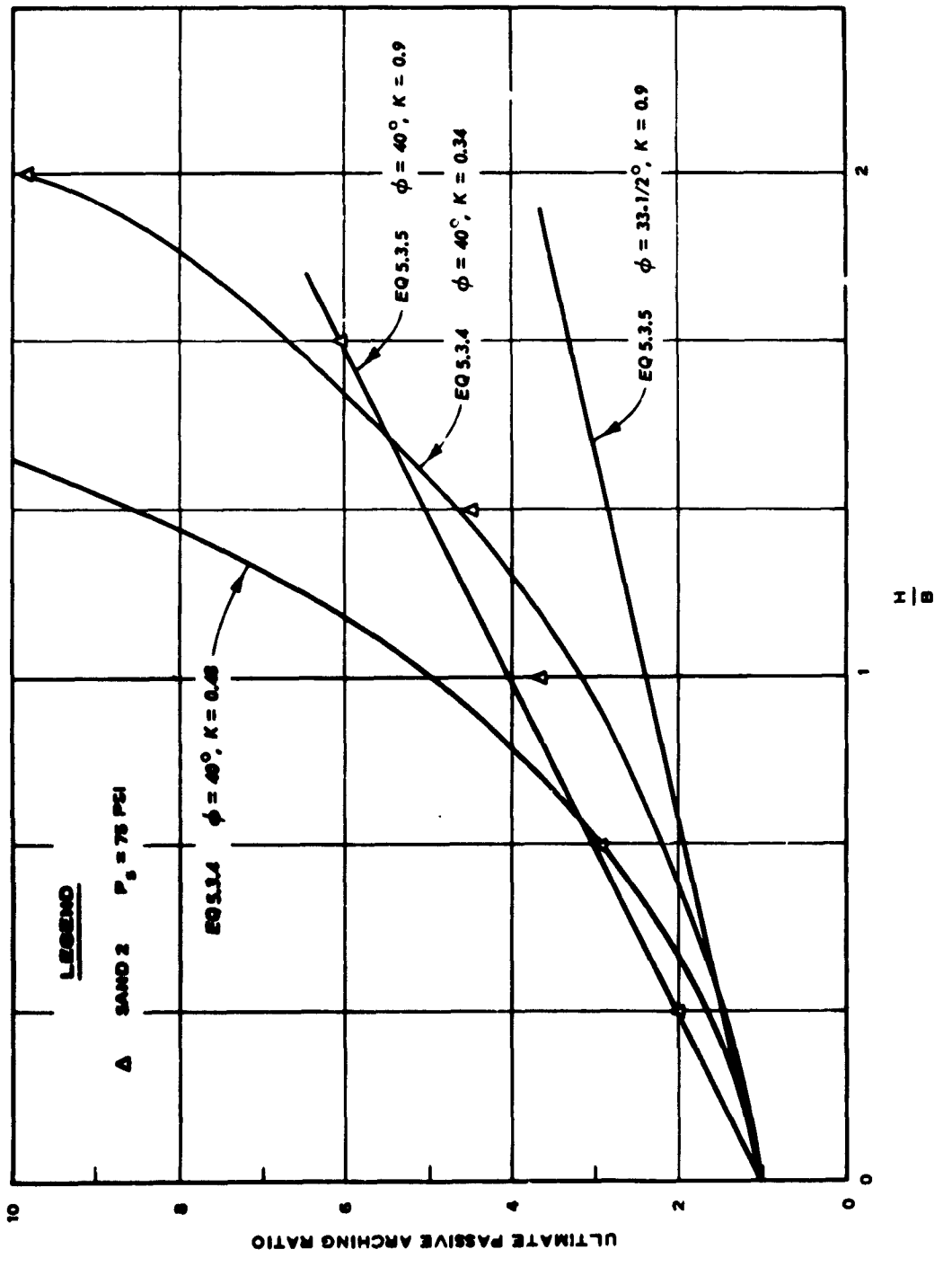
LEGEND
SAND 2 P_s = 75 PSI
EQ 5.3.4 ϕ = 40°, K = 0.48
EQ 5.3.5 ϕ = 40°, K = 0.9
EQ 5.3.4 ϕ = 40°, K = 0.34
EQ 5.3.5 ϕ = 33.1/2°, K = 0.9
ULTIMATE PASSIVE ARCHING RATIO
H/B
0
2
4
6
8
10
0
1
2

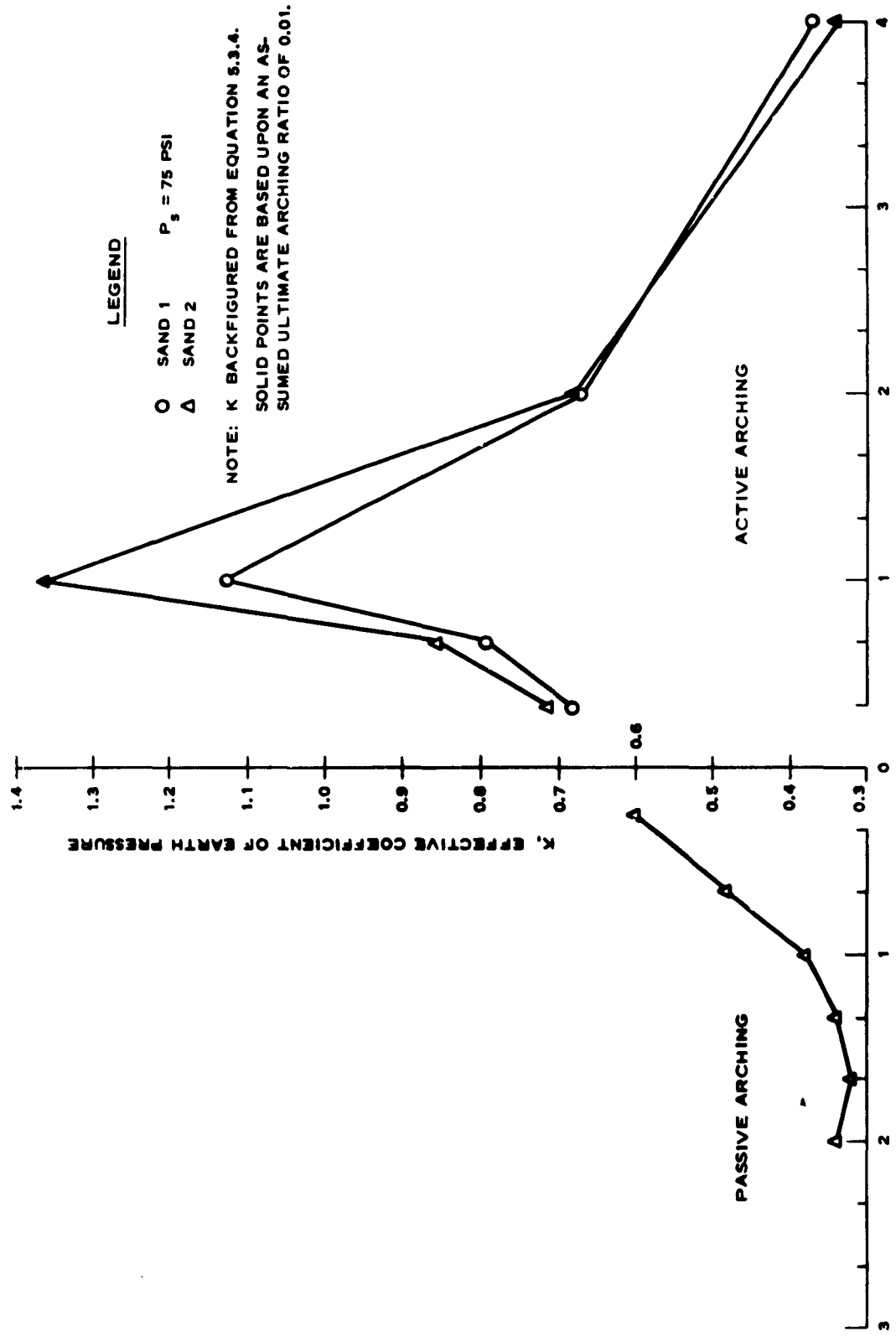

Fig. 5.8 Influence of H/B on effective coefficient of earth pressure

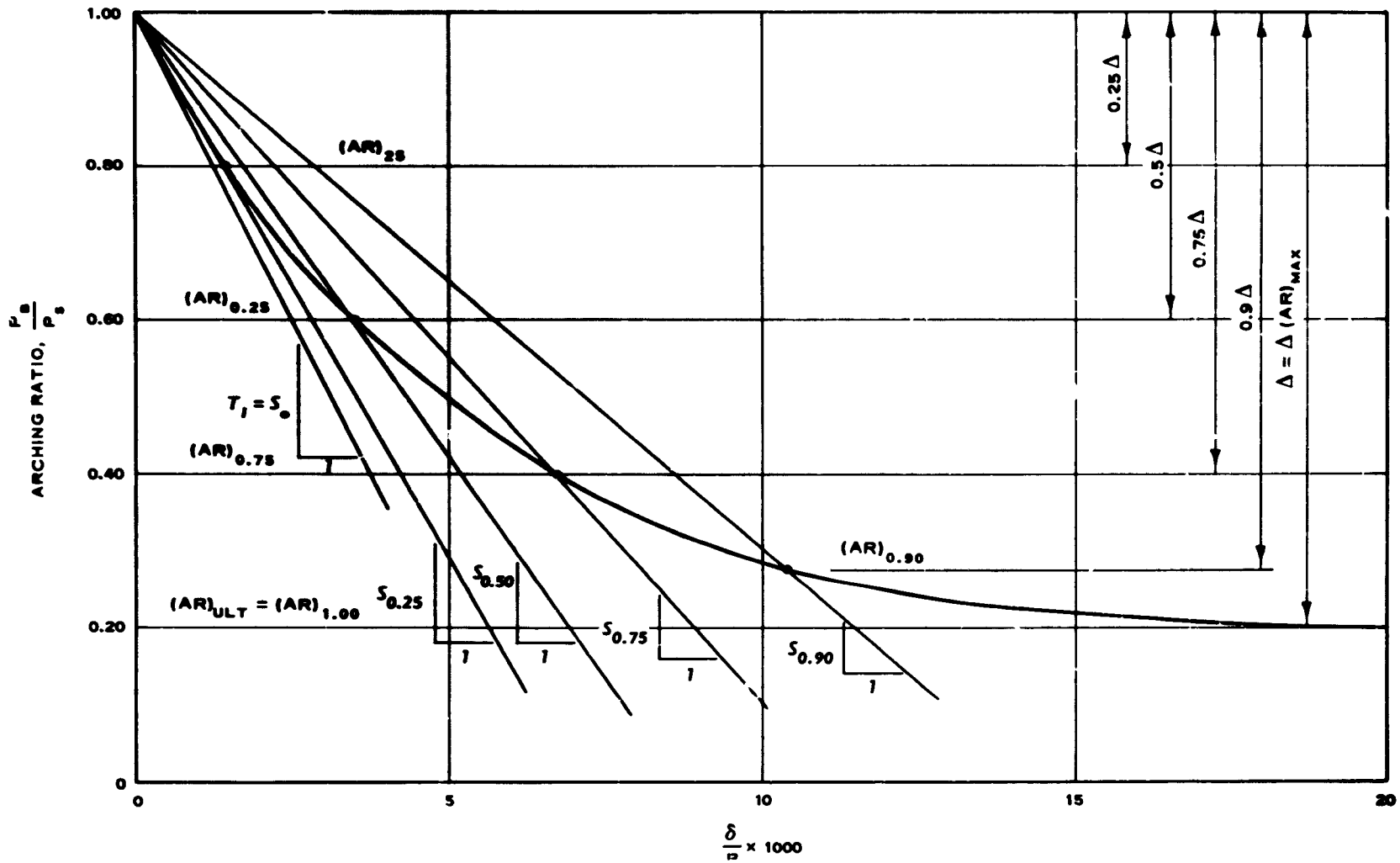
1.00
0.80
0.60
0.40
0.20
0
0
5
10
15
20
ARCHING RATIO, $\frac{f'_s}{f'_s}$
$\frac{\delta}{D} \times 1000$
$(AR)_{25}$
$(AR)_{0.25}$
$(AR)_{0.75}$
$(AR)_{0.90}$
$(AR)_{ULT} = (AR)_{1.00}$
$T_i = S_o$
$S_{0.25}$
$S_{0.50}$
$S_{0.75}$
$S_{0.90}$
1
1
1
1
0.25Δ
0.5Δ
0.75Δ
0.9Δ
$\Delta = \Delta (AR)_{MAX}$

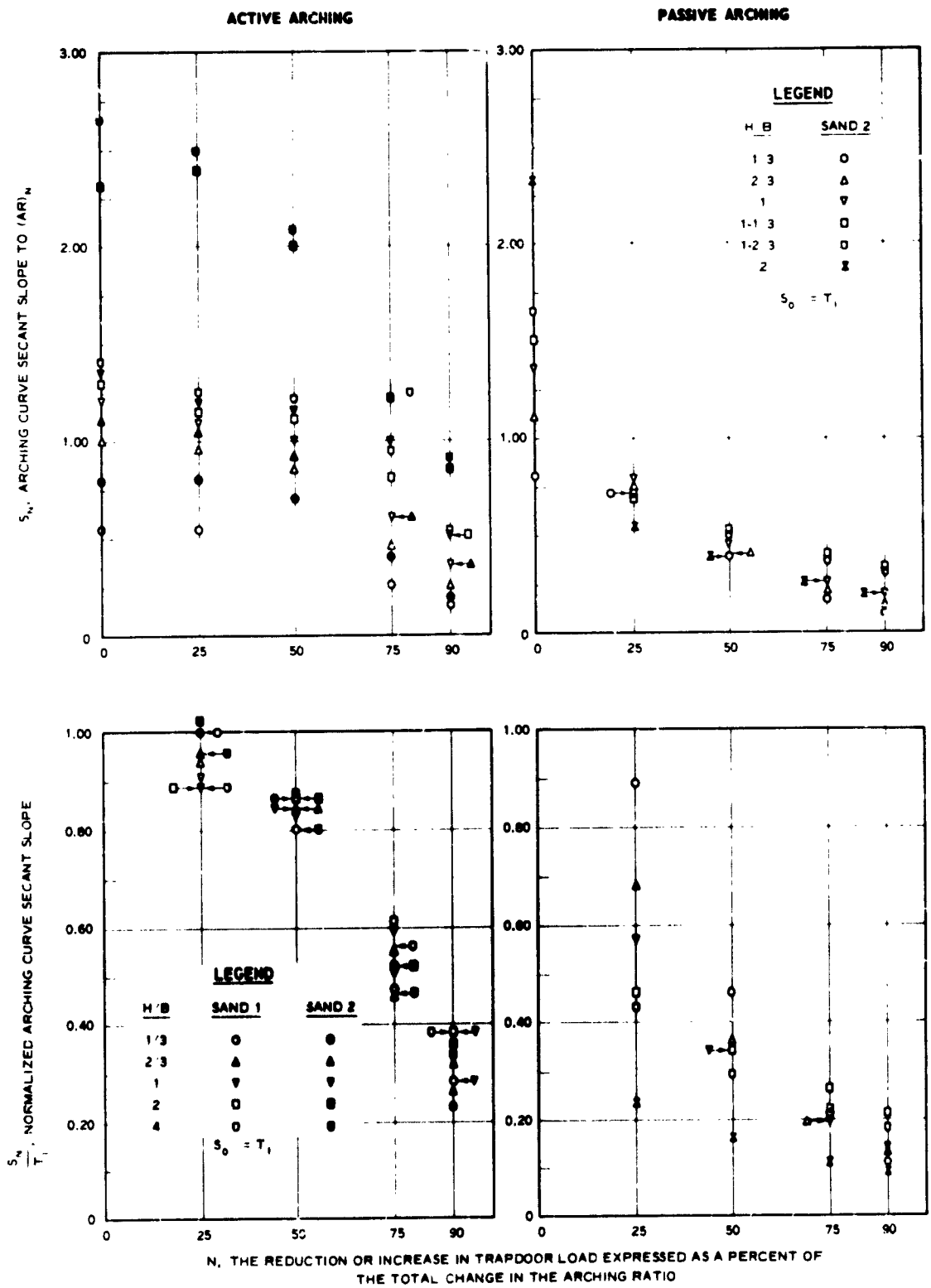

Fig. 5.10 Relation between arching curve secant slopes and percent of ultimate change in arching ratio

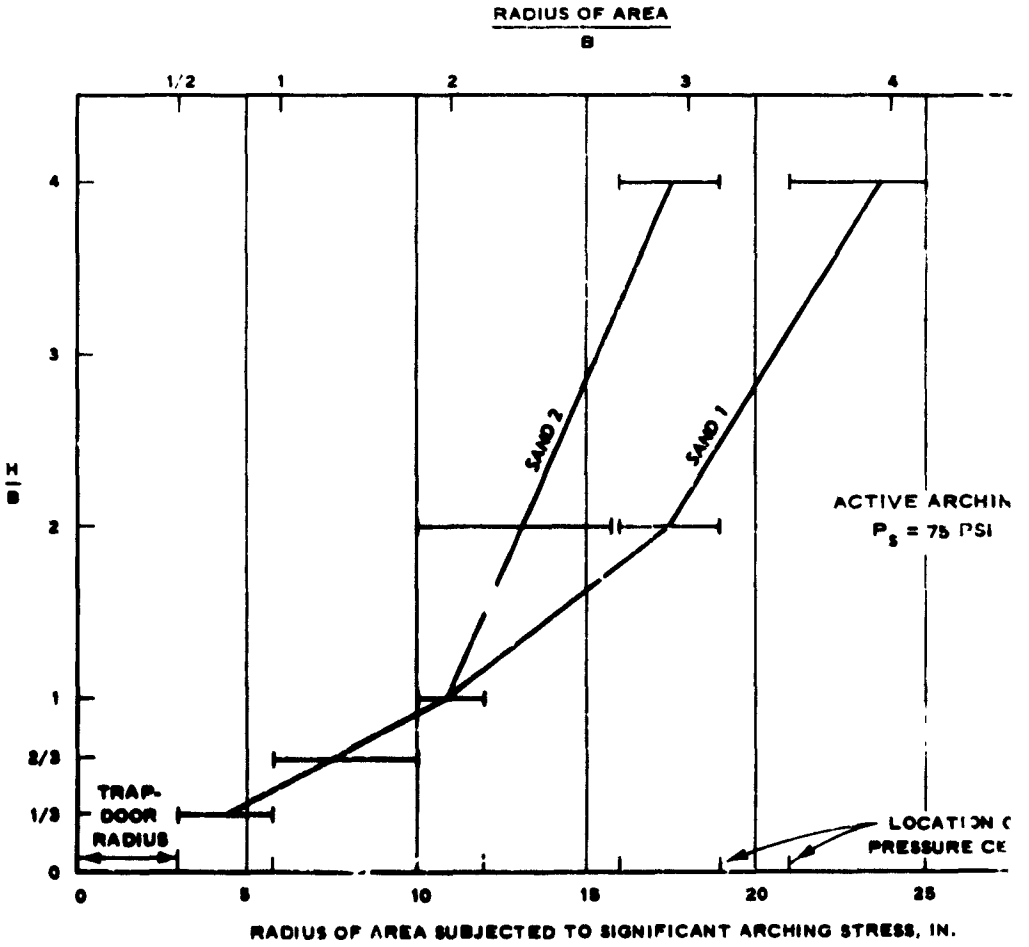

Fig. 5.11 Influence of H/B ratio on size of area subjected to a arching stress

APPENDIX A: IN-PLACE CALIBRATION OF PRESSURE CELLS AND OBSERVATIONS OF SIDEWALL FRICTION

A.1 General

As mentioned in Section 3.3, the pressure cells used to evaluate changes in vertical stress due to arching were effectively calibrated in place during the pressure-buildup phase of each test. For cells which experienced only increases in pressure during the test, these calibrations proved acceptable as discussed in Section A.2. Certain cells, however, experienced pressure decreases during some tests which invalidated direct application of the loading calibrations. The adjustment made in this situation is discussed in Section A.3. Section A.4 contains observations of the influence of sidewall friction which are based upon orderly variations in the calibration curves as the depth of cover increased.

A.2 Pretest, In-Place Calibrations

Figs. A.1 and A.2 are summaries of the calibration curves obtained for the soil pressure cells prior to each test. The abscissa of the plots is the normalized output of the pressure cells, which is the deflection of the galvanometer trace, as recorded on the oscillograph, divided by the deflection associated with a precision calibration resistor. One cell of each pair which was located at a set distance from the trapdoor center is represented. All calibration curves of each cell are essentially the same except those calibrations in which the depth of cover became great enough that sidewall friction caused the calibration to change. Calibrations which are essentially the same have not been plotted individually, but are represented by a bar which indicates the amount of scatter due to soil placement and other experimental errors. The curves associated with

depths of cover great enough that the influence of sidewall friction w apparent are plotted as the average of several calibrations at each de of cover. Two particularly important points should be noted. First, linearity in the later portions of each of these curves indicates the error involved in the extrapolating beyond the limits of calibration moderate pressure increases is minor. Second, for equal values of d the surface pressure (P_s) associated with a given output in sand 2 ca tions is higher than the value of P_s associated with the same outpu sand 1 calibrations. This is in accord with the greater arching cap of sand 2, as indicated by Figs. 4.5 and 4.17.

A.3 Special Calibrations

The distribution of arching stress for those tests in whi certain pressure cells experienced reductions in pressure could not b interpreted directly from the pretest calibrations. Three special ca tion tests in which the trapdoor was not allowed to deflect were cond so that the loading and unloading curves could be obtained. These te were conducted using a 2-in. depth of sand 2 (a new specimen was buil each test) and a maximum surface pressure of 73 psi. The shallow dep cover is considered adequate because of the small size of the pressur diameter (H/B for the cell is at least 4) and the repeatability of th calibrations discussed in Section A.2 for a wide range of depths. Th ibration curves for pressure cells 2 and 8 are shown at the top of Fi All tests produced essentially the same curve for cell 2, while the s test on cell 8 is slightly different from the others. Since the prob is that of judging the amount of unloading which took place by using the loading calibration curves available for each test, the curve at

bottom of Fig. A.3 was plotted. This curve shows the relation between the reduction in pressure from 73 psi as read from a loading calibration curve, and the reduction as read from an unloading calibration curve for the same level of normalized output. The data points indicate that the error associated with using a loading calibration to evaluate unloading is fairly constant for a given pressure reduction regardless of differences in individual cells or variations in calibration curves. The curve at the bottom of Fig. A.3 was used with the pretest calibrations in order to estimate pressure reductions.

A.4 Influence of Sidewall Friction

Since the minimum H/B for the pressure cells was about 4, the plane of equal settlement for ultimate arching was always well below the surface. Therefore, changes in cover should not change the calibration curves. However, the calibration curves did change with H in an orderly fashion as indicated by Figs. A.1 and A.2. Friction between the sand and the walls of the test chamber causes a transfer of vertical stress to the walls, resembling silo-type arching. On a given horizontal plane, the area over which the vertical pressure is distributed is believed to be an annulus with an outer diameter equal to the diameter of the chamber and an inner diameter which is equal to the outer diameter at the surface and which decreases with depth. For very shallow tests, most of the soil pressure cells were within the undisturbed zone, but as the depth was increased the disturbed zone gradually enveloped them. This envelopment is believed to be the major reason for the variation with depth of the calibration curves. By using the calibration obtained during a test to interpret the pressure changes for that test, the influence of the

sidewalls on the pressure redistribution was accounted for. Howeve changes in calibration curves may be used to estimate the extent of undisturbed zone as a function of cover. Fig. A.4 represents the l on the extent of the undisturbed zone as they may be inferred from calibrations. Due to certain large jumps in the depth of cover and spacing of pressure cells it is impossible to do more than establ on the location of the zone separating the disturbed and undisturbe tions of the specimen.

Fig. A.4 indicates that the line of separation cannot po be a single straight line. This is probably due to increasing effe sidewall roughness with depth as a result of the joints between the Although the line of separation may well be a curve, one possible a mation composed of two line segments has been placed in Fig. A.4.

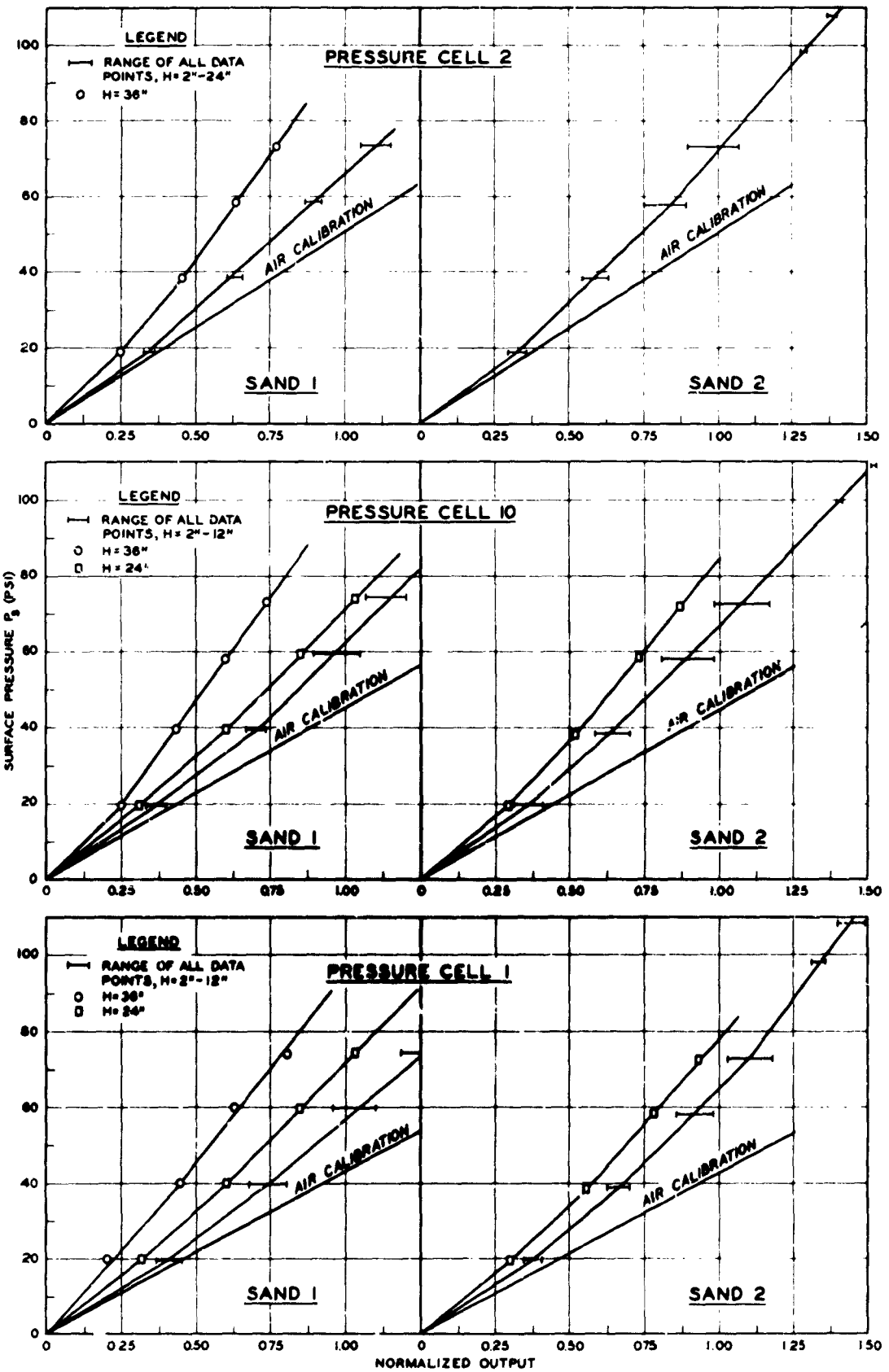

Fig. A.1 Pretest calibrations of pressure cells 2, 10, and 1

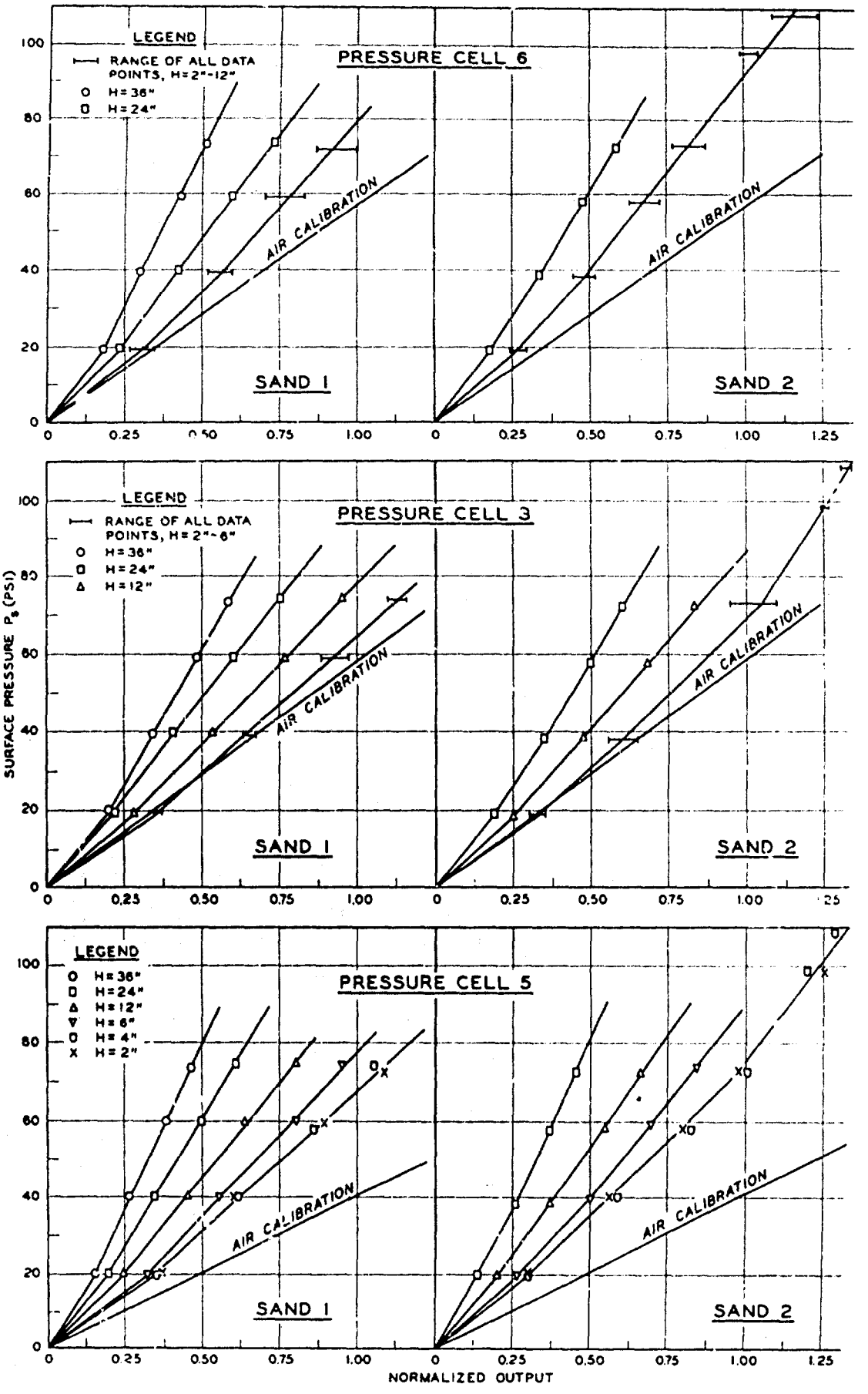

Fig. A.2 Pretest calibrations of pressure cells 6, 3, and 5

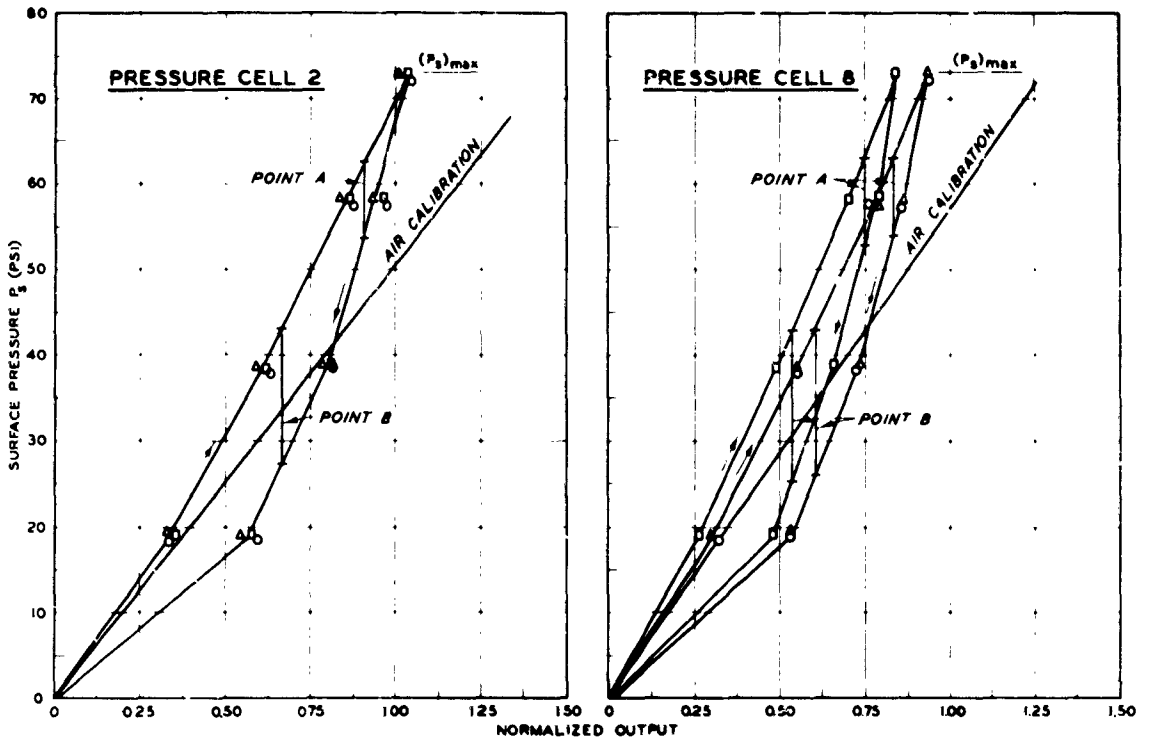

a. THREE, LOADING-UNLOADING, IN-PLACE CALIBRATIONS OF PRESSURE CELLS 2 AND 8.

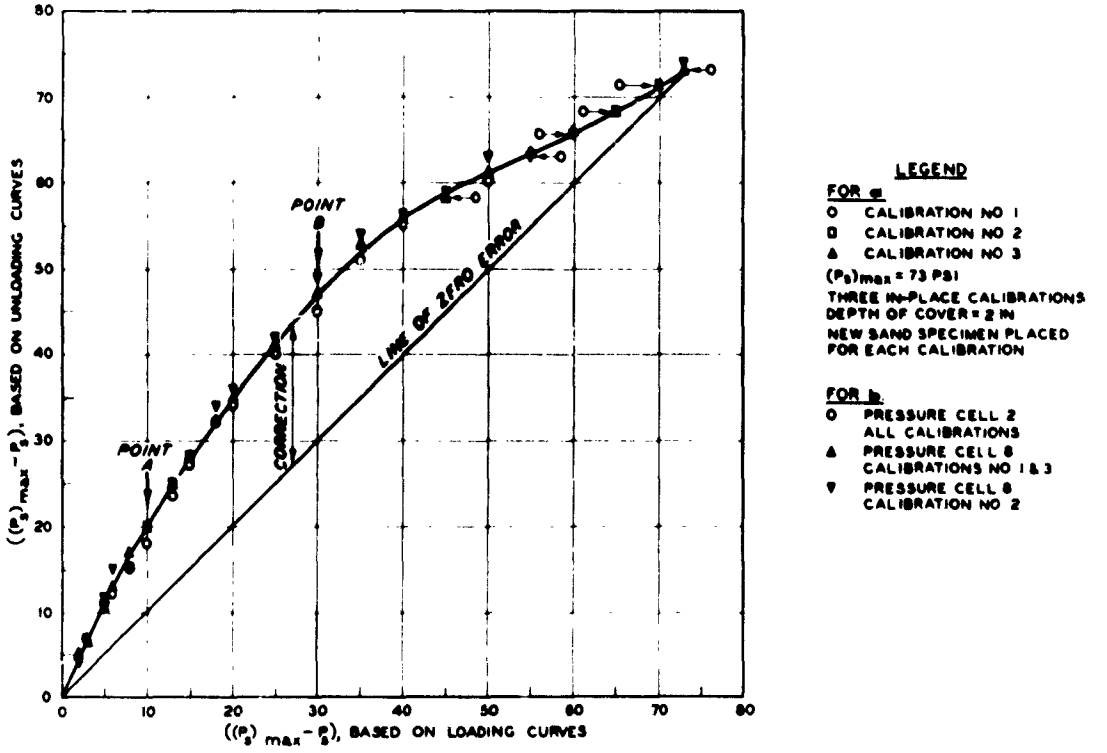

b PLOT OF CORRECTIONS FOR PRESSURE DECREASES BASED ON LOADING CALIBRATION

Fig. A.3 Error associated with use of loading calibration to estimate unloading

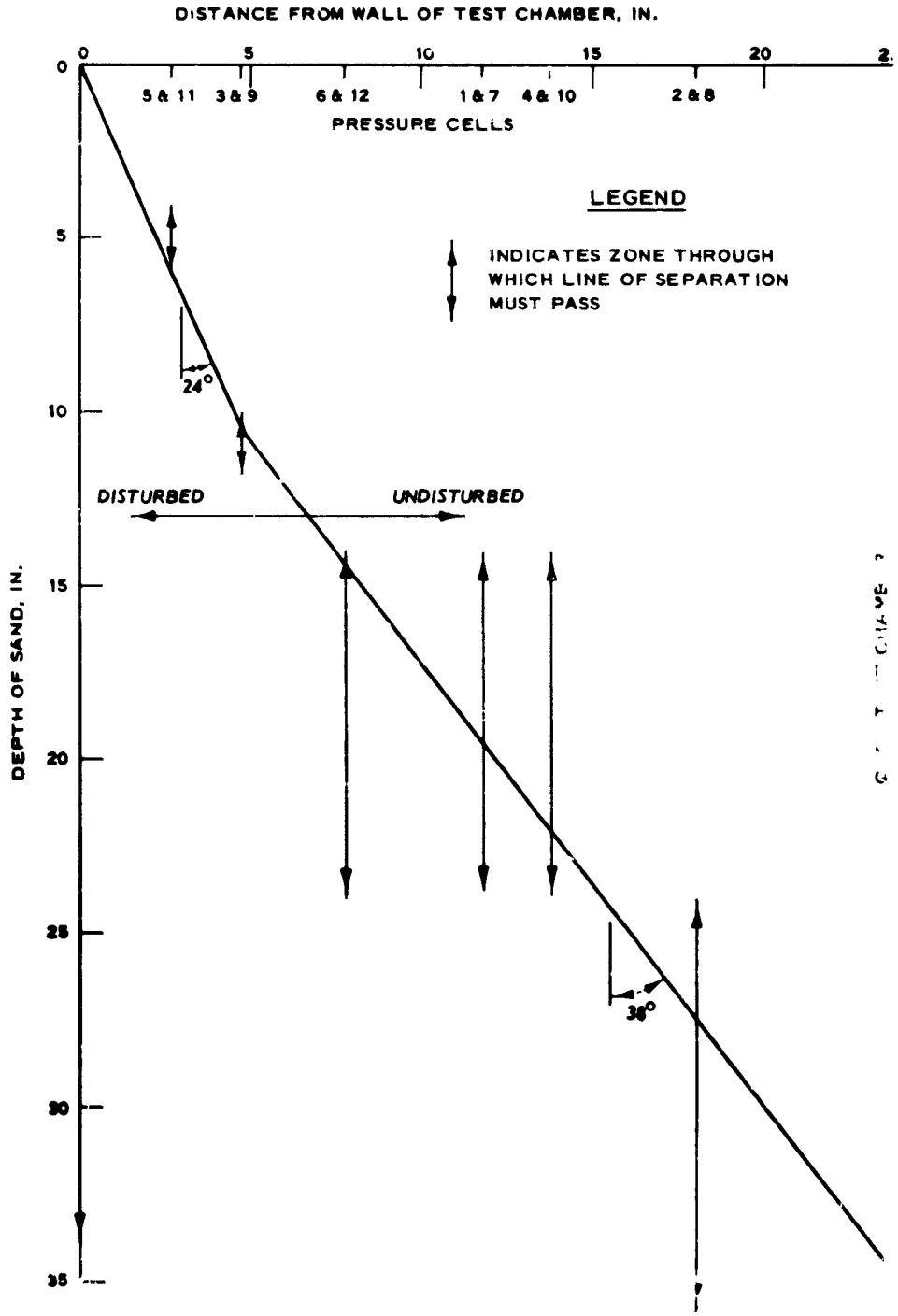

Fig. A.4 Influence of sidewalls on pressure distribution

APPENDIX B: PRELIMINARY TESTS

B.1 General

Preliminary active arching tests were conducted in a rectangular bin with transparent walls as mentioned in Section 1.3. Several advantages are associated with tests conducted in such a configuration: visual observation of the soil through the glass sidewalls is possible; a number of analytical solutions for this geometry are available; the stress changes associated with arching are large, hence subject to more accurate measurement; and smaller quantities of sand are required. It was originally believed that these advantages would lead to insight which would at least facilitate the conduct of the axially symmetrical te , series, and possibly make it unnecessary. However, the influence o' sidewall friction proved great enough to negate these advantages. Sev ral attempts were made to reduce the influence of friction, but it was decided that it would be more advantageous to proceed with the axially symmetrical tests in which frictional effects were minimized by locating the trapdoor away from the vicinity of the walls.

B.2 Test Apparatus

A test bin 54-1/4 in. long and 8-1/4 in. wide (interior dimensions), as shown in Fig. B.1 and B.2, was used for the tests. The overall interior depth of the bin was 24 in., but the design was such that any soil depth less than 24 in. could be used. The sidewalls of the bin were double-strength window glass backed by Plexiglas sheets 5/8 in. thick. The Plexiglas sheets were supported by the grid of steel plates shown in Fig. B.1. Trapdoors 6 in. and 3 in. long, which ran from wall to wall,

were used for these tests. The trapdoor itself was a hollow, metal which was supported by a column of load-carrying elements consisting the trapdoor support plate, load cell, and jack (Fig. B.3). The loa carrying column was supported by a stiff platform hung from the bas the soil container. Deflections of the trapdoor support plate were monitored by two spring-loaded LVDT's like those described in Secti The LVDT's were supported by the system of brackets and rods show Fig. B.3. Prior to each test, the LVDT's were given a two-step ca tion by inserting shims of known thickness (0.010 and 0.026 in.) be the end of the LVDT core and the trapdoor support plate. Pressure applied to the surface of the sand by the thin rubber bag shown in Fig. B.4. The top surface of the bag was restrained by a 3/8-in.- steel plate, with approximately the same plan dimensions as the i of the test bin. The steel plate was held down by the pressure rea members (inverted T sections, see Fig. B.2) which bolted to the top the apparatus. Hardwood spacer blocks transmitted the load between steel plate and the pressure reaction members. The apparatus could up for any desired depth of sand by varying the length of these blo The base of the apparatus contained several flush-mounted pressure of the same type used in the axially symmetrical tests (Section 3.

B.3 Sand and Sand-Placement Procedures

Reid-Bedford Model sand (sand 1) was the medium used for these tests (Section 3.4). The sand was placed in layers of known which were approximately 2-1/4 in. thick. The layers were leveled a screed and then vibrated, as shown in Fig. B.5, by passing a sma vibrator fastened to a wooden block with a width slightly less than

chamber over the sand layer. Vibration was continued until the thickness of the layer decreased to 2 in. The resulting density of the layer was 104.2 pcf. Subsequent layers were placed in the same manner.

B.4 Results of Tests

Figs. B.6-B.9 contain the major results of the tests, arching curves for values of H/B between 1 and 3. Certain conclusions, similar to those based on the axially symmetrical tests, can be drawn. Most of the observed reduction in load took place during the initial deflections of the trapdoor. The form of the arching curves was changed very little for values of H/B greater than 1-1/2. Further interpretation of the data is very difficult. The combined effects of sidewall friction and the loss of load due to elastic deflections in the load-carrying column during pressure buildup cannot be separated. It seems certain than one or both influence the initial arching ratio, which was never much greater than 0.8, the shape of the arching curve, and the ultimate arching ratio.

In order to investigate the significance of wall friction on the test results, several special tests were conducted with lubricated bin walls. The results of these tests are shown in Fig. B.6. In all special tests the lubricant was separated from the sand by a sheet of vinyl film less than 0.001 in. thick. Light machine oil was used as the lubricant in some of the tests. As Fig. B.6 indicates, the general results were essentially the same as those obtained from tests conducted without a friction-reducing scheme. However, during pauses in the lowering of the trapdoor, an increase in load at essentially constant deflection was noted. Since this creep was not noted during routine tests, it is probably associated with the lubricant layer at the

boundary. Subsequently a special test was conducted with a model a smooth layer of petroleum jelly on the sidewalls. The arching cur this test was considerably higher than those previously observed. addition to this, the creep observed during pauses of 3 to 4 sec w greater than before. The existence and importance of wall friction demonstrated by this test, but there was no way of measuring its m with the apparatus. This uncertainty and the problems associated the lubrication technique lead to the conclusion that an axially rical geometry is much more suitable for a systematic study of ar. No motion of the sand grains was ever observed through the glass w of the container at the deflections associated with all loss of

Fig. B.1 Apparatus for plane tests

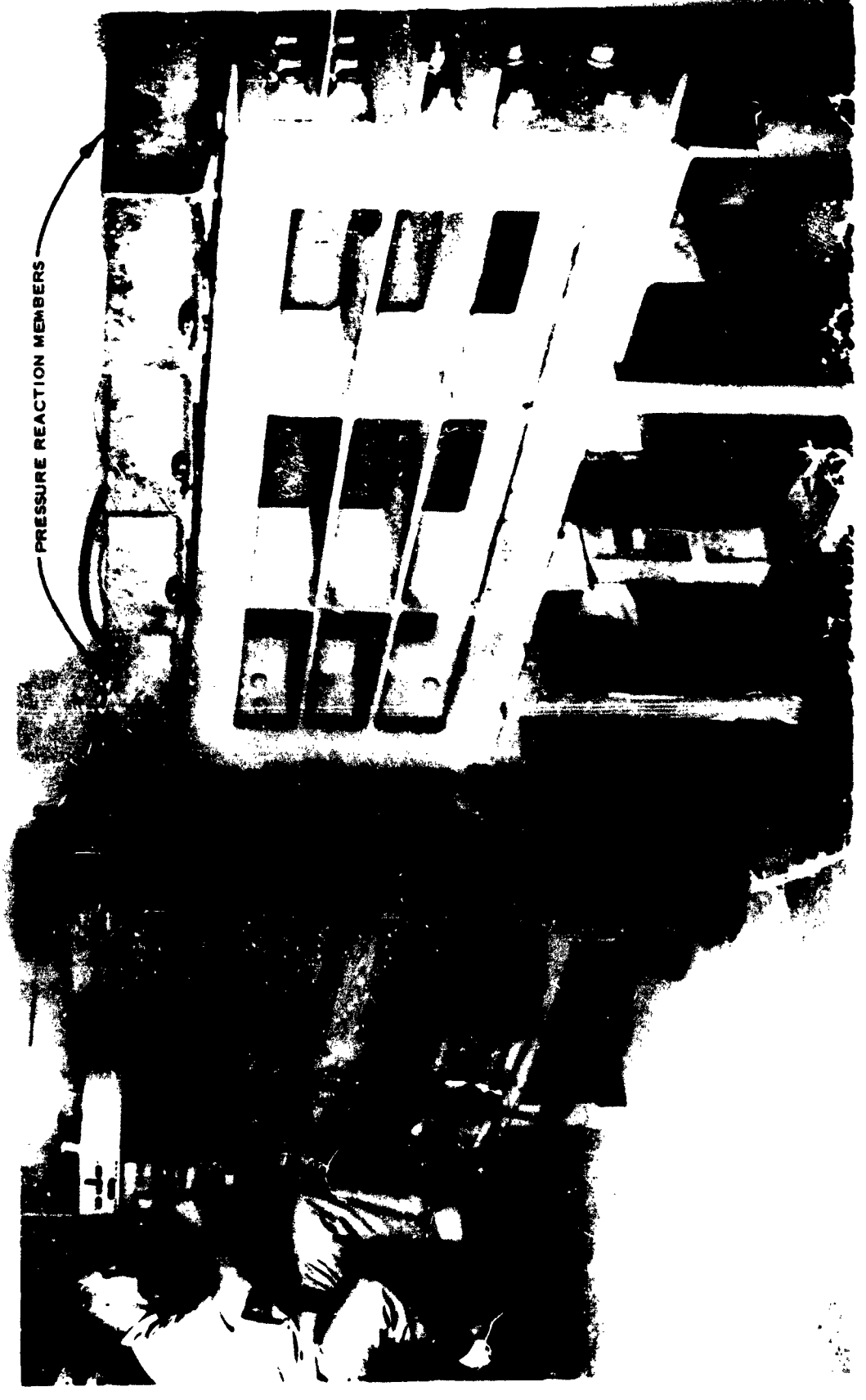
PRESSURE REACTION MEMBERS

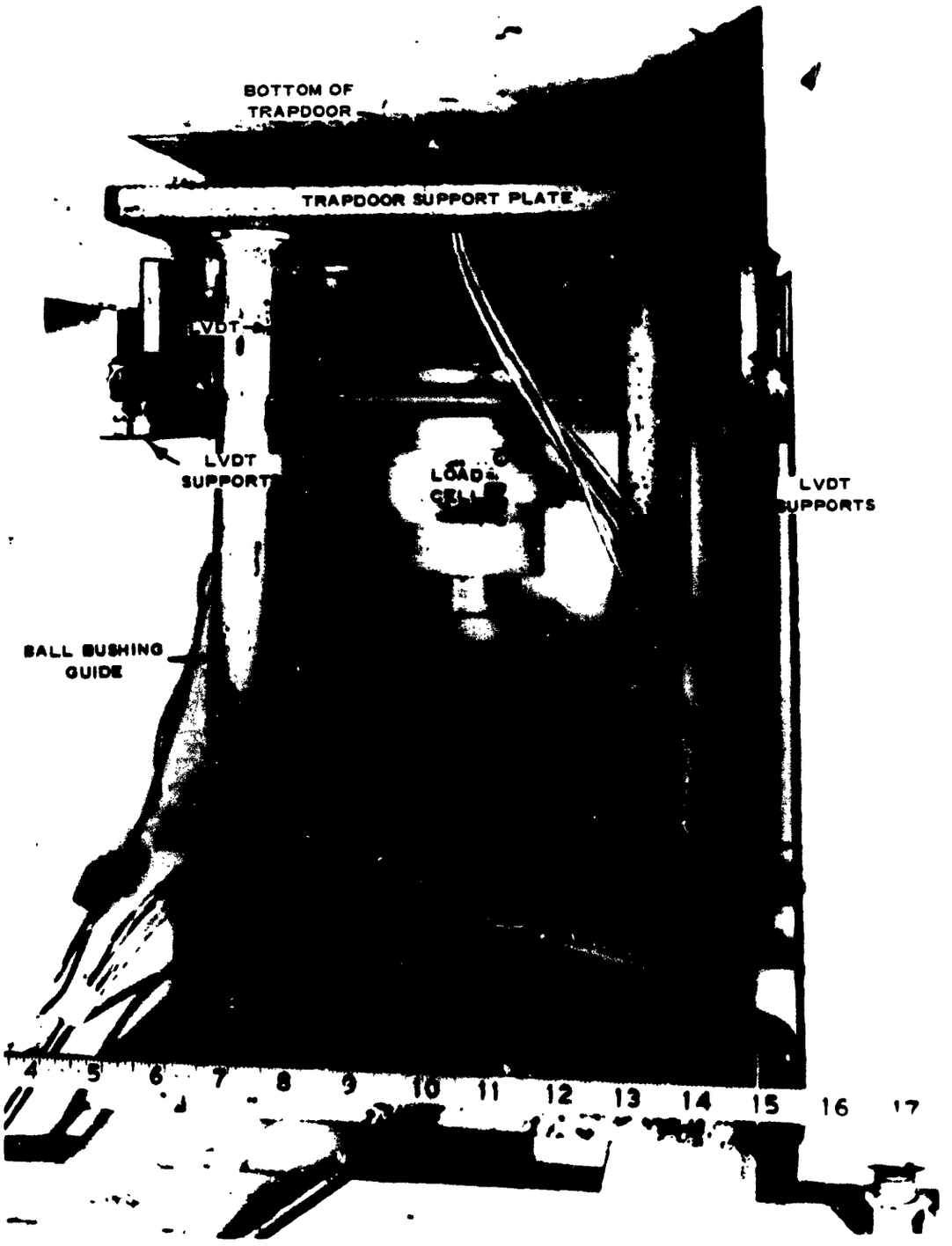

Fig. B.3 Closeup of load support element and deflection measurement system

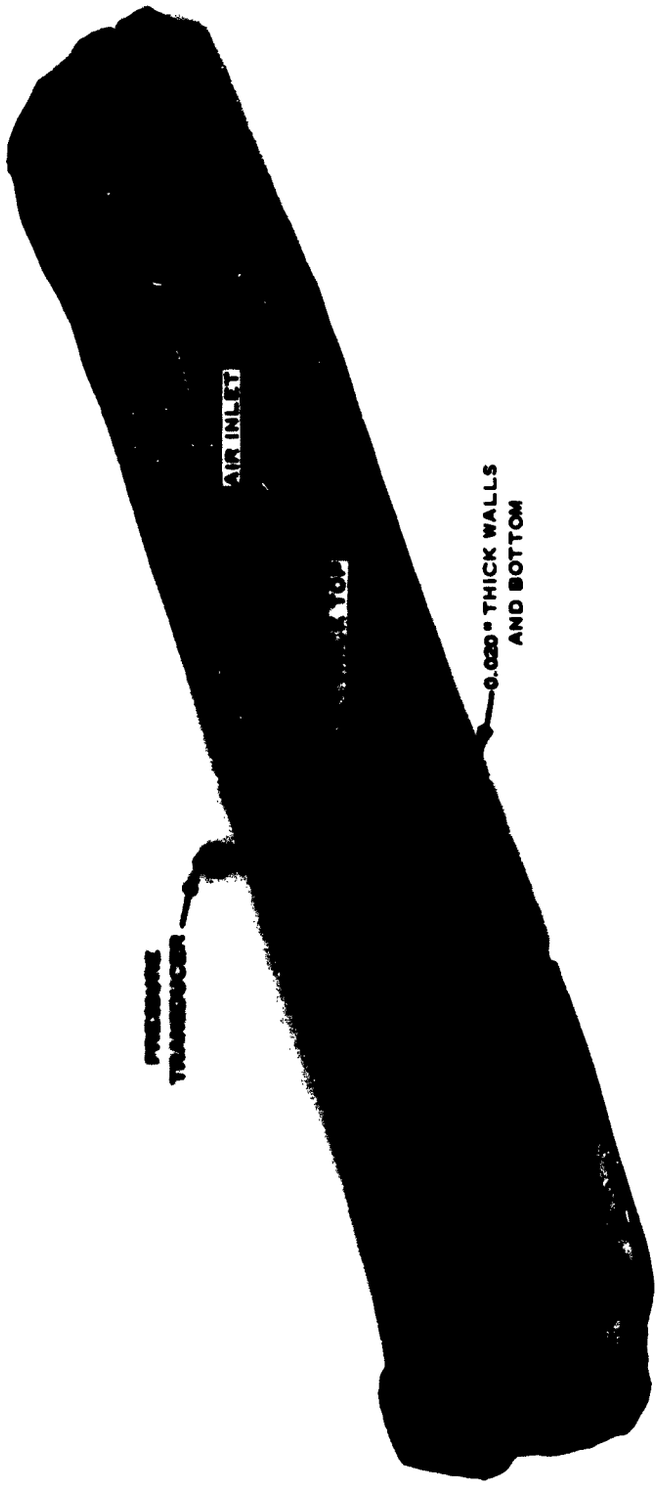
AIR INLET
0.020" THICK WALLS
AND BOTTOM
PRESSURE
TRANSDUCER

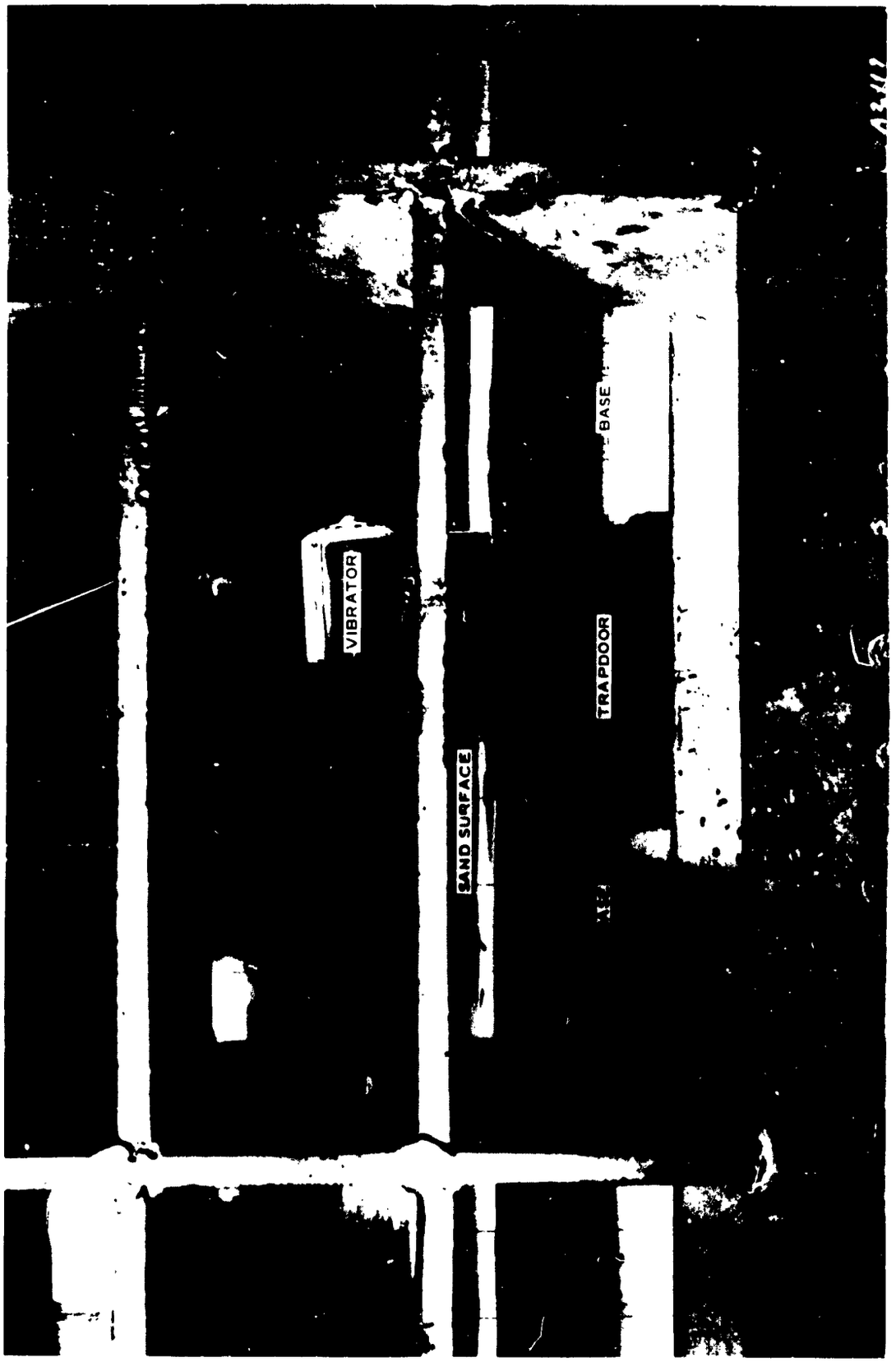

Fig. 3.

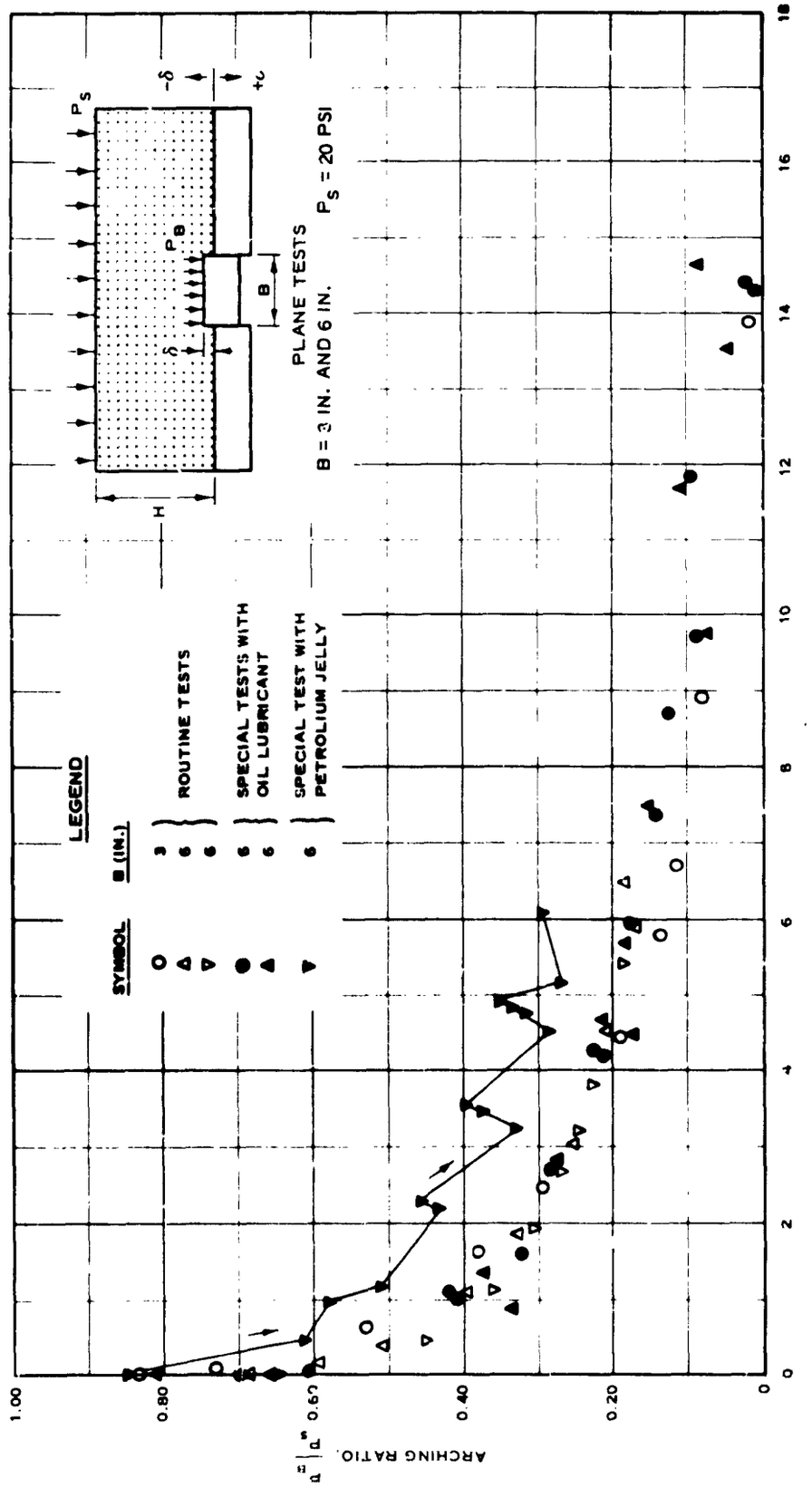
LEGEND
SYMBOL
B (IN.)
ROUTINE TESTS
SPECIAL TESTS WITH OIL LUBRICANT
SPECIAL TEST WITH PETROLIUM JELLY
PLANE TESTS
B = 3 IN. AND 6 IN.
P_S = 20 PSI
P_S
P_B
B
H
δ
$-\delta$
$+\delta$
ARCHING RATIO $\frac{\sigma}{\sigma_s}$
1.00
0.80
0.60
0.40
0.20
0
0
2
4
6
8
10
12
14
16
18

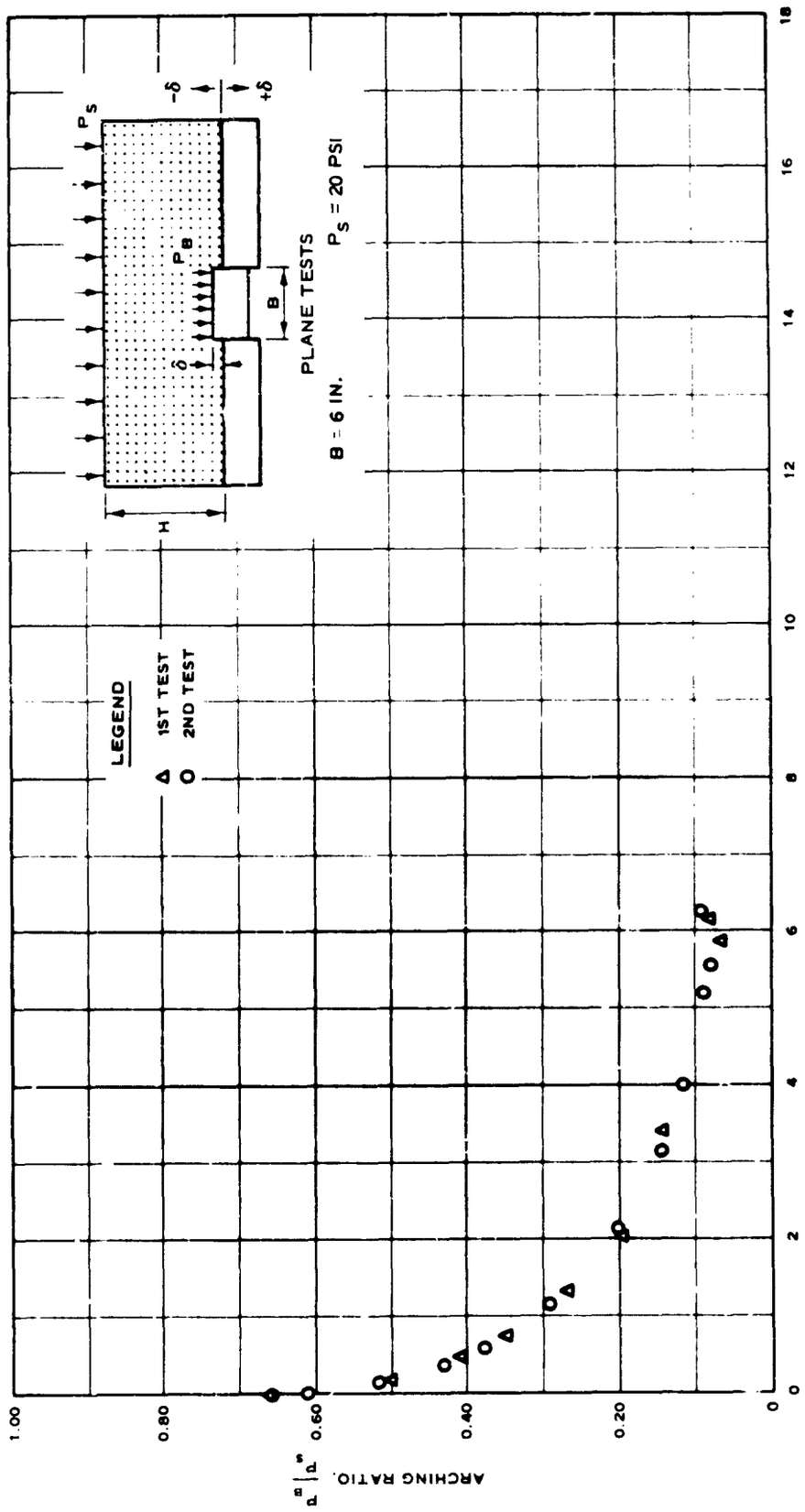

Fig. B.7 Dimensionless plot of pressure vs. deflection for active arching tests with sand 1, H/B = 1-1/2 , plane geometry

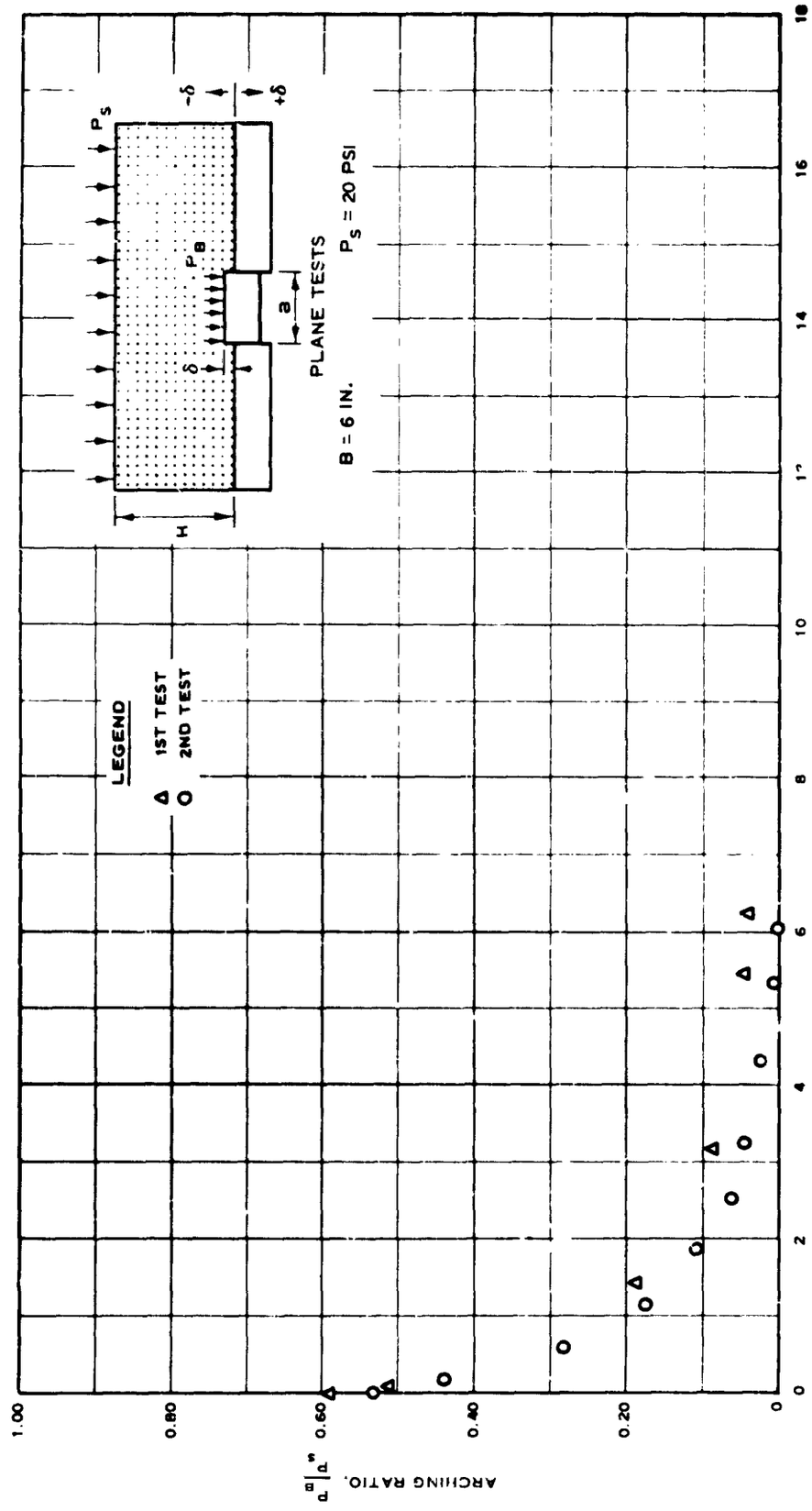
ARCHING RATIO, $\frac{P_v}{P_s B}$
1.00
0.80
0.60
0.40
0.20
0
0
2
4
6
8
10
12
14
16
18
LEGEND
1ST TEST
2ND TEST
PLANE TESTS
P_s = 20 PSI
B = 6 IN.
P_s
P_v
$-\delta$
$+\delta$
a
H

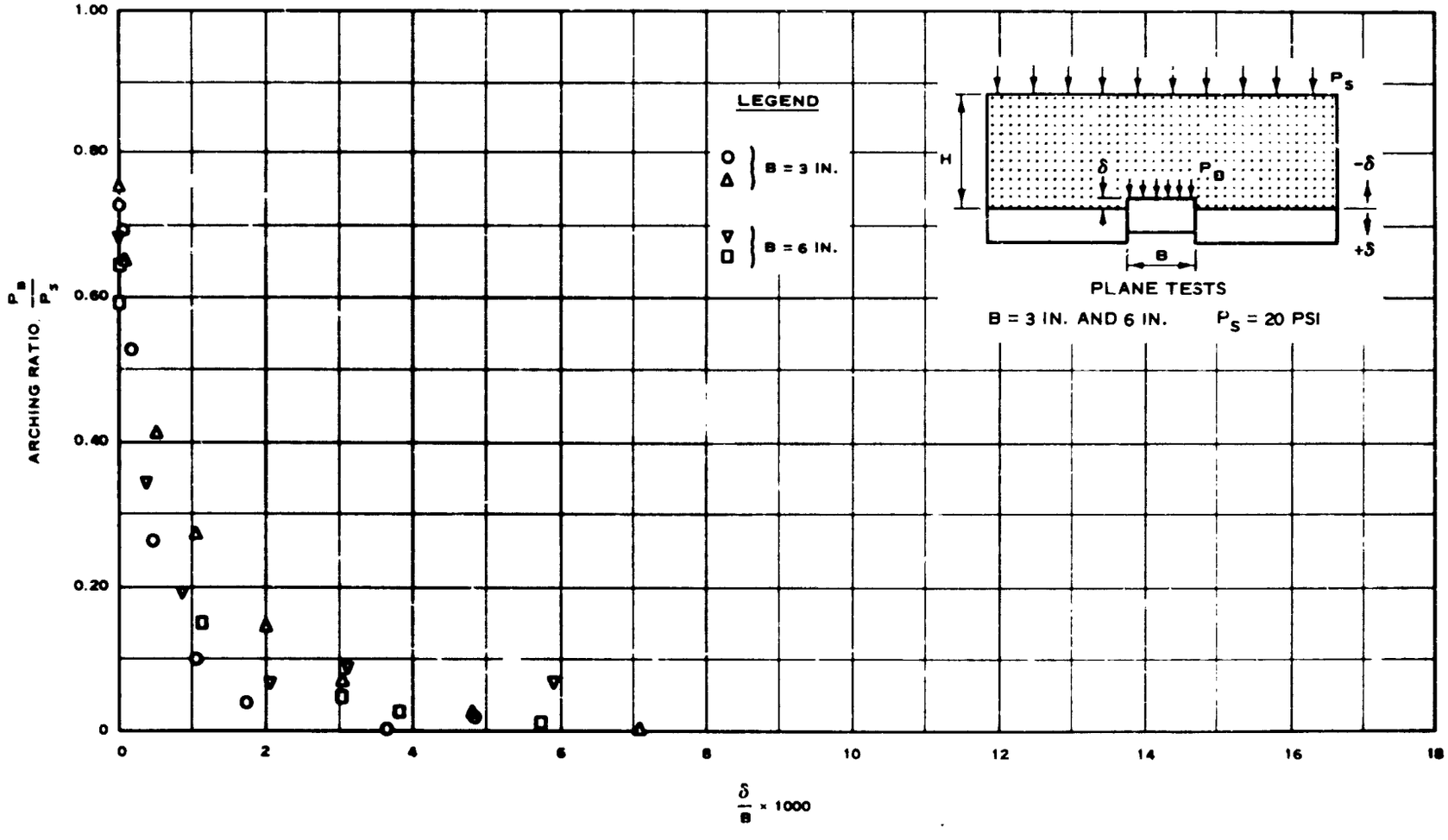

Fig. B.9 **Dimensionless** plot of pressure vs. deflection for active arching tests with sand 1, H/B = 3 , plane geometry

VITA

James Walsh McNulty was born on 17 December 1934 in Orange, New Jersey, and grew up in Lyndhurst, New Jersey. Following one year attendance at St. Peter's College in Jersey City, New Jersey, he entered the United States Military Academy at West Point, New York, in 1952. He was graduated from the Military Academy in 1956 with the degree of Bachelor of Science and received the commission of Second Lieutenant, Regular Army in the Corps of Engineers. He has served as a Platoon Leader and Company Executive Officer in an Engineer Construction Battalion with the United States Army on Guam and Taiwan and as an Airborne Engineer Platoon Leader and Company Commander at Fort Bragg, North Carolina. He has attended the Engineer Officers Basic Course at Fort Belvoir, Virginia, and has completed Parachutist and Ranger training at Fort Benning, Georgia. He received the degree of Master of Science in Civil Engineering from the University of Illinois in 1961. Since February 1962, he has been assigned to the U. S. Army Engineer Waterways Experiment Station at Vicksburg, Mississippi where he has worked on various research and development projects in the Nuclear Weapons Effects Division. At present he is a Captain, Regular Army, Corps of Engineers. He is a member of the Society of Military Engineers and the Association of the United States Army.